Characterisation of antagonist binding sites on chemokine receptor CCR4

Jonathan Mark Viney

Ph.D. Thesis

2012

Leukocyte Biology Section, National Heart and Lung Institute
Faculty of Medicine
Imperial College
London SW7 2AZ
United Kingdom

Submitted for the Doctor of Philosophy degree at Imperial College London

Declaration of originality

I, Jonathan Mark Viney, confirm that the work presented in this thesis is my own. Information derived from other sources is appropriately referenced. Images or figures taken from these sources have been given copyright permission and are credited accordingly.

Abstract

CCR4 is a chemokine receptor notably expressed on T helper 2 and regulatory T cells. CCR4 binds the chemokines CCL17 and CCL22. These are involved in T cell homeostasis and inflammatory diseases including asthma and atopic dermatitis, making CCR4 a potential therapeutic target. Previous studies suggested that CCL22 is dominant over CCL17 with respect to ligand-induced internalisation and desensitisation of CCR4. The biology of CCR4 was investigated in this project using point mutational studies. A C-terminal lysine within the conserved helix VIII region was determined to be dispensable for CCL22-induced chemotaxis but required for CCL17-induced chemotaxis, suggesting that the two chemokines stabilised distinct receptor conformations. The highly conserved GluVII:06 of helix VII was shown to be critical for chemokine binding and receptor function.

Seven small molecule allosteric antagonists of CCR4, supplied by GlaxoSmithKline, were hypothesised to bind either a classical intrahelical site (site 1) within the receptor or a novel intracellular site (site 2). 22 amino acids were predicted to be involved in the binding of the antagonists. Antagonist binding was indirectly investigated by inhibiting either function or chemokine binding of the receptor mutants. Mutation of leucine 118 in transmembrane helix III significantly reduced CCR4 sensitivity to site 1 antagonism in chemotaxis and chemokine-binding assays. Mutants of phenylalanine 305 and leucine 307 at the end of transmembrane helix VII also showed a reduction in antagonist 2 sensitivity.

Direct investigation of the effects of mutation on antagonist binding was performed using tritium-labelled antagonists. Mutation of GluVII:06 prevented site 1 antagonist binding to CCR4. Further investigation of site 1 antagonist binding was hindered by high non-specific binding of the compounds. A low-affinity site for the tritium-labelled site 2 antagonist was identified on untransfected cells, possibly within endogenously expressed chemokine receptors. This antagonist therefore may have potential as a broad-spectrum chemokine receptor inhibitor.

Table of contents

List of figures

List of tables

Acknowledgments

I would like to thank Dr James Pease for supervising my time at Imperial College, and for the guidance he gave me during my project. I would also like to thank the members of the Pease group, both past and present, for their help and support. In addition, the people of Leukocyte Biology made my time in the department very enjoyable.

I would also like to thank Dr David Hall for his supervision of my project, and his help during the time I spent at GlaxoSmithKline. I am grateful to Rob Slack for his assistance with practical techniques and to Nick Barton for the feedback on my project.

The Biotechnology and Biological Sciences Research Council (BBSRC) along with GlaxoSmithKline provided the funding for my project, for which I am very thankful.

Lastly, I would like to thank my friends and family. In particular I would like to thank Dr Ripu Bains for her continued support over the past four years.

List of abbreviations

ANOVA:	Analysis of variance
APC:	Antigen presenting cell
ATL:	Adult T-cell leukaemia
β_2AR:	β_2-adrenergic receptor
BCA:	Bicinchoninic acid
BSA:	Bovine serum albumin
cAMP:	Cyclic adenosine monophosphate
CD:	Cluster of Differentiation
CHO:	Chinese Hamster Ovary cell line
CI:	Chemotactic index
CPM:	Counts per minute
CTLA-4:	Cytotoxic T-lymphocyte antigen 4
C-terminus:	Carboxy terminus
DARC:	Duffy antigen receptor for chemokines
DMSO:	Dimethyl sulphoxide
DNA:	Deoxyribonucleic acid
DPM:	Disintegrations per minute
ECL:	Extracellular loop
EDTA:	Ethylenediaminetetraacetic acid
ERK:	Extracellular signal-related kinase
FACS:	Fluorescence Activated Cell Sorter
FCS:	Foetal calf serum
FITC:	Fluorescein Isothiocyanate
FRET:	Fluorescence resonance energy transfer
GAG:	Glycosaminoglycan
GDP:	Guanosine diphosphate
GPCR:	G protein-coupled receptor
GRK:	G protein-coupled receptor kinase
GSK:	GlaxoSmithKline
GTP:	Guanosine triphosphate
HA:	Haemagluttinin

HEPES:	N-(2-hydroxyethyl)piperazine-N'-(2-ethanesulfonic acid) hemisodium salt
hERG:	Human ether-a-go-go related gene
HIV:	Human Immunodeficiency Virus
HTLV-1:	Human T-cell leukaemia virus type 1
ICAM:	Intracellular adhesion molecule
ICL:	Intracellular loop
IFN:	Interferon
Ig:	Immunoglobulin
IL:	Interleukin
JAK:	Janus kinase
kDa:	kiloDalton
L1.2:	Murine pre-B L1.2 cell line
LB:	Luria broth
LFA:	Lymphocyte function-associated antigen
LPS:	Lipopolysaccharide
LTB_4:	Leukotriene B_4
mAb:	Monoclonal antibody
MAPK:	Mitogen-activated protein kinase
MEF:	Murine embryonic fibroblast
MDC:	Macrophage-derived chemokine
MHC:	Major histocompatibility complex
mRNA:	Messenger ribonucleic acid
ND:	Not done
NMR:	Nuclear magnetic resonance
NR:	No response
NS:	Not significant
NSB:	Non-specific binding
N-terminus:	Amino terminus
PAR:	Protease-activated receptor
PEI:	Polyethylenimine
PBS:	Phosphate buffered saline
PCR:	Polymerase chain reaction
PTX:	*Pertussis* toxin

RNA:	Ribonucleic acid
RPM:	Revolutions per minute
RT:	Room temperature
SEM:	Standard error of the mean
SPA:	Scintillation proximity assay
STAT:	Signal transducer and activator of transcription
TB:	Total binding
TAE:	Tris-acetate buffer
TARC:	Thymus and activation-regulated chemokine
T_H:	Helper T cell
TNF:	Tumour necrosis factor
TM:	Transmembrane domain
T_{reg}:	Regulatory T cell
VLA:	Very late antigen
VCAM:	Vascular cell adhesion molecule
WT:	Wild-type
XCL/CCL/CXCL/CX_3CL:	Chemokine ligand
XCR/CCR/CXCR/CX_3CR:	Chemokine receptor

1 – Introduction

1.1 – The immune system

The immune system exists to protect organisms from invasion by microorganisms such as bacteria and viruses. Leukocytes, more generally known as white blood cells, are one of the factors responsible for carrying out the functions of the immune system. Leukocytes can be broadly grouped into two categories based on whether they function in the innate or adaptive immune response, although both branches of the immune system are intricately linked. The innate response is the first line of defence against pathogens, taking place within minutes of an infection. The innate response involves processes including pattern recognition of common non-self molecular structures, such as bacterial cell wall proteins. In contrast, the adaptive response takes hours or even days to initiate, due to the fact that somatic rearrangement of genes is required to generate molecules to bind the foreign antigen (Chaplin, 2003; Barton, 2008).

The leukocytes of the innate immune system include granulocytes (named due to the presence of large granules in their cytoplasm) such as neutrophils, eosinophils and basophils. Neutrophils phagocytose microorganisms, and can release granules containing reactive oxygen and nitrogen species to disrupt the physical structure of the microorganism (Nathan, 2006). Eosinophils also release granules to counter infections of parasitic organisms such as helminths; the main constituents of these granules are major basic protein and various other toxic products that induce tissue damage (Rothenberg and Hogan, 2006). Basophils are a source of histamine, which when released causes smooth muscle contraction and vasodilation, leading to the characteristic swelling and redness associated with allergy (Schroeder, 2009). Mast cells are also a source of histamine, which they release in response binding of at least two molecules of the immunoglobulin IgE which have been cross-linked by antigen (Williams and Galli, 2000; Abraham and St John, 2010).

Other cell types involved in the innate immune response are the monocytes, macrophages and dendritic cells. Like the granulocytes, they are derived from a myeloid lineage. Monocytes produce inflammatory cytokines and can differentiate into macrophages and dendritic cells. Macrophages are phagocytic cells that can clear apoptotic cells and microbes. Dendritic cells are professional antigen presenting cells that residue in tissues such as the skin, where they phagocytose infectious organisms and display antigen on their cell surface after processing. Dendritic cells migrate to

the lymphoid organs where they interact with B and T cells, thus engaging the adaptive immune response (Geissmann et al., 2010).

To trigger the adaptive immune response, antigen needs to be encountered by B cells, T cells and antigen presenting cells (APCs). APCs such as dendritic cells take up antigen from the tissues, after which they migrate via the lymphatic system to the secondary lymphoid organs which include the spleen and lymph nodes. Here the dendritic cells present antigen in order to activate the adaptive immune response. The adaptive immune response has two major branches; humoral immunity mediated by B cells, and cell-mediated immunity involving the production of cytokines and killing cells in a process mediated by cytotoxic T cells, macrophages and natural killer cells (Murphy, 2011).

In cell-mediated immunity, APCs such as dendritic cells and macrophages encounter antigen in the tissues, and then display it on their cell surface in complex with major histocompatibility (MHC) proteins. For example, an APC that has encountered antigen in the tissue migrates via the lymphatic vessels to the secondary lymphoid organs. Here, the APC encounters naïve T cells that have entered the organ from the bloodstream via a process called diapedesis. Intracellular antigens, such as those from viruses are displayed with MHC type I proteins. Extracellular antigens, such as those from bacteria, are displayed with MHC type II proteins. For example, a macrophage that has phagocytosed a virus-infected cell displays viral antigens in complex with MHC I; these are presented to naïve T cells which causes them to differentiate into $CD8^+$ antiviral cytotoxic T cells. A dendritic cell that has phagocytosed bacterial antigen displays it in complex with MHC II to naïve T cells, causing them to differentiate into CD4 T helper cells. These cells then help B cells in mediating humoral immunity.

In humoral immunity, antigen is encountered by B cells. Like professional APCs such as dendritic cells, B cells migrate to the lymph nodes. B cells interact with helper T cells in the germinal centers, leading to proliferation of the B cells and subsequent production of antibodies. Antibodies perform a variety of functions, including the can opsonisation of microorganisms in order to facilitate phagocytosis by cells such as macrophages, neutralise toxins and viruses. Opsonisation involves the binding of the Fab region of antibody to the microorganism, after which the Fc region of the antibody is bound by a receptor on the surface of the phagocyte. This

facilitates phagocytosis. Antibodies also activate other cell types such as mast cells (Murphy, 2011).

T helper (T_H) cells are important for the initiation and maintenance of adaptive immunity. These can be split into various subtypes, including T_H1 and T_H2 cells. Upon contact with an antigen-presenting cell, secretion of interleukin-12 stimulates the naïve T cell to differentiate into a T_H1 cell, while interleukin-4 stimulates T_H2 differentiation. T_H1 cells secrete cytokines such as interferon-γ (IFN-γ), which has antiviral activity in addition to stimulating macrophages to kill phagocytosed bacteria. T_H2 cells secrete the cytokines IL-4, IL-5 and IL-13. These promote antibody production by B cells, eosinophil migration and activation, further T_H2 differentiation, and synthesis of the antibody IgE, thus furthering the humoral response (Murphy, 2011). Another subset of T cells known as T_H17 cells also plays a role in inflammation. T_H17 cells produce the pro-inflammatory cytokine IL-17, and mediate neutrophil and macrophage recruitment during infections. They also have shown to be involved in autoimmune diseases such as multiple sclerosis (Dong, 2008).

The immune system is highly complex and involves the coordination of multiple cell types throughout all the tissues of the body. It is through the action of chemokines and their receptors that many immune cells reach their target destinations within the tissues. For example, chemokines are required for dendritic cell immune surveillance throughout the tissues and for their migration to the lymphoid organs in order to present antigen to T cells. Chemokines are also required for the migration of phagocytic cells to sites of bacterial infection, in addition to a whole host of other processes. Chemokines are therefore an important factor in the immune system as they allow its component cells to carry out their effector functions.

1.2 – Chemokines

Chemokines, *chemo*tactic cyto*kines*, are a family of low molecular weight proteins that range from 8 to 10 kDa in size (Harrison and Lukacs, 2007). Chemokines guide the migration of cells expressing chemokine receptors, in a process termed chemotaxis. Chemotaxis is the migration of a cell along an increasing concentration gradient of a chemoattractant substance. There are over 40 known chemokines present in humans; these are divided into four subfamilies based upon the number and position of conserved N-terminal cysteine residues, which provide stabilisation of the chemokine tertiary structure through the formation of disulphide bonds (Laing and Secombes, 2004). Most chemokines, despite their diversity in sequence, share a similar tertiary structure; an N-terminal 6-10 amino acid signalling domain, an N-loop binding domain, a three-stranded β-sheet, followed by a C-terminal helix (Allen et al., 2007). Figure 1-1 shows the tertiary structure of CXCL8, which is representative of other chemokines (Fernandez and Lolis, 2002).

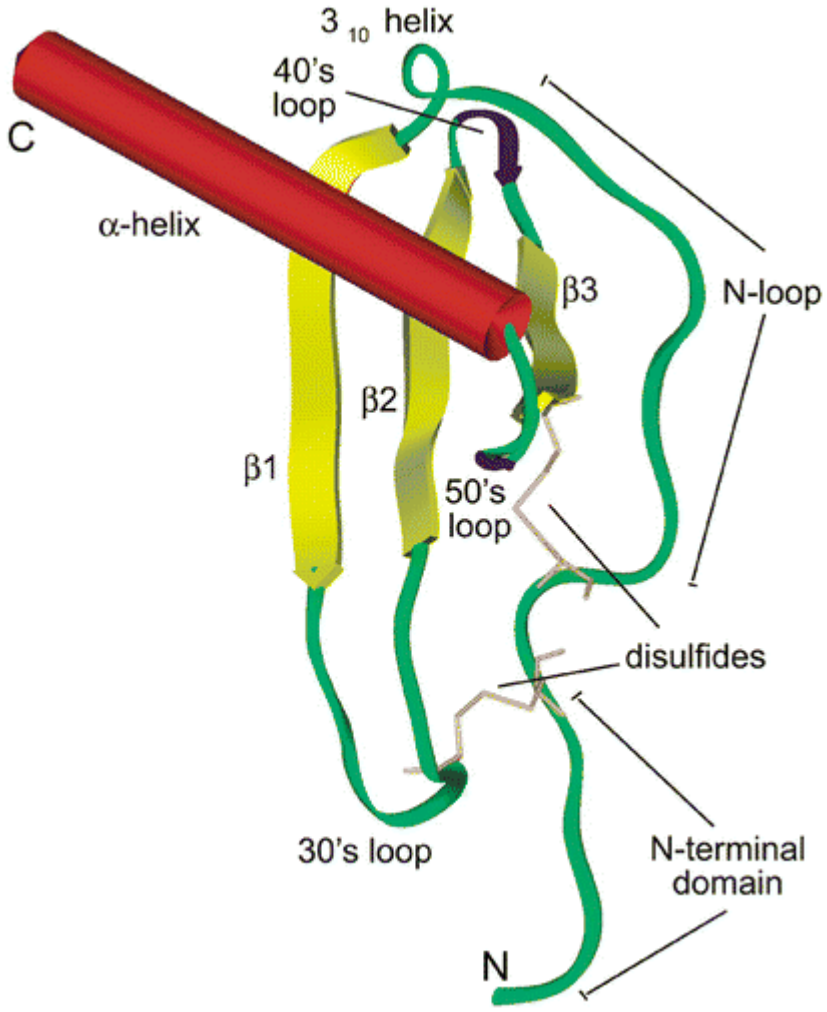

Figure 1-1 – Tertiary structure of CXCL8

Ribbon structure of CXCL8, with the various domains labelled (Fernandez and Lolis, 2002).

There are four chemokine subfamilies; CC, CXC, XC and CX_3C. These are named due to the arrangement of the first pair of cysteines. The cysteines in the CC subfamily are adjacent, while in the CXC subfamily they are separated by one amino acid. Three amino acids separate the cysteines of the CX_3C subfamily, while the first cysteine is absent in chemokines of the XC subfamily (Murphy et al., 2000). As shown in figure 1-1, the cysteines create intramolecular disulphide bonds that provide stabilisation of the chemokine tertiary structure.

Chemokines can also be loosely organised according to their function. Inflammatory chemokines are those involved in migration of cells during an infection, allergic reaction or other inflammatory stimulus; these chemokines are not constitutively expressed but rather are induced by the inflammatory processes. Homeostatic chemokines however are constitutively expressed; these chemokines direct the migration of cells involved in immune system development, immune surveillance, and immunological memory (Moser and Willimann, 2004). Table 1-2 shows the chemokines classified by sub-family along with their functions, and the receptors they bind.

Systematic name	Other names	Function	Chromosome	Receptors
CC subfamily				
CCL1	I-309	I	17q11.2	CCR8
CCL2	MCP-1	I	17q11.2	CCR2
CCL3	MIP-1α, LD78α	I	17q11.2	CCR1, CCR5
CCL3L1	LD78β	I	17q12	CCR1, CCR3, CCR5
CCL3L2	LD78β	I	17q12	
CCL4	MIP-1β	I	17q12	CCR5
CCL4L1	AT744.2	I	17q12	
CCL4L2		I	17q12	
CCL5	RANTES	I, Pt	17q12	CCR1, CCR3, CCR5
CCL7	MCP-3	I	17q11.2	CCR1, CCR3, CCR5
CCL8	MCP-2	I	17q11.2	CCR1, CCR3, CCR5
CCL11	Eotaxin	D	17q11.2	CCR3, CCR5
CCL13	MCP-4	I	17q11.2	CCR2, CCR3
CCL14	HCC-1	P	17q12	CCR1, CCR3, CCR5
CCL15	HCC-2, Leukotactin	P	17q12	CCR1, CCR3
CCL16	HCC-4	U	17q12	CCR1, CCR2, CCR5, CCR8, H4
CCL17	TARC	D	16q13	CCR4
CCL18	PARC	H	17q12	PITPNM3
CCL19	MIP-3β, ELC	H	9p13.3	CCR7
CCL20	MIP-3α, LARC	D	2q36.3	CCR6
CCL21	SLC, 6Ckine	D	9p13.3	CCR7
CCL22	MDC	D	16q13	CCR4
CCL23	MPIF-1	P	17q12	CCR1, FPRL-1
CCL24	Eotaxin-2	H	17q11.23	CCR3
CCL25	TECK	H	19p13.2	CCR9
CCL26	Eotaxin-3	I	7q11.23	CCR3, CX_3CR1
CCL27	CTACK, ILC	H	9p13.3	CCR10
CCL28	MEC	H	5p12	CCR10, CCR3
CXC subfamily				
CXCL1	Gro-α	I, ELR	4q13.3	CXCR2
CXCL2	Gro-β	I, ELR	4q13.3	CXCR2
CXCL3	Gro-γ	I, ELR	4q13.3	CXCR2
CXCL4	PF-4	Pt, non-ELR	4q13.3	CXCR3-B
CXCL4L1	PF4V1	Pt, non-ELR	4q13.3	CXCR3-B
CXCL5	ENA-78	I, ELR	4q13.3	CXCR2
CXCL6	GCP-2	I, ELR	4q13.3	CXCR1, CXCR2
CXCL7	NAP-2	Pt, I, ELR	4q13.3	CXCR1, CXCR2
CXCL8	IL-8	I, ELR	4q13.3	CXCR1, CXCR2
CXCL9	MIG	I, non-ELR	4q21.1	CXCR3
CXCL10	IP-10	I, non-ELR	4q21.1	CXCR3
CXCL11	I-TAC	I, non-ELR	4q21.1	CXCR3, CXCR7
CXCL12	SDF-1α/β	H, non-ELR	10q11.21	CXCR4, CXCR7
CXCL13	BLC, BCA-1	H, non-ELR	4q21.1	CXCR5, CXCR3
CXCL14	BRAK, bolekine	H, non-ELR	5q31.1	Unknown
CXCL16	SR-PSOX	I	17p13.2	CXCR6
CXCL17	DMC	U	19q13.2	Unknown
Other subfamilies				
XCL1	Lymphotactin, ATAC, SCM-1α	D	1q24.2	XCR1
XCL2	SCM-1β	D	1q24.2	XCR1
CX_3CL1	Fractalkine	I	16q13	CX_3CR1

Table 1-2 – Summary table of chemokines, their functions, and receptors

Chemokines are classified by subfamily. Both systematic and other names are shown. Abbreviations; I – inflammatory, H – homeostatic, D – dual inflammatory/homeostatic, U – unknown, P – plasma or platelet chemokine activated by cleavage, Pt – platelet chemokines, ELR – contains the ELR motif, H4 – histamine receptor 4, PITPNM3 – phosphatidylinositol transfer protein membrane associated 3, FPRL-1 – formyl peptide receptor-like 1. Adapted from Zlotnik and Yoshie, 2012.

Inflammatory chemokine production is induced when inflammatory mediators such as TNF-α, IFN-γ or antigens are present. TNF-α production by mast cells during inflammation (Gordon and Galli, 1990) has been demonstrated to induce the production of ELR-motif neutrophil-attracting chemokines (Lakshminarayanan et al., 1997; Smart & Casale, 1994). These chemokines, which include the inflammatory chemokine CXCL8, bind the receptors CXCR1 and CXCR2 expressed on neutrophils. Once they have migrated to the source of the initial inflammatory stimulus, neutrophils perform a variety of functions including phagocytosis of microorganisms and the release of toxic anti-bacterial proteins such as elastase, myeloperoxidase, cathepsins, and defensins (Lacy, 2006). IFN-γ has been shown to induce the production of CXCL9, CXCL10 and CXCL11, which are chemotactic for activated T cells expressing the receptor CXCR3 (Flier et al., 1999). Such T cells include the T_H1 subset of T helper cells, which promote antiviral immunity by activating macrophages and NK cells.

The CC group contains both inflammatory and homeostatic chemokines. CCL2, which is induced by the pro-inflammatory cytokine IL-1, is chemotactic for inflammatory monocytes expressing CCR2 (Luster and Rothenberg, 1997). Other examples of pro-inflammatory CC chemokines include CCL5, which at low concentrations attracts memory T cell expressing CCR5 (Schall et al., 1990); these cells can then rapidly induce an inflammatory response. CD45R0-expressing memory T cells are those that have previously encountered antigen, and as such are able to quickly respond to a second antigen exposure.

The homeostatic chemokines CCL19 and CCL21 direct migration of CCR7-expressing dendritic cells throughout the lymphoid tissues during immune surveillance, as well as guiding T cells into the lymph nodes (Förster et al., 2008). It is within the lymph nodes that dendritic cells present antigen to naive T cells, causing them to differentiate into effector T cells.

T cells development involves the differentiation of haematopoietic progenitor cells into thymocytes, which occurs in the bone marrow. These thymocytes then migrate into the thymus, where they develop into T cells through several differentiation steps, including the expression of cell-surface antigens such as CD4 and CD8, as well as the T cell receptor. Mature T cells are then able to differentiate into effector T cells after antigen presentation by cells such as dendritic cells (Zúñiga-Pflücker, 2004). The migration of thymocytes into the thymus is a homeostatic

process that is directed by chemokines. The chemokines CCL17 and CCL22, which bind the receptor CCR4, have been shown to attract thymocytes during their development in the thymus (Chantry et al., 1999; Annunziato et al., 1999).

CCL17 and CCL22 also function as inflammatory chemokines; CCR4 is expressed on T_H2 cells (Bonecchi et al., 1998), regulatory T cells (Iellem et al., 2001) and mast cells (Juremalm et al., 2002), which suggests a role in allergic disease. T_H2 cells, as described in section 1.1, are important mediators of the adaptive immune response, in that they secrete cytokines such as IL-4, IL-5, and IL-13 that encourage antibody production and class switching by B cells and induce eosinophil activation. Indeed, CCR4-positive cells are recruited to the skin in atopic dermatitis and are associated with the pathogenesis of the disease due to their inflammatory roles (Kakinuma et al., 2001; Vestergaard et al., 2000). Thus, chemokines such as CCL17 and CCL22 have dual functions, as both homeostatic and inflammatory mediators of migration.

Another method of chemokine classification is by genetic similarity. Most chemokines cluster in particular regions on the chromosomes, and there are two major clusters of either CXC or CC chemokines. The CXC cluster is located on chromosome 4q13.3-q21.1, and is split into the GRO and IP-10 regions based upon the representative chemokine for each region. The CC cluster is located on chromosome 17q11.2 and is split into the MCP and MIP regions. This CXC/CC clustering also broadly matches the inflammatory/homeostatic division of the chemokines. There also exist CC and XC mini-clusters; the CC mini-cluster on chromosome 16 for example contains dual-action inflammatory/homeostatic chemokines CCL17 and CCL22 (Nomiyama et al., 2010). The chromosomal locations of the chemokines are shown in table 1-2. This clustering of CC and CXC chemokine alludes to their origins; gene duplication and subsequent genetic diversion undoubtedly occurred during the evolutionary past of chemokines, leading to the diverse number and types we see today.

1.2.1 – Chemotaxis

Chemokines guide the migration of cells expressing their receptors along a gradient of increasing concentration. This process, chemotaxis, is used by many cell types in order to traverse the body and the tissues within. Amoebae such as *Dictyostelium discoidium* also use this process to migrate toward bacteria (Devreotes and Zigmond, 1988). In multicellular organisms, the immune system in particular utilises chemotaxis in order to selectively attract different leukocytes to areas of inflammation (Rot and von Andrian, 2004).

Chemotaxis is one component of a multi-step process known as transendothelial migration. Cells that leave the bloodstream and enter the tissues must squeeze through the endotheliu; this migration depends on a variety of factors and mediators. A leukocyte passing through a blood vessel is initially captured by a group of proteins expressed on endothelium known as selectins. The L, P and E selectins tether the leukocyte, initiating a process known as rolling. The leukocyte slows its movement and begins to roll across the endothelium under shear stress from blood flow; interestingly this shear stress is required for rolling behaviour, as the cells detach if blood flow is interrupted. Chemokines and adhesion molecules expressed on the endothelium then initiate activation and arrest of the rolling leukocyte. Chemokines are presented on the endothelial surface by glycosaminoglycans (GAGs), and bind with high affinity to chemokine receptors, causing the leukocyte to stop rolling and begin crossing the endothelial barrier. Integrins such as VLA-4 and LFA-1 mediate leukocyte adhesion during this process. The leukocyte can cross the endothelium by either the paracellular or transcellular route; the former involves migrating between endothelial cells, whereas the latter involves the leukocyte passing through an endothelial cell (Ley et al., 2007). A summary of this process is shown in figure 1-3.

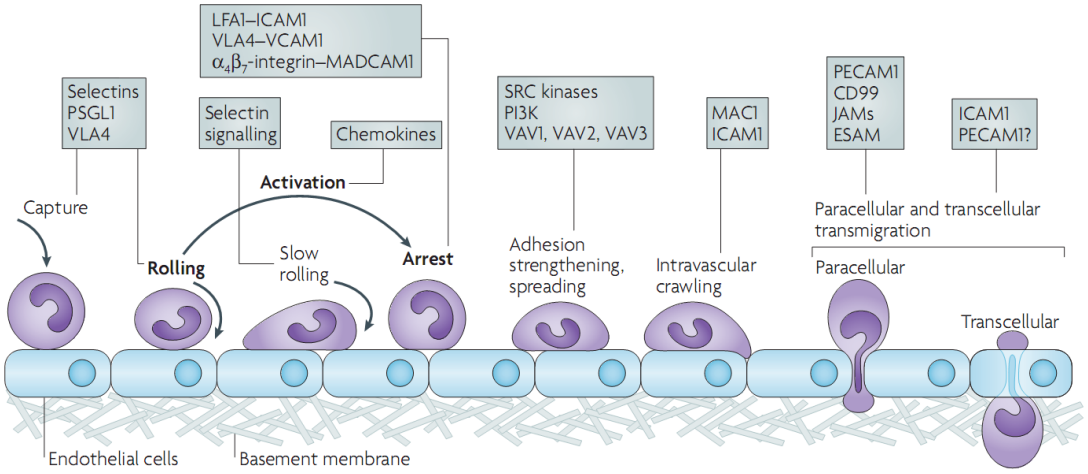

Figure 1-3 – The steps of leukocyte migration

The main steps of leukocyte migration are shown; the three original steps are bolded. The mediators of each step are shown in the grey boxes. A leukocyte is captured by the endothelium by selectins, which initiates rolling under shear stress. Chemokines activate the leukocyte, and integrins mediate arrestin. Migration then occurs via the paracellular or transcellular route. ESAM - endothelial cell-selective adhesion molecule; ICAM1 - intercellular adhesion molecule 1; JAM - junctional adhesion molecule; LFA1 - lymphocyte function-associated antigen 1; MAC1 - macrophage antigen 1; MADCAM1 – mucosal vascular addressin cell-adhesion molecule 1; PSGL1 - P-selectin glycoprotein ligand 1; PECAM1 - platelet/endothelial-cell adhesion molecule 1; PI3K - phosphoinositide 3-kinase; VCAM1 - vascular cell-adhesion molecule 1; VLA4 -very late antigen 4. From Ley et al., 2007.

Once out of the blood vessel and through the endothelium, the leukocyte responds to chemokine gradients present in the tissue, and undergoes chemotaxis toward the source of the chemokine where it can carry out its effector function.

During the process of migration, lymphocytes probe the surface of endothelial cells in order to create transcellular pores through which to migrate (Carman et al., 2007). It has also been shown that shear forces generated by blood flow enhance the formation of these filopodia during lymphocyte crawling across the endothelial surface (Shulman et al., 2009). More recent research however has shown that chemokines such as CCL2 exist in vesicles just below the apical surface of the endothelial cells, and these are probed by lymphocyte filopodia (Shulman et al., 2011). As the lymphocyte migrates through the endothelium the vesicles are consumed by these protrusions; the authors hypothesised that this allows the cell to remain responsive to chemokine stimulation as only specific parts of the lymphocyte membrane are exposed to chemokine at one time. They also showed that the arrest of crawling lymphocytes on the endothelium was independent of G proteins, which are involved in the transduction of chemokine receptor signals. This signifies that lymphocyte arrest is not dependent on chemokine receptors, unlike transendothelial migration. Instead, integrins were shown to be essential for lymphocyte arrest, since the blocking of integrins prevented this process (Shulman et al., 2011).

1.3 – G protein-coupled receptors

GPCRs are one of the largest families of proteins; more than 1% of human genes code for GPCRs (Venter et al., 2001). As such, the functions of these receptors and the ligands they bind vary greatly. GPCRs communicate a host of signals from ligands such as photons, lipid hormones, neurotransmitters, and proteins (Lagerström and Schiöth, 2008). Previous classification systems grouped GPCRs into subfamilies based on physiological and structural features. Once such system is shown in figure 1-4 (Bockaert and Pin, 1999). A more recent system grouped GPCRs into five families according to the GRAFS phylogenetic categorisation system; the Glutamate (G), Rhodopsin (R), Adhesion (A), Frizzled/Taste2 (F), and Secretin (S) families (Bjarnadóttir et al., 2006; Schiöth and Fredriksson, 2005).

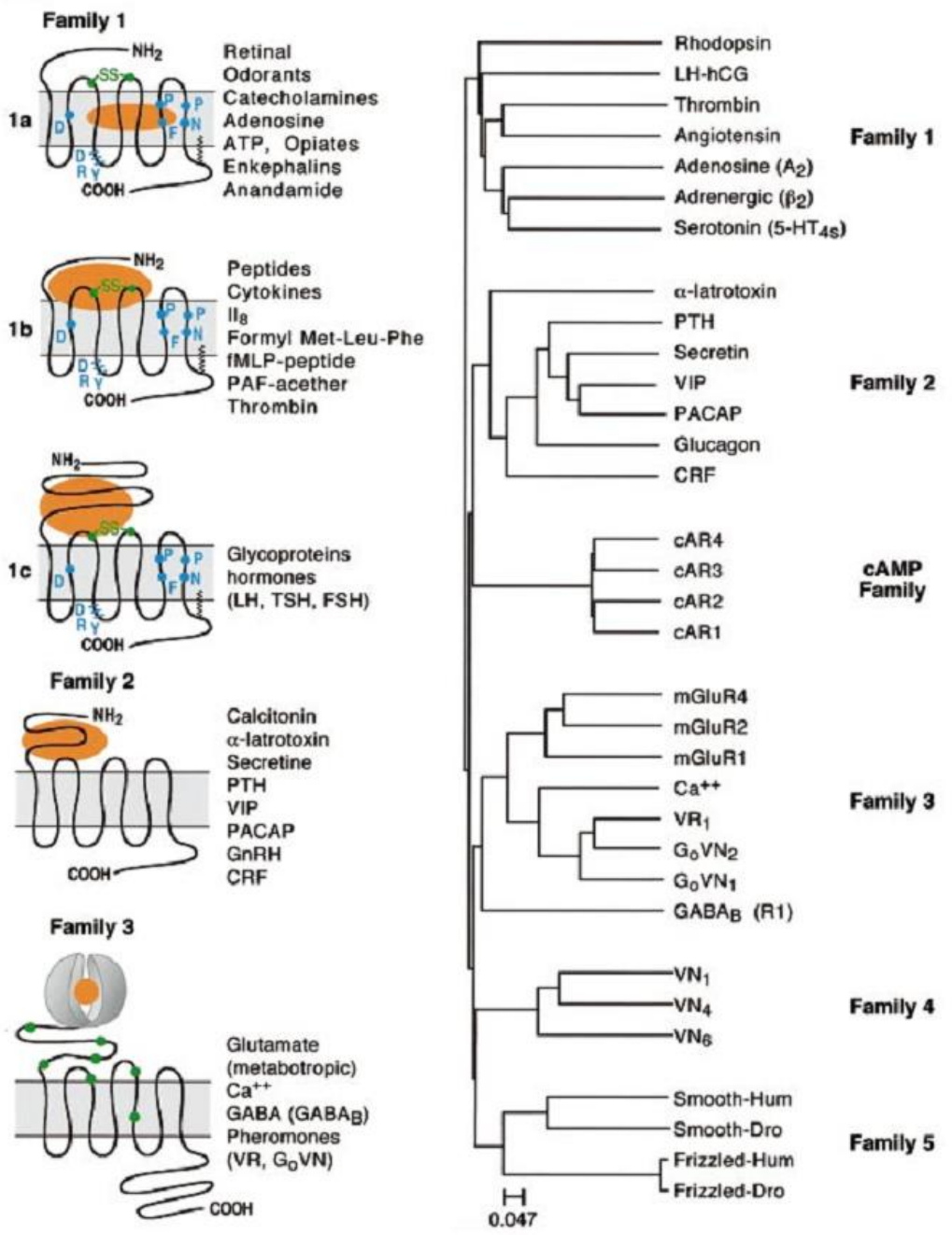

Figure 1-4 – GPCR ligand types and family tree

Three families of GPCRs are apparent based on their amino-acid sequences. Family 1 contains most GPCRs; 1a receptors bind small ligands in the transmembrane domains; 1b receptors bind larger peptides using the N-terminus, extracellular loops and transmembrane domains; 1c receptors bind ligand with their large N-terminus. The unrelated family 2 receptors bind ligand in a similar manner to family 1c. The family 3 receptors bind ligand using a lobed region on their N-terminus. From Bockaert and Pin, 1999.

The *Frizzled/Taste2* family contains 10 frizzled receptors and the smoothened receptor present in *Drosophila melanogaster*, as well as the 25 human Taste2 receptors. The latter are involved in the taste of bitter compounds. The *Secretin* family of GPCRs consists of 15 hormone-binding receptors such as the calcitonin receptor, secretin receptor, and parathyroid receptor. Each member of this family binds its cognate peptide hormone via its large N-terminal domain. The *Glutamate* receptor family consists of 22 proteins, which include the sweet and umami taste receptors TAS1R1-3. These receptors bind ligand with their large 'Venus fly-trap' N-termini. The second largest class of GPCRs, the *Adhesion* family, has 33 members that are divided into 8 subgroups. Most of these receptors are orphan receptors, in that their endogenous ligands are still unknown (Lagerström and Schiöth, 2008).

The *Rhodopsin* family is the largest GPCR family, containing approximately 670 receptors. This family is highly diverse and contains receptors that are involved in a myriad of processes that include vision, olfaction, adrenaline production, calcium release, water homeostasis and cell migration (Lagerström and Schiöth, 2008). The *Rhodopsin* receptors have comparatively short N-termini compared to other families such as the *Adhesion* receptors. This N-terminus binds ligand along with the extracellular loops and portions of the transmembrane domains. The *Rhodopsin* family is further divided into four groups – α, β, γ, and δ - that are based upon the specific type of ligand the receptor binds. The α-group receptors bind biogenic amines, and include the histamine, dopamine, serotonin and cannabinoid receptors. These receptors contain a ligand-binding pocket within the transmembrane bundle (Strader et al., 1989; Swaminath et al., 2004). The β-group receptors bind peptides, which are larger than the molecules that the α-group receptors bind. This group includes endothelin and oxytocin receptors (Lagerström and Schiöth, 2008). Due to the larger ligands that these receptors bind, the N-terminus and extracellular loops are involved in ligand binding in addition to sites within the transmembrane domains. The γ-group receptors contain members that bind peptides and lipid-like compounds (Fredriksson et al., 2003), and include the chemokine receptors, which direct cell migration. Lastly, the δ-group contains the olfactory and thrombin receptors (Fredriksson et al., 2003).

Rhodopsin was the first GPCR to be identified and cloned (Nathans and Hogness, 1983), and is responsible for the detection of light in photoreceptor cells. In most GPCRs, ligand binds the orthosteric site within the transmembrane domain,

leading to conformational change and receptor signalling through heterotrimeric G proteins. The ligands of these GPCRs can dissociate from the receptor and return it to its inactive form. Rhodopsin however is different in that the receptor consists of the protein opsin covalently bound to the chromophore retinal. The bound retinal of rhodopsin is isomerised upon exposure to photons from its *cis* form to its *trans* form, which induces conformational change within the opsin molecule, leading to receptor activation and subsequent downstream signalling (Nathans & Hogness, 1983; Okada & Palczewski, 2001; Palczewski et al., 2000). Therefore, it is a conformational change in the covalently-bound ligand that leads to receptor activation rather than the binding of ligand itself. The *trans*-retinal is eventually hydrolysed, causing it to dissociate from opsin. This is replaced by newly-synthesised *cis*-retinal (Palczewski et al., 2000).

GPCRs have seven α-helical domains that span the cell membrane, an extracellular amino terminus (N-terminus), an intracellular carboxy terminus (C-terminus), and three extracellular and intracellular loops linking the transmembrane domains. When activated by ligand, GPCRs shift into a conformation that allows coupling to G proteins through their intracellular face, which then allows signal transduction. Residues in the intracellular loops, C-terminus and intracellular ends of the transmembrane domains bind these heterotrimeric G proteins. The G proteins consist of α, β, and γ subunits. GDP is normally bound to the Gα subunit of the G protein; when the GPCR shifts to an active conformation and recruits the G proteins, GDP dissociates and is replaced by GTP. This then causes the Gβγ complex to dissociate from Gα-GTP. Once dissociated from each other, the Gα subunit and Gβγ complex can activate or inhibit different downstream signalling partners (Johnston and Siderovski, 2007).

In mammals there are four families of Gα proteins ($G\alpha_{i/o}$, $G\alpha_{q}$, $G\alpha_{12}$, and $G\alpha_{s}$), as well as five β and twelve γ subunits. These can activate or inhibit various signalling partners, which include; phospholipase C, phosphatidylinositol 3-kinase, adenylyl cyclase, potassium channels, calcium channels, GPCR kinases, as well as the MAPK and JAK/STAT kinase pathways (Offermanns, 2003). Following activation of these signalling partners, secondary messengers are produced. Adenylyl cyclase activation leads to cAMP production, which then activates protein kinase A; this then phosphorylates a host of other proteins leading to cellular function. Another

secondary messenger that is produced is inositol triphosphate, which causes the release of calcium from intracellular stores within the endoplasmic reticulum. Calcium then activates further signalling partners, including the small GTPase Ras, which activates pathways such as the ERK/MAPK cascade, leading to gene transcription (Chao et al., 1992; Cullen & Lockyer, 2002). The immune system in particular relies on $G\alpha_i$ signalling through chemokine receptors; this was determined through the use of *Pertussis* toxin, which uncouples $G\alpha_i$ proteins from GPCRs (Spangrude et al., 1985; Burns, 1988).

1.3.1 – GPCR structure and signalling

Bacteriorhodopsin was identified as a seven transmembrane domain protein based on electron microscopy, which showed the presence of seven α-helices lying perpendicular to the cell membrane (Henderson and Unwin, 1975). Bovine rhodopsin was compared to bacteriorhodopsin and the sequence conservation between the two receptors, particularly the presence of hydrophobic residues, suggested that it had a seven transmembrane domain structure. Only once the receptor was crystallised and its three-dimensional structure analysed was the seven transmembrane domain structure confirmed (Palczewski et al., 2000). Figure 1-5 shows the crystal structure of rhodopsin. This structure however was of an inactive receptor, crystallised in the dark with retinal in its *cis* form. Covalently bound *cis*-retinal acts as an inverse agonist of rhodopsin, locking the GPCR structure into an inactive conformation (Tesmer, 2010). Structures of active receptors were needed in order to shed more light on how GPCRs functioned.

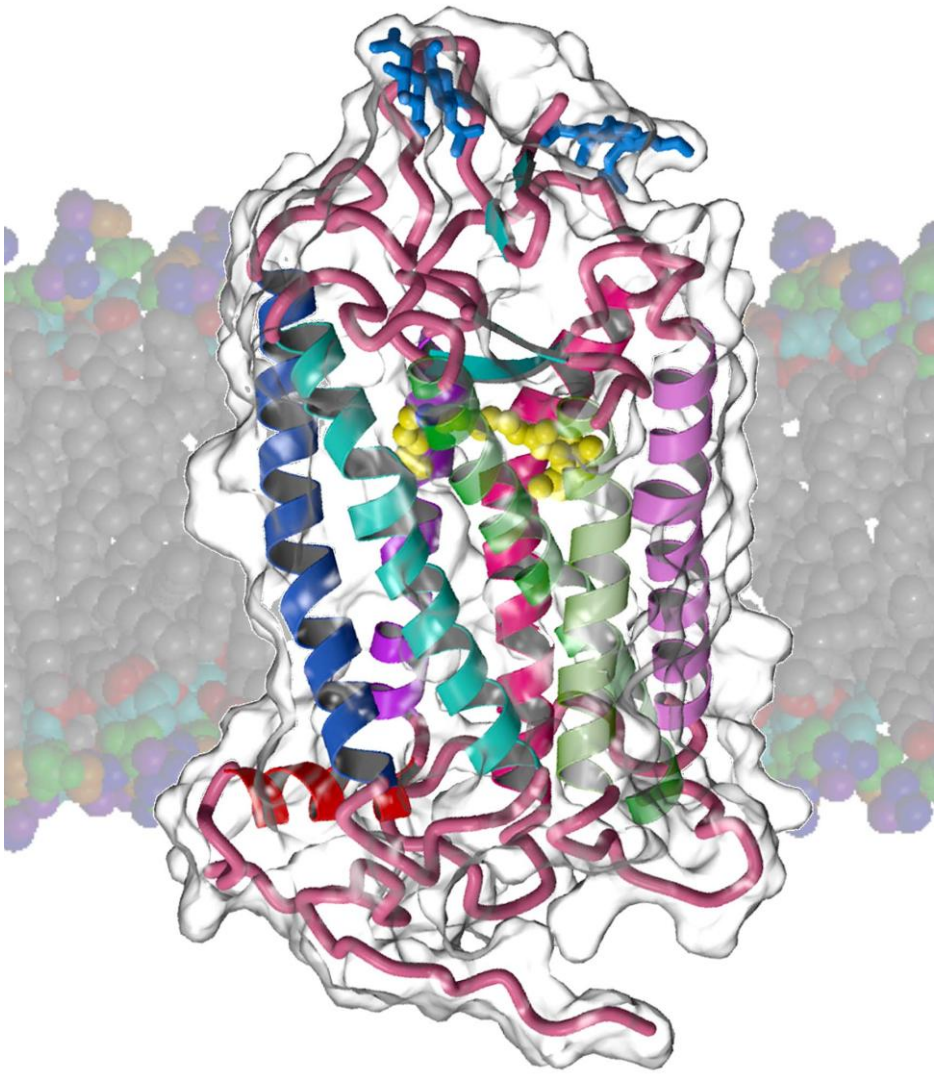

Figure 1-5 – Crystal structure of bovine rhodopsin

Ribbon drawing of the structure of bovine rhodopsin, shown parallel to the cell membrane. The intracellular C-terminus is shown at the bottom and the extracellular N-terminus at the top. The seven transmembrane domains are shown in the centre, along with covalently-bound retinal in yellow. © miyano@riken

Other GPCR structures have indeed since been solved, such as the human β_2-adrenergic receptor (β_2AR). In order to crystallise the β_2AR, much of the third intracellular loop was replaced with a more rigid structural domain; this was done in order to reduce basal activity levels of the receptor which hindered crystallisation attempts. However, as with rhodopsin, this crystal structure could not provide a full picture of G protein coupling. Since the intracellular loops are required for G protein binding, the replacement of the third loops therefore removed a key structural element in this binding (Rasmussen et al., 2007; Rasmussen et al., 2011; Rosenbaum et al., 2007; Warne et al., 2008).

In conjunction with sequence analysis of other GPCRs, the crystal structures of these receptors revealed several motifs that were both highly conserved and potentially important for receptor structure and function. One example is an eighth helix, located at proximal end of the C-terminus of the receptor. Helix VIII is amphipathic, meaning that it possesses both hydrophilic and lipophilic properties. This explains the observation that helix VIII lies parallel to the membrane, with charged residues clustering on the cytosolic side of the helix, whereas hydrophobic residues such as phenylalanine, methionine, and leucine are on the side of the helix facing the lipid membrane (Palczewski et al., 2000).

Squid rhodopsin (Murakami and Kouyama, 2008) and the human A_{2A} adenosine receptor (Jaakola et al., 2008) were also crystallised, but again these were done so in inactive states. The squid rhodopsin structure revealed several motifs that were not present in the bovine structure; transmembrane helices V and VI extended into the cytoplasm, which was believed to be required for G protein coupling. Overall 9 helices were observed, 7 transmembrane and two cytoplasmic. Another feature unique to squid was the presence of a short 3_{10} helix – a less common helical motif compared to the α-helix – linking helices VIII and IX. This short linker helix was thought to be involved in the folding of the seven transmembrane domains by acting as an anchor for these helices (Murakami and Kouyama, 2008).

The NPXXY motif is another example of a conserved motif in GPCR structures, located at the cytoplasmic end of helix VII. Hydrophobic interactions were shown to occur between the tyrosine of this motif and a phenylalanine of the amphipathic C-terminal helix VIII. These interactions were hypothesised to be required for receptor function (Fritze et al., 2003; Palczewski et al., 2000). Before the publication of the rhodopsin structure, previous mutational studies had demonstrated

the importance of this conserved region in receptor expression, ligand binding and receptor activity. An M3 muscarinic receptor mutant that had the proline of the NPXXY motif mutated to alanine had reduced levels of receptor activation, in terms of phosphatidyl inositol hydrolysis (Wess et al., 1993). In the β_2-adrenergic receptor, mutation of the asparagine of this motif to alanine resulted in uncoupling from G proteins, loss of agonist binding, and poor cell-surface expression. Mutation of the proline to alanine reduced receptor coupling and decreased the level of kinase activity following receptor activation (Barak et al., 1995). Subsequent studies and crystal structures of other GPCRs confirmed the importance of this NPXXY motif in receptor function.

Another highly conserved motif is the E/DRY motif. This is present in many GPCRs, located in the second intracellular loop at the end of helix III. It consists of either a glutamic acid or aspartic acid followed by an arginine and a tyrosine. Like the NPXXY motif, its conservation in other receptors is indicative of potential function. In rhodopsin, a salt bridge was identified between the E/DRY motif and a glutamic acid located in helix VI. This was believed to form an 'ionic lock', fixing the receptor in an inactive conformation (Palczewski et al., 2000). Bovine opsin was crystallised without bound ligand, and the structure revealed a broken ionic lock. This structural rearrangement, including others such as the rotation of helix VI and stabilising interactions between other transmembrane domains, were believed to be part of the receptor activation process involving recruitment of G proteins (Park et al., 2008). Crystallisation of opsin in complex with a synthetic G protein showed an outwardly rotated helix VI, breaking the ionic lock. The R of the E/DRY motif was shown to not interact with the E/D of this motif and helix VI residues, but instead interacted with the main binding crevice of the G protein. The rotated helices and interaction of the arginine were also stabilised in part by the NXXPY motif (Scheerer et al., 2008).

The human chemokine receptor CXCR4 has also had its crystal structure solved (Wu et al., 2010). Previously no other chemokine receptors had been crystallised and therefore all models were based upon more distantly-related receptors such as rhodopsin or the β_2-adrenergic receptor. The CXCR4 structure provided far more insight into how chemokine receptors may be structurally organised and what similarities and differences they have when compared to other GPCRs. Compared to

the β_2-adrenergic receptor and adenosine receptor, the extracellular portion of helix I of CXCR4 is shifted towards the centre of the transmembrane bundle. The residues of the helices that face inwards are involved in ligand binding. It was revealed in the CXCR4 structure that helix II makes a tighter turn than was previously believed based on homology models. This means that residues of helix II that face the ligand-binding pocket were inaccurately predicted, since the models did not account for this rotation. This is significant since it changes what amino acids were believed to contact ligand upon binding. Surprisingly, despite the high level of conservation with other receptors, helix VII was shorter than in other structures, ending after the NPXXY motif. In addition, the CXCR4 structure lacked the short C-terminal helix VIII. However, since CXCR4 contains only a partially conserved motif in this region, the authors suggested that this eighth helix may only form under certain conditions (Wu et al., 2010). The crystal structure of CXCR4 is shown in figure 1-6.

More recently, the crystal structures of the δ-, κ-, and μ-opioid receptors have been solved (Granier et al., 2012; Wu et al., 2012; Manglik et al., 2012), along with the structure of the nociceptin receptor (Thompson et al., 2012). These receptors are members of the *Rhodopsin* family of GPCRs. The former three share approximately 70% sequence identity with each other, while the nociceptin receptor shares approximately 60% sequence identity with the other three. All four receptors are involved in the central nervous system, regulating process such as pain, mood, and homeostasis (Filidoza and Devi, 2012).

The δ-opioid receptor, like the other opioid receptors, has two distinct structural regions in its ligand binding pocket; the lower portion of the pocket is highly conserved and recognises the core of the ligand and determines ligand efficacy, while the upper portion of the pocket is more divergent between receptors and determines ligand selectivity (Granier et al., 2012).

The κ-opioid receptor shows strong conservation with the δ-opioid receptor but structurally is more similar to the dopamine receptors than to the other opioid receptors. It contains the previously mentioned C-terminal helix VIII, which lies parallel to the membrane. The κ receptor also lacks the glutamic acid/aspartic acid of the DRY motif; however the ‘ionic lock’ is still present in the form of an interaction between the arginine of this region and a threonine in helix VI. The κ receptor also contains the highly conserved NPXXY motif at the intracellular end of helix VII (Wu et al., 2012).

The μ-opioid receptor also lacks the salt bridge formed by the glutamic or aspartic acid of E/DRY motif with a residue in transmembrane helix VI. However, the arginine of this motif forms a salt bridge with the aspartic acid, which in turn forms a polar interaction with another arginine in intracellular loop 2 in a similar manner to that in the β_2-adrenergic receptor. The arginine of the E/DRY motif also forms an interaction with a threonine in helix VI, as in the κ-opioid receptor. Like the κ receptor, the μ receptor has a deep and narrow ligand-binding pocket compared to other crystal structures such as CXCR4 (Manglik et al., 2012).

The nociceptin receptor is less similar to the other opioid receptors than they are to each other, and has more proline residues through the transmembrane helices. This causes several kinks to develop, which causes the helices to be shifted compared to other receptors. For example, helix V is shifted compared to the κ- and μ-opioid receptors, giving a larger gap between helices VI and V, which in turn results in a larger binding pocket. Helices VI and VII are also titled further in towards the orthosteric binding pocket when compared to CXCR4 (Thompson et al., 2012).

These structures therefore have provided valuable insight into the activation mechanisms of GPCRs, including the conserved motifs that are required for G protein interaction. Despite the variety of *Rhodopsin* class GPCRs, they share broadly similar activation mechanisms. In terms of GPCR activation, the conserved motifs previously described all act in concert in the shift from an inactive receptor state to an active one.

In summary, binding of an agonist to the ligand-binding pocket of the receptor induces large-scale conformational changes in the receptor structure, which translates into intracellular signalling. In general, the movement of helix VI in particular is important for this process, as it rotates during receptor activation, allowing G protein access due to the breaking of the aforementioned ionic lock created by interactions between the E/DRY motif and residues within helix VI. The arginine of this motif acts as a micro-switch, since breakage of the ionic lock causes this amino acid to interact directly with G proteins. A micro-switch is a highly conserved residue of a GPCR that exists in distinct conformations and thus forms different interactions depending upon the activation state of the receptor (Nygaard et al., 2009). A diagram of the ligand binding pocket of GPCRs based on crystal structures and homology modelling is shown in figure 1-7. This shows the diversity of ligand-binding domains between class A GPCRs; while the receptors share the same seven transmembrane-

domain architecture the diversity of the extracellular face allows discrimination between different ligand types.

In addition to the arginine of the E/DRY motif, various other ‘micro-switches’ are also involved in receptor activation. TrpVI:13, a tryptophan located at the bottom of helix VI is believed to act as one such micro-switch; upon receptor activation the side chain of this amino acid rotates away from helix VII, where it is facing when the receptor is in an inactive conformation, to be stabilised in a new position by a phenylalanine in helix V. In addition, TyrVII:20 of the NPXXY motif also acts as a micro-switch. In rhodopsin, this tyrosine interacts with helix VIII in an inactive conformation, and with the rotated helix VI in the active conformation. In the inactive conformations of the β_2-adrenergic and adenosine receptors however, this tyrosine forms hydrogen bonds with a water molecule located between helices I, II, VI and VII (Nygaard et al., 2009). Thus, the various structural domains and micro-switches of GPCRs work in concert to translate ligand binding into a functional response.

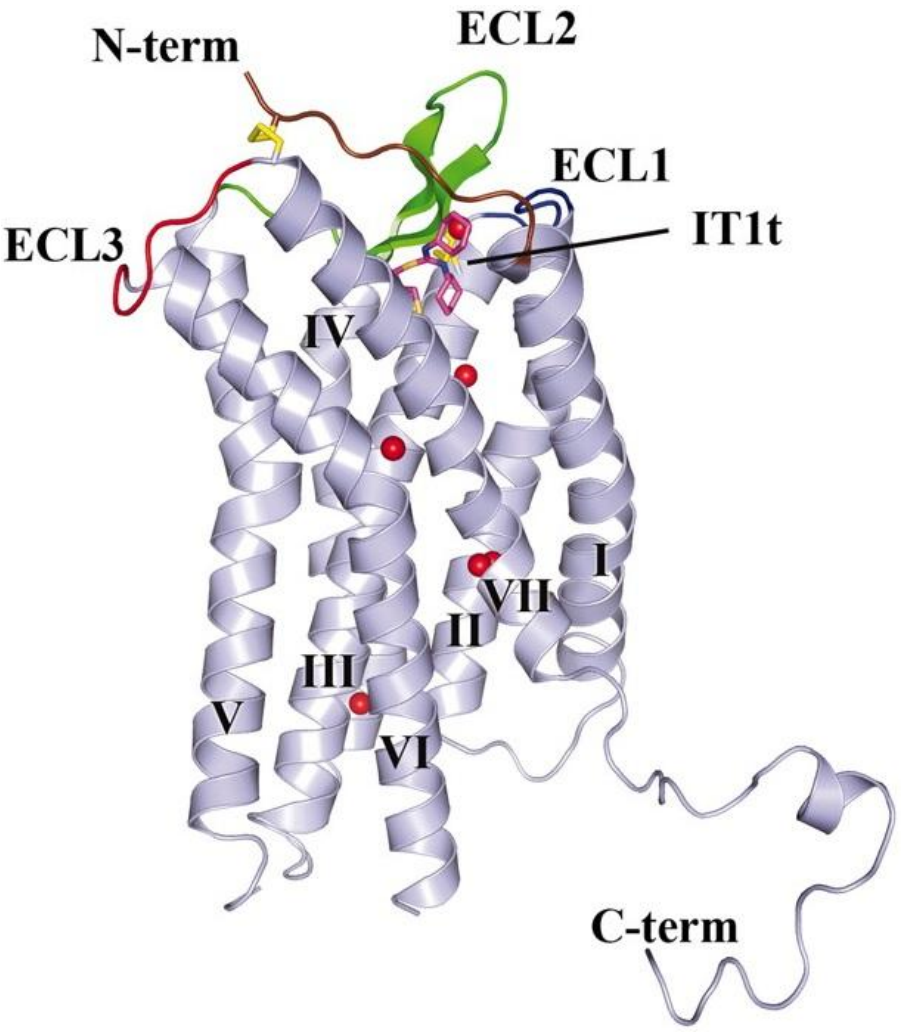

Figure 1-6 – Crystal structure of the chemokine receptor CXCR4

Ribbon drawing of the CXCR4 crystal structure, in complex with the inhibitor IT1t. The N-terminus and three extracellular loops are highlighted in brown, blue, green and red. Disulphide bonds between extracellular domains are shown in yellow. Red circles show water molecules located within the structure. From Wu et al., 2010.

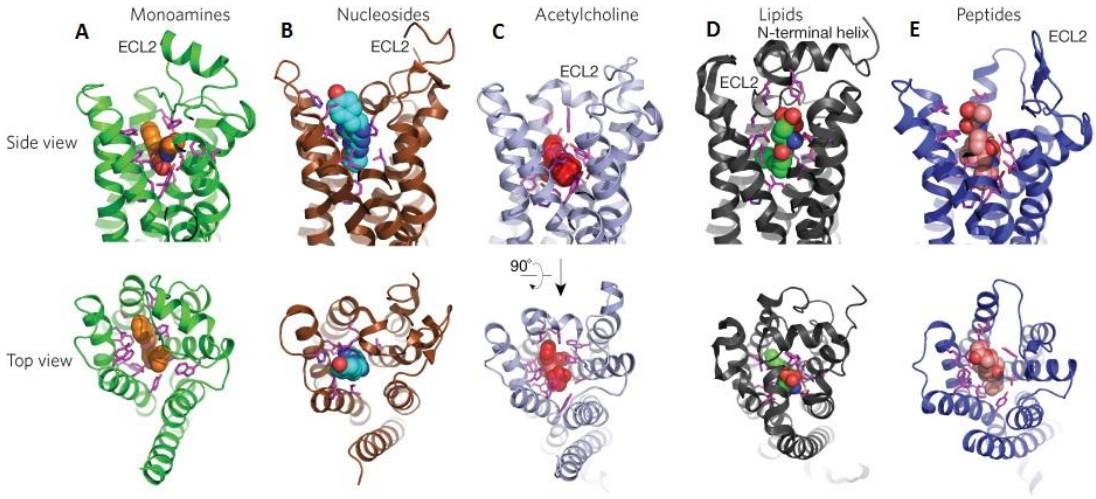

Figure 1-7 – Diversity of the ligand binding pockets of class A GPCRs

Side and top views of the ligand binding domains of the β_2-adrenergic receptor bound to carazolol (A), the A_{2A} adenosine receptor bound to ZM24138 (B), the M2 muscarinic receptor bound to quinuclidinyl benzilate (C), the sphingosine-1-phosphate receptor bound to ML056 (D), and the μ-opioid receptor bound to β-funaltrexamine (E). The variation in ligand binding domains allows discrimination between different ligand types, and leads to pockets of varying depth. Note the differences in position of extracellular loop 2 in particular. Adapted from Granier and Kobilka, 2012.

1.3.2 – Chemokine receptors

Chemokine receptors are a class of *Rhodopsin* GPCRs, of the γ sub-group. Like other GPCRs, they contain seven membrane-spanning α-helices, three extracellular loops, an extracellular N-terminus, three intracellular loops, and an intracellular C-terminus. Chemokine receptors couple to G proteins in the same manner as other GPCRs, and following chemokine binding to the N-terminus and extracellular loops, cell migration is induced. Chemotaxis, the migration of cells along an increasing concentration gradient of chemoattractant, is one of the main effector functions of chemokine binding to chemokine receptors. It is via chemotaxis that many cell types migrate through tissues in the body (see section 1.2.1).

Chemokine receptors are present on multiple cell types, particularly immune cells such as leukocytes. CXCR1 and CXCR2 were the first chemokine receptors to be identified, and are predominantly expressed on neutrophils (Holmes et al., 1991; Murphy & Tiffany, 1991). Chemokine receptors were then identified as *Rhodopsin* class (formerly class A) GPCRs (Vassilatis et al., 2003). So far, 18 chemokine receptors have been identified that couple to $G\alpha_i$ proteins, with a further five exhibiting atypical behavior (Zlotnik and Yoshie, 2012).

One such atypical receptor is D6. This chemokine receptor is known to bind 12 CC chemokines, although it does not signal in response to their binding. D6 does not signal due the lack of the DRYLAIV motif in its second extracellular loop; as was described in section 1.3.1 this motif is critical for receptor coupling to G proteins and thus signalling. D6 undergoes constitutive internalisation and recycling to the membrane via the endosomes, which is where the receptor-bound chemokine is removed and targeted for degradation in the lysosomes. D6 therefore acts as a chemokine scavenger and regulates levels of inflammatory chemokines (Nibbs et al., 2009).

Another such atypical chemokine receptor is DARC (Duffy antigen receptor for chemokines). This receptor binds many inflammatory chemokines of both the CC and CXC classes. Like D6, it lacks the DRYLAIV motif and thus cannot couple G proteins or induce signalling. However in contrast to D6, DARC promotes migration by acting as a transporter of chemokines. DARC was shown to be localised intracellularly with chemokines, suggestive of a role in their internalisation. It was also shown that it underwent transcytosis, transporting chemokines from one side of

endothelial cells to the other. Thus, by moving tissue-derived chemokines to the luminal side of the endothelium, DARC supports the chemotaxis of leukocytes in the blood vessels (Pruenster et al., 2009).

Chemokine receptor classification follows that of chemokines; there are four families – CC, CXC, CX_3C and XC – that are based on the relative position of cysteine pairs within the chemokine. While chemokines are denoted CCL/CXCL/CX_3CL/XCL, their cognate receptors are denoted CCR/CXCR/CX_3-CR/XCR.

To date, 18 chemokine receptors have been identified that induce chemotaxis via G proteins. A further 5 atypical receptors have also been identified that do not induce chemotaxis. As there are 48 known chemokines, some chemokines evidently bind to more than one receptor. For example, the receptor CCR1 binds the chemokines CCL3, CCL5, CCL7, CCL8, CCL13, CCL14, CCL15, CCL16, and CCL23. Other receptors such as CXCR4 only bind one chemokine, in this case CXCL12. To add a further layer of complexity to this system, some chemokines bind to multiple receptors; CCL5 for example binds to CCR1, CCR3 and CCR5 (Zlotnik and Yoshie, 2012). The chemokines and their cognate receptors are shown in table 1-2.

This phenomenon of multiple chemokines binding to one receptor, and multiple receptors binding one chemokine, has been commonly described as chemokine 'promiscuity' and suggests a redundancy within the system (Lukacs et al., 1999; Power et al., 1995; Mantovani, 1999). Chemokines were first characterised by their ability to stimulate chemotaxis *in vitro*, before the complexity of receptor subtypes was realised. For example, before the different T-cell subsets such as T_H1, T_H2, T_{reg}, and T_H17 cells were discovered, $CD3^+$ (cluster of differentiation notation for the T-cell receptor) T-cells were assayed for chemotactic ability to various chemokines. Some of the receptors that T_H1 cells express include CXCR3 and CCR5, while T_H2 and T_{reg} cells express CCR4 and CCR8 (Bonecchi et al., 1998; Iellem et al., 2001). T_H17 cells express CCR6 (Lim et al., 2008; Singh et al., 2008). Therefore, a mixed population of these cells migrated to a large number of chemokines due to the range of receptors expressed on the differing T-cell types. Without the knowledge that different sub-populations of cells existed, it was surmised that the different chemokines were performing redundant functions (Schall and Proudfoot, 2011).

The multiple chemokines and receptors may therefore not be redundant, but rather guide the migration of specific cell subsets with each performing specific functions. For example, the naturally occurring CCR5Δ32 mutation leads to a truncation of the last 32 amino acids from the C-terminus of CCR5. People with this mutation appear healthy, and in fact have increased resistance to HIV-1 infection since the virus uses CCR5 as a coreceptor for entry into T cells. This may have suggested that CCR5 was therefore playing a redundant role since a severe truncation of CCR5 that rendered it non-functional had no effect on health. However it was then discovered that people carrying the truncated form of CCR5 had an increased susceptibility to West Nile virus (Glass et al., 2006). CCR5 is expressed on T_H1 cells, and was believed to play a role in restraining West Nile virus infection (Loetscher et al., 1998; Glass et al., 2006). Chemokine receptors therefore may have non-redundant roles that are not immediately apparent.

1.3.2.1 – Posttranslational modification of chemokine receptors

Chemokine receptors undergo posttranslational modifications in the Golgi apparatus or endoplasmic reticulum, and these processes have essential biological roles. *N*-glycosylation is a process in which carbohydrates are linked to the nitrogen atoms of asparagine (N) residues, whereas *O*-linked glycosylation involves linkage of carbohydrates to the hydroxyl-oxygen of serine (S) and threonine (T) residues (Spiro, 2002). Tyrosine residues also can be sulphated (Moore, 2009).

Glycosylation has been shown to be required for the intracellular trafficking of certain GPCRs. Mutants of the β_2-adrenergic receptor in which sites of glycosylation were removed showed a 50% reduction in trafficking to the cell surface, however receptors that did reach the membrane showed no impairment in coupling to G proteins, indicating that the oligosaccharide additions were only necessary for receptor export to the cell surface and not receptor function (Rands et al., 1990).

CCR5 was one of the first chemokine receptors to be shown to undergo glycosylation and sulphation. The chemokine receptor was shown to contain O-linked oligosaccharides such as sialic acid but not N-linked oligosaccharides. Inhibition of sulphation did not reduce cell-surface expression of CCR5 but did however reduce binding affinity of the chemokines CCL3, CCL4 and CCL5, as did mutation of

potentially sulphated tyrosines to phenylalanine (Farzan et al., 1999). Later studies confirmed these data, and also showed that O-linked glycosylation was also required for chemokine binding (Bannert et al., 2001).

Similar results were shown in the case of murine CCR8. Mutants of this chemokine receptor in which potentially sulphated N-terminal tyrosines were mutated to phenylalanine had reduced ligand-binding capacity. Sulphation was believed to add extra negative charges to a region of the receptor that was already acidic, thereby facilitating interactions with CCL1, which like other chemokines is basic. The replacement of tyrosines with phenylalanines not only removed the sulphation sites, it introduced hydrophobic side-chains that were proposed to disrupt ionic interactions with the chemokine, further demonstrating the importance of tyrosine residues in the N-terminus of the chemokine receptor, which as described along with the extracellular loops binds chemokine. Like the β_2-adrenergic receptor mutants, CCR8 mutants in which glycosylation sites were removed showed reduced trafficking to the cell surface (Gutiérrez et al., 2004).

The atypical chemokine receptor D6 was also shown to be glycosylated, however unlike CCR8 and other receptors (Farzan et al., 1999; Farzan et al., 2002; Fong et al., 2002; Preobrazhensky et al., 2000), this modification was not required for ligand binding. Glycosylated and deglycosylated D6 showed identical binding of the chemokine CCL3, as did D6 mutants that had glycosylation sites removed (Blackburn et al., 2004). With the exception of D6, chemokine receptor glycosylation and sulphation has shown to be important for ligand binding.

Palmitoylation is another form of modification that can modulate the biological activities of receptors. Palmitoylation is the addition of a palmitate, a fatty acid, to cysteine residues. Bovine rhodopsin was the first GPCR demonstrated to be palmitoylated, on two cysteines in its C-terminus (Ovchinnikov et al., 1988). Subsequent research showed that CCR5 was also palmitoylated on its C-terminus, and that disruption of this modification led to a reduction in cell-surface expression and proteolytic degradation of the receptor (Percherancier et al., 2001; Blanpain et al., 2001). Since cysteines in the C-termini are conserved in approximately 80% of GPCRs, palmitoylation likely has important functions in other chemokine receptors.

1.3.2.2 – Chemokine receptor signalling

Chemokine binding to chemokine receptors is believed to occur in two steps. In the first step, the chemokine binds with high affinity to the N-terminus of the receptor. In the second step, the chemokine also binds to the extracellular loops of the receptor with low affinity. This model was postulated after the switching of CCR2/CCR5 N-termini and extracellular loops showed the high affinity interactions require the N-terminus; for example, CCR2 with its N-terminus exchanged with that of CCR5 only bound its ligand, CCL2, with low affinity (Monteclaro and Charo, 1997).

Subsequently, it was determined that different regions of the chemokine interact with specific residues of the extracellular loops, in addition to the transmembrane domains. The second extracellular loop of CCR5 was found to be important for ligand selectivity; the core domain of the chemokine interacted with the loop, and point mutants of the second extracellular loop were able to bind CCL5 but not CCL3 (Blanpain et al., 2003).

Other domains within the receptor helices were also required for function. The TXP motif is a highly conserved motif in the transmembrane helix II of chemokine receptors, and the proline of this motif is required for maintenance of helical structure and in turn chemokine binding and activity (Govaerts et al., 2001). An aromatic cluster of amino acids around the TXP motif in transmembrane helices II and III were mutated in CCR5, which led to a reduction in chemokine activation but not binding (Blanpain et al., 2003). These aromatic residues were required for the interhelical interactions necessary to stabilise helical conformations in ligand-induced activation (Govaerts et al., 2003).

Chemokine binding results in the receptor coupling to G proteins, which induces subsequent downstream signalling. As will be described, ligand binding to the N-terminus of the receptor results in a conformational shift of the transmembrane helices; in particular helices 3 and 6 tilt inwards which results in an opening up of the C-terminal face of the receptor. This allows signalling proteins such as G proteins to bind the receptor.

Chemokine receptors predominantly signal through $G\alpha_i$ proteins; migration of leukocytes *in vitro* and *in vivo* is significantly reduced after treatment with *Pertussis* toxin (PTX), a bacterial endotoxin that uncouples $G\alpha_i$ proteins from GPCRs by catalysing the ADP-ribosylation of the $G\alpha_i$ protein; this makes it unable to

exchange GDP for GTP and thus renders it inactive (Burns, 1988). After PTX treatment, lymphocyte and neutrophil motility was significantly reduced in chemotaxis assays (Spangrude et al., 1985), as was lymphocyte migration into the spleen (Cyster and Goodnow, 1995) and lymph nodes (Spangrude et al., 1984). PTX treatment was later shown to specifically inhibit chemokine receptor signalling; CXCL8 signalling was abolished after treatment with the toxin (Wu et al., 1993). In CXCR4, $G\alpha_i$ proteins were shown to bind to the third intracellular loop of the receptor (Roland et al., 2003).

As described in section 1.3, $G\alpha_i$ proteins inhibit the signalling protein adenylyl cyclase. They also activate Rac, which is a member of the GTPase family of proteins that acts in the G protein signalling cascade (Belisle & Abo, 2000; Benard et al., 1999). As a result of Rac activation, actin polymerisation occurs, which is essential for cell motility (Viola and Luster, 2008). It also appears that different isoforms of $G\alpha_i$ have opposing functions; in T cells, the $G\alpha_{i2}$ isoform was required for CXCR3-mediated chemotaxis, since deletion of this protein ablated the chemotactic response. In mice, deletion of the $G\alpha_{i3}$ isoform however resulted in an increase in receptor signalling and the chemotactic response, indicating that it played an antagonistic role in CXCR3-mediated signalling (Thompson et al., 2007).

Chemokine receptor signalling is a tightly regulated process. Due to the complexity of the chemokine system, in which different cells and tissues express varying levels of multiple chemokines, and the cells that respond can express a large combination of different receptor types, there needs to be a system in place to attenuate receptor signalling in order to fine-tune the chemotactic responses of migrating cells.

One such mechanism for regulating this signalling activity is by receptor desensitisation, through the action of GPCR kinases (GRKs) and β-arrestins. β-arrestins are proteins initially thought to only function by desensitising GPCRs by blocking interaction with G proteins (Lefkowitz and Whalen, 2004). Murine β-arrestin-knockout cell lines however showed that internalisation of the β_2-adrenergic receptor was significantly reduced, indicating that these proteins not only bound the C-terminus of GPCRs but mediated their endocytosis as a mechanism of receptor regulation (Kohout et al., 2001).

In order for β-arrestins to bind the GPCR and initiate endocytosis, they require GRKs to phosphorylate serine and threonine residues on the intracellular loops and C-terminus of the receptor, which leads to the binding of β-arrestins. This recruitment of β-arrestins thus prevents further G protein signalling due to the inability of the G proteins to couple with the receptor. The β-arrestins also serve as a scaffold for other proteins that in turn cause the receptor to internalise, leading to a reduction in signalling and therefore prevention of overstimulation of the cell (Borroni et al., 2010; Vroon et al., 2006). β-arrestins recruit clathrin and its adaptor AP2, allowing receptor endocytosis to proceed via clathrin-coated pits, which are membrane invaginations that internalise the receptor (Borroni et al., 2010). β-arrestins have been shown to regulate signalling of the chemokine receptors CCR5 (Aramori et al., 1997), CXCR1 (Barlic et al., 1999), CXCR4 (Cheng et al., 2000), as well as the internalisation of the non-signalling receptor D6 (Galliera et al., 2004).

β-arrestins have also been shown to signal as well as mediate receptor endocytosis. In addition to functioning as a scaffold for clathrin and its adaptor protein AP2 in order to induce endocytosis, β-arrestins also recruit signalling partners such as kinases in order to activate G protein-independent pathways. Such kinases include c-Jun amino-terminal kinase (JNK) and extracellular-signal-related-kinases/mitogen-activated protein kinases (ERK/MAPK). These kinases then go on to phosphorylate and activate other signalling partners leading to processes (Reiter and Lefkowitz, 2006).

Murine lymphocytes which were knockouts of β-arrestin and GRKs had impaired chemotactic ability; the β-arrestin2 and GRK6 knockout T and B cells showed significantly reduced CXCR4-induced migration to CXCL12, while GRK5 knockouts were no different to WT cells (Fong et al., 2002). CXCR4-mediated chemotaxis to CXCL12 was enhanced by the transfection of cells with β-arrestin 2, and this effect was determined to be due to the action of p38 MAPK since a dominant-negative mutant of this kinase blocked the chemotactic effect of the β-arrestin (Sun et al., 2002). A similar role was found for p38 MAPK in the signalling the viral chemokine receptor US28, which is constitutively phosphorylated by GRKs. The C-terminus of US28 including the β-arrestin-interacting domain were required to activate p38 MAPK (Miller et al., 2003).

These studies indicate that in addition to the desensitising roles described previously, β-arrestins and GRKs can be involved in receptor signalling through G protein-independent pathways.

The role of GRKs and β-arrestins has been investigated in the chemokine receptor CCR7. CCR7, which is notably expressed on dendritic cells, binds the chemokines CCL19 and CCL21. CCL19 induces receptor internalisation, whereas CCL21 does not (Bardi et al., 2001); CCL19 was later determined to also cause receptor desensitisation by the recruitment of GRKs, leading to phosphorylation of the CCR7 C-terminus (Kohout et al., 2004). Interestingly, both chemokines induce chemotaxis through CCR7, meaning that the differential activity of these ligands is likely not through G proteins.

This phenomenon of differential activity of ligands through a single receptor is known as biased agonism or functional selectivity; the premise of this being that different ligands stabilise unique receptor conformations leading to the recruitment of different signalling proteins and kinases, ultimately producing 'biased' signalling outputs (Kenakin, 2009).

As described previously in section 1.3.1, several key domains and micro-switches were identified as being important for the receptor activation process. Some of these sites were identified using GPCR crystal structures, whereas others used metal-ion chelators to determine key receptor domains. Histidine residues were introduced at sites of interest within the receptor, and zinc or copper chelated between them to form a bridge. This allowed helix-helix interactions to be studied, and led to the proposition of the global toggle switch model. This model states that the intracellular segments of the GPCR move outwards while the extracellular segments of the transmembrane helices move inwards; specifically, the extracellular portions of helices VI and VII tilt towards helix III (Schwartz et al., 2006; Hoffmann et al., 2008).

The model of receptor toggles and switches ties in with the notion of biased agonism, in that the full repertoire of micro-switches may not necessarily be toggled after ligand binding, and that different ligands activate different sets of switches (Nygaard et al., 2009). For example, to use the above example of CCL21 and CCL19 inducing different effects upon GRKs and resulting receptor phosphorylation levels, it may be the case that CCL19 activates a slightly different set of micro-switches in the

receptor architecture compared to CCL21, thus affecting subtle conformational changes and therefore the recruitment of downstream signalling partners.

The β_2-adrenergic receptor has been shown to signal in a biased manner. Some ligands of this receptor activate both G protein- and β-arrestin-mediated signalling pathways. Three ligands however were found to show a bias towards the β-arrestin pathway. The ligands CPB (N-cyclopentylbutanephrine), isoetharine, and ethylnorepinephrine showed a greater degree of β-arrestin recruitment and activation of β-arrestin-dependent kinases relative to G protein activation, when compared to other ligands (Drake et al., 2008).

The biased pathways of β_2AR signalling were characterised by fluorine-19 nuclear magnetic resonance (^{19}F-NMR). This involved labelling cysteines in helices V, VII and VIII with 2,2,2-trifluoroethanethiol. The movements of the receptor helices altered the chemical shifts of the labelled cysteines; by comparing the variation in shifts resulting from different agonists binding to the receptor, it could be determined that some agonists induced different receptor conformations to others. For example, the β-arrestin biased ligand isoetharine produced shifts in helix VII, whereas the unbiased agonist isoproterenol did not produce such a shift (Liu et al., 2012). Previous studies have shown that GRK phosphorylation of β_2AR – which is necessary for β-arrestin recruitment – occurs on helix VII, and that the G_α subunit contacts helices V and VI of the receptor without contacting helix VII (Nobles et al., 2011; Søren et al., 2011; Westfield et al., 2011).

Together, these data indicate that the different ligands of the β_2AR stabilise distinct conformations leading to biased signalling outputs. Biased signalling through chemokine receptors such as CCR7 may therefore occur in a similar manner, due to both structural conservation between GPCRs and the shared repertoire of signalling proteins they recruit.

1.3.2.3 – Helix VIII

Like other GPCRs, chemokine receptors contain a highly conserved region downstream of helix VII. This region in other receptors such as rhodopsin is known as helix VIII, an amphipathic alpha helix running parallel to membrane due to a concentration of lipophilic residues on one side and hydrophilic residues on the other side. However, as described in section 1.3.1, the crystal structure of the chemokine

receptor CXCR4 did not reveal the presence of this helix, when compared to the structures of the human β_2-adrenergic receptor, the human A_{2A} adenosine receptor, and bovine rhodopsin. In addition, compared to other chemokine receptors this region is less conserved in CXCR4; in particular it lacks a phenylalanine at the end of helix VIII and a putative cysteine palmitoylation site further downstream which would anchor the helix in the membrane. This may account for the lack of the helix observed in the receptor structure. While some other chemokine receptors lack this phenylalanine they possess other hydrophobic amino acids such as leucine or isoleucine which are believed to play a similar role in helix VIII formation (Wu et al., 2010).

Helix VIII however was identified in other GPCR structures, such as bovine rhodopsin, the human β_2-adrenergic receptor, the human adenosine A_{2A} receptor, squid rhodopsin, the murine δ-, and μ-opioid receptors, and the human κ-opioid receptor (Cherezov et al., 2007; Granier et al., 2012; Jaakola et al., 2008; Manglik et al., 2012; Murakami & Kouyama, 2008; Palczewski et al., 2000; Wu et al., 2012).

The C-terminal helix VIII has been shown to play an important role in GPCR function. Leukotriene B_4 (LTB_4) is a chemotactic lipid inflammatory mediator that signals through the GPCRs BLT1 and BLT2. Like other GPCRs, BLT1 has a putative C-terminal helix VIII downstream of helix VII. Receptor mutants of BLT1 in which the helix VIII region was truncated or substituted bound a greater level of LTB_4 than WT BLT1 despite comparable surface expression. In addition, the mutant receptors showed prolonged calcium signalling compared to WT receptors (Okuno et al., 2003). Molecular modelling and helical wheel analysis predicted that an interaction between a tyrosine in helix VII and a phenylalanine in helix VIII stabilised the inactive BLT1 conformation by keeping helix VIII at a right-angle to membrane. Therefore, mutation of this region prevented this stabilisation, thus accounting for the increases seen in receptor activation (Okuno et al., 2003, 2005). Point mutations of leucines of this region indicated that helix VIII inhibits LTB_4-dependent internalisation of BLT1 in addition to inhibiting the inactive receptor conformation (Aratake et al., 2012).

The protease-activated receptors (PARs) are an interesting subtype of *Rhodopsin* family, in that in order to be activated they have to be proteolytically cleaved. For example, PAR1 is cleaved by proteases such as thrombin at its N-terminal extracellular domain, revealing a tethered ligand that activates the receptor.

Activated PAR1 then induces processes such as platelet aggregation (Vu et al., 1991). Molecular modelling of PAR1 predicted a C-terminal helix VIII, while truncations of this region resulted in a receptor that activated poorly in response to thrombin. More fine-grained analysis of this region involved point mutagenesis of potentially critical amino acids to determine their specific contribution to receptor function. Mutation of glutamic acid 377 and aspartic acid 379 in helix VIII – which were predicted to form an interaction with intracellular loop 1 and helix VII, respectively – resulted in reduced receptor activation. The authors of this study postulated a 7-8-1 mechanism, in which helix VII interacted with helix VIII, which in turn interacted with intracellular loop 1, resulting in PAR1 activating G_q proteins (Swift et al., 2006).

Similar results were obtained with the β_1-adrenergic receptor (β_1AR). This receptor shares 48% sequence similarity with its related receptor, β_2AR. Helix VIII was identified in β_2-AR (Rosenbaum et al., 2007), and is strongly conserved between the two receptors, indicating that β_1AR likely also possesses this C-terminal motif. Like β_2AR and rhodopsin, it was predicted that polar side chains of helix VIII such as arginine, lysine and glutamine would be clustered on the side facing the cytoplasm. Point mutations of amino acids in this region disrupted ligand binding to the receptor; mutation of the polar aspartic acid 382 to a non-polar leucine reduced ligand binding by 200-fold. Neutralising or reversing the charge of arginine 384 by mutating it to glutamine or glutamic acid resulted in a constitutively active receptor that was resistant to desensitisation. Like aspartic acid 382, this arginine was predicted to be on the cytosolic face of helix VIII, and due to their roles in receptor activation believed to be sites of G protein coupling (Delos Santos et al., 2006).

Similar roles have been observed for helix VIII in other GPCRs. In the thyrotropin-releasing hormone receptor it was shown to be phosphorylated by GRKs (Gehret et al., 2010); helix VIII in the bradykinin receptor was shown to be involved in receptor trafficking and signalling (Feierler et al., 2011); and residues within this region of the cannabinoid receptor 1 were required for ligand binding (Ahn et al., 2010).

The viral chemokine receptor ORF74 is encoded by the Kaposi sarcoma-associated herpesvirus 8 and shares a high degree of homology with human chemokine receptors, and with CXCR2 in particular. ORF74 is constitutively active and binds multiple human chemokines including CXCL1, CXCL8, CXCL10, CXCL11, and CXCL12. Some of these chemokines, such as CXCL1, act as agonists

by increasing the activity of the receptor, while others such as CXCL12 act as inverse agonists and reduce the activity of the receptor. The broad range of ligands for ORF74 supports its role in tumourigenesis. ORF74 is also constitutively active, and acts as an oncogene by using chemokine signalling to drive endothelial proliferation and inflammatory cell recruitment (Holst et al., 2001).

As in many other GPCRs, helix VIII of ORF74 plays an important role in receptor function and chemokine binding. Despite showing normal levels of cell-surface expression, a helix VIII truncation mutant of ORF74 showed significantly reduced receptor activation in response to CXCL1 and CXCL10. This mutant also lost the ability to bind CXCL8, while retaining the ability to bind CXCL11. A point mutant of glutamic acid 323 produced similar results. These results indicated that helix VIII of ORF74 and the residue E323 in particular contact G proteins and that their removal rendered the receptor unable to couple to these proteins and induce signalling. CXCL8 binding was ablated since it has been could only bind ORF74 when it was coupled to G proteins; CXCL10 binding was retained since it did not require coupling to G proteins (Verzijl et al., 2006).

In summary, helix VIII plays a critical role in many GPCRs including the chemokine receptor ORF74. Helix VIII is involved in many aspects of receptor function, including ligand binding, trafficking to the cell surface, and desensitisation of signalling. Polar residues on the cytosolic side of helix VIII likely contact G proteins, as demonstrated in multiple crystal structures and mutational studies.

The absence of helix VIII in CXCR4 structure was believe to be due to the lack of a cysteine residue downstream of this region (Wu et al., 2010). It was described in section 1.3.2.1 that chemokine receptors such as CCR5 are palmitoylated on C-terminal cysteines. Due to the lipophilic nature of these palmitate groups, they would likely serve to anchor parts of the C-terminus to the membrane. Since helix VIII in other GPCRs has been shown in other GPCRs to lie parallel to the membrane, this palmitoylation likely plays a role in this orientation. The CXCR4 C-terminus contains no cysteine residues, unlike other chemokine receptors. Therefore, considering this and the highly conserved sequences of this region, helix VIII likely exists in other chemokine receptors.

1.4 – CCR4

The 360 amino-acid chemokine receptor CCR4 was first cloned from the basophil cell line KU-812 (Power et al., 1995). At the time, only five other chemokine receptors had been identified; CXCR1 and CXCR2 (Holmes et al., 1991; Murphy & Tiffany, 1991), CCR5 (Neote et al., 1993), CCR2 (Charo et al., 1994), and the Duffy antigen receptor for chemokines (DARC) (Neote et al., 1993). Sequence comparisons showed CCR4 had 49% identity to CCR5 and 47% identity to CCR2. CCR4 was later discovered to respond to the chemokines CCL17 (TARC; thymus and activation-regulated chemokine) (Imai et al., 1997) and CCL22 (MDC; macrophage-derived chemokine) (Imai et al., 1998). Both chemokines bound selectively to CCR4-transfected cells, and induced cell migration and calcium release.

The ligands CCL17 and CCL22 have been reported to exert differential effects upon the receptor; CCL22 treatment induced significant receptor internalisation whereas CCL17 did not, when surface expression was assessed by flow cytometry. Confocal microscopy showed intracellular pools of CCR4 following CCL22 treatment but not after CCL17 treatment. This internalisation required lipid rafts; filipin, an inhibitor of raft-mediated endocytosis, prevented CCL22-induced internalisation. *Pertussis* toxin (PTX), which uncouples G proteins from receptors, did not affect internalisation. This indicated that the CCL22-induced internalisation did not require G protein coupling (Mariani et al., 2004). These data suggest that the ligands have differential activity through the receptor.

As described in section 1.3.2.2, GPCRs can signal through both G protein- and β-arrestin-mediated pathways. It also has been shown that the signalling of a ligand through a receptor does not necessarily lead to the equal activation of both pathways. Some ligands induce more G protein-biased signalling outputs while others lead to β-arrestin-biased outputs. This biased agonism may be a product of subtly different receptor conformations induced by different ligands for a receptor. Figure 1-8 shows the difference between balanced and biased agonism.

In the case of CCR4, the described data show that CCL22 induces a greater level of CCR4 internalisation compared to CCL17, indicative of potential β-arrestin-biased recruitment in response to CCL22 binding to the receptor. The selective activity of GRKs has been shown for CCR7 with respect to phosphorylation of its C-terminus in response to CCL19 but not CCL21(Kohout et al., 2004), and CXCR4-

mediated chemotaxis required β-arrestins (Fong et al., 2002b; Sun et al., 2002). Since these chemokine receptors show outputs that involve β-arrestins and biased ligand-induced signalling, the CCR4 data suggest that it too signals differentially in response to its ligands CCL17 and CCL22.

In addition, the highly conserved helix VIII region is likely located in the C-terminus of CCR4. This helix VIII has been identified in the C-terminus of *Rhodopsin*-type GPCRs and as described has many important roles in receptor function and ligand binding.

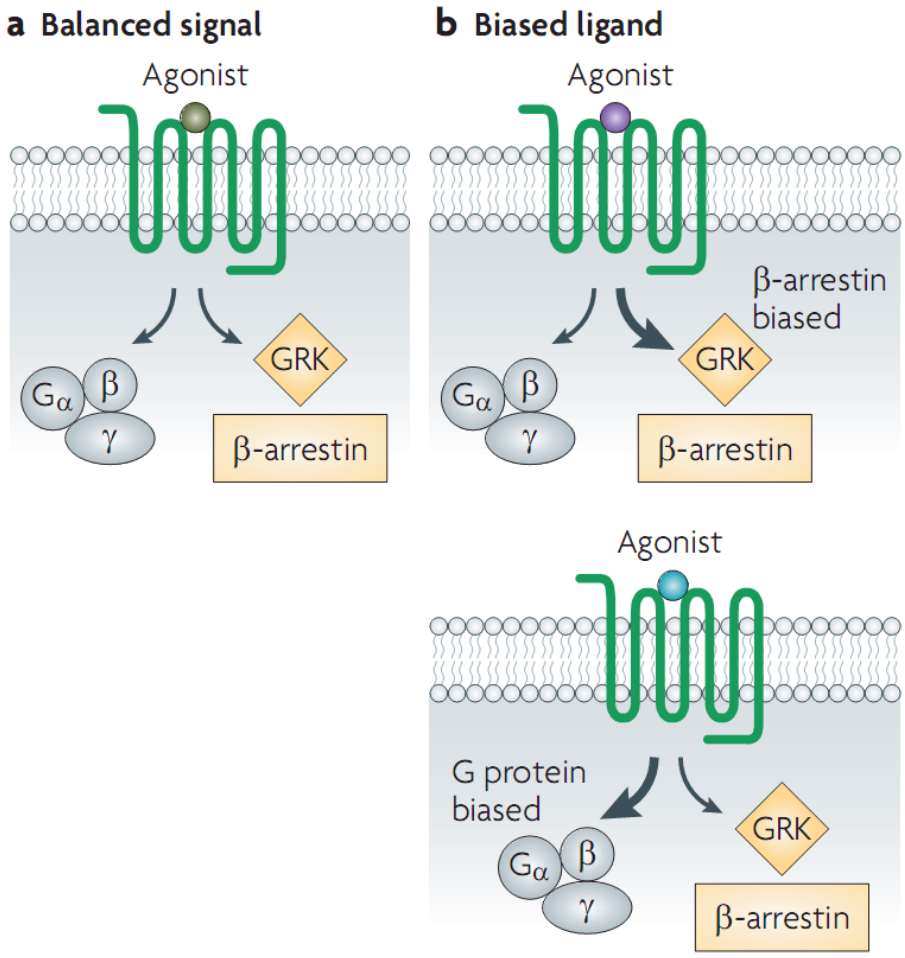

Figure 1-8 – Biased agonism through a GPCR

In balanced signalling (a), an agonist induces equal levels of G protein- and β-arrestin-mediated signalling. In biased agonism however (b), an agonist can induce a greater level of β-arrestin signalling (top) or a greater level of G protein signalling (bottom). Adapted from Rajagopal et al., 2010.

1.4.1 – CCR4 and its ligands in the immune system

Most chemokine genes are clustered into 2 groups on the chromosomes; a CXC cluster on 4q13.3, and a CC cluster on 17q12. These clusters contain chemokines that are mainly involved in inflammatory responses (Zlotnik and Yoshie, 2012). CCL17 and CCL22 however are located on 16q13 (Nomiyama et al., 1998). This suggests that these chemokines, and thus CCR4, have a role in homeostasis since other known homeostatic chemokines are also located outside of the CC inflammatory cluster. For example, CCL19 and CCL21, which bind CCR7, are located on 9p13 (Nagira et al., 1997; Yoshida et al., 1998). These chemokines direct migration of CCR7-expressing dendritic cells during immune surveillance and passage through the lymphatic tissues (Förster et al., 2008).

Indeed, CCR4-expressing T_{reg} cells (Iellem et al., 2001) are involved in immune homeostasis. T_{reg} cells express the transcription factor Foxp3, which is critical for their suppressive function; *Foxp3* knockout mice show a paucity of these cells and develop autoimmune diseases and cancers. The immune responses to foreign antigens also became stronger in these mice (Sakaguchi et al., 2008). Foxp3 enhances transcription of factors associated with immune suppression such as Cytotoxic T-Lymphocyte Antigen 4 (CTLA-4); this protein transmits inhibitory signals to T cells upon T_{reg} contact (Waterhouse et al., 1995). Therefore, the lack of these cells removed attenuating mechanisms resulting in the development of a strong immune response.

T_{reg} cells also require the presence of the cytokine interleukin 2 (IL-2); mice lacking this cytokine have similar phenotypes to *Foxp3* knockouts (Sakaguchi et al., 2008). Since IL-2 is produced by activated T cells, which are the targets of T_{reg} cells, IL-2 serves as a positive feedback mechanism to control the T cell response; if the T cell population becomes too large the resulting levels of IL-2 lead to T_{reg} development and thus suppression of the response (Laurence et al., 2007).

In addition to their role in immune homeostasis, CCR4, CCL17, and CCL22 are involved in inflammatory reactions, indicating that the chemokines have dual function. CCR4 is also expressed by T_H2 cells (Bonecchi et al., 1998), which are involved in the immune responses to allergens and parasites; these cells release cytokines such as interleukin 4 (IL-4) and 5 (IL-5) (Mosmann and Sad, 1996; Mosmann et al., 1986). IL-4 is required for T_H2 cell differentiation, while IL-5

mediates eosinophil activation. Eosinophils subsequently release cytotoxic granules in an effort to combat parasite infection (Sanderson, 1992). Both CCL17 and CCL22 are produced by dendritic cells, which are used to attract both regulatory (T_{reg}) and inflammatory (T_H2) CCR4-expressing T cells (Tang and Cyster, 1999; Sallusto et al., 1999).

Mast cells are another cell type involved in the inflammatory response. Mast cells express the receptor FcεRI, which binds the Fc portion of the antibody IgE with high affinity. B cells produce this antibody, which after binding to mast cells and cross-linking by antigen induces degranulation, a process by which granules containing mediators such as histamine are released into the extracellular medium. This leads to capillary dilation and thus swelling, redness and recruitment of other inflammatory cells (Williams and Galli, 2000). Mast cells have since been shown to express CCR4, both on those derived from cord blood (Juremalm et al., 2002), and on those obtained from the airways of patients with allergic asthma (Kaur et al., 2005). CCR4 and therefore its chemokines may be involved in the actions of these inflammatory cells during the immune response to allergens.

1.4.2 – CCR4 and its ligands in disease

As has been described, GPCRs constitute 1% of all human genes and are involved in a wide variety of cellular processes. It is therefore unsurprising GPCRs are also involved in disease; indeed, half of all clinically-used drugs target GPCRs (Gurevich and Gurevich, 2008). Chemokine receptors, due to their important role in the immune system are thus implicated in allergy, autoimmunity, inflammatory conditions and other associated pathologies. CCR4 and its ligands are associated with several diseases such as asthma, atopic dermatitis, allergic rhinitis, and some cancers.

Asthma is an inflammatory disease, typically characterised by eosinophilic inflammation, elevated IgE and T_H2 cytokine production, airway hyperresponsiveness (AHR), and mucus secretion (Heijink and Van Oosterhout, 2005; Lloyd and Hessel, 2010). CCR4-expressing T_H2 cells are a major component of the disease. In asthma, allergen that passes through the epithelial barrier of the lungs is processed by dendritic cells and presented to T cells, leading to the generation of helper cells. T_H2 cells, while not the only subset involved in the pathogenesis of asthma, are important drivers of inflammation. They secrete the cytokines IL-4, IL-5 and IL-13. IL-4

promotes further T_H2 activation, IL-5 activates eosinophils, and IL-13 stimulates B cells to produce the antibody IgE. IgE binds mast cells with high affinity, leading to histamine and cytokine release, causing swelling and further cell recruitment (Qian and Wahl, 2009).

CCR4-positive cells have been identified in the skin (Campbell et al., 1999a) and implicated in atopic dermatitis. Patients with the disease had increased levels of CCL17, which correlated with increased eosinophils numbers since $CCR4^+$ T_H2 cells induce eosinophilia via the action of IL-5. In the skin lesions, CCL17 was present in dendritic cells, keratinocytes and endothelial cells (Vestergaard et al., 2000; Kakinuma et al., 2001), indicating that local cells were inducing CCR4-positive cell migration to the site of inflammation.

CCR4 is also implicated in the pathogenesis of various cancers such as adult T-cell leukemia (ATL). ATL is caused by the human T-cell leukaemia virus type 1 (HTLV-1), which infects $CD4^+$ T-cells. The majority of HTLV-1-infected cells express CCR4, which then migrate to CCL17 or CCL22 in the tissues and act as T_{reg} cells, contributing to tumour survival by limiting the host immune response (Yoshie, 2005).

1.4.3 – CCR4 as a therapeutic target

Due to its role in disease, CCR4 is a potential target for therapeutic intervention. Since in diseases such as asthma and atopic dermatitis there is a large influx of CCR4-expressing T_H2 cells into the afflicted tissue, blocking CCR4-dependent migration could provide a way to ameliorate disease states; by limiting the number of T_H2 cells, production of the cytokines IL-4, IL-5 and IL-13 would be reduced, thus preventing further exacerbation of the immune response. Since some cancers rely on CCR4-directed metastasis (Olkhanud et al., 2009), inhibition of this receptor would aid in the therapy of these diseases. In addition, in diseases such as Hodgkin's lymphoma, CCR4-expressing T_{reg} cells are recruited in order to dampen local immune responses and aid the tumour in immune evasion (Ishida et al., 2006). Recently, the anti-CCR4 antibody mogamulizumab has gained marketing approval for treatment of adult T-cell leukemia (Ishida and Ueda, 2011; Beck and Reichert, 2012).

The effect of blocking or removing CCR4 or CCR4-positive cells has been investigated in several studies. T_H2 cells from CCR4-deficient mice were adoptively transferred to WT mice, after which they showed a failure to migrate to the lung in response to allergen exposure, in addition to showing a reduction in the level of T_H2 cytokines IL-4, IL-5 and IL-13. Levels of CCL17 were also significantly reduced compared to WT mice (Mikhak et al., 2010). This shows that CCR4 was required for maintenance of the T_H2 response. Similar results were observed after blockade of CCL17 and CCL22 in mice, which resulted in reduced $CD4^+$ T cell and eosinophil recruitment and cytokine production (Kawasaki et al., 2001; Lloyd et al., 2000).

Conflicting studies have also been performed that do not show CCR4 blockade ameliorating disease states. For example, treatment of allergic airways disease in guinea pigs by CCR4 blockade with the 10E4 antibody did not reduce the number of CCR4-positive cells migrating to the lung. Eosinophil numbers and chemokine production was also unaffected (Conroy et al., 2003). In addition, CCR4 knockout mice showed no difference to WT mice in a model of allergic airways disease. Interestingly however the same mice showed resistance to endotoxic shock induced by the bacterial membrane component lipopolysaccharide (LPS). These mice showed decreased mortality and production of macrophage-associated cytokines such as TNF-α in response to LPS (Chvatchko et al., 2000).

There are several factors to consider when attempting to block CCR4 for therapeutic purposes. Antagonising CCR4 on T_H2 cells may result in compensation by the receptor CCR8, since it is also expressed on this T cell subset (Roos et al., 1997; Iellem et al., 2001; Panina-Bordignon et al., 2001). CCR8 expression has also been shown to increase in asthma, along with its ligand CCL1 (Mutalithas et al., 2010; Montes-Vizuet et al., 2006). This has been proposed to explain the failure of CCR4-blocking studies.

Studies of CCR8 have also shown variable results; some studies of CCR8 knockout mice have shown no difference to WT mice whereas others showed a reduction in airways inflammation (Goya et al., 2003; Gonzalo et al., 2012; Chensue et al., 2001; Chung et al., 2012). If CCR4 and CCR8 are indeed compensating for one another in these studies, it may be necessary to block both chemokine receptors in order to reduce T_H2 cell migration. The observed variability in CCR4 and CCR8 studies may also be due to the different models used and also a result of blocking of all CCR4- and CCR8-expressing cells. CCR4 and CCR8 are also expressed on T_{reg} cells, and blocking these in addition to T_H2 cells may counteract any anti-inflammatory effects; T_{reg} cells act to attenuate the immune response, and their blockade could have the potential to exacerbate rather than ameliorate inflammatory conditions. Thus it would be desirable to block T_H2 cells but not T_{reg} cells. A method of selectively targeting cell populations would prove invaluable in developing therapeutic chemokine receptor antagonists.

1.4.4 – Small molecule antagonists of CCR4

Agonists and antagonists are ligands that either promote or block receptor activation. These are typically classified as either orthosteric or allosteric. Orthosteric ligands bind to the same site as the endogenous ligand, and thus have to compete with it for receptor binding. Allosteric ligands however bind to site distinct from the ligand-binding site and modulate receptor function from there (Müller et al., 2012). Agonists and antagonists of both classes have been investigated for their therapeutic benefit due to their ability to alter receptor function.

In the context of chemokine receptors, receptor antagonists are a well-researched group of ligands since many chemokine- and chemokine receptor-related diseases involve the infiltration of unwanted inflammatory cells. By antagonising the chemokine receptors responsible for directing the migration of these cells, it may be possible to ameliorate disease states and symptoms. For example, as previously described in section 1.4.2, asthma involves the influx of large numbers of CCR4-expressing T_H2 cells into the lung. These cells then propagate an immune response to allergen resulting in the accumulation of eosinophils and other inflammatory cells that cause damage to the tissues. By blocking CCR4 with an antagonist the aim would be to prevent this T_H2-mediated response.

Small molecule drugs are of interest to pharmaceutical companies since their small size allows them to be administered orally, rather than intravenously as is done for larger molecules such as antibodies. Allosteric antagonists of chemokine receptors are of particular interest as they provide a feasible way for a small molecule to block the function of large proteins. In addition, unlike orthosteric antagonists, allosteric antagonists cannot be competed with; in a disease state, there may be a large excess of endogenous ligand meaning that the dose of orthosteric antagonist necessary to inhibit the receptor response would be quite large. By using an allosteric antagonist this problem could be bypassed; by modulating receptor function to prevent it from binding ligand, the receptor response could be blocked with a comparatively lower dose. Another important property of allosteric ligands is that they are probe dependent, meaning that their effects on different orthosteric ligands are not the same (Scholten et al., 2012). For example, a small molecule metal ion chelator complex has been shown to enhance CCL3 binding for CCR1 while also blocking CCL5 binding (Jensen et al., 2008).

As described in section 1.3.2.2, endogenous orthosteric ligands of GPCRs can be biased agonists of the receptors. For example, the C-terminus of CCR7 is phosphorylated by GRKs in response to binding by CCL19 but not CCL21 (Kohout et al., 2004). Other examples include the preferential activation of β-arrestin signalling over G protein signalling by some β_2-adrenergic receptor ligands and not others (Drake et al., 2008). This phenomenon relates to the concept of allostery, in that different ligands modulate the receptor in a way that results in differential signalling outputs. Allosteric antagonists in the same fashion can modulate the different signalling pathways for the same ligand; for example, an allosteric modulator of a glutamate receptor enhanced the calcium mobilisation induced by its orthosteric agonist but decreased the level of kinase activation (Zhang et al., 2005). It may then also be possible for an allosteric antagonist to selectively inhibit the responses of one orthosteric ligand and not another. To use the example of chemokines and their role in disease, it may be possible to target the response of CCR4 to CCL17, which as shown is a ligand highly expressed in atopic skin diseases, but leave the CCR4 response to CCL22 unaffected. Selectively inhibiting the response to specific ligands may therefore provide a way to reduce the side-effects associated with less targeted therapies (Galandrin et al., 2007).

Many allosteric chemokine receptor antagonists have been developed, for receptors including CCR1 (Vaidehi et al., 2006; de Mendonça et al., 2005), CCR2 (Mirzadegan et al., 2000), CCR4 (Andrews et al., 2008), CCR5 (Garcia-Perez et al., 2011; Watson et al., 2005), CXCR1/CXCR2 (Bertini et al., 2012), CXCR3 (Scholten et al., 2012), and many others (Scholten et al., 2012).

Notable examples include the CCR5 inhibitor Maraviroc, which is an allosteric antagonist of CCR5. Maraviroc binds to a region within the transmembrane helices of CCR5 and prevents it from binding the chemokine CCL3. CCR5 serves as a co-receptor for HIV entry, and Maraviroc has been licensed for HIV therapy. The allosteric mechanism of inhibition of CCL3 binding also prevents CCR5 from binding the viral gp120 glycoprotein; Maraviroc induces conformational changes that prevent the second extracellular loop of CCR5 from interacting with a loop structure in gp120 (Garcia-Perez et al., 2011). Maraviroc is both the first chemokine receptor antagonist to pass clinical trials and the first anti-retroviral drug that does not target viral proteins.

AMD3100, a CXCR4 antagonist, was also developed for HIV treatment since some strains of the virus use CXCR4 to enter macrophages, but later withdrawn due to toxicity issues. In mice, CXCR4 and its ligand CXCL12 were shown to be required for the retention of haematopoietic stem cells in the bone marrow, most likely to maintain a reserve of these cells and support their survival (Sugiyama et al., 2006). This stem cell retention was disrupted in human patients treated with AMD3100, leading to the mobilisation of these cells from the bone marrow into peripheral tissues. As a result of this, AMD3100 was licensed as plerixaflor/Mozobil for autologous bone marrow transplant patients suffering from non-Hodgkin lymphoma and multiple myeloma (De Clercq, 2010).

Despite these successes, many chemokine receptor antagonists have failed to pass clinical trials for several reasons. One such reason is toxicity or unwanted side-effects; the CCR5 antagonist aplaviroc entered clinical trials for HIV-1 treatment but resulted in high liver toxicity (Allegretti et al., 2012). A CCR3 antagonist was discontinued due to it also inhibiting the human ether-a-go-go related gene (hERG) ion channel (Pease, 2011). The hERG protein is a potassium-selective ion channel involved in cardiac function, specifically the beating of the heart. Since several hERG inhibitors led to arrhythmia and death, other antagonists in development are screened for anti-hERG activity and discontinued if this activity is too high (Sanguinetti and Tristani-Firouzi, 2006).

Poor efficacy has also been a problem in chemokine receptor antagonist development. The development of the CCR1 antagonist BX 471 for multiple sclerosis was stopped in Phase II trials after it failed to show efficacy. A similar lack of efficacy was shown for GW701897B, a CCR3 antagonist indicated for allergic rhinitis. A CXCR3 antagonist, AMG487, also proved ineffective in Phase II trials for psoriasis (Pease and Horuk, 2009; Allegretti et al., 2012).

Several factors may have contributed to these antagonists not producing the desired therapeutic outcome. One such factor relates to the apparent redundancy in the chemokine system, as described in section 1.3.2. For example, CCR1 and CCR2 both guide the migration of macrophages, and since these cells are involved in the pathogenesis of rheumatoid arthritis both receptors were targeted for therapy as it was believed they were performing redundant functions. However, CCR1 has been shown to be the main driver of macrophage recruitment into arthritic joints, despite the

presence of CCR2 on these cells. This therefore explains the negative results of CCR2 antagonists for rheumatoid arthritis (Schall and Proudfoot, 2011).

The correct dosage of antagonist is another factor that must be taken into account when trying to inhibit chemokine receptors. It has been postulated that in order to effectively inhibit a response the levels of drug in the blood must be high enough to bind over 90% of the target receptors, since positive feedback can result from even a small number of unoccupied receptors. Indeed, antagonists of CCR1 used at high doses have shown positive clinical effects (Schall and Proudfoot, 2011).

1.4.4.1 – Intrahelical and intracellular allosteric antagonists

Allosteric antagonists typically bind a site within the transmembrane bundles of the receptor. Examples of antagonists binding in this fashion include the CCR1 and CCR3 antagonist UCB36526 (de Mendonça et al., 2005; Wise et al., 2007), the CCR1 antagonist BX471, and the CCR5 antagonist Maraviroc (Dorr et al., 2005; Watson et al., 2005). These antagonists typically contain a positively charged amine group that binds a conserved glutamine in helix VII of the receptors. Within the transmembrane bundle exists a major and minor binding pocket for the antagonists; the former is defined by helices I, II, III and VI while the latter is defined by helices III, IV, V, VI and VII. The functional groups of the antagonists then bind to other amino acids that line these binding pockets. It is through binding to this site that the antagonists prevent receptor activation, specifically by preventing helix VI from rotating outwards to facilitate ligand binding. This prevents the breakage of the ionic lock that exists between the DRYLAIV motif and a glutamic acid in helix VI in many GPCR structures; this then prevents subsequent G protein activation (Nygaard et al., 2009; Thiele et al., 2011).

Figure 1-10 shows the diversity of antagonist-binding pockets of GPCRs, based on crystal structures. Despite the preservation of the seven transmembrane domain structures of these receptors, the ligand binding pockets can vary quite significantly, due to variations in amino acid side chains that line the pockets and also the relative shifts in helix and extracellular loop conformations. For example, the adenosine A_{2A} receptor has a much shallower pocket than the adrenergic receptors, while the histamine H_1 receptor has an even deeper binding pocket.

Interestingly, it has been shown that the ligand-binding pockets are relatively inflexible. Analysis of GPCR structures suggests that these pockets have restricted conformational rearrangements; for example, the β_2-adrenergic receptor ligand-binding pocket was largely similar when crystallised with different antagonists and inverse agonists. While some ligands, such as CVX15 bound to CXCR4 shown in figure 1-9, induce larger helix shifts, small molecules generally do not lead to large conformational rearrangements. This therefore suggests that small molecule antagonists inhibit function by subtly affecting receptor conformation, and that different antagonists for a receptor would each occupy a largely similar binding pocket rather each binding to a specific portion of the receptor (Katritch et al., 2012).

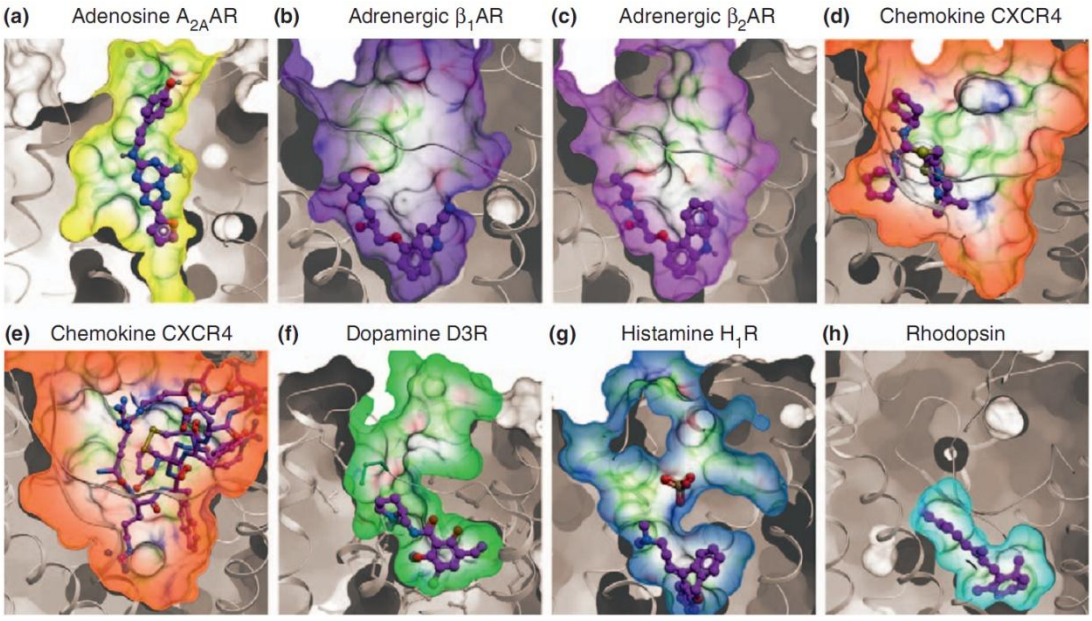

Figure 1-9 – Antagonist binding pockets of GPCRs

Diversity of the shape of the ligand-binding pocket of different GPCRs, based on crystal structures. Adenosine A2A receptor (a) forms a channel with the antagonist ZM241385 positioned vertically. The β_1- and β_2-adrenergic receptors (b and c) have similar and highly accessible pockets that share the same residues for cyandopindolol and carazolol. CXCR4 has a large and open pocket than can bind the small molecule IT1t (d) and the large peptide CVX15 (e). Dopamine D3 receptor (f) has distinct extracellular and core sub-pockets; the latter is occupied by eticlopride. The histamine H_1 receptor (g) has a deeper pocket than the other receptors. Rhodopsin (h) has a small, hydrophobic, and enclosed retinal-binding pocket. All pockets are shown in the same orientation. From Katritch et al., 2012.

Seven allosteric antagonists of CCR4 have been supplied by GlaxoSmithKline. Four of these are hypothesised to target the intrahelical site between the transmembrane domains of CCR4. Their structures are shown in figure 1-10. These are believed to act via the classical mode of allosteric antagonism, in which the antagonist binds within the transmembrane bundle and prevents the receptor from shifting into an active conformation, thus blocking its activation.

In addition to the antagonists that target the classical intrahelical site of the receptor, a novel class of antagonists was developed that bound the C-terminus of CCR4. Based on C-terminus exchanges of CCR4 and CCR5, it was found that the antagonists were specific for the C-terminus of CCR4. The compounds were modified to ester and carboxylic forms in order to test this; the more lipophilic esters could pass through the membrane and antagonise the receptor while the less lipophilic carboxylic acids could not do so and thus had reduced efficacy. Treatment of cells with saponin to permeabilise the membrane or using membrane-based assays gave similar results, indicating that these compounds did indeed bind the CCR4 C-terminus (Andrews et al., 2008).

GlaxoSmithKline has supplied three antagonists that are hypothesised to bind to this novel intracellular site of CCR4. The structures of these antagonists are also shown in figure 1-10.

A

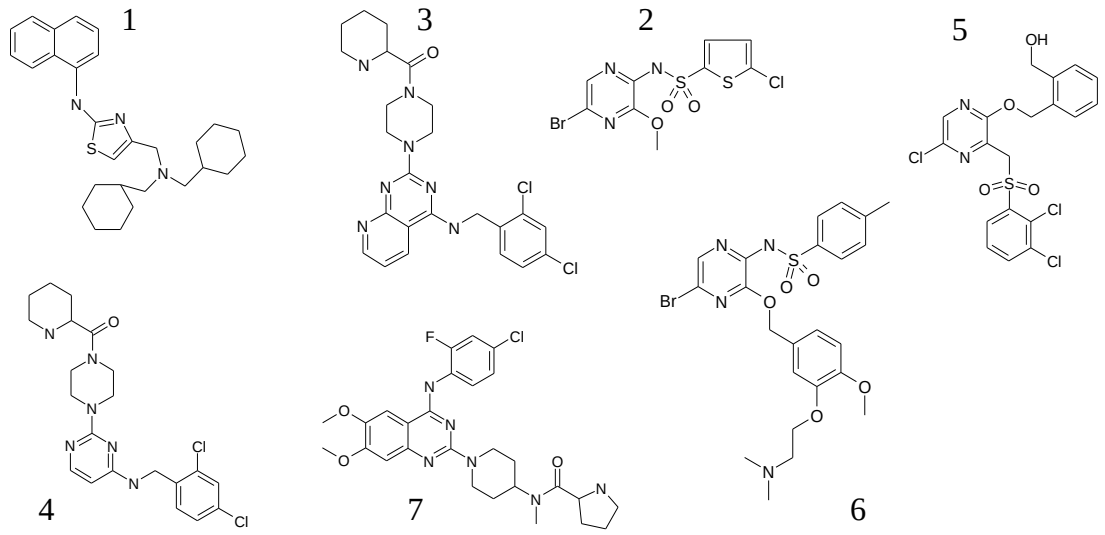

B

Compound	Source patent
1	US7144903B2 (Amgen)
2	WO2003051870A1 (Astra Zeneca)
3	WO2004020584A2 (Bristol-Myers-Squibb)
4	WO2004020584A2 (Bristol-Myers-Squibb)
5	WO2003059893A1 (Astra Zeneca)
6	US20060004010A1 (Ono)
7	WO2007111227A1 (Astellas)

Figure 1-10 – Structures of CCR4 antagonists

Seven allosteric CCR4 antagonists were supplied by GlaxoSmithKline, the structures of which are shown in panel A. Antagonists 1, 3, 4, and 7 are hypothesised to bind to the site within the transmembrane helices. Antagonists 2, 5 and 6 are hypothesised to bind to the novel site identified in the C-terminus of CCR4. Panel B shows the source patent for each of the antagonists.

1.5 – Project hypotheses and aims

The three hypotheses of this project are as follows:

- There is a structural basis for the CCL17 and CCL22 selectivity seen in ligand-induced endocytosis and desensitisation assays.
- The ‘site 1’ group of allosteric CCR4 antagonists bind to a site within the transmembrane domains of the receptor.
- The ‘site 2’ antagonists bind to a site on the C-terminus of CCR4.

The first aim of this project was to investigate the biology of the chemokine receptor CCR4. This was performed using different CCR4 antibodies to explore the differences reported in receptor expression between these antibodies, and to compare the differing effects of the two ligands CCL17 and CCL22 on receptor internalisation and function. Mutation of amino acids within the seventh transmembrane domain and C-terminus was also performed in order to determine their contribution to receptor expression, chemokine binding, and receptor function.

GlaxoSmithKline has supplied seven allosteric antagonists of CCR4, four of which are hypothesised to bind to the intrahelical site within the transmembrane bundle of the receptor, while the remaining three are hypothesised to bind the novel C-terminal site.

The second and third aims of the project were to investigate the intrahelical and intracellular antagonists to validate the hypotheses that they bind the two allosteric sites. This was performed by mutating regions of the receptor that were predicted to bind the antagonists. The mutants were then tested for cell surface expression, chemokine binding, and functional abilities. Functional mutants were investigated for their ability to be inhibited by the antagonists, the rationale being that a mutant of a key antagonist-binding region would confer sensitivity of the receptor to the compound. Radiolabelled antagonists were also used to directly test the interaction of the antagonists with the mutant receptors.

2 – Materials and Methods

2.1 – Materials

2.1.1 – Reagents

All reagents unless otherwise stated were purchased from Sigma-Aldrich (Poole, UK). Media, PBS, and media additives were from Gibco (Invitrogen, Paisley, UK). Chemokines were from Peprotech (London, UK). The anti-HA ascites fluid was from Covance (Crawley, UK), the IgG1 antibody from Sigma-Aldrich, and the FITC-conjugated polyclonal goat anti-mouse immunoglobulins (Fab'2 fragments) from Dako (Glostrup, Denmark). Radiolabelled chemokines were from Perkin-Elmer Life Sciences (Waltham, MA, USA). CCR4 antagonists and radiolabelled antagonists were synthesised by GlaxoSmithKline (Stevenage, UK). Restriction enzymes, DNA ladders, R buffer, and *Pfu* polymerase were from Fermentas (Glen Burnie, MD, USA).

2.1.2 – Kits

The Fast Plasmid Mini Kit was from Eppendorf (Stevenage, UK). The HiSpeed Plasmid Maxi Kit was from Qiagen (Crawley, UK). The QuikChange site-directed mutagenesis kit was from Stratagene (Santa Clara, CA, USA). The Pierce BCA Protein Assay Kit was from Thermo Scientific (Rockford, IL, USA).

2.1.3 – Media, buffers and solutions

"Complete" RPMI:	500 ml RPMI 1640+GlutaMAX+HEPES
	10% heat-inactivated certified FCS (50 ml)
	50,000 units penicillin (5 ml 10,000 units/ml)
	50 mg streptomycin (5 ml 10 mg/ml)
	50 µM β-mercaptoethanol (500 µl 50 mM)
	1 mM sodium pyruvate (5 ml 100mM)
	1x non-essential amino acids (5ml 100x)
Ampicillin:	100 mg/ml in H_2O
LB broth:	1 litre dH_2O
	10 g LB powder
	100 mg ampicillin (1ml 100 µg/ml) after autoclaving

LB agar:	1 litre H_2O
	10 g LB broth powder
	15 g agar powder
	100 mg ampicillin (1ml 100 µg/ml) after autoclaving
50xTAE:	242 g Tris base
	750 ml deionised water
	57.1 ml glacial acid
	100 ml 0.5M EDTA
FACS buffer:	PBS (500 ml)
	0.25% BSA (1.25 g)
	0.01% sodium azide (500 µl of 10%)
HEPES buffer:	50 mM HEPES
	1 mM EDTA
	in water, pH=7.4 using KOH
A2 buffer:	50 ml HEPES buffer
	1 tablet protease inhibitor cocktail (Roche, UK)
SPA buffer:	20 mM HEPES
	100 mM NaCl
	10 mM $MgCl_2$
	in water, pH 7.4 (NaOH)
Filtration agonist buffer:	20 mM HEPES
	100 mM NaCl
	10 mM $MgCl_2$
	10 µg/ml saponin
	0.1% BSA
	in water, pH=7.4 (KOH)
Filtration antagonist buffer:	20 mM HEPES
	100 mM NaCl
	10 mM $MgCl_2$
	10 µg/ml saponin
	in water, pH=7.4 (KOH)
Whole-cell binding buffer:	0.1% BSA (0.2 g)
	0.05% NaN_3 (1 ml/10%)
	in RPMI 1640 (200 ml), pH 7.4 (NaOH)

2.2 – Methods

2.2.1 – Cell biology

2.2.1.1 – Culture of L1.2 cells

The murine L1.2 pre-B lymphoma and Hut78 T cell lines were cultured in liquid suspension in complete RPMI. Cells were kept in a humidified incubator, at 37°C, 5% CO_2. The cells were maintained at a density between 0.5 x 10^6/ml and 1 x 10^6/ml, to ensure that they were in a log growth phase, as higher cell densities often resulted in suboptimal transfection efficiencies. Cell density was determined by mixing 10 µl trypan blue with 10 µl cells and counting using a haemocytomer and inverted microscope (Zeiss, Cambridge, UK). Trypan blue selectively stained dead cells blue, allowing them to be factored in when assessing viability. Complete RPMI was stored at 4°C.

2.2.1.2 – Transient transfection of L1.2 cells with CCR4-containing plasmid DNA

All steps were performed in a tissue culture cabinet, with the exception of the electroporation step. L1.2 cells were counted using a haemocytometer. 1.5 x 10^7 cells were transferred to a sterile 50 ml tube, and centrifuged at 310 g, 21°C, for 5 minutes. 50 µl (10.5 mg/ml) tRNA and 1 µg DNA per 1x10^6 cells were added to the bottom of a sterile cuvette with a 0.4 cm electrode gap (BTX Harvard Apparatus, Holliston, MA, USA). The supernatant of the centrifuged cells was decanted, and the pelleted cells resuspended in 800 µl RPMI, transferred to cuvette, and incubated at room temperature for 20 minutes. The cuvette was placed in a BioRad Gene-pulser (BioRad, Hercules, CA, USA), electroporated at 330 volts, 975 µF, and incubated at room temperature for 20 minutes. The contents of the cuvette were transferred to a T-75 tissue culture flask containing 15 ml complete RPMI, and incubated for 5 hours at 37°C. 150 µl 1M sodium butyrate was added to the flask to give a final concentration of 10 mM, and the cells incubated overnight at 37°C. The number of cells transfected could be varied depending on assay requirements; the maximum recommended per cuvette was 4 x 10^7 cells.

2.2.2 – Molecular biology

2.2.2.1 – Primer design

Individual primer pairs were designed to generate CCR4 mutants, and synthesised by Invitrogen. Primers were approximately 35bp in length, and corresponded to the target residue and flanking regions. The codon of the target residue was altered in the primer sequence. For example, mutation of glutamic acid 290 to alanine (E290A) involved changing the codon from GAA to GCA. Reverse complementary primers were also designed. Primer length was varied by several base pairs to ensure a higher percentage of cytosine and guanine compared to adenine and thymine. This gave the primers a higher melting temperature (Tm). The Tm was determined by using the formula supplied by the Stratagene QuikChange Site-Directed Mutagenesis Kit:

$$Tm = 81.5 + 0.41(\%GC) – 675/N - \%mismatch$$

Where N is primer length in bases, and values for %GC and %mismatch are whole numbers.

2.2.2.2 – Site-directed mutagenesis of WT CCR4 DNA template

A 50 µl reaction mixture was composed using the reagents from the kit and the custom-designed primers. It was made in a 250 µl thin-walled PCR tube and placed in the thermal cycler (MJ Research, Waltham, MA, USA):

5 µl 10X buffer
1 µl dNTPs
1 µl *Pfu* DNA polymerase
1 µl forward primer (10 µM)
1 µl reverse primer (10 µM)
40 µl sterile water

The reaction mixture was run on this programme:

1) 95°C for 30 seconds
2) 55°C for 1 minute
3) 68°C for 6 minutes
4) Go to step 2, repeat 15 times
5) 4°C indefinitely

1 µl *DpnI* (10 units/µl) (Invitrogen) was added to the reaction mixture. Incubation at 37°C for one hour digested parental DNA. This was used to transform *E. coli*. The resulting DNA from a mini-prep was sent for sequencing to Eurofins (Germany); once the mutation of CCR4 was confirmed, a maxi-prep culture was seeded using the previously transformed bacteria. This was then used to generate a larger volume of mutant CCR4 DNA.

2.2.2.3 – Transformation of Escherichia coli *with CCR4 DNA*

DH5α One-Shot supercompetent *E. coli* (Invitrogen) were removed from -80°C storage and thawed on ice. A 50 µl *E. coli* aliquot and 1 µl (10 ng/µl) plasmid DNA were pipetted into a 15 ml tube, swirled to mix, incubated on ice for 30 minutes, heat shocked in a 42°C water bath for 45 seconds, and incubated on ice for 2 minutes. 0.5 ml SOC medium (Invitrogen) was added, and the tube placed in a 37°C shaker at 200 RPM for one hour. An ampicillin agar plate was left to dry in a 37°C incubator during the incubation. 250 µl of the bacterial culture was pipetted onto the plate, and spread evenly using a sterile glass rod. The plate was incubated overnight at 37°C.

2.2.2.4 – Bacterial culture

2 ml LB broth and 2 µl 100 mg/ml ampicillin (Boehringer Ingelheim, Ingelheim am Rhein, Germany) were added to a sterile 15 ml tube. A single bacterial colony from an agar plate was picked using a sterile pipette tip, and the tip ejected into the 15 ml tube, which was incubated in a 37°C Innova 4000 shaker (New Brunswick Scientific, Enfield, CT, USA) at 200 RPM overnight.

2.2.2.5 – Mini-prep of bacterial culture

The Eppendorf Fast Plasmid Mini Kit (Eppendorf, UK) was used to obtain 20 µl purified DNA from 2 ml bacterial culture, with a typical yield of approximately 200 ng/µl.

2.2.2.6 – Restriction digest of purified plasmid DNA

Purified plasmid DNA from a mini-prep was digested to ensure the presence of the CCR4 insert. The following were added to a tube, mixed, and incubated for 1 hour at 37°C:

1 µl *Hind* III (10 units/µl)
1 µl *Xho* I (10 units/µl)
2 µl R buffer
5 µl DNA
11 µl H_2O

2.2.2.7 – Agarose gel electrophoresis of restriction digest product

A stock of 1% agarose in 1xTAE was composed by dissolving 5 g of agarose powder (Helena Biosciences, Gateshead, UK) in 500 ml of 1xTAE by heating in a microwave.

This mixture was then adjusted to 1 litre in volume by adding deionised water. 7 µl ethidium bromide (10 mg/ml) was added to the molten agarose. This was used to fill a gel mould fitted with a comb. Once cooled, the comb was removed and the gel placed in a horizontal electrophoresis tank and submerged in 1xTAE. 5 µl 1kb DNA ladder (Fermentas) was loaded into the leftmost well. 4 µl loading dye (Fermentas) was added to the restriction digest, mixed, and loaded in the well adjacent to the ladder. The electrophoresis machine was set at 100V for approximately 40 minutes. A UV transilluminator was used to visualise the bands.

2.2.2.8 – Maxi-prep of bacterial culture

Once the authenticity of the CCR4 insert was confirmed by sequencing (Eurofins, Ebersberg bei München, Germany), 0.5 ml of culture was added to a flask containing 100 ml LB broth and 200 µl of 100 mg/ml ampicillin, and incubated in a 37°C Innova 4430 shaker (New Brunswick Scientific) at 200 RPM overnight. This culture was used to generate 1.5 ml plasmid DNA, using the Qiagen HiSpeed Plasmid Maxi Kit. A typical yield was approximately 1000 ng/µl.

2.2.2.9 – Measurement of CCR4 surface expression using flow cytometry

16 hours following transfection of CCR4 DNA, the cells were counted and transferred to a 50 ml tube and centrifuged at 310 g for 5 minutes. The supernatant was discarded, and the cells resuspended in simple RPMI at a density of 10^7 cells/ml.

2 x 100 µl of cells were pipetted into FACS tubes and centrifuged at 4ºC at 310 g for 5 minutes. The supernatant was discarded. The cell pellets were resuspended in 100 µl of 5 µg/ml anti-HA ascites fluid or IgG1 antibody. They were then incubated on ice for 30 minutes, and centrifuged at 310 g for 5 minutes. The supernatant was discarded, and both pellets resuspended in 100 µl of 2 µg/ml FITC-conjugated polyclonal goat anti-mouse immunoglobulins (Fab'2 fragments), and incubated on ice for 30 minutes. 500 µl FACS buffer was added to the tubes, which were centrifuged at 310 g for 5 minutes. The supernatant was then discarded, the pellet resuspended in 450 µl FACS buffer and analysed using a FACSCalibur or FACSFortessa flow cytometer (BD Biosciences, San Jose, CA, USA).

2.2.3 – Functional assays

2.2.3.1 – Chemotaxis of CCR4-transfected cells to increasing chemokine concentrations

The chemotaxis assay was performed on transfected cells. Once expression had been confirmed by staining and flow cytometry, a 96 well chemotaxis plate (Neuroprobe, Gathersburg, MD, USA) was blocked by adding 30 µl 1% BSA (0.1 g in 10 ml simple RPMI) to each well, and incubating at room temperature for 30 minutes. Solutions of 0.1 nM, 1 nM, 10 nM and 100 nM chemokine (CCL17 and CCL22 (Peprotech, London, UK) from 10 µM stocks) in RPMI containing 0.1% BSA were prepared. The 1% BSA was removed from the plate and 31 µl chemokine solution added to the wells in duplicate, in addition to 0.1% BSA as a buffer control. The membrane of the chemotaxis plate was attached on top of the wells, and 20 µl cell droplets (at 10^7/ml) were pipetted onto this contact point. The lid of the plate was attached, and the plate was placed in a humidified box and incubated for 5 hours at 37°C. After incubation, the lid and membrane were removed, and the cell droplets scraped off of the top of the membrane. A well-funnel was placed over the chemotaxis plate, and a 96 well OptiPlate (Perkin Elmer) was placed on top. The plates were inverted and centrifuged at 310 g for 5 minutes, to transfer the chemotaxis plate well contents into the wells of the OptiPlate. 20 µl CellTiter-Glo (Promega, Southampton, UK) was added to each well, and the plate sealed with an adhesive TopSeal covering. The OptiPlate was placed on a shaking table for 10 minutes, to lyse the cells. The plate was analysed by detecting luminescence levels, using a TopCount NXT (Perkin Elmer). The results from this were used to determine the chemotactic index (CI), which is the mean of the duplicates divided by the mean of the buffer duplicates.

2.2.3.2 – Dose-dependent inhibition of chemotaxis

A chemotaxis assay was set up using a fixed concentration of chemokine and an increasing concentration of antagonist. A chemotaxis plate was blocked and the transfectants prepared as described previously. A solution of 1 nM CCL17 or CCL22 (10 nM in the case of mutants that showed a reduced chemotactic potency) was made in RPMI containing 0.1% BSA. Serial dilutions of 10 mM antagonist stocks were the

made using this chemokine solution, at concentrations of 1 nM, 3 nM, 10 nM, 30 nM, 100 nM, 300 nM, 1 µM, 3 µM, 10 µM and 30 µM. After the plate was blocked, these were pipetted into the wells in duplicate, along with negative buffer controls and positive chemokine-only controls. Following the 5 hour incubation, the cells were stained with CellTiter-Glo and luminescence detected, as described previously. The values of the mean of the buffer duplicates were subtracted from the remaining means, which were then expressed as percentage of the positive controls. These data were then analysed with non-linear regression using the GraphPad Prism statistical package to generate a $\log IC_{50}$. The $\log IC_{50}$ values for the mutant and WT transfectants were compared using an unpaired two-tailed t-test.

2.2.4 – Receptor binding assays

2.2.4.1 – Preparation of cell membranes for filtration and scintillation proximity binding assays

1-1.2 x 10^8 L1.2 cells were transfected with WT or mutant CCR4 and assayed the following day for receptor expression, as described previously. Once expression was confirmed, the cells were centrifuged at 310 g for 5 minutes, resuspended in 10 ml simple RPMI, and centrifuged again. The supernatant was discarded and the pellet snap-frozen in liquid nitrogen. The frozen pellet was stored at -80°C if required.

The pellet was resuspended in 10 volumes of buffer A2; typically the cell pellet measured 1 ml in volume, therefore 10 ml of A2 was added. The cells were then homogenised by 3 x 45 second bursts in a pre-chilled blender (Waring, Torrington, CT, USA), with 2 minutes on ice between each burst and 5-10 minutes on ice after the final burst, to allow foam to dissipate.

The homogenised cells and washings from the blender (with A2 buffer) were then transferred to 50 ml falcon tubes, which were spun at 500g for 20 minutes in a pre-chilled 4°C centrifuge. The supernatant was withdrawn and spun at 48,000g for 30 minutes in a pre-chilled 4°C ultracentrifuge. The resulting pellet from the centrifuged supernatant was resuspended in 50 mM HEPES buffer, at 4x the volume of the original cell pellet. The pellet was resuspended by vortexing for 5 seconds, forcing it through a 10 ml syringe against the tube base, then forcing through a 0.6 mm needle using a 10 ml syringe. The membrane suspension was then distributed into 200 µl aliquots and stored at -80°C until use. The same process was repeated for naïve L1.2 cells.

2.2.4.2 – BCA (bicinchoninic acid) assay to determine membrane suspension concentration

An aliquot of membrane suspension was removed from -80°C storage and thawed on ice. BSA standards were composed in PBS at the following concentrations: 0.1, 0.2, 0.4, 0.5, 0.6, 0.8, 1, 1.25, 1.5, 1.75, and 2 mg/ml. 10 µl duplicates were pipetted into a 96 well plate. 10 µl duplicates of membrane suspension were then added to the plate, in addition to 1:3, 1:6 and 1:9 dilutions of the suspension. The $CuSO_4$ and BCA reagents from a Pierce BCA Protein Assay Kit

(Thermo Scientific, Rockford, IL, USA) were mixed at a ratio of 1:50, and 200 µl added to each well. The plate was incubated at 37°C for 30 minutes. Absorbance was read at 562 nm (540 nm reference), using a Safire microplate reader (Tecan, Männedorf, Switzerland). The absorbance values from the BSA standards were analysed using linear regression, and from this the concentration of the membrane suspension was determined.

2.2.4.3 – Scintillation proximity assay (SPA) using cell membranes

SPA involved incubating membranes with radiolabelled antagonist, scintillant beads, and either vehicle to measure total binding or unlabelled antagonist to measure non-specific binding. This assay was performed in 96 well polypropylene assay blocks (Coring, USA), with a final assay volume of 101 µl.

The two radiolabelled antagonists, ^{3}H-3 and ^{3}H-5, required two different types of SPA beads; ^{3}H-3 required wheatgerm agglutinin beads (WGA; GE Healthcare, Chalfont St Giles, UK) whereas ^{3}H-5 required washed yttrium silicate beads (YSi; GE Healthcare). The beads were resuspended in SPA buffer along with thawed membrane suspension to give a final assay concentration of 10 mg/ml. Membrane suspension concentration varied from 5 µg/well to 40 µg/well. After a 30 minute incubation, 50 µl of the bead/membrane mixture was added to the wells along with 50 µl radiolabelled ligand solution at a final assay concentration of 1 nM. To total binding wells, 1 µl DMSO was added. To non-specific binding wells, 1 µl unlabelled antagonist was added; from the 10 mM stocks this gave a final assay concentration of 100 µM. The assay was incubated at room temperature for 30 minutes, after which the assay plate was read using a MicroBeta 1450 Trilux scintillation counter (Perkin Elmer).

2.2.4.4 – Filtration binding assay using cell membranes

Filtration binding involved incubating membranes, radiolabelled antagonist and either buffer (total binding) or unlabelled antagonist (non-specific binding) and then using a filter under vacuum pressure to separate the membranes. This assay was performed in 96 well propylene assay blocks, with an assay volume of 500 µl.

The membrane suspension was thawed on ice. 50 µl of a 10% DMSO in buffer solution was added to the TB wells, and a 100 µM antagonist/10% DMSO in buffer solution was added to the NSB wells (antagonist stocks at 10 mM); these resulted in 1% DMSO and 10 µM antagonist final assay concentration. 50 µl radiolabelled antagonist solution (^{3}H-3 stocks at 27 µM, ^{3}H-5 stocks at 19 µM) was added to the wells to give a final assay concentration of 1 nM, after which 400 µl membrane solution was added to mix. The membrane solution was composed at a concentration 1.25x that of the final assay concentration, to account for the dilution factor.

The plate was sealed and shaken at room temperature for 2 hours, after which the contents on the wells were filtered through glass fibre mats under vacuum pressure using a Brandel harvester. ^{3}H-3 wells were filtered through GF/C-type mats (Brandel Inc, Gathersburg MD, USA) pre-soaked in 0.3% polyethylenimine (PEI) for 2 hours. ^{3}H-5 wells were filtered through GF/B-type mats pre-soaked with pure H_2O. The filter mats were dried for 30 minutes at 60ºC, after which the filter pieces placed in scintillation vials. 4ml liquid scintillant (Perkin Elmer) was added to each tube, which were then read on a Tri-Carb 2900 TR liquid scintillation counter (Canberra Packard, Pangebourne, UK). The resulting data were recorded as disintegrations per minute (DPM). Radioactive counts from free ligand were measured by adding 3 x 50 µl aliquots to scintillation vials along with scintillation fluid. This was used to accurately determine the concentration of radiolabelled ligand added to each well.

2.2.4.5 – Whole-cell radiolabelled chemokine binding assay

L1.2 cells transfectants were incubated in 96 well round-bottomed polypropylene plates with 0.1 nM ^{125}I-chemokine and either buffer (total binding) or 100 nM unlabelled chemokine (non-specific binding). Chemokine and cell dilutions were composed in whole-cell binding buffer. Assay volume was 50 µl.

20 µl buffer was added to the total binding wells, and 20 µl of 250 µM chemokine solution was added to the non-specific binding wells to give a final assay concentration of 100 nM. 5 µl 1 nM radiolabelled chemokine solution was added to each well to give a final assay concentration of 0.1 nM. Cells were resuspended in buffer at 6 x 10^{7}/ml; 25 µl (1.5 million cells) was added to each well and the contents of the well mixed by pipetting.

The plate was incubated for 90 minutes at room temperature, during which time a 0.5 M NaCl in buffer salt wash was composed (5 g NaCl in 10 ml RPMI). Tubes were prepared for centrifugation by pipetting 100 µl of Nyosil M-25 oil (TAI Lubricants, Hockessin DE, USA) into 0.5 ml capped tubes. After incubation, 50 µl salt wash was added to each well, mixed, and 80 µl removed and layered on top of the Nyosil oil. The lids were closed and the tubes centrifuged at 10,000 g for 3 minutes. This resulted in the cells collecting at the bottom of the tube with the supernatant remaining on top of the oil. After centrifugation, canine nail clippers were used to cut off the base of the tube containing the cell pellet into LP3 tubes for use in a Canberra Packard Cobra 5010 gamma counter (Canberra Packard).

2.3 – Statistical analyses

Unless otherwise stated, data are presented as the mean ± standard error of the mean (SEM). Data were plotted using Prism v4.03 (GraphPad, CA, USA). Statistical analyses were performed using Microsoft Excel (CA, USA) and Prism. Statistical thresholds of 0.05, 0.01 and 0.001 are denoted as *, ** and ***, respectively for the results of the t-tests.

3 – The biology of CCR4

3.1 – Introduction

CCR4 is a chemokine receptor in the *Rhodopsin* GPCR family (Power et al. 1995; Murphy et al. 2000) notably expressed by T_H2 and T_{reg} cells (Bonecchi et al., 1998; Iellem et al., 2001). CCR4 has also been shown to be expressed on mast cells (Juremalm et al., 2005; Kaur et al., 2005), platelets (Abi-Younes et al., 2001) and monocytes (Katschke et al., 2001). CCR4 has two ligands, CCL17 (TARC) and CCL22 (MDC), which bind the receptor and induce migration of CCR4-expressing cells (Imai et al., 1997, 1998; Andrew et al., 1998).

CCR4 can act as both a homeostatic and inflammatory chemokine receptor. In terms of its homeostatic capacity, the CCR4 ligand CCL22 has been shown to play a role in the migration of thymocytes, haematopoetic progenitor cells, during development in the medulla of the thymus (Chantry et al., 1999; Campbell et al., 1999b). Both CCL17 and CCL22 are produced by dendritic cells, which attract various T cell populations in the lymphoid organs (Tang and Cyster, 1999; Sallusto et al., 1999). As for its inflammatory role, CCR4-directed migration of T_H2 cells has been widely documented in diseases such as asthma and atopic dermatitis (Vijayanand et al., 2010; Saeki and Tamaki, 2006). CCR4 is strongly implicated in cancers such as leukaemia and lymphoma; CCR4-positive cells are involved in the pathogenesis of Hodgkin lymphoma (Ishida et al., 2006) and adult T-cell leukaemia (Yoshie, 2005).

Chemokine receptors, like all GPCRs, depend on various structural motifs in order to function. In various studies, regions of interest were mutated and the resulting effects on receptor trafficking, expression, signalling, function and ligand binding were investigated. In addition to mutational studies, receptor chimeras were created in which specific domains of receptors were swapped, allowing dissection of the function of a particular motif.

As described in section 1.3.2, the N-terminus and extracellular loops of the receptor are responsible for chemokine binding. These regions can be modified by glycosylation and sulphation, which has been shown in many receptors to be required for both receptor trafficking and function (see section 1.3.2.1). Mutations of the N-terminus and extracellular loops of the receptor have been used to identify motifs that are critical for chemokine binding. For example, the amino acid glutamic acid 3 (E3) at the distal end of the CXCR6 N-terminus was shown to be important for receptor

expression; mutation of this to glutamine reduced cell-surface expression of CXCR6 by 25%. The N16A mutation of CXCR6, in which an N-terminal asparagine was mutated to alanine, showed significantly reduced cell-surface expression, chemokine binding and migration compared to WT CXCR6. N16 of CXCR6 was identified as a site of N-linked glycosylation; tunicamycin, an inhibitor of this process, had the same effect on receptor expression, function and binding (Petit et al., 2008).

The chemokine receptor US28 is encoded by human cytomegalovirus (HCMV). It shows strong homology with CCR1 and CCR2 and binds a large number of chemokines, including CCL5, CCL3, CCL4, CCL2, and CX_3CL1 (Kuhn et al., 1995; Kledal et al., 1998), indicating that it may function as a scavenger of chemokines. Truncation of 14 amino acids of the N-terminus of US28 removed the ability of the receptor to bind chemokines. Further investigation by point mutagenesis of specific amino acids to alanine revealed that phenylalanine 14 of US28 is important for interaction with the N-loop of CCL4. In addition, mutation of tyrosine 16 of US28 to alanine resulted in significantly reduced cell-surface expression and chemokine binding, likely due to the removal of sulphation sites (Casarosa et al., 2005). These studies on CXCR6 and US28 show that regions within the N-termini of chemokine receptors are critical for chemokine binding, both due to direct interaction and through the effects of post-translational modifications such as glycosylation and sulphation.

The extracellular loops of chemokine receptors are also involved in chemokine binding, and mutational studies have been performed to examine these regions in detail. These loops contain cysteine residues which are thought to be involved in structural stabilisation of the receptor by forming disulphide bonds; two cysteines, located in the first and second extracellular loops of many chemokines receptors are known to form a disulphide bond (Ji et al., 1998). Substitution of these cysteines for serine removes the ability for bond formation due to the lack of sulphur in serine. Cysteine to serine substitution in CCR6 resulted in significantly reduced receptor expression, and confocal microscopy revealed that the majority of mutant receptors were unable to leave the cytoplasm and reach the cell surface, indicating a defect in intracellular trafficking. Further analysis showed that mutant receptors were insensitive to CCL20-induced migration except at high concentrations, and were less able to bind the chemokine (Ai and Liao, 2002). Mutation of glutamate 254 in the

third extracellular loop of CX_3CR1 to alanine resulted in significantly reduced CX_3CL1 binding, demonstrating the importance of this acidic residue in the chemokine-chemokine receptor interaction. Mutation of aspartic acid 266, also in the third extracellular loop, did not affect chemokine binding but did affect receptor activation; mutant transfectants migrated to 1 nM CX_3CL1 at half the level of WT transfectants despite showing normal cell-surface expression (Chen et al., 2006). These data demonstrate that the extracellular loops of chemokine receptors have important roles in both chemokine binding and receptor activation. This fits with the two-step model of chemokine binding, described in section 1.3.2.2, which states that chemokine first binds the N-terminus of the receptor with high affinity, and then the extracellular loops with lower affinity (Monteclaro and Charo, 1997).

The transmembrane domains of chemokine receptors also serve important functions in chemokine binding, receptor activation and signalling. Chemokines have been shown to interact with the transmembrane bundle; mutations of phenylalanine 85 in helix II and leucine 104 and phenylalanines 109 and 122 in helix III significantly reduced CCL3 binding to CCR5 (Blanpain et al., 2003). The transmembrane domains are important in maintaining receptor tertiary structure, and are thus required for maintaining receptor signalling, since coupling to signalling partners is dependent on receptor conformation. Thus, disruption of stabilising interactions by mutagenesis has revealed several important domains required for receptor activation.

The TXP motif is a highly conserved motif, located in the second transmembrane domain of many chemokine receptors. The amino acid proline, due to its cyclic side chain structure, causes a kink in a helical structure when it is present. Because of this, it was hypothesised that this highly conserved amino acid, along with the conserved threonine upstream, was involved in receptor function and chemokine binding. The mutation of these two amino acids in CCR5 resulted in significantly reduced binding of CCL3 and CCL4 to the receptor, in addition to reduced chemotactic ability. Interestingly, CCL5 binding was not as drastically affected by the mutations, indicating that this mode of receptor activation is dependent on specific chemokine structures (Govaerts et al., 2001). While in CCR5 this motif is involved in chemokine binding, the TXP motif was shown in CCR1 to instead be involved in receptor activation. Leucine 87 of CCR1 lies within the TXP motif, and when this

amino acid was mutated to alanine the chemokine CCL3 was still able to bind the receptor. However, the L87A mutant did not induce chemotaxis, despite the normal binding of the chemokine (de Mendonça et al., 2005). Therefore, the role of this conserved motif varies between different chemokine receptors.

E290 is a highly conserved glutamic acid located near the top of the seventh transmembrane domain of CCR4. Following the Baldwin numbering scheme, this residue is referred to as GluVII:06, since it is the sixth amino acid in the seventh transmembrane in many receptors (Kledal et al., 1998; Nygaard et al., 2009). GluVII:06 acts as a major contact point for chemokines, and its mutation often results in the inability of the receptor to bind its ligand. For example, following mutation of GluVII:06 (E286) of CCR8 to glutamine the cell-surface expression of the receptor was significantly reduced along with its ability to induce chemotaxis to the chemokine CCL1 (Fox et al., 2006). The same mutation of GluVII:06 (E287) in CCR3 gave a similar phenotype (Wise et al., 2007). However, this mutation in CCR5 did not abolish chemotaxis of mutant receptor-transfected cells to CCL3 (de Mendonça et al., 2005). Interestingly, mutation of GluVII:06 (E274) in CXCR6 rendered the receptor unable to bind the soluble form of CXCL16 but still able to bind the membrane-bound from. This suggests that the receptor discriminates between different forms of the chemokine and that only the soluble form required GluVII:06 (Petit et al., 2008).

The intracellular loops of chemokine receptors also play an important role in receptor function. One region in particular is the conserved DRYLAIV motif, located in the second intracellular loop. This motif consists of either a glutamic acid or an aspartic acid, followed by an arginine and then a tyrosine. This motif is highly conserved amongst chemokine receptors, indicating a potential role in function (Murphy et al., 2000; Rovati and Neubig, 2007). Mutation of the DRYLAIV motif in CCR3 resulted in a receptor that was non-functional; both an alanine triple mutation and individual point mutants of this region rendered the receptor unable to induce migration to CCL11 (Auger et al., 2002). As described in section 1.3.1, the intial glutamic acid/aspartic acid of the DRYLAIV motif forms an ‘ionic lock’ with residues in transmembrane helix VI. Ligand binding, inducing conformational changes in receptor structure, disrupts this lock and allows G protein coupling (Rovati and Neubig, 2007). The arginine of this motif, in addition to contributing to the previously described salt bridge, is believed to function as a micro-switch in receptor

activation, forming part of a binding pocket for Gα proteins (Nygaard et al., 2009). Therefore, the mutation of DRYLAIV motif residues disrupts these interactions and hinders receptor activation.

The cytoplasmic end of transmembrane helix VII and the C-terminal helix VIII are also required for receptor function. The conserved NPXXY motif in helix VII functions as another micro-switch, similar to the DRYLAIV motif. The tyrosine of this motif interacts with a phenylalanine in helix VIII when the receptor is in an inactive state, forming pi-stacking interactions. Upon ligand binding the tyrosine rotates outward to interact with helix VI and stabilise its conformational shift. Mutations of this region in rhodopsin reduced levels of receptor activation (Fritze et al., 2003; Nygaard et al., 2009), and mutation of the tyrosine of this region in CCR5 significantly reduced the chemotactic response of transfected cells to CCL5 (Kraft et al., 2001).

Deletion of portions of the C-terminus of the helix VIII region of the viral chemokine receptor ORF74 caused reduced activity of the receptor, while complete C-terminal truncation resulted in an inactive receptor. The ORF74 receptor is constitutively active, and CXCL8 binding was shown to require the receptor to be coupled to $G\alpha_q$ proteins. By removing the C-terminus, coupling could not occur, and CXCL8 binding was ablated. However, CXCL10 retained the ability to bind since it did not require G protein coupling (Verzijl et al., 2006). These data indicate that this region mediates chemokine binding in addition to being involved in receptor activation. While it is well established that N-terminal binding of ligand influences receptor conformation to recruit C-terminal proteins, this finding is interesting as it shows that C-terminal coupling to G protein is required for N-terminal chemokine binding.

This chapter describes experiments in which CCR4 expression and function was assayed on cells expressing CCR4 endogenously, or on L1.2 cells transfected with a plasmid containing the CCR4 gene. Due to the previous research highlighting the importance of key amino acids, mutants of CCR4 were made. Lysine 310, within the conserved C-terminal region helix VIII, was mutated to asparagine. GluVII:06 (E290), a highly conserved amino acid within the seventh transmembrane domain was mutated to alanine, aspartic acid, and glutamine. These mutants were then compared to the WT receptor with respect to chemokine binding and function.

3.2 – Results

3.2.1 – CCR4 cell-surface expression

In order to study the expression and function of CCR4, the *CCR4* gene needed to be transfected into a cell line and the protein subsequently expressed. *CCR4* was previously cloned into the pcDNA3 vector. This was used to transiently transfect the L1.2 cell line.

The pcDNA3 vector contains the sequence for the HA epitope tag upstream of the gene insert. Epitope tags are often used in molecular biology assays to label proteins without adversely affecting tertiary structure or function. While these tags can be placed anywhere within the protein sequence, they are usually placed at either the carboxy or amino terminus of the protein, in order to minimise effects on the target protein. The HA tag was derived from the haemagglutinin epitope of the influenza virus (protein sequence YPYDVPDYA). Tagged proteins can be used as normal in various assays such as flow cytometry, immunohistochemistry and Western blotting.

Antibodies for CCR4 are commercially available, which rely on the presence of epitopes on the receptor which are currently unmapped. In this project, several mutants of CCR4 were generated, and many of the sites of mutation were within the transmembrane helices and extracellular loops of the protein. The mutations could have potentially affected receptor structure, and as such altered or masked the epitopes required for anti-CCR4 antibodies to bind. Therefore, using an antibody against the HA tag allowed for detection of the receptor without the mutation compromising binding of a conformationally sensitive antibody.

The L1.2 cells into which the *CCR4*-containing pcDNA3 vector was transfected have previously been used for similar studies (Meiser et al., 2008; Pease et al., 1998; Wise et al., 2007). These cells serve well as a transfection system; they double in 16 hours, which allows the culture of large numbers in a relatively short amount of time compared to other cell lines; they grow in liquid suspension, which allows for a greater speed of manipulation; they are derived from a leukocyte line, and are therefore a suitable system in which to express chemokine receptors; they are easy to transfect by electroporation, and can be treated with sodium butyrate to increase gene expression and thus functional responses.

The cell-surface expression of transfected WT CCR4 is shown in figure 3-1. This figure shows the result of flow cytometry performed using anti-HA antibodies and an IgG1 isotype control. The isotype stain in figure 3-1 (filled curve) had a median fluorescence of 6.9, indicating a low degree of staining. The HA antibody however showed high receptor staining, as signified by the right-shift of the histogram (solid line). This had a median of 75.6. Subtracting the non-specific value from the HA value gave a median specific fluorescence value of 68.7. From this it can be concluded that L1.2 cells express CCR4 on their surface following transient transfection, and that this can be detected with the HA antibody.

The Hut78 human T-cell line was also assessed by flow cytometry for CCR4 expression. Since Hut78 cells express the receptor endogenously, *CCR4* is contained within genomic DNA rather than the pcDNA3 vector. Therefore the protein does not possess the HA tag used for antibody staining in the transient transfection system. Two CCR4 antibodies, 1G1 and 10E4, were used in place of the HA antibody to detect the receptor on these cells. Figure 3-2 shows the results of antibody staining of Hut78 cells with these antibodies; panel A shows 1G1 staining while panel B shows 10E4 staining. 1G1 staining shows a much lower CCR4 levels compared to 10E4; it had a median specific fluorescence of 6.6 whereas 10E4 had a median specific fluorescence of 175.9.

The phenomenon of differing CCR4 expression with the 1G1 and 10E4 antibodies was also apparent after chemokine-induced receptor internalisation. Following chemokine binding, receptors can undergo endocytosis via caveolae or clathrin-coated pits (see section 1.3.2.2). This removal of the receptor from the cell surface is believed to act as a form of regulation, preventing over-stimulation of the cell (Neel and Richmond, 2005; Borroni et al., 2010). CCL22 has previously been reported to induce CCR4 internalisation, when assayed with the mAb 1G1. CCL17 however induced no CCR4 internalisation (Mariani et al., 2004). To investigate this whether this phenomenon was also apparent after 10E4 staining, Hut78 cells were incubated with 100 nM CCL17 or CCL22 for 30 minutes to induce receptor internalisation. The cells were then washed and stained with either 1G1 or 10E4, and CCR4 cell-surface levels analysed by flow cytometry and compared to untreated cells. The results of this are shown in figure 3-3. 1G1 staining showed a significant reduction in CCR4 cell-surface levels after CCL22 treatment, to 20% of untreated levels. CCL17 treatment showed a trend towards a reduction, however this was not

significant. 10E4 staining however showed a significant reduction in CCR4 cell-surface levels for both CCL17 and CCL22 treatment; levels were 60% and 50% of WT, respectively. 10E4 thus detected significant CCR4 internalisation after both CCL17 and CCL22 treatment, whereas 1G1 only detected significant internalisation on the CCL22-treated cells.

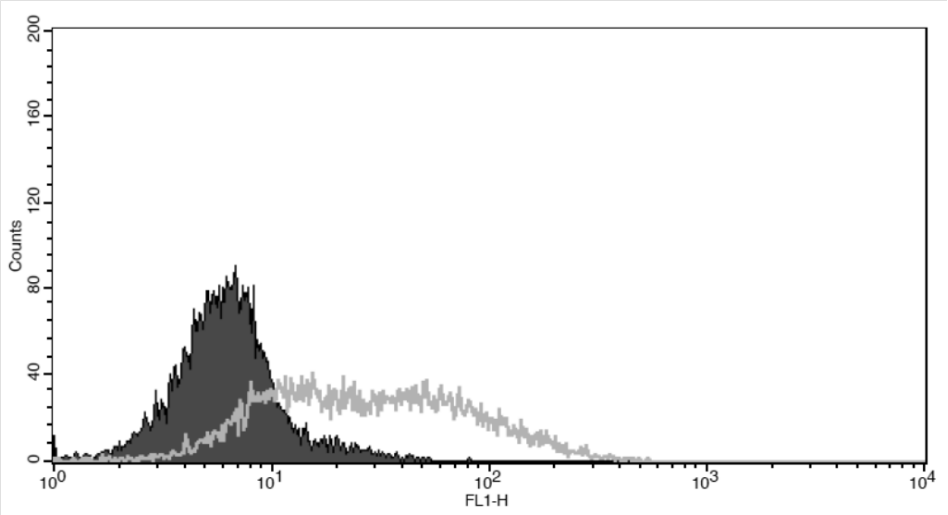

Figure 3-1 – L1.2 cells transfected with HA WT CCR4 DNA express the receptor on their surface

The histogram shows the cell surface expression of WT CCR4. The filled curve shows the isotype control IgG1 stain. Mean fluorescence – 6.9. The solid line shows the HA stain. Mean fluorescence – 75.6. Mean specific fluorescence – 68.7. Data are from a typical experiment and representative of at least three independent experiments.

A

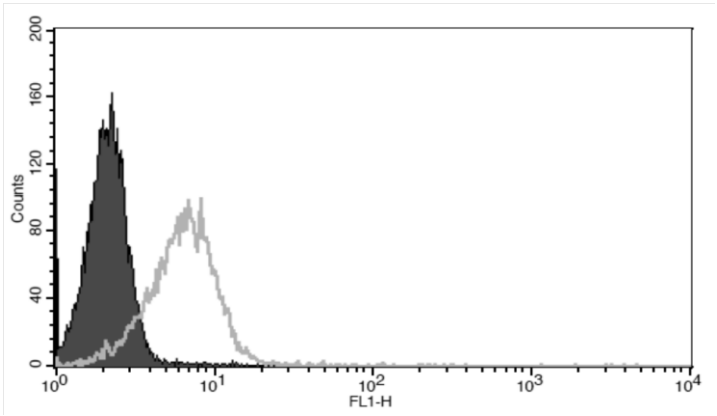

B

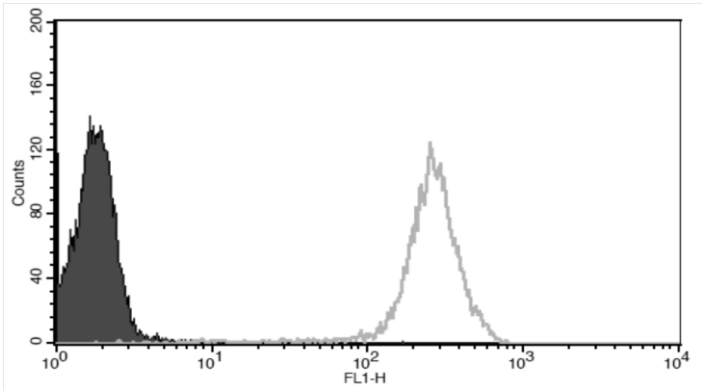

Figure 3-2 – The 10E4 antibody detects a greater level of CCR4 expression than the 1G1 antibody

Cell-surface expression of CCR4 on the Hut78 human T cell line. Panel A shows the isotype IgG1 control stain (filled curve) and anti-CCR4 1G1 stain (solid line). Median specific fluorescence - 6.6. Panel B shows the isotype IgG2a (filled curve) and anti-CCR4 10E4 stains (solid line). Median specific fluorescence – 175.9. A FITC-conjugated secondary antibody was used in both A and B. Data are from a typical experiment and representative of at least three independent experiments.

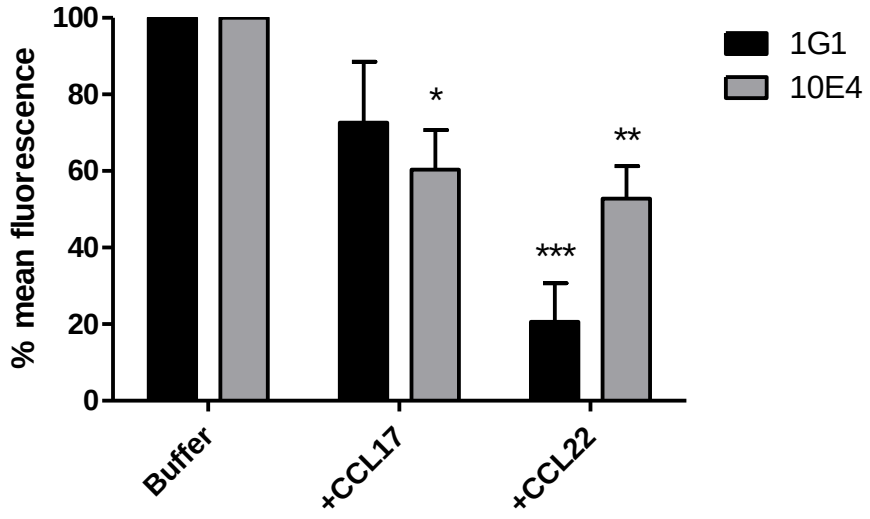

Figure 3-3 – Detection of CCL17-induced internalisation of CCR4 is dependent upon the use of the 10E4 antibody

Hut78 cells were stained with 1G1 (black bars) or 10E4 (grey bars) after treatment with 100 nM CCL17 or CCL22 for 30 minutes, and compared to untreated cells. Data are shown as a percentage of the untreated control, and are the mean ± SEM of three independent experiments, which were analysed by two-way ANOVA. Significance stars *, ** and *** represent p values of 0.05, 0.01, and 0.001 respectively.

3.2.2 – Chemotaxis of CCR4-expressing cells

After confirmation of cell-surface expression, WT CCR4-transfectants were then tested for their ability to undergo chemotaxis to soluble CCL17 and CCL22, the two ligands of the receptor. The chemotaxis assay was used to investigate this. This employed a membrane that was designed to mimic the endothelium; it had pores of 5 μm in diameter through which the cells had to actively transmigrate. This assay was useful for determining the functionality of the transfected receptor, in that it discriminated between cells that were able to migrate and those that were not.

Figure 3-4 shows the results of this chemotaxis assay. Data are expressed as chemotactic index (CI), which is the ratio of the response relative to buffer. The CCR4-expressing cells migrated to both chemokines in the 0.1 nM – 100 nM range, but did not migrate to buffer alone. Maximal migration was observed at 1 nM for CCL17 and CCL22. While both chemokines were of the same potency, CCL22 was the more efficacious of the two ligands, a larger CI was induced at 1 nM than CCL17 (CIs of 60 and 45, respectively). Concentrations higher than 1 nM elicited a reduction in migration, giving the typical bell-shaped curve observed previously in chemotaxis assays (James Pease, personal communication).

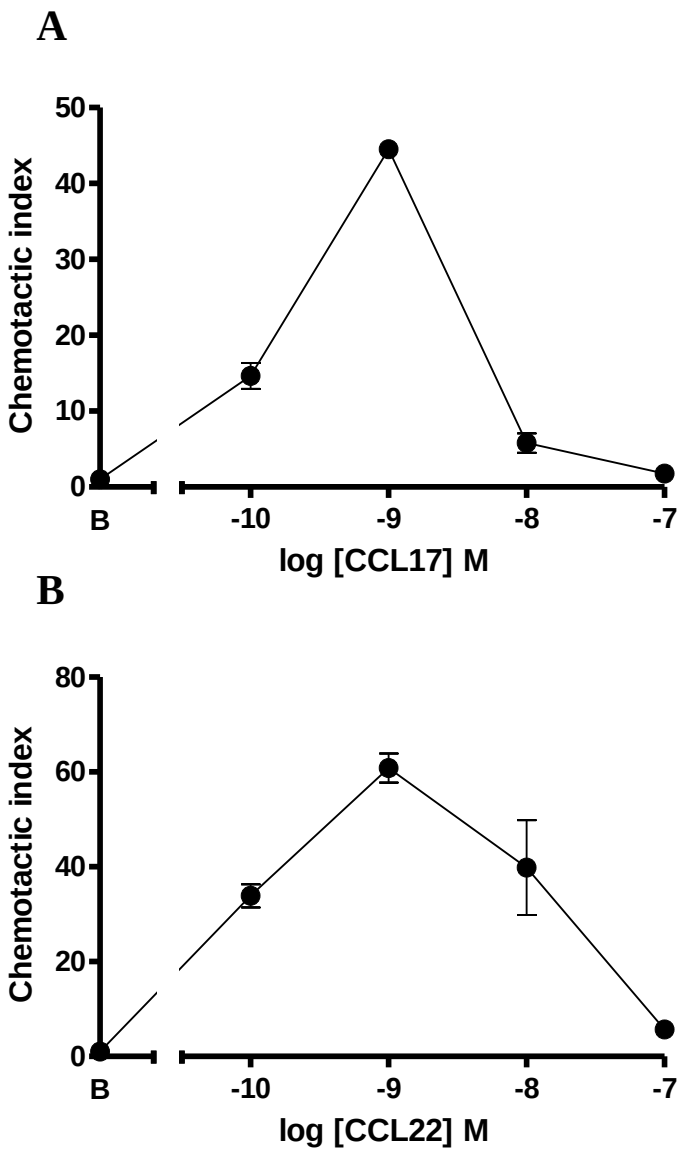

Figure 3-4 – CCL17 and CCL22 have similar potencies and efficacies in chemotaxis assays

WT CCR4 transfectants were tested for their ability to migrate towards buffer (B on the *x*-axes) and increasing concentrations of the two chemokines CCL17 (panel A) and CCL22 (panel B). Data are the means ± SEM of three independent experiments.

3.2.3 – Binding of CCL17 and CCL22 to CCR4

CCR4-transfected cells were assessed for their ability to bind soluble CCL17 and CCL22. Figure 3-5 shows total and non-specific binding of ^{125}I-CCL17 and ^{125}I-CCL22 to WT CCR4 transfectants. A higher number of counts per minute (CPM) was observed for ^{125}I-CCL17 binding when compared to ^{125}I-CCL22; means of 3260 and 1070, respectively. ^{125}I-CCL22 however had a higher level of non-specific binding.

To investigate the affinity of the chemokines for the receptor, saturation assays using increasing concentrations of radiolabelled chemokine would have been performed. These assays determine the K_d, which is the dissociation constant. The K_d indicates the strength of binding between the ligand and its receptor; if a high concentration is required to bind ligand and receptor, it shows that the strength of binding is low, which means that the K_d value is high. If a low concentration is required, it shows a strong binding affinity, giving a low K_d value. Therefore, the smaller the K_d, the stronger the binding affinity of the ligand for the receptor.

Due to practical limitations, assays were performed in which binding of 0.1 nM radiolabelled chemokine was inhibited with increasing concentrations of unlabelled chemokine. The results of this are shown in figure 3-6, in which CCL17 and CCL22 were used to inhibit ^{125}I-CCL17 and ^{125}I-CCL22 binding, respectively. Figure 3-7 shows the inhibition of ^{125}I-CCL17 (A) and ^{125}I-CCL22 (A) binding with both unlabelled CCL17 and CCL22.

The dose-response curves from figures 3-6 and 3-7 were initially used to calculate IC_{50} values, which is the concentration at which binding is inhibited to 50% of maximum. The Cheng-Prussof equation allows the K_i, the equilibrium dissociation constant for the binding of the unlabelled ligand, to be calculated from the IC_{50} (Cheng and Prusoff, 1973):

$$K_i = \frac{IC_{50}}{1 + ([radioligand]/K_d)}$$

Under the assumption that radiolabelled and unlabelled chemokine have the same binding affinity, (Motulsky and Christopoulos, 2004), the K_d and K_i are equal. This therefore converts the equation to:

$$K_d = IC_{50} - [radioligand]$$

However, the assumption that the radiolabelled and unlabelled chemokine had the same affinity was not true in this case. The specific activities of both ^{125}I-CCL17 and ^{125}I-CCL22 were similar – 2200 and 2110 Ci/mmol, respectively. Despite this similarity in specific activities, ^{125}I-CCL17 had higher specific binding that ^{125}I-CCL22 (3000 counts versus 300 counts; figure 3-6). This suggests that ^{125}I-CCL17 has a higher affinity for CCR4 than ^{125}I-CCL22. However, figure 3-7 shows that both CCL17 and CCL22 inhibit ^{125}I-CCL17 and ^{125}I-CCL22 binding with similar potency. This therefore indicates that the affinities of the radiolabelled and unlabelled chemokines are not the same; if they were, similar specific binding values would have been observed for both ^{125}I-CCL17 and ^{125}I-CCL22. Because of this, figures 3-6 and 3-7 cannot be considered as homologous competition assays, meaning that the K_d and B_{max} for each ligand could not be calculated.

A concentration of 0.1 nM radiolabelled chemokine was used in figures 3-5, 3-6 and 3-7. This value is likely well below the K_d concentration of these ligands. This therefore allows for the approximation that the IC_{50} equals K_i. The K_i, the inhibitor constant, is the binding affinity of the inhibitor, which in this case is the unlabelled chemokine. IC_{50} values cannot be compared to one another, whereas K_i values can be compared. K_i values were thus generated for figures 3-6 and 3-7.

Figure 3-6 shows that ^{125}I-CCL17 binding was inhibited by unlabelled CCL17 with a logK_i of -7.89 ± 016 (A), while ^{125}I-CCL22 binding was inhibited by unlabelled CCL22 with a logK_i of -8.18 ± 0.31 (B).

Figure 3-7 shows the inhibition of both ^{125}I-CCL17 and ^{125}I-CCL22 with unlabelled CCL17 and CCL22. This was performed on CEM-4 cells, a human T cell line that endogenously expresses CCR4 (Cronshaw et al., 2004; Viney et al., in preparation). Since the competing ligands were different, this assay could be used to determine whether the two occupy the same binding site on the receptor (Swillens et al., 1995). If both ligands bound the same site, they would have been able to displace each other, leading to a sigmoidal dose-response curve similar to those seen for figure

3-6. If the two ligands occupied different sites, then there would be no dose-dependent competition with the radiolabelled ligand. Figure 3-7A shows that CCL17 and CCL22 inhibit ^{125}I-CCL17 binding with similar potencies; the log K_i values were -8.67 and -8.76 respectively. These values were not significantly different when analysed using a t-test ($p = 0.91$). The two chemokines also inhibited ^{125}I-CCL22 binding with similar potencies; the log K_i values were -8.50 and -8.57, respectively ($p = 0.99$).

Despite this similarity in potency, ^{125}I-CCL22 binding could not be fully inhibited. Panel A shows that CCL17 and CCL22 fully competed with ^{125}I-CCL17; binding was reduced to 6% and 5% of maximum by 100 nM CCL17 and CCL22, respectively. Panel B however shows that CCL17 could not fully compete with ^{125}I-CCL22; while 100nM CCL22 reduced binding to 12.8% of maximum, 100 nM CCL17 reduced binding to only 33.5% of maximum. This difference was statistically significant when analysed using a t-test ($p=0.01$).

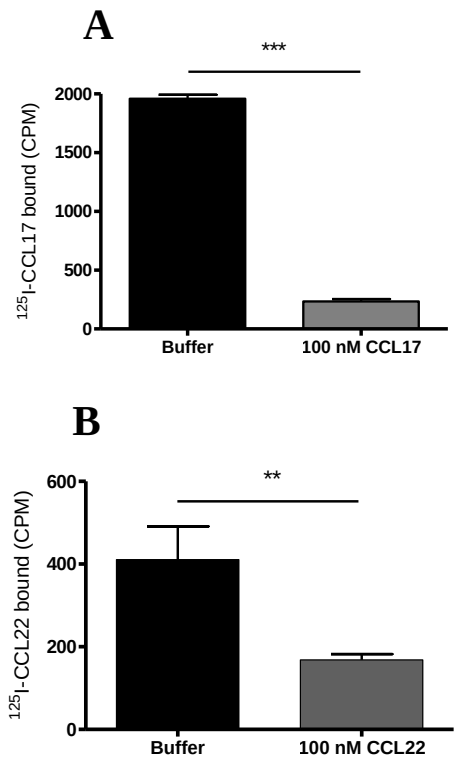

Figure 3-5 – Both CCL17 and CCL22 bind CCR4 transfectants

WT-CCR4 transfectants were tested for their ability to bind ^{125}I-CCL17 (A) or ^{125}I-CCL22 (B) in the presence/absence of unlabelled chemokine. Data are the means ± SEM of three independent experiments, which were analysed by one-way ANOVA.

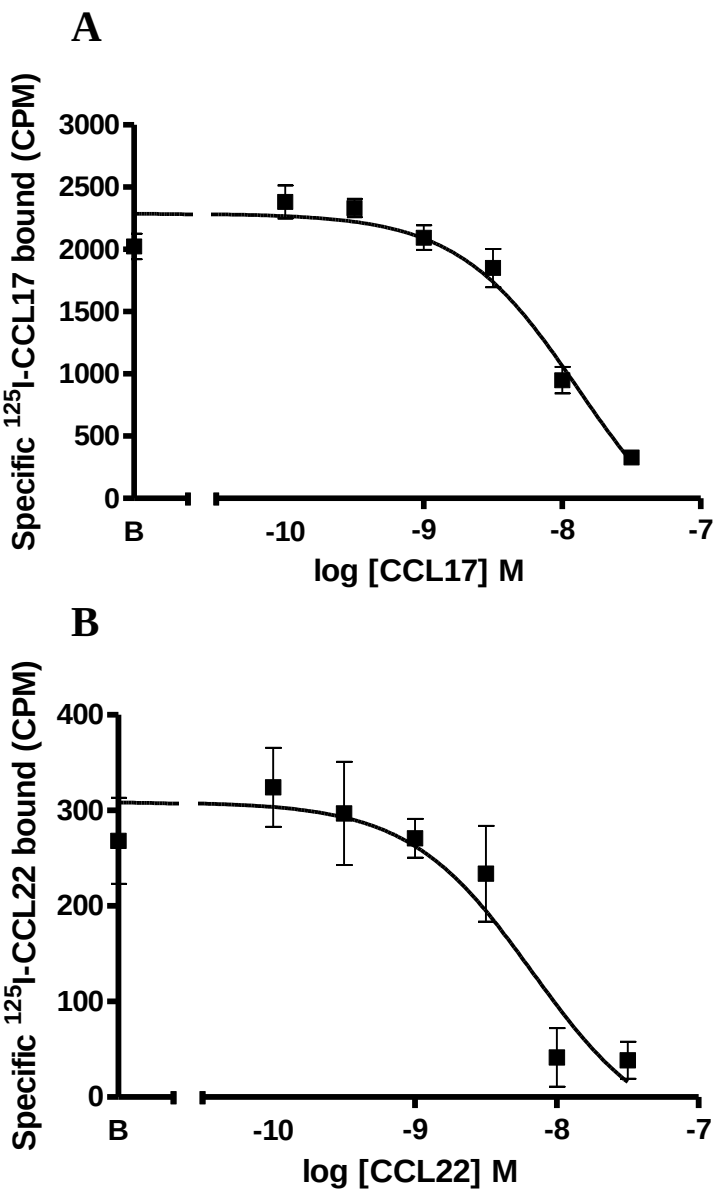

Figure 3-6 – ^{125}I-CCL17 and ^{125}I-CCL22 can be dose-dependently competed with unlabelled chemokine for binding to CCR4 transfectants

Increasing concentration of unlabelled chemokine was competed with radiolabelled chemokine in order to investigate the ability of the chemokines to bind CCR4 on transfected L1.2 cells. Panel A: ^{125}I-CCL17 binding competed with increasing concentrations of CCL17 ($\log K_i$ = -7.89 ± 0.16). Panel B: ^{125}I-CCL22 binding competed with increasing concentrations of CCL22 ($\log K_i$ = -8.18 ± 0.31). Data are the mean ± SEM of three independent experiments.

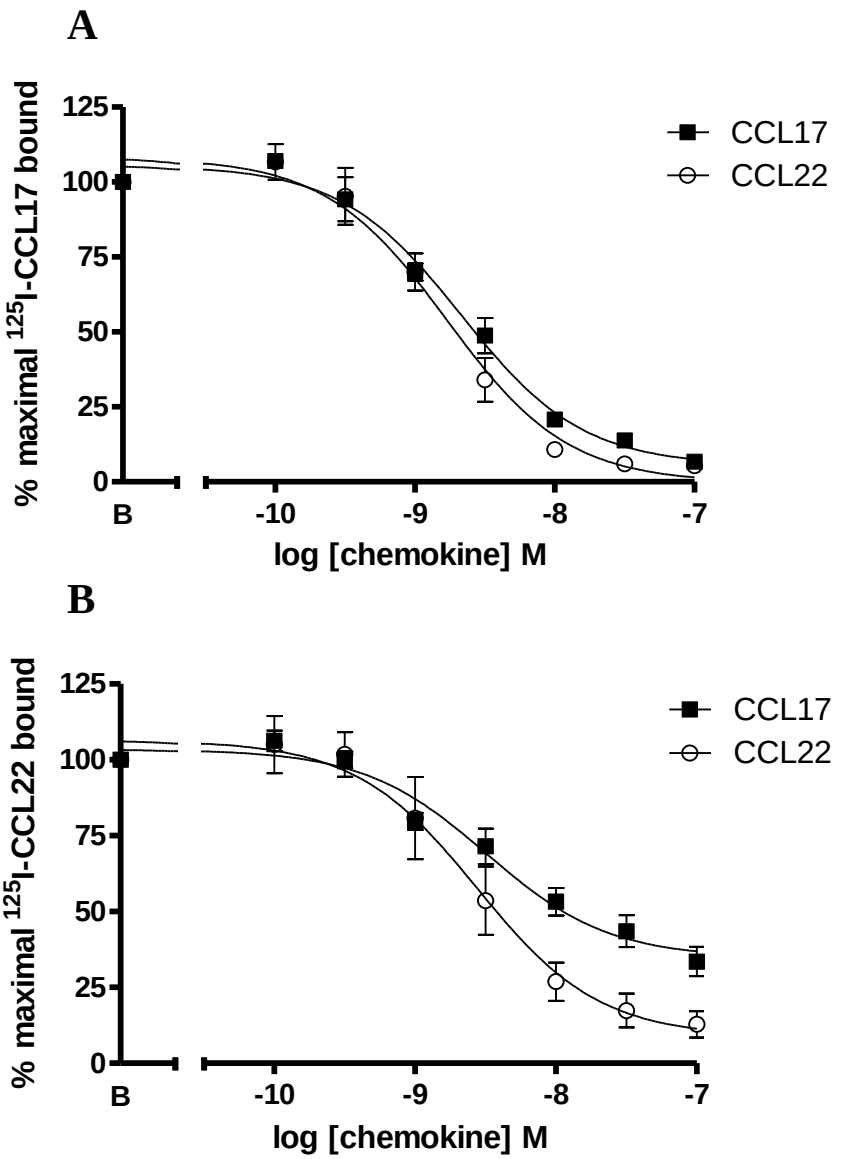

Figure 3-7 – CCL17 is unable to fully displace ^{125}I-CCL22 from CEM-4 cells in homologous competition assays

Homologous and heterologous binding curves on CEM-4 cells. Panel A: ^{125}I-CCL17 was competed with increasing concentrations of CCL17 ($logK_i$ = -8.67 ± 0.07) or CCL22 ($logK_i$ = -8.76 ± 0.09). Panel B: ^{125}I-CCL22 was competed with increasing concentrations of CCL17 ($logK_i$ = -8.50 ± 0.12) or CCL22 ($logK_i$ = -8.57 ± 0.15). Data are mean ± SEM of three independent experiments. From (Viney et al., in preparation).

3.2.4 – Mutation of GluVII:06 (E290) ablates binding and chemotactic ability of CCR4-transfected cells

GluVII:06 of CCR4 (E290) is located in the seventh transmembrane domain. It is conserved among other GPCRs, including chemokine receptors, and has been shown to play an important role in receptor function. Fox et al. (2006) demonstrated that GluVII:06 in CCR8 (E286) was critical for cell-surface expression and receptor function. When mutated to glutamine, expression levels and chemotactic responses were abolished. An analogous mutation in CCR3 produced the same effect (Wise et al., 2007). However, similar mutation of GluVII:06 in CCR1 (E287) did not perturb chemokine binding of functional responses of the receptor (de Mendonça et al., 2005).

GluVII:06 (E290) of CCR4 was mutated to alanine (E290A), aspartic acid (E290D) and glutamine (E290Q). Glutamic acid is a negatively charged amino acid. Glutamine is uncharged, but with a side chain of similar size to glutamic acid. Aspartic acid is similarly charged and has a smaller side chain. Alanine is uncharged and has an even smaller side chain. By mutating glutamic acid to these three amino acids, the contribution of both size and charge of E290 to receptor function could be determined.

Once the three CCR4 mutants had been generated, they were transfected into L1.2 cells. Their cell surface expression was assessed and compared to WT (figure 3-8A). The three mutations affected surface expression to varying degrees. E290A and E290D were expressed at lower levels that WT, E290D significantly so at approximately 50% of WT levels. E290Q was expressed at higher levels than WT. When the mutants were assessed for chemotactic ability, it was found that none of cells expressing the three mutants migrated to either CCL17 or CCL22 (panels B and C); two way ANOVA showed that the chemotaxis responses for all three mutants were significantly reduced compared to WT transfectants. WT transfectants migrated to CCL17 and CCL22 with chemotactic indices of 10 and 30, respectively. However, all three of the E290 mutants did not migrate to either CCL17 or CCL22, since the response did not significantly increase above background levels.

Following this, the cells were assayed for chemokine binding, to investigate whether the lack of chemotaxis was due to the inability of the chemokine to bind to the mutated receptors. As described previously, transfected cells were incubated with

radiolabelled ligand and either buffer or excess unlabelled chemokine to provide a measure of total and non-specific binding. WT transfectants showed significant differences between both CCL17 and CCL22 total and non-specific binding, indicating that chemokine binding occurred. Non-specific binding for ^{125}I-CCL17 and ^{125}I-CCL22 binding was approximately 7% and 40%, respectively. All three E290 mutant transfectants had reduced total binding values approximating the level of non-specific binding, such that there was no significant difference between the two values. This indicated that all three E290 mutants did not bind 0.1 nM of the radiolabelled chemokine; this could be explained by a reduction in affinity for ligands, and also explains the inability of the mutant receptors to induce chemotaxis to the chemokines.

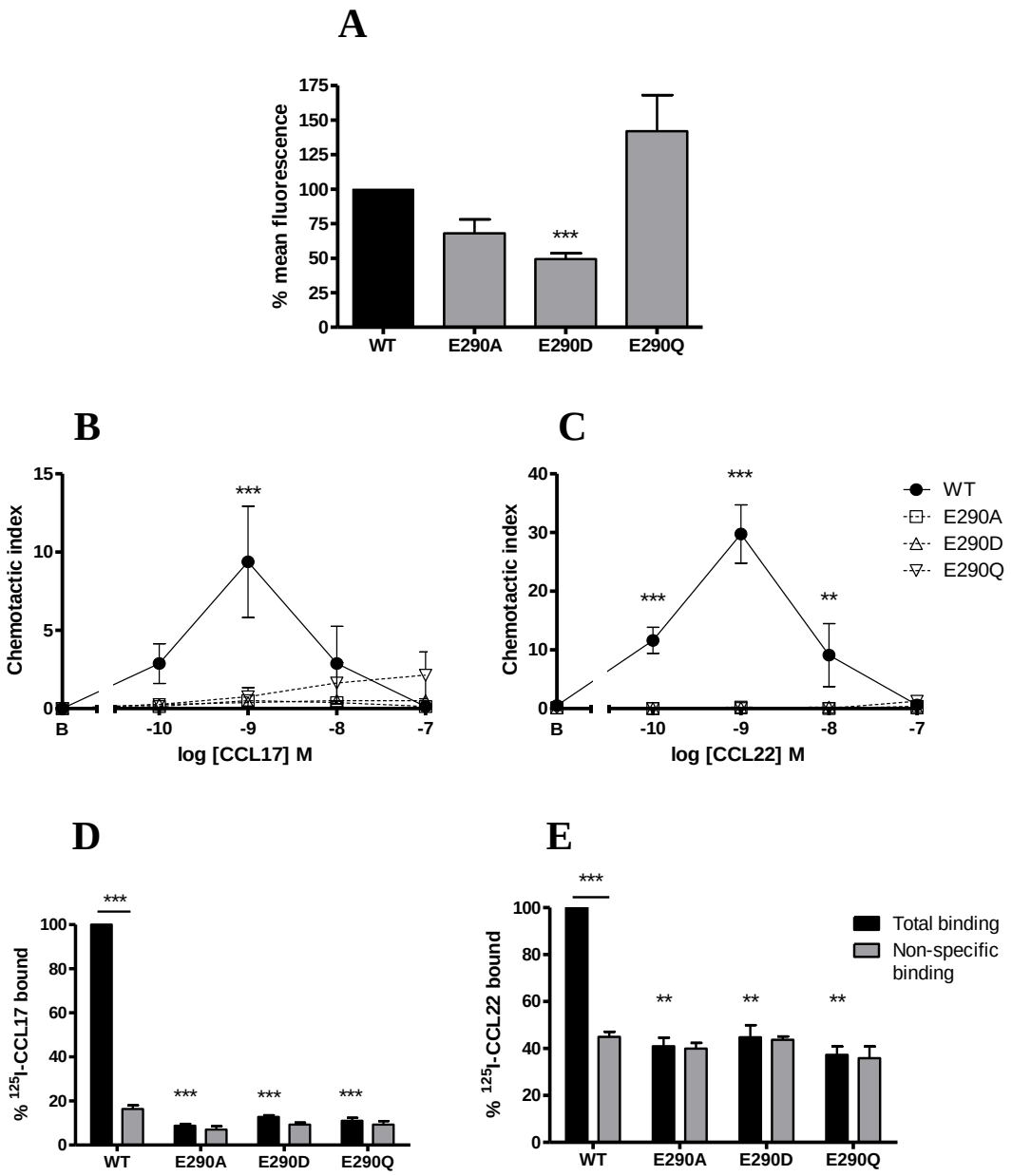

Figure 3-8 – Mutation of GluVII:06 (E290) ablates chemokine binding and functional responses of transfected cells.

CCR4 transfectants were analysed for cell-surface expression (panel A) and then assessed for their chemotactic ability in response to CCL17 (B) and CCL22 (C). Total and nonspecific binding was then assessed with 0.1 nM ^{125}I-CCL17 (D) and ^{125}I-CCL22 (E). Data are mean ± SEM of three independent experiments, which were analysed with a two-tailed t-test or two-way ANOVA. Significance stars *, ** and *** represent p values of 0.05, 0.01, and 0.001 respectively.

3.2.5 – Mutation of K310N does not affect chemokine binding, but ablates chemotactic ability toward CCL17

The amino acid lysine 310 (K310) in the C-terminus of CCR4 was mutated to asparagine (K310N). K310 is located in helix VIII, an important structural motif in the C-terminus that is highly conserved across several GPCRs. Helix VIII has been implicated in receptor signalling, ligand activity and antagonist activity (see section 1.3.2.3). The mutation to asparagine was chosen because lysine and asparagine have different ionisation states at physiological pH (Salchow et al., 2010), but do not differ enough structurally for a mutation to adversely affect helical structure. The fact that the side chain of asparagine is not a proton donor or acceptor under physiological conditions means that any ionic interactions with other amino acids would be disrupted. Therefore the lysine to asparagine mutation allowed study of the ionic interactions involved in receptor activity without causing a breakdown in the structure of helix VIII.

K310N mutation did not significantly affect expression of the receptor; expression levels of the mutant were comparable to WT when assayed by flow cytometry (figure 3-9 A). Panels B and C show the migration of transfectants to CCL17 and CCL22. WT transfectants migrated to increasing concentrations of CCL17 and CCL22, with peak chemotactic indices at 1 nM of 45 and 60, respectively. K310N transfectants did not migrate dose-dependently to CCL17, and the chemotactic index for 1 nM was 4.6, which was not significantly different to migration to buffer alone. K310N transfectants did however migrate dose-dependently to CCL22, albeit with reduced efficacy. The chemotactic index for these transfectants for 1 nM CCL22 was 30, which was significantly lower than the chemotactic index for WT transfectants.

To determine whether the lack of chemotactic response to CCL17 and the reduced chemotactic response to CCL22 was due to a loss of binding, K310N transfectants were incubated with radiolabelled chemokine and an increasing concentration of unlabelled chemokine. Panel D shows WT and K310N transfectant binding to ^{125}I-CCL17, and panel E shows binding to ^{125}I-CCL22. In both cases, WT CCR4 transfectants bound higher levels of radiolabelled chemokine; WT transfectants bound 2250 counts of ^{125}I-CCL17 whereas K310N bound 1500 counts; this difference was statistically significant when analysed using a t-test ($p=0.02$). WT

bound 300 counts of ^{125}I-CCL22, K310N bound 200 counts; this difference was not statistically significant (p=0.1).

In the same manner as figures 3-6 and 3-7, the $\log K_i$ values were calculated for the inhibition of ^{125}I-CCL17 and ^{125}I-CCL22 binding by unlabelled CCL17 and CCL22. CCL17 inhibited binding of ^{125}I-CCL17 to both WT and K310N CCR4 with similar potencies; the $\log K_i$ values were -7.89 and -7.93, respectively. These values were not significantly different, with a p value of 0.62 when analysed using a t-test. The difference between CCL22 inhibition of ^{125}I-CCL22 binding to WT and K310N was also not significantly different (p = 0.73).

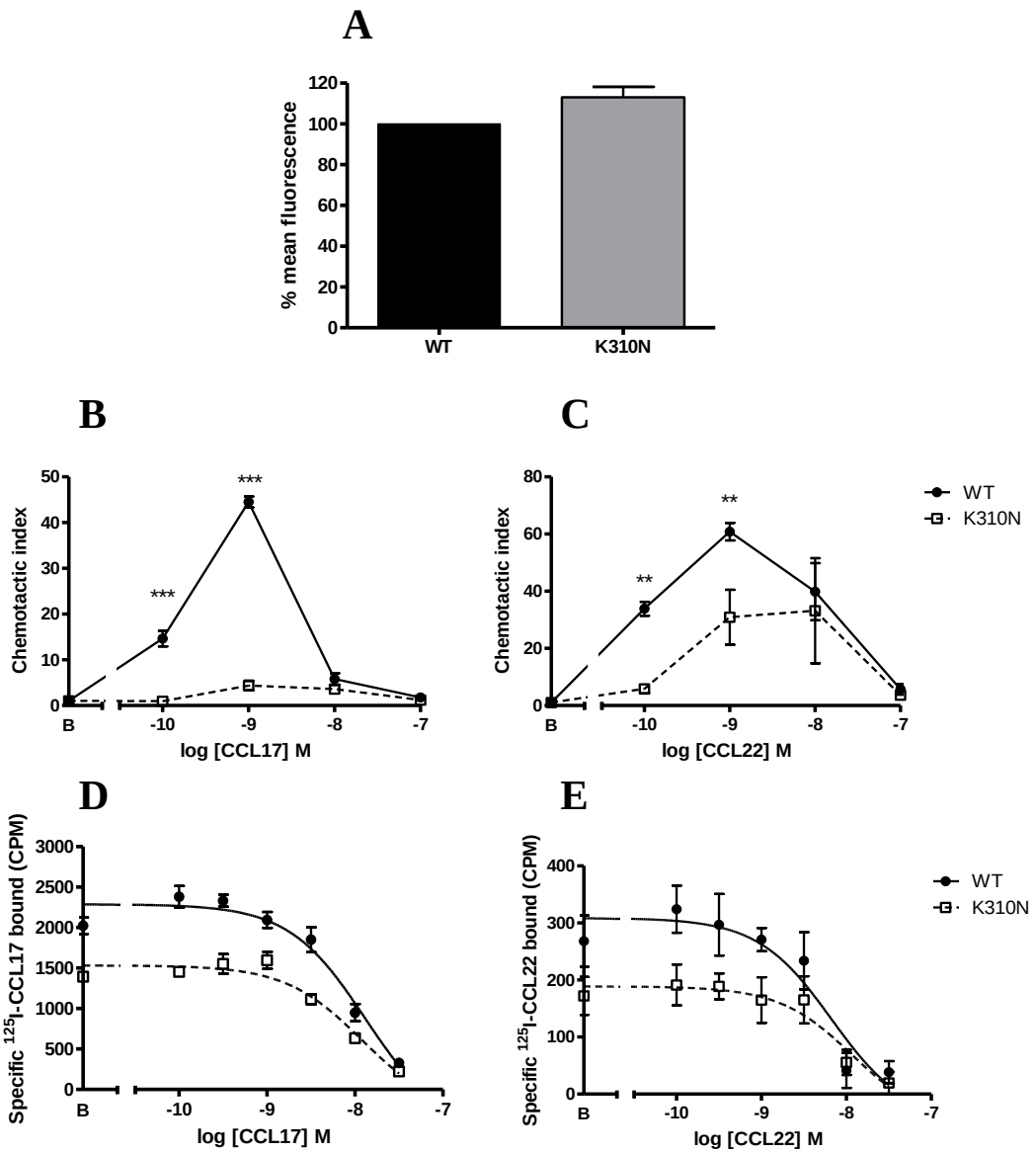

Figure 3-9 – K310N mutation ablates chemotactic response to CCL17 but not CCL22. WT and K310N CCR4 transfectants were analysed for cell-surface expression by flow cytometry (panel A), then assessed for their ability to induce chemotaxis toward the ligands CCL17 (B) and CCL22 (C). Homologous competition curves were generated to compare chemokine binding of WT and K310N. CCL17 (D) – WT: $\log K_i$ = -7.89 ± 0.16. K310N: $\log K_i$ = -7.93 ± 0.17. CCL22 (E) – WT: $\log K_i$ = -8.18 ± 0.31. K310N: $\log K_i$ = -7.93 ± 0.42. Data are the means ± SEM of three independent experiments. Significance stars *, ** and *** represent p values of 0.05, 0.01, and 0.001 respectively.

3.3 – Discussion

3.3.1 – L1.2 and T cell lines express functional CCR4

CCR4, a chemokine receptor normally expressed on T_H2 cells and Treg cells, was transiently transfected into L1.2 cells and successfully expressed on the cell surface (figure 3-1). The L1.2 cells, a pre-B cell lymphoma line, have previously been used in similar studies to investigate other chemokine receptors (Mueller et al., 2008; Pease et al., 1998; Wise et al., 2007). CCR4 has been transfected into 300-19 cells, a human pre-B cell line (Sebastiani et al., 2005), as well as HEK293 cells (Wang et al., 2006).

Compared to previous studies, CCR4 is expressed at reduced levels compared to other receptors; CXCR3 transfected into L1.2 cells and gave a much higher degree of cell-surface expression than seen here with CCR4 (Nedjai et al., 2012). Similar results have been observed for other chemokine receptors, such as CXCR1 and CXCR2, when transfected into the same cells (James Pease, personal communication). The reasons for this disparity between chemokine receptor cell-surface expression levels are unclear; the L1.2 cells may not possess the full repertoire of cellular machinery necessary to express the receptor at a level normally seen on cells that endogenously express it. Hut78 cells, which are a T cell line, express CCR4 at a higher level (figures 3-1 and 3-2). It has been previously demonstrated that different chemokine receptors are expressed at different levels on the same cells; for example, lung CD4+ cells were shown to have higher expression levels of CCR5, CCR6 and CXCR4 compared to CCR4 and CCR7 (Campbell et al., 2001). When a specific CD4+ T cell subtype was examined, T_H2 cells were shown to have relatively low levels of CCR1, CXCR2 and CCR3 compared to CCR4 and CCR5 (Sebastiani et al., 2005). Eosinophils also had varying expression levels of different chemokine receptors; CCR3 being the most highly expressed compared to others such as CCR1, CCR2 and CCR4 (Nagase et al., 2001). The data in this chapter that show L1.2 cells express CCR4 relatively poorly compared to other receptors such as CXCR3 (personal communication) or compared to T cell lines that endogenously express it, may be indicative of general variation in expression levels between receptors.

Sodium butyrate was used to increase cell-surface expression levels; addition of this short-chain fatty acid has been shown to increase transfection efficiency and

resulting protein expression in several cell lines; HeLa cell transcription was increased by a factor of 30 (Gorman and Howard, 1983). The improved efficiency was the result of increased enhancer-dependent transcription through the SV40 promotor present on the transfected plasmid.

In agreement with previous findings, CCR4 was also shown to be endogenously expressed on Hut78 cells, a T cell line (figure 3-2). Whereas L1.2 transfectant CCR4 expression was determined using an antibody specific to the HA tag on the N-terminus of the receptor, detection of CCR4 on Hut78 cells was performed with CCR4-specific antibodies 1G1 and 10E4. 1G1 was commercially available, whereas 10E4 was developed by Millennium Pharmaceuticals (Jopling et al., 2002) and is no longer in production.

The 10E4 epitope was mapped to N-terminus of CCR4 (Jopling et al., 2002), whereas information regarding the epitope of 1G1 was unavailable. However, when considering the difference in CCR4 expression that was observed when staining the same cells with the two antibodies (figures 3-2A and B); it is likely that they bound different epitopes. This difference in CCR4 expression was also observed by Jopling et al. (2002) in the original identification of the 10E4 antibody, and later in CEM-4 and L1.2 cells (Viney et al., in preparation).

The antibody-dependent difference in CCR4 cell-surface expression was also observed after treatment with chemokine. Figure 3-3 shows CCR4 expression on Hut78 cells after CCL17 or CCL22 treatment when assayed with either 1G1 or 10E4. While 10E4 showed a significant reduction in CCR4 levels after treatment with both CCL17 and CCL22, 1G1 only showed a significant reduction after treatment with CCL22. CCL22 has previously been described as ‘dominant’ over CCL17 with respect to CCR4 internalisation (Mariani et al., 2004); CCL22 treatment of T_H2 cells induced a 62.6% level of CCR4 internalisation, whereas CCL17 only induced a 4.5% level of internalisation. However these results were obtained by staining the cells with the 1G1 antibody; figure 3-3 shows that when stained with 10E4 CCL17 can also internalise a significant proportion of CCR4. These results suggest that 10E4 detects a larger population of CCR4 than 1G1, which would account for the increased expression seen here on Hut78 cells in figure 3-2, as well as in the original 10E4 identification report (Jopling et al., 2002). Taken together, it could be surmised that

10E4 is binding a major CCR4 population that is internalised by both CCL17 and CCL22.

Transfected CCR4 was shown to be functional; L1.2 transfectants migrated to soluble CCL17 and CCL22 (figure 3-4). The classic bell-shaped dose-response showed that as concentration of chemokine increased, the number of cells migrating also increased. However this response peaked at 1 nM chemokine, after which cell migration decreased. This type of response generally believed to be due to saturation of chemokine receptors across the cell membrane, leading to a loss of directionality of the cells. Since a cell can sense as little as a 2% difference in concentration between its anterior and posterior ends, an overabundance of chemokine would lead to a loss of response (Devreotes and Zigmond, 1988). Both CCL17 and CCL22 chemotactic responses peaked at 1 nM, indicating that both chemokines were equally potent. The maximal responses however were not identical for the two chemokines. 1 nM CCL17 induced a chemotactic index of 45, whereas 1 nM CCL22 induced a chemotactic index of 61. This shows that CCL22 was a more efficacious ligand, inducing a greater degree of cell migration compared to CCL17. Similar findings have previously been reported in CCR4; in chemotaxis assays, 500 ng/ml CCL22 induced migration of 10,000 L1.2 cells compared to the same concentration of CCL17 inducing migration of L1.2 4000 cells (Mariani et al., 2004). CCL22 was also shown to induce full arrest of rolling cells under shear conditions, whereas CCL17 only induced partial arrest of cells (D'Ambrosio et al., 2002).

Following confirmation of CCL17- and CCL22-induced chemotaxis, the binding properties of these chemokines were investigated. 0.1 nM chemokine labelled with radioactive iodine 125 (^{125}I) was incubated with CCR4 transfectants and either buffer or 100 nM unlabelled chemokine. Figure 3-5 shows the results of this.

To determine receptor affinity (K_d) and density (B_{max}), the ideal assay to perform would have been a saturation binding assay. This would have involved measuring total and non-specific binding at several radiolabelled ligand concentrations. Due to the large volumes of radiolabelled ligand required for saturation binding assays, homologous competition assays can be used as an alternative in order to estimate K_d and B_{max}. These involve using a fixed concentration of radiolabelled ligand and an increasing concentration of unlabelled chemokine. These assays require several assumptions: that there was no

cooperativity; that radiolabelled ligand was not depleted; that non-specific binding was proportional to radiolabelled ligand concentration; and that the unlabelled and radiolabelled ligands had identical affinity for the receptor.

Cooperativity is the phenomenon in which the affinity of a ligand for its receptor changes dependent on ligand concentration (Motulsky and Christopoulos, 2004). Since, there is no published evidence for CCR4 or other chemokine receptors exhibiting cooperative binding, it is assumed that no cooperativity occurred in the binding assays presented here.

Ligand depletion is a phenomenon that occurs when more than 10% of the added radiolabelled ligand binds during the assay incubation. This means that the free concentration of ligand is not equal to the added concentration (Daugherty et al., 2000). Ligand depletion can be tested by measuring the radioactivity emitted from free ligand; in the case of the whole-cell binding assay, after centrifugation the radiation emitted from the free ligand was measured. This was then compared to the counts measured from ligand incubated without cells, in which no binding would have occurred. The two values were identical, indicating that no depletion had occurred in the CCR4 binding assays.

The third assumption, that non-specific binding was proportional to ligand concentration, has been shown to be true in multiple systems (Motulsky and Christopoulos, 2004).

The final assumption - that the ligands had identical affinity - is quite a major one since it assumes that the iodinated chemokine has not been structurally altered. Since the iodination process attached iodine molecules to tyrosine residues within the protein, it would be unlikely if this did not have some degree of an effect on chemokine-receptor interaction. However, the chemokines were iodinated through the use of the enzyme lactoperoxidase, which is considered a more gentle way of achieving iodination than by other methods; as such, protein function is more likely to remain conserved than if another method was used (Bennett and Horuk, 1997).

Despite this, the data in the CCR4 binding assays shown in figures 3-5, 3-6 and 3-7 indicate that the radiolabelled chemokines do not bind CCR4 with the same affinity as unlabelled chemokines, as described in section 3.2.3. The K_d of the ligands could therefore not be determined. The K_i was therefore used to compare the potency of ^{125}I-chemokine inhibition by the unlabelled chemokines. It was shown that both unlabelled ligands inhibited ^{125}I-CCL17 and ^{125}I-CCL22 binding with similar

potencies. This indicates that the two ligands occupied the same binding site on CCR4, as they were both able to displace the radiolabelled chemokines. It was shown however that CCL17 could not fully displace ^{125}I-CCL22, suggesting that a population of receptors may exist that only bind CCL22.

The data also suggest that the addition of radioactive iodine to the chemokines significantly perturbs their structure enough to cause a change in affinity for CCR4. This finding has implications for future assays performed with the radiolabelled chemokines, since it is often assumed that the labelled and unlabelled ligands bind the receptor in the same manner.

3.3.2 – GluVII:06 (E290) within transmembrane domain 7 is critical for CCR4 function

Mutation of the GluVII:06 (E290) at the top of transmembrane domain 7 was carried out due to its conservation in other receptors and the important role it plays in chemokine-induced signalling. In the data shown here, mutation of this residue in CCR4 to alanine, aspartic acid or glutamic acid removed the ability of the receptor to bind either chemokine, and thus prevented chemotaxis (figure 3-8). These results clearly show that the charge and shape of the side group is necessary for chemokine binding and thus receptor function.

Mutations of GluVII:06 in other receptors had similar effects; this residue in CCR2, E291, was shown to be important for chemokine function. When mutated to alanine and glutamine, CCL2 binding was significantly reduced in potency (Mirzadegan et al., 2000). The acidic side chain of GluVII:06 was believed to interact with basic residues in CCL2. Mutation to alanine and glutamine, amino acids with uncharged side chains, would have removed this acid-base interaction, leading to the loss of binding.

However, mutation of GluVII:06 of CCR1 and CCR5 to alanine and glutamine did not perturb chemotaxis of transfectants; the CCR1 and CCR5 mutants were still able to induce chemotaxis to the chemokine CCL3 (Hall et al., 2009; de Mendonça et al., 2005). GluVII:06 of CCR1 was believed to interact with the basic lysine and arginine side chains of CCL3, however the data show that this residue is not essential for chemokine binding (de Mendonça et al., 2005). CCR1 and CCR5 thus seem to differ to other chemokine receptors in that GluVII:06 is not an essential interaction point for chemokines.

Mutation of GluVII:06 (E287) of CCR3 induced a less efficacious chemotactic response to CCL11 than WT CCR3; approximately half the number of cells migrated in a chemotaxis assay (Wise et al., 2007). Receptor modelling implicated GluVII:06 (E287) of CCR3 in the binding of proline 2 (P2) of CCL11; disruption of this interaction may explain the reduced efficacy of the chemokine. However, since some function was retained, it can be concluded that chemokine binding was not fully ablated in the CCR3 mutant, unlike data shown here for CCR4. Again this demonstrates that the same conserved residues have differing roles in different receptors.

When placed in context with other chemokine receptor mutants, it is likely that the CCR4 GluVII:06 mutations presented here have disrupted a network of bonds that are required for receptor conformations that can recognise chemokine, leading to the receptor being unable to bind either ligand. Since the binding assays were carried out with 0.1 nM radiolabelled chemokine, it may be the case that binding is only perturbed at this particular concentration. The mutations may have just removed high-affinity binding of the chemokines, and an increased concentration may reveal some degree of binding occurring due to the retention of low-affinity binding. A two-step binding model has been previously been proposed, and mutation of GluVII:06 may have removed the ability of the chemokine to bind in the second higher affinity stage (Monteclaro and Charo, 1997).

Other point mutants on the extracellular end of transmembrane domains and in the extracellular loops also have been shown to prevent the receptor from binding ligand. In most *Rhodopsin*-type GPCRs, a disulphide bond is formed between two highly conserved cysteines, one located in ECL2 and the other at the top of transmembrane helix III (Palczewski, 2000). This bond provides structural stabilisation of the receptor; in the rat M1 muscarinic receptor, mutation of these cysteines to serines prevented ligand binding (Savareses et al., 1992). Mutation of these to alanine in the M3 receptor as well as the β_2-adrenergic receptor had a similar effect; ligand binding affinity and receptor expression were significantly reduced, suggesting reduced stability of receptor conformation (Zeng et al., 1999; Noda et al., 1994). Two acidic residues within the second extracellular loop of CXCR3, D195 and E196, were postulated to form a salt bridge and provide structural stabilisation of ligand-binding conformations of the receptor. Interestingly, when mutated the receptor had impaired CXCL10 binding but not CXCL11 binding, indicating that certain receptor motifs and thus conformations are chemokine-specific (Nedjai et al., 2012). The studies demonstrate that several key amino acids within the receptor, when mutated, perturb ligand binding.

3.3.3 – CCL17 and CCL22 stabilise distinct conformations of CCR4

Since many chemokine receptors bind more than one ligand, and some chemokines bind to multiple receptors, the chemokine system has often been described as redundant or promiscuous (Lukacs et al., 1999; Power 2003). It was also postulated that this apparent redundancy made the chemokine system robust, in that genetic mutations or other factors reducing one chemotactic signal would result in compensation by another signal (Mantovani, 1999). However, these descriptions were used before some of the complexities of the chemokine network were fully realised. As previously described in section 1.3.2, mixed populations of cells were assayed for chemotactic function and the resulting responses to multiple ligands were interpreted as evidence of redundancy (Schall & Proudfoot, 2011).

Since it can be argued that chemokines and their receptors may not be performing redundant functions, that instead the chemokine network is highly complex, it could also be argued that multiple ligands for the same receptor have distinct roles. Indeed, chemokines that bind the same receptor have been shown to induce different effects. CCL19 and CCL21, the two ligands for CCR7, have similar binding affinities and induce chemotaxis with the same potency (Sullivan et al., 2000; Yoshida et al., 1998; Ott et al., 2004). However only CCL19 induced receptor internalisation, whereas CCL21 treatment had no effect on receptor levels (Bardi et al., 2001). Subsequent research showed that this internalisation is coupled with receptor desensitisation. Receptor desensitisation involves the phosphorylation of the C-terminus of the GPCR by GPCR kinases (GRKs), leading the recruitment of arrestins, which then allow attenuation of GPCR signalling by way of G protein decoupling and recruitment of other binding partners. CCR7 was shown to be desensitised by CCL19 but not CCL21; CCR7-expressing membranes showed a reduced ability to signal through G proteins after treatment with CCL19, whereas CCL21 signalling was unaffected. A greater level of receptor phosphorylation was shown to occur after CCL19 treatment when compared to CCL21 treatment, indicating that the two ligands induce different effects upon the receptor (Kohout et al., 2004). Subsequent research showed that arrestin 3 co-localised with CCR7 following CCL19-induced internalisation, whereas arrestin 3 was not associated with CCL21 (Byers et al., 2008). Since the two ligands are differentially expressed, CCL19 within the high endothelial venules and CCL21 within the T-cell zones

(Campbell and Butcher, 2000), their differing effects upon the receptor likely reflect distinct biological roles.

Another chemokine receptor, CCR5, was also shown to be differentially phosphorylated and internalised by its ligands; CCL5 induced a greater degree of receptor phosphorylation and internalisation than CCL3, which itself was more effective at doing so than CCL4. As with CCR7, this receptor phosphorylation was carried out by GRKs acting on C-terminal serine residues (Oppermann et al., 1999).

These data on chemokine receptors show that the activity of different ligands through the same receptor is not redundant; each induce different effects on the receptor which likely have *in vivo* significance. Therefore, considering these findings in context with the data presented here on CCR4 may suggest that it too is differentially activated by its ligands.

It has been reported that CCL22 induces a greater degree of receptor activation and desensitisation than CCL17; in both T_H2 cells and CCR4-transfected L1.2 cells CCL22 induced a greater degree of calcium mobilisation than CCL17. In addition to this, CCL22 treatment of cells desensitised the calcium response to subsequent CCL17 treatment, whereas treatment of CCL17 followed by CCL22 did not produce the same magnitude of receptor desensitisation (Ambrosio et al., 2002; James Pease, personal communication). This may indicate that the different binding potencies and chemotactic efficacies of CCL22 and CCL17 demonstrated here are not solely due to receptor-chemokine interactions; downstream G protein signalling is likely differentially activated by the two chemokines, which may explain the larger efficacy of CCL22-induced chemotaxis seen in figure 3-4.

Figure 3-7 shows heterologous competition assays of CCR4-expressing CEM-4 cells. While CCL17 and CCL22 could fully compete with ^{125}I-CCL17, only CCL22 could fully compete with ^{125}I-CCL22, suggesting that a population of receptors exists that is unable to bind CCL17. These data are reminiscent of those previously reported regarding CXCR3 and its ligands, CXCL9, CXCL10 and CXCL11. These three chemokines exhibited different potencies when competed with the radiolabelled chemokines. CXCL10 and CXCL11 could displace ^{125}I-CXCL10 with equal potency; however CXCL9 did so with a lower potency. CXCL11 could fully displace ^{125}I-CXCL11, but CXCL9 and CXCL10 could not; as well as showing lower potency, these chemokines did not fully displace the ^{125}I-CXCL11 even at micromolar

concentrations (Nedjai et al., 2012; Cox et al., 2001; Xanthou et al., 2003). It was also shown that CXCL11 bound to uncoupled CXCR3, unlike CXCL9 and CXCL10. It was concluded that CXCL11 bound to a different, allotopic, site on the receptor and thus was not binding in a classical competitive manner (Cox et al., 2001).

Since the allotopic binding of CXCR3 ligands is dictated by coupling to G proteins (Cox et al., 2001), the same was hypothesised to be true of CCR4 and its differential ligand binding. When treated with *Pertussis* toxin to uncouple the receptor from G proteins, the same phenomenon was observed; despite a reduction in ^{125}I-chemokine binding, there existed a population of receptors that still bound ^{125}I-CCL22 despite being uncoupled and incubated with excess CCL17 (James Pease, personal communication). Therefore it can be concluded that the results shown in figure 3-7 regarding the differential binding of CCL17 and CCL22 signify that the ligands bind different receptor states; CCL22 may be able to bind both coupled and uncoupled receptors while CCL17 only binds coupled receptors.

Figure 3-9 shows the effect of the K310N mutation on CCR4 expression, chemotaxis, and binding. Since the lysine to asparagine mutation did not affect receptor expression when compared to WT CCR4 (figure 3-9A), it can be surmised that any ionic interactions dependent on the lysine side group were not essential for receptor expression. The mutation did however affect the functionality of the receptor; the chemotactic response to CCL17 was ablated (figure 3-9B). Despite the lack of response to CCL17, responses to CCL22 were intact (figure 3-9C). While efficacy to this ligand was significantly reduced by the mutation, a large response was still observed.

Our initial conclusion regarding these data was that the mutation had disrupted chemokine binding, leading to the loss of chemotaxis to CCL17 and the reduced response to CCL22. However it was shown that the K310N mutants retained the ability to bind chemokine. CCL17 and CCL22 showed similar $\log K_i$ values in binding assays, indicating that the mutation had not affected chemokine binding affinity, although this would need to be confirmed by performing saturation binding assays.

This result was interesting for several reasons. The first reason is that such a mutation does not normally lead to a receptor capable of responding to one ligand and not the other; data presented in chapters 4 and 5 show that most point mutations either render the receptor completely non-functional or have no affect on chemotaxis. Many

receptor point mutants of CCR4 did not induce chemotaxis to ligand, and after investigation it was determined that was due to a lack of binding (see chapters 4 and 5). For example, the GluVII:06 (E290) mutants shown in figure 3-8 were unable to bind chemokine, rendering them non-functional. This phenomenon is discussed in section 3.3.2.

The K310N mutant however retained the ability to bind both chemokines but did not induce chemotaxis to CCL17. Therefore, signalling in response to CCL17 binding had been disrupted by the mutation. The fact that the $\log K_i$ values were not affected by the mutation despite a reduction in total ^{125}I-chemokine binding suggests that K310 is involved in receptor activation.

Receptor mutations have previously been reported to prevent ligand-induced signalling while not affecting ligand binding. As described in section 1.3.1, the highly conserved DRYLAIV motif located at the end of transmembrane helix II of most GPCRs plays a critical role in receptor signalling and is believed to form an 'ionic lock' (Rovati and Neubig, 2007; Palczewski, 2000). When this region is mutated, receptor signalling can be drastically affected. For example, mutation of this region in somatostatin receptor 5, a hormone-responsive GPCR, led to markedly reduced calcium signalling and cAMP production (Peverelli et al., 2009). Mutation of the arginine in this region to asparagine in CCR5 did not affect CCL4 binding - the affinity of the chemokine for the mutant was unaltered compared to the WT receptor - but signalling was lost, indicated by the lack of G protein coupling and chemotaxis (Lagane et al., 2005).

These findings indicate that the interaction between the DRYLAIV motif and transmembrane helix VI is an important and conserved one that plays a major role in receptor activation. Since these mutations can affect receptor function, it is not unimaginable that a mutation such as K310N in CCR4 could also do the same. Since the DRYLAIV mutations disrupted ionic interactions between helices and prevented G protein coupling, the mutation of K310 within the highly conserved helix VIII region could feasibly disrupt recruitment of other signalling partners.

The C-termini of other GPCRs, including chemokine receptors, have been implicated in receptor function. The conserved helix VIII region in particular has been shown to have an important role. A truncation mutant of CCR7, in which the C-terminus was removed, removed the ability of the receptor to activate G proteins and

thus induce chemotaxis, implying that a G protein activation motif lies within this region. Further analysis narrowed down this region to an 11 amino acid motif at the proximal end of the C-terminus, directly after the seventh transmembrane domain (Otero et al., 2008), which is the location of the putative helix VIII (see section 1.3.2.3). Similar truncations of these regions in CCR3, CCR5 and CXCR3 gave similar results, including poor cell migration and calcium mobilisation (Sabroe et al., 2005; Kraft et al., 2001; Dagan-Berger, 2006; Colvin et al., 2006). Non-chemokine receptor GPCRs also rely on signalling through helix VIII; for example, mutations of residues within the eighth helix of the thrombin receptor PAR1 disrupted ionic interactions with residues in transmembrane helix VII and intracellular loop 1, and prevented signalling through $G\alpha_q$ proteins (Swift et al., 2006).

Analysis of the crystal structure of squid rhodopsin adds weight to the hypothesis of helix VIII signalling via G proteins, and in particular implicates the homolog of K310 in CCR4. Several residues of squid rhodopsin, including D132 and R133 of the DRYLAIV motif as well as K321 of helix VIII, interacted with the amphiphilic compound octylglucoside; a detergent used in the preparation of protein crystals. This binding was believed to mimic $G\alpha_q$ binding and provide stabilization of the cytoplasmic domain of the receptor, thus facilitating signalling (Murakami and Kouyama, 2008). These studies suggest that K310 of CCR4 may also be involved in G protein signalling. However the results presented here, that mutation of an eighth helix residue leads to differential ligand activity, are novel. No references to single mutations having this effect on GPCR function could be found in the literature; however these data may support the notion of biased agonism.

Biased agonism is the term given to the observation that different ligands for a receptor do not activate the same repertoire of downstream signalling partners. Rather, each agonist stabilises distinct receptor conformations that in turn activate pathways specific to that ligand (Kenakin, 2009). The β_2-adrengergic receptor, like other GPCRs, is conformationally flexible when not bound to an agonist. The model proposes that the catechol ring of norepinephrine first stabilises interactions between transmembrane helices V and VI. This allows an amine nitrogen to interact with an aspartic acid in helix III, which then allows the receptor to bind the β-hydroxyl group of norepinephrine (Swaminath et al., 2004).

As described previously, GPCRs couple to G proteins in order to signal, as well as binding arrestins and other proteins. It has been demonstrated that different

receptor agonists induce different levels of G protein and arrestin recruitment; some agonists show a G protein or arrestin bias. The β_2-adrenergic receptor shows identical activation of G proteins and recruitment of arrestins when bound to most ligands, however three ligands in particular induced a biased phenotype; isoetharine, CPB (N-cyclopentylbutanephrine) and ethyl-norepinephrine induced a greater degree of arrestin recruitment relative to G protein activation (Drake et al., 2008). Also, as previously described, CCL19 and CCL21 both induce G protein signalling through CCR7 while only CCL19 induces receptor phosphorylation and arrestin recruitment (Kohout et al., 2004).

When the data shown here regarding CCR4 are placed in context with the research described above regarding biased agonism and ligands inducing unique receptor conformations, we hypothesise that CCR4 is stabilised into two distinct conformations by the chemokines CCL17 and CCL22. Figure 3-10 shows this model. We propose that there are two distinct CCR4 populations. The major species (R1) signals in response to both CCL17 and CCL22 while the minor species (R2) signals only in response to CCL22. This model accounts for the data shown in this chapter and those in unpublished data (Viney et al., in preparation); a second population of receptors able to respond to CCL22 alone would explain why CCL17 treatment cannot desensitise the receptor against subsequent CCL22 treatment. Also, the inability of the CCL17 to fully compete with CCL22 for binding (figure 3-7) would again by explained by this model. Since this incomplete displacement left 20% of ^{125}I-CCL22 bound, we propose that R2 compromises the same proportion of total receptor numbers. 10E4 detected a larger level of CCR4 than 1G1 (figure 3-2), and was able to detect CCL17-induced internalisation (figure 3-3), again implying that it can recognise different receptor conformations. Since K310 mutation removed chemotactic responsiveness of the receptor to CCL17 but not CCL22, while still maintaining binding, we propose that this residue is required for functionality of R1; when mutated R2 is still able to respond to CCL22 and induce chemotaxis.

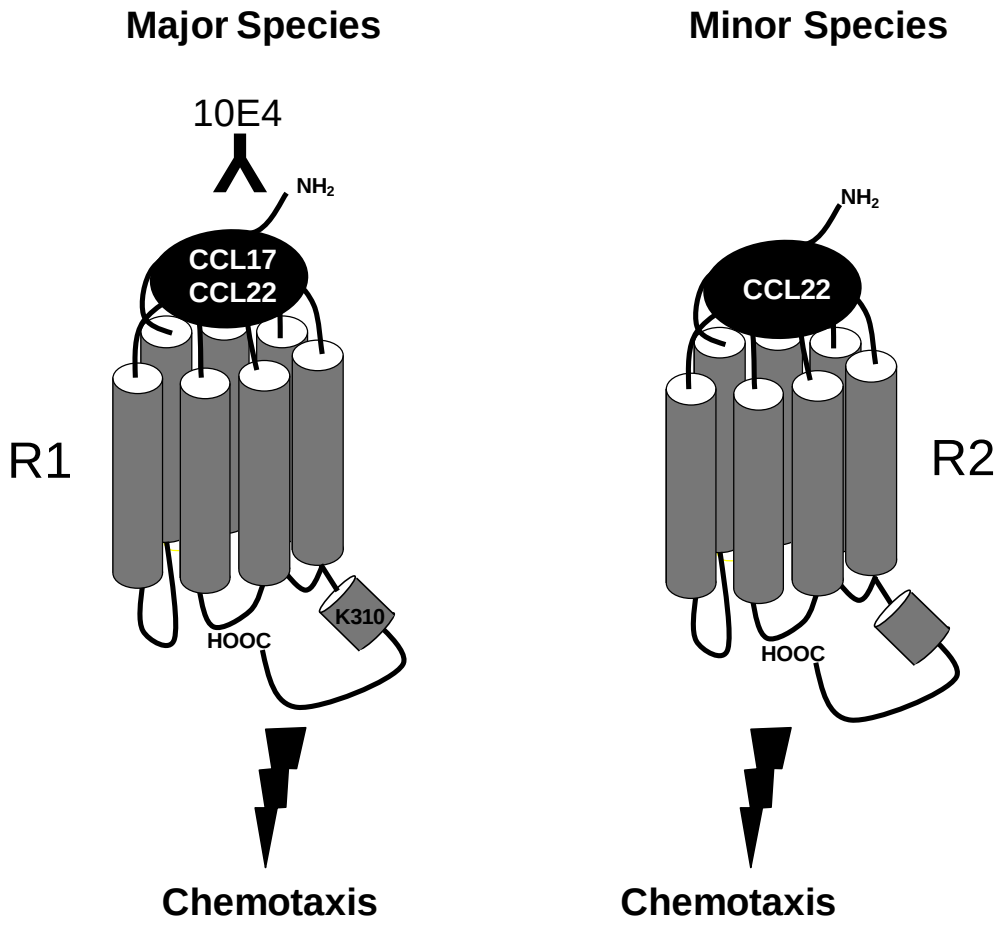

Figure 3-10 – Two-population model of CCR4

Two species of CCR4 are proposed to exist; one that responds to CCL17 and CCL22 (R1; left) and another that only responds to CCL22 (R2; right). R1 is the major species, comprising 80% of receptors. It is detected by the 10E4 antibody and its function is mediated by K310 in the C-terminus. R2 comprises 20% of receptors, is not detected by 10E4, and does not require K310 for function.

3.3.4 – Summary

In summary, L1.2 cells serve as a platform for functional CCR4 expression. The 10E4 and 1G1 antibodies were shown to detect different levels of cell-surface CCR4 on Hut78 cells, and different levels of chemokine-induced internalisation. The C-terminal K310N mutation of CCR4 ablated chemotactic responses to CCL17 but not CCL22. These data, along with unpublished data (Viney et al., in preparation), suggest that CCL17 and CCL22 stabilise distinct conformations of CCR4. In addition, the conserved residue GluVII:06 (E290) located with transmembrane domain 7 was shown to be critical for chemokine binding and thus receptor function.

4 – Investigation of intrahelical CCR4 antagonists by receptor point mutation

4.1 – Introduction

In the preceding chapter, CCR4 was shown to be expressed on the surface of L1.2 cells after transient transfection. CCR4 was shown to bind both CCL17 and CCL22, and induce migration toward these chemokines. The K310N, E290A, E290D and E290Q point mutants were investigated for their effects on receptor function. In this chapter, the activities of several CCR4 antagonists will be discussed in relation to other point mutants of CCR4.

Since GPCRs comprise such a large family of cell-surface receptors and bind a huge array of ligands, they unsurprisingly are involved in the pathogenesis of many diseases, and as such are important targets for therapeutic intervention. Current GPCR antagonists in therapeutic use include beta blockers, which antagonise β-adrenergic receptors. Upon stimulation these receptors can cause increases in heart rate and blood pressure. As such, beta blockers are used to antagonise these receptors to treat conditions such as angina or high blood pressure (Frishman, 2003). As described in section 1.1, histamine release by mast cells and basophils leads to the swelling and redness associated with an allergic reaction. A common treatment for this reaction is through the use of histamine H_1 receptor inverse agonists; these reduce the functional output of the receptor and thus limit histamine-associated effects such as swelling (Leurs et al., 2002).

Agonists or antagonists for GPCRs thus have the potential to ameliorate disease states by counteracting the signalling pathways associated with them. For example, in diseases such as asthma and atopic dermatitis, CCR4-expressing T_H2 cells contribute to pathology by secreting the cytokines IL-4, IL-5 and IL-13, which lead to eosinophil recruitment and antibody production. By developing antagonists against CCR4 it is hoped that symptoms associated with $CCR4^+$ cells could be reduced (see section 1.4.3). As previously described, antagonists can be classified as either orthosteric or allosteric. Orthosteric antagonists bind to the endogenous agonist binding site on the receptor, and therefore compete with the receptor ligand. Allosteric antagonists however bind to a site distinct from the agonist, preventing receptor activation without competing with the ligand (see section 1.4.4).

Seven allosteric CCR4 antagonists have been supplied by GlaxoSmithKline (GSK). Four of these antagonists - denoted antagonists 1, 3, 4, and 7 - are hypothesised to bind to a site within the transmembrane bundle of the receptor known

as site 1. The remaining three antagonists are hypothesised to bind to an intracellular site, known as site 2, which will be discussed in chapter 5. The binding of antagonists to the transmembrane bundle, referred to as intrahelical or ‘classical’ binding, is the principal mechanism by which receptor antagonists were believed to act and inhibit receptor function. The adenosine, dopamine, neurokinin, opiod and serotonin receptors are all examples of GPCRs that have had allosteric modulators for them identified or developed (reviewed in Conn et al., 2009). Several allosteric antagonists for chemokine receptors have also been identified that also bind this site, for targets including CCR1, CCR3 and CCR5 (de Mendonça et al., 2005; Wise et al., 2007; Vaidehi et al., 2006; Dorr et al., 2005; Dragic et al., 2000).

The four intrahelical antagonists described here are lipophilic amines. The structures of the antagonists are shown in figure 4-1. The compounds all contain several simple aromatic rings. Antagonist 3 is a derivative of antagonist 4, while antagonists 1 and 7 are of different structural classes.

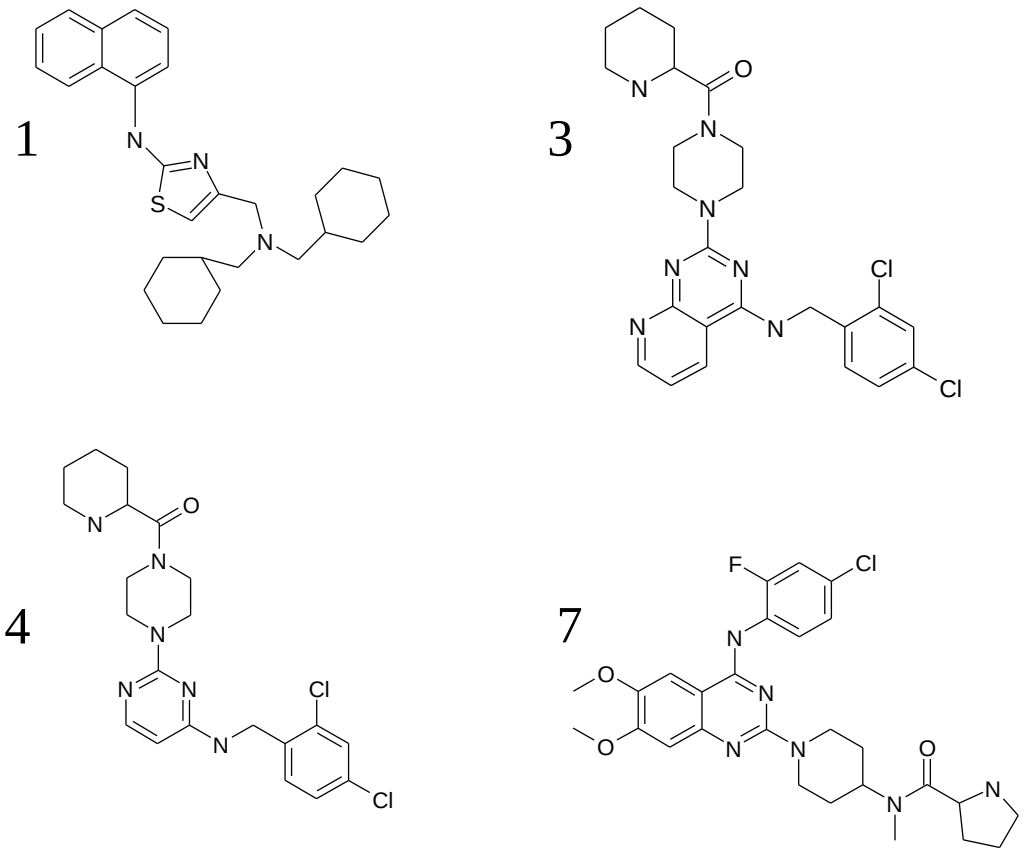

Figure 4-1 – Site 1 antagonists

The structures of the four site 1 (intrahelical) allosteric antagonists are shown. These were supplied by GlaxoSmithKline (GSK), and were hypothesised to bind within the transmembrane bundle of CCR4.

Molecular modelling performed by scientists at GlaxoSmithKline identified several amino acids of CCR4 potentially involved in antagonist binding. Figure 4-2A shows a cartoon of CCR4, with its extracellular N-terminus and three extracellular loops (ECL), seven transmembrane (TM) domains, and intracellular C-terminus and three intracellular loops (ICL). Seventeen amino acids were predicted to be points of contact for the site 1 antagonists; these are highlighted in green. Eight of these were located within transmembrane helix III, indicating its potential importance in antagonist activity. Four were located in the second extracellular loop, while the rest were in transmembrane domains 2, 4, 5 and 7. Panel B of this figure shows a molecular model of the predicted interaction of the site 1 compounds with the transmembrane domains of CCR4.

The seventeen highlighted amino acids were comprised of seven different types; leucine, isoleucine, serine, tyrosine, phenylalanine, lysine and glutamic acid. Lysine is positively charged and glutamic acid negatively charged, due to their respective amino and carboxyl side groups. Serine and tyrosine are weakly polar, due to the presence of electronegative groups causing an uneven distribution of electrons in their side chains. Leucine, isoleucine and phenylalanine are strongly hydrophobic due to their non-polar side chains, explaining their positions in or near the transmembrane domains of the receptor.

A

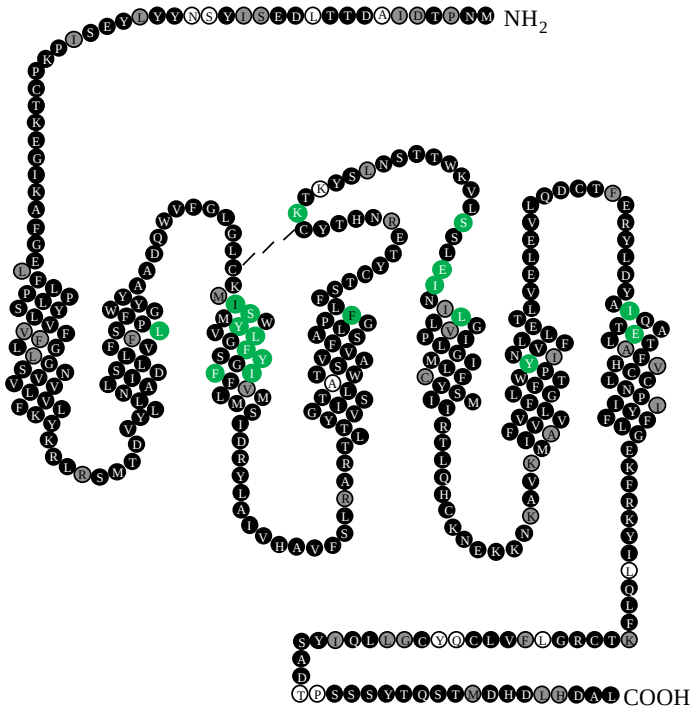

B

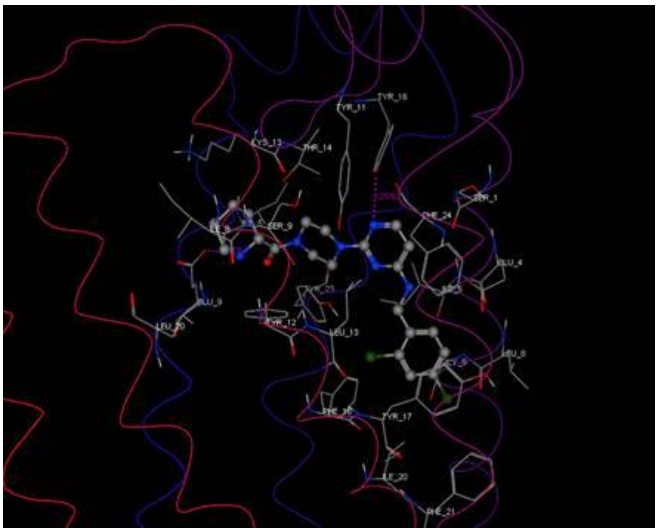

Figure 4-2 – Model of site 1 antagonist binding

(A) A cartoon of CCR4 showing the extracellular N-terminus and 3 extracellular loops, seven transmembrane domains, and the intracellular C-terminus and 3 intracellular loops. Highlighted in green are the seventeen predicted contact points of site 1 antagonists, located in transmembrane domains 2, 3, 4, 5 and 7, as well as extracellular loop 2. (B) Molecular modelling performed by GSK, showing the predicted interactions of the site 1 compounds with the transmembrane domains of CCR4. From Nick Barton (personal communication).

To investigate the contribution of these amino acids to antagonist binding and thus antagonist activity, point mutants of these residues were made. The rationale behind this method was that by mutating the particular side chain of an amino acid of interest, the properties that lent it to antagonist binding were removed. For example, tyrosine 117 (Y117) within the 3rd transmembrane domain was predicted to be a point of contact for the site 1 antagonists. The structure of tyrosine is shown in figure 4-3A; it contains a phenol group, which is fairly bulky compared to other amino acid side chains. In order to determine the contribution of this tyrosine to antagonist binding, it was mutated to alanine (Y117A). Functional studies were then performed on Y117A and compared to WT CCR4 in which the tyrosine remained. The structure of alanine is shown in figure 4-3B; it has a CH_3 group, which compared to tyrosine's phenol group is much smaller in size. In addition to size, the side chains of the amino acids also affect charge and polarity. Alanine is neutral and non-polar, whereas tyrosine is neutral and polar. This polarity is due to the hydroxyl group present in the side chain.

Another mutation, Y117F, was also made; this involved mutation of tyrosine to phenylalanine, the structure of which is shown in figure 4-3C. Phenylalanine, like tyrosine, also contains a large benzene ring in its side chain. However the lack of the hydroxyl group in phenylalanine renders this amino acid neutral and non-polar. These two mutations allowed dissection of the relative contribution of size and polarity to antagonist binding; by performing assays on both and comparing them to WT CCR4 it could be ascertained which property, if any, was important for antagonist binding. Glutamic acids 205 (E205) and 290 (E290) were mutated to alanine, aspartic acid and glutamine in order to dissect the contribution of size and charge of the side chain of this amino acid. Mutation to aspartic acid maintained the charge while removing the bulk associated with the glutamic acid. Mutation to glutamine retained the bulk of glutamic acid while removing the charge. Mutation to alanine removed both the bulk and charge of glutamic acid.

Previous studies have used receptor mutation to investigate antagonist binding and activity as well as receptor function, the latter described in section 1.1. The antagonist UCB36526 was predicted to bind several amino acids within the transmembrane domains of CCR1, analogous to the site 1 CCR4 compounds presented here. The E287Q, Y113A, and Y41A CCR1 mutants showed resistance to UCB36526 in chemotaxis assays; 100 nM of the compound completely inhibited the

wild-type response to CCL3 but did not inhibit the mutant responses. Molecular modelling of the receptor-antagonist interaction suggested the formation of a salt bridge between E287 and the quaternary nitrogen of the compound (de Mendonça et al., 2005). The same antagonist was shown to inhibit CCR3 responses, and as with CCR1, the conserved E287 and Y113 residues were required for its activity (Wise et al., 2007). Y113A of CCR1 was also critical for the activity of another antagonist, BX 471 (Vaidehi et al., 2006).

Figure 4-3G shows the site 1 residues implicated in antagonist binding along with the mutations of these residues. Most mutations were to alanine, which as described is small, neutral, and non-polar. This mutation therefore removed any specific effects of size, charge or polarity of that amino acid. Tyrosines 117, 122 and 258 were mutated to both alanine and phenylalanine. In addition to this, glutamic acid 205 (E205) was mutated to alanine (E205A), aspartic acid (E205D), and glutamine (E205Q), the structures of which are shown in figure 4-3D-F. In section 3.2.4 the rationale for this strategy was explained in reference to the three E290 mutants; mutation to these three amino acids allowed the relative contribution of side chain size and charge on antagonist binding to be determined.

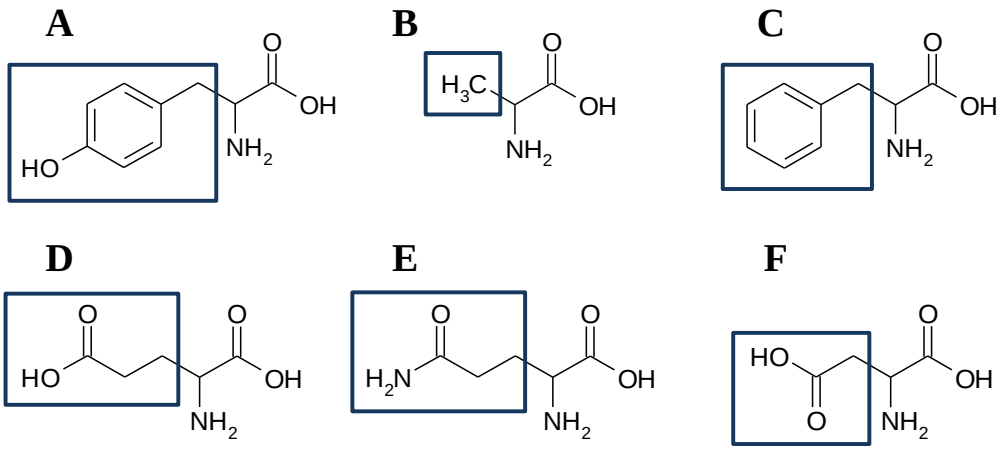

Location	TM2	TM3	TM4	ECL2	TM5	TM6	TM7
Mutation	L92A	I113A	F173A	K188A	L209A	Y258A	I286A
		S114A		S202A		Y258F	E290A
		Y117A		E205A			E290D
		Y117F		E205D			E290Q
		L118A		E205Q			
		F121A		I206A			
		Y122A					
		Y122F					
		I125A					
		F126A					

Figure 4-3 – Site 1 amino acid point mutations

Structures of amino acids; tyrosine 117 (A) was mutated to alanine (B) and phenylalanine (C). Glutamic acid 290 (D) was mutated to alanine, glutamine (E), and aspartic acid (F) and glutamine. Side chains of the amino acids are shown in boxes. Panel G shows a summary table of the site 1 point mutants along with their location in the receptor.

4.2 – Results

4.2.1 – Cell-surface expression of site 1 CCR4 point mutants

Since the intrahelical CCR4 antagonists were believed to contact sites within the transmembrane bundle, point mutants of these residues were made by performing site-directed mutagenesis on the *CCR4* insert within the pcDNA vector. These mutants were then transiently transfected into L1.2 cells and the following day their cell-surface expression measured using antibody staining and flow cytometry. In total, 25 point mutants were made of 18 residues. Figure 4-4 shows the cell surface expression of the various CCR4 point mutants after transfection. Receptor mutation had a wide variety of effects on cell-surface expression. L92A and L118A showed significantly increased levels of expression, with L92A expressed at 150% of WT CCR4 levels. Most of the point mutants showed no difference in expression; F121A, I113A, K188A, S202A, I206A, Y117A, Y117F, I125A, Y122F, F126A, E205A, E205D, E205Q and I286A all had expression levels comparable to WT, although Y117F, I125A and E290Q showed a trend to an increase. The remaining mutants S114A, Y122A, Y258A, Y258F, F173A, L209A, E290A and E290D were expressed at lower levels than WT. Y122A, Y258A and E290A showed the most marked reduction, expressing at 50% of WT levels. These data are summarised in table 4-5, which shows the change in cell-surface expression of a mutant relative to WT CCR4.

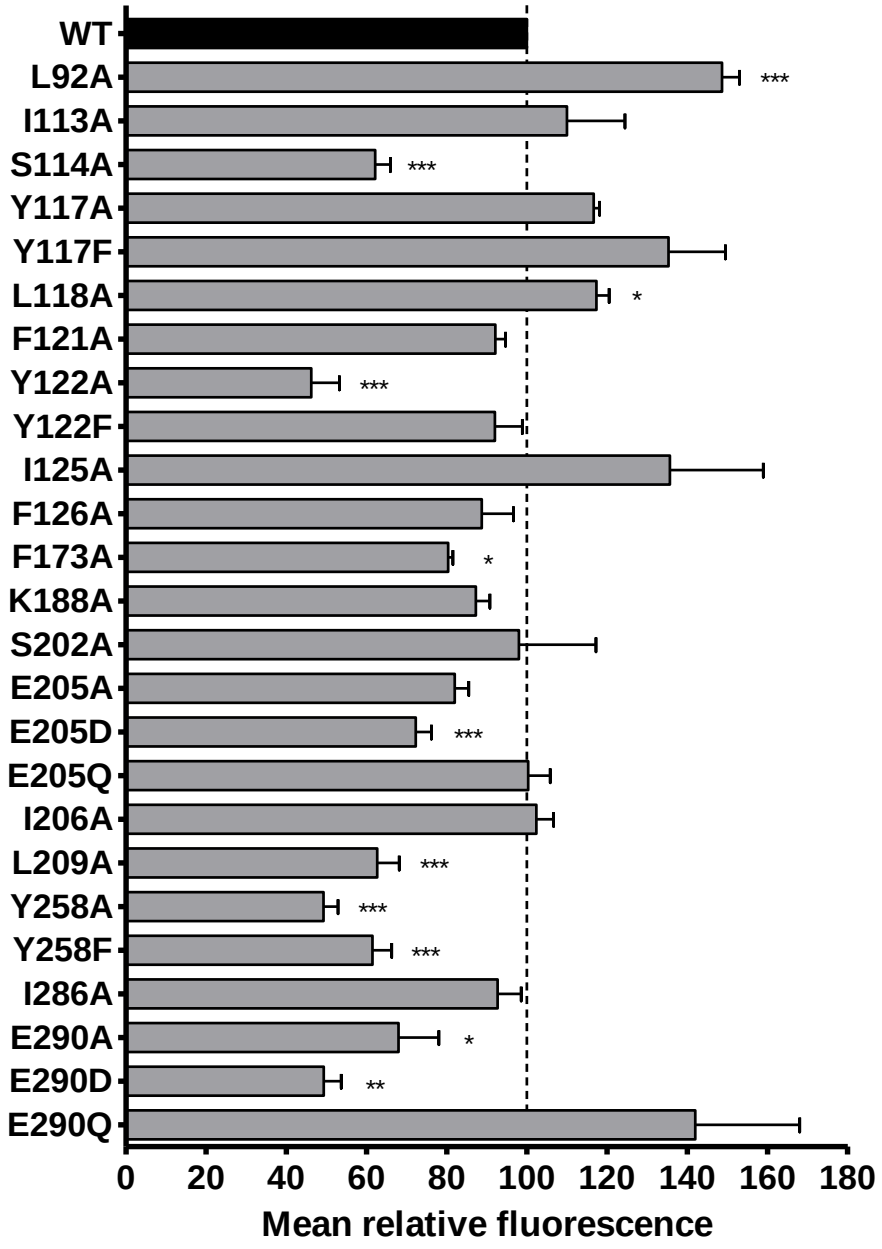

Figure 4-4 – CCR4 point mutants show variability in cell-surface expression levels

L1.2 cells were transiently transfected with WT and mutant CCR4 pcDNA and the following day analysed for cell surface expression by flow cytometry. The black bar shows WT CCR4, grey bars show individual point mutants. Data are presented as percentage of WT expression, and as the mean ± SEM of three independent experiments. Data were analysed by one-way ANOVA. Significance stars *, ** and *** represent p values of 0.05, 0.01, and 0.001 respectively.

Mutant	Relative expression	Mutant	Relative expression
L92A	↑	**S202A**	-
I113A	-	**E205A**	↓
S114A	↓	**E205D**	↓
Y117A	-	**E205Q**	-
Y117F	-	**I206A**	-
L118A	↑	**L209A**	↓
F121A	-	**Y258A**	↓
Y122A	↓	**Y258F**	↓
Y122F	-	**I286A**	-
I125A	-	**E290A**	-
F126A	-	**E290D**	↓
F173A	↓	**E290Q**	-
K188A	-		

Table 4-5 – Changes in cell-surface expression of CCR4 site 1 point mutants

A summary table of the relative cell-surface expression changes from figure 4-4. - = no change relative to WT, ↑ = increase relative to WT, ↓ = decrease relative to WT.

4.2.2 – Migratory potential of site 1 CCR4 point mutant transfectants to CCL17 and CCL22

After cell-surface expression was determined, the point mutant transfectants were assessed for their ability to migrate to soluble CCL17 and CCL22 in chemotaxis assays. These assays used concentrations of CCL17 and CCL22 ranging from 0.1 to 100 nM; it was previously shown in WT CCR4 L1.2 transfectants that the typical response observed during chemotaxis assays peaked at 1 nM (figure 3-4). The mutants were compared to WT across this concentration range.

Figure 4-6 shows the results of the chemotaxis assays of the mutants compared to WT CCR4. Some mutants, such as I113A, showed no difference in terms of migration to both CCL17 and CCL22 when compared to WT CCR4. Other mutants that exhibited this behaviour were K188A, S202A, Y258F, F173A, and E205Q. Other mutants showed no chemotactic response to either ligand; L29A, Y117A, Y122A, Y258A and the three E290 mutants did not induce migration above baseline levels. Another effect of receptor mutation was to decrease the potency of the chemokine relative to the WT response; for example, F121A mutation shifted the peak response of both CCL17 and CCL22 rightwards to 10 nM rather than its normal peak at 1 nM. The chemotactic responses of the mutants E205D, I206A, Y117F, I125A, Y122F, F126A, I286A, and E205A all showed a reduction in potency to one or both chemokines. The chemotactic response of I268A to CCL22, while reduced in potency compared to the WT response, showed an increase in efficacy; the chemotactic index at 1 nM was 15 for WT CCR4, compared to 65 at 10 nM for I286A. These results are summarised in table 4-7; the table shows what effects each mutation had on the efficacy and potency of each chemokine response.

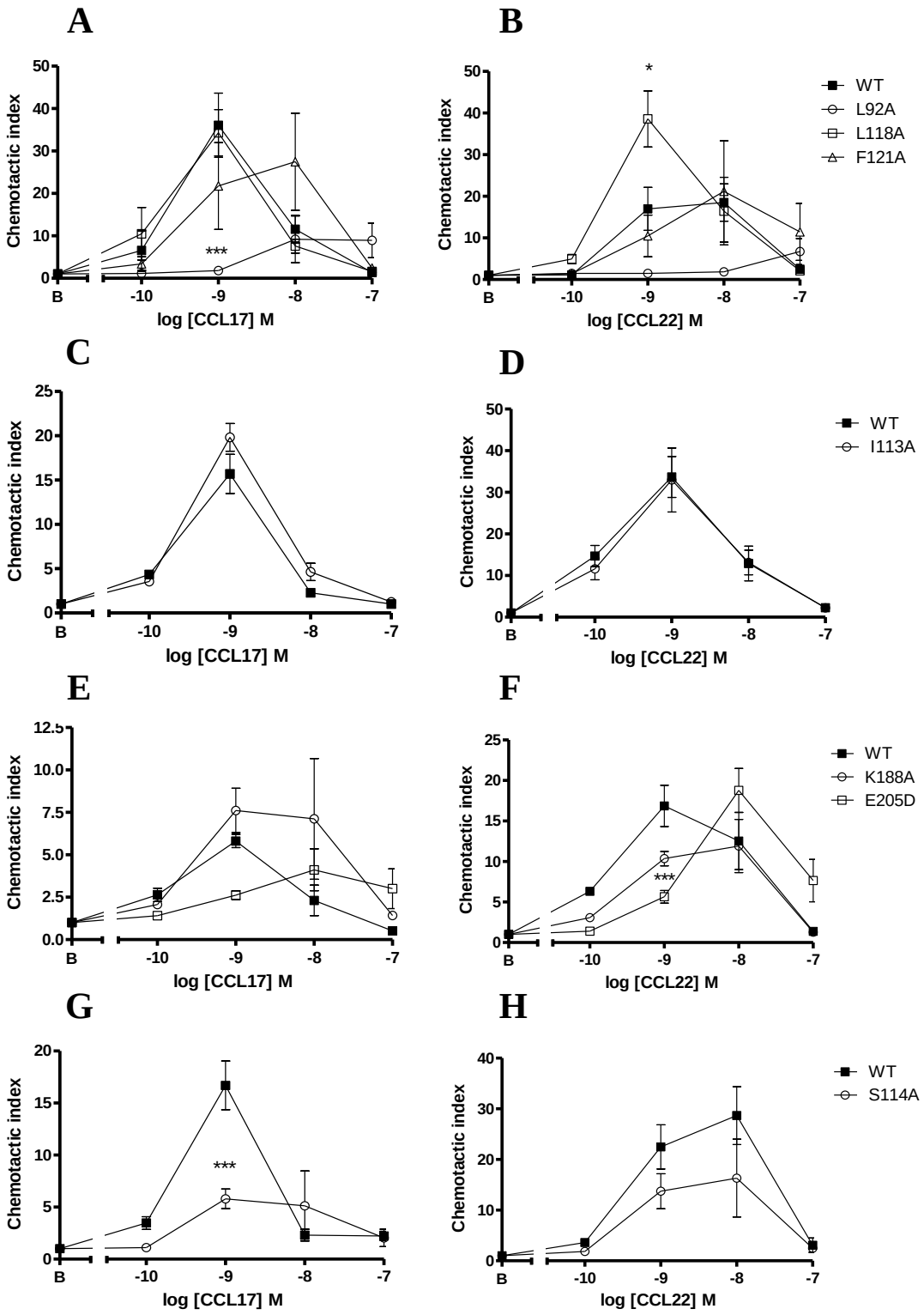
A
B
C
D
E
F
G
H
Chemotactic index
log [CCL17] M
log [CCL22] M
B
-10
-9
-8
-7
***
*
WT
L92A
L118A
F121A
I113A
K188A
E205D
S114A

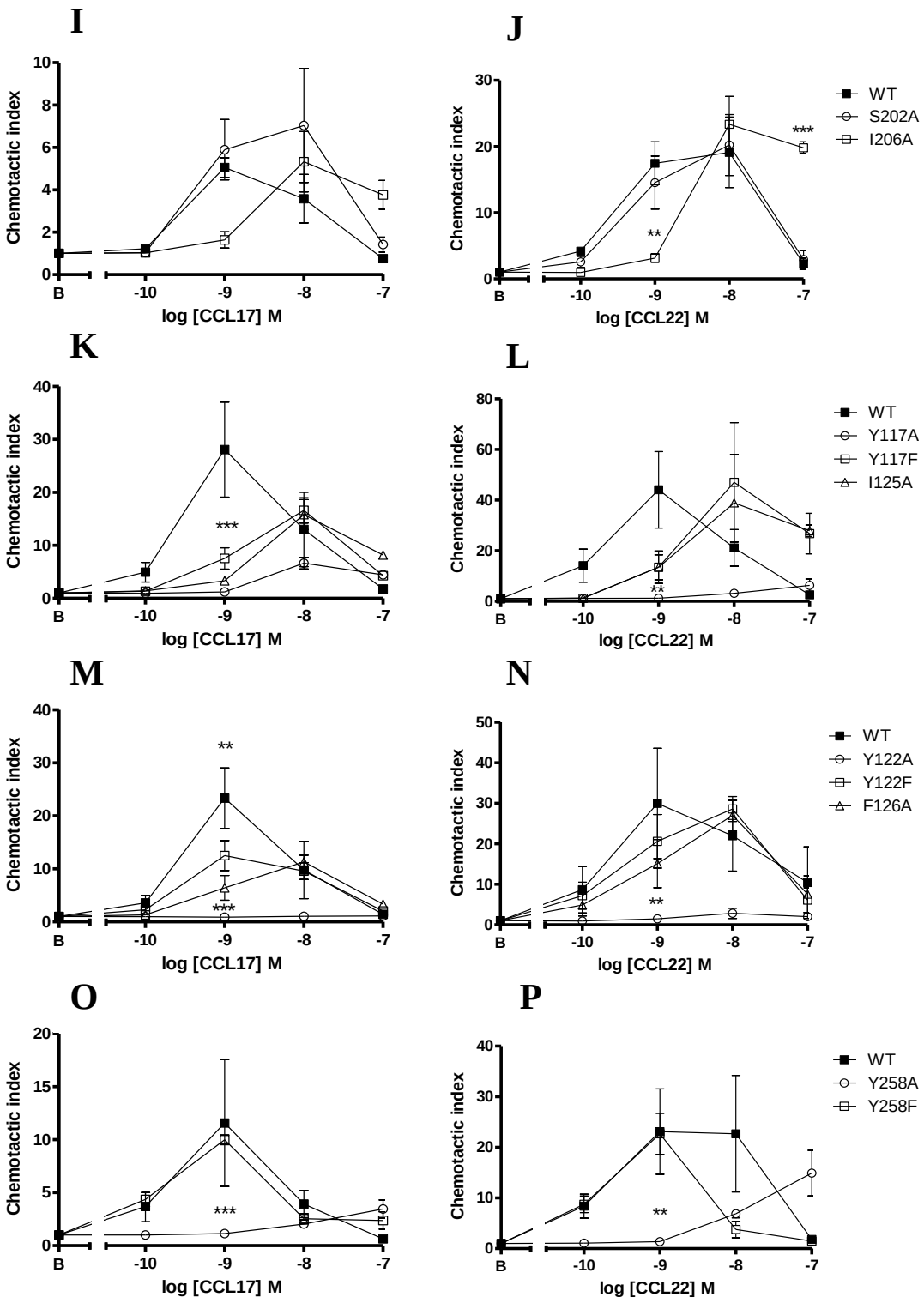
I
J
K
L
M
N
O
P
Chemotactic index
log [CCL17] M
log [CCL22] M
B
-10
-9
-8
-7
WT
S202A
I206A
Y117A
Y117F
I125A
Y122A
Y122F
F126A
Y258A
Y258F
*
**
***

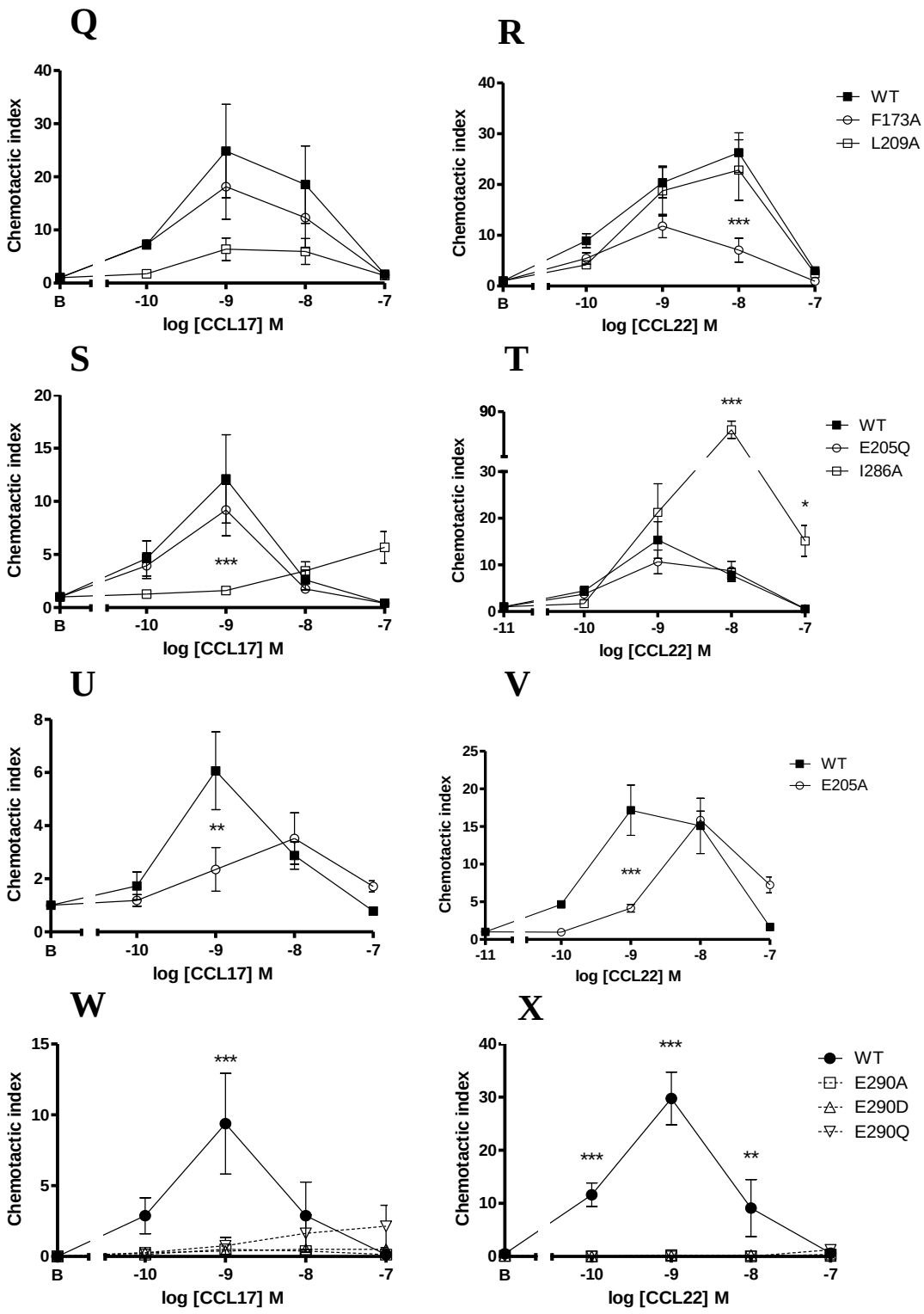
Q
Chemotactic index
log [CCL17] M
R
log [CCL22] M
WT
F173A
L209A
S
E205Q
I286A
T
U
E205A
V
W
E290A
E290D
E290Q
X

Figure 4-6 – CCR4 point mutation affects chemotaxis of transfectants to both CCL17 and CCL22

Following analysis of cell-surface expression, WT and mutant CCR4 transfectants were assessed for their ability to migrate to soluble CCL17 (left-hand column) and CCL22 (right-hand column). WT responses are shown as filled squares; mutants as open circles, squares and triangles. Data are the mean ± SEM of three independent experiments, and were analysed by two-way ANOVA. Significance stars *, ** and *** represent p values of 0.05, 0.01, and 0.001 respectively.

	CCL17		CCL22			CCL17		CCL22	
CCR4 mutant	Efficacy	Potency	Efficacy	Potency	**CCR4 mutant**	Efficacy	Potency	Efficacy	Potency
L92A	NR	NR	NR	NR	**S202A**	-	-	-	-
I113A	-	-	-	-	**E205A**	↓	↓	↓	↓
S114A	↓	-	-	-	**E205D**	↓	↓	↓	↓
Y117A	NR	NR	NR	NR	**E205Q**	-	-	-	-
Y117F	↓	↓	-	↓	**I206A**	-	↓	-	↓
L118A	-	-	↑	-	**L209A**	↓	-	-	-
F121A	-	↓	↓	↓	**Y258A**	NR	NR	NR	NR
Y122A	NR	NR	NR	NR	**Y258F**	-	-	-	-
Y122F	↓	-	-	↓	**I286A**	↓	↓	↑	↓
I125A	↓	↓	-	↓	**E290A**	NR	NR	NR	NR
F126A	↓	↓	-	↓	**E290D**	NR	NR	NR	NR
F173A	-	-	-	-	**E290Q**	NR	NR	NR	NR
K188A	-	-	-	-					

Table 4-7 – Changes in chemotactic response of site 1 point mutant transfectants

A summary table of the data from figure 4-6; the effect of point mutations on efficacy and potency of the chemotactic response. - = no change, NR = no response, ↑ = increase in efficacy/potency, ↓ = decrease in efficacy/potency.

4.2.3 – Binding of radiolabelled chemokines to site 1 CCR4 point mutant transfectants

After functional assays had been performed, the ability of chemokine to bind WT and mutant CCR4 was assessed. Cells expressing the receptor were incubated with radiolabelled ligand and either buffer or unlabelled ligand, after which they were centrifuged through oil. This separated the cells from the free ligand, and the counts from the resulting cell pellet measured. To investigate chemokine binding, radioactive iodinated CCL17 and CCL22 (^{125}I-CCL17 and ^{125}I-CCL22) were used in these assays.

Figure 4-8 (panels A and B) shows the total and non-specific binding of WT CCR4 and the Y117A, Y122A and Y258A mutants. WT CCR4 bound both chemokines; there was a significant difference between the total and non-specific binding values for ^{125}I-CCL17 and ^{125}I-CCL22. The ^{125}I-CCL22 binding window was smaller than for ^{125}I-CCL17; there was 45% non-specific ^{125}I-CCL22 binding compared to 20% for ^{125}I-CCL17. The three mutants did not bind chemokine, as there was no significant difference between the total and non-specific binding values. In addition, the values for these were similar to the non-specific WT values, indicating that only non-specific binding was being detected. Similar results were observed for the mutants E205A, E205D and Y117F in panels C and D, and mutants L92A and I286A in panels G and H. These mutants had no significant difference between total and non-specific binding, indicating that they did not bind chemokine. E205Q and Y122F (panels C and D) however did bind chemokine, along with L118A (panels E and F). E205Q and L118A showed a significant difference between total and non-specific binding for both chemokines, with a window comparable to WT CCR4 in that total binding reached 100%. Y122F however had a smaller binding window; the total binding value was 58% for ^{125}I-CCL17 and 62% for ^{125}I-CCL22. Panels I and J show the E290 mutants, which as previously described in figure 3-9, did not bind either ^{125}I-CCL17 or ^{125}I-CCL22.

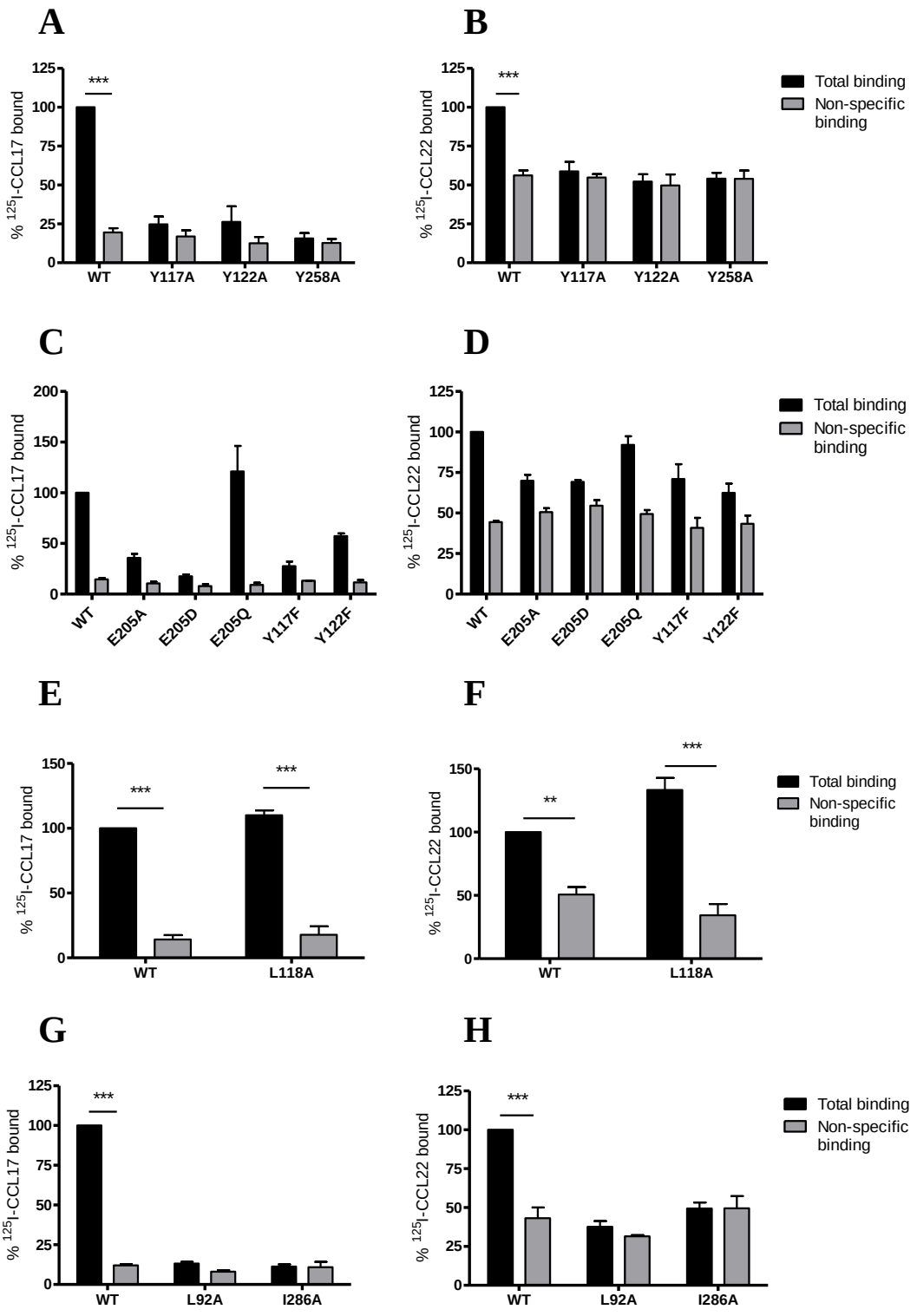
A
B
C
D
E
F
G
H
% 125I-CCL17 bound
% 125I-CCL22 bound
Total binding
Non-specific binding
***
**
WT
Y117A
Y122A
Y258A
E205A
E205D
E205Q
Y117F
Y122F
L118A
L92A
I286A

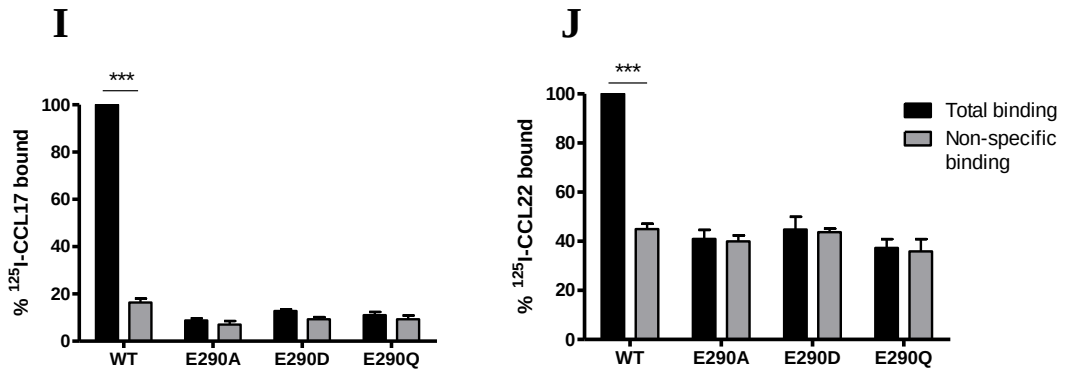

Figure 4-8 – Whole-cell chemokine binding of CCR4 point mutant transfectants

CCR4 transfectants were incubated with ^{125}I-CCL17 (left-hand column) or ^{125}I-CCL22 (right-hand column) and buffer (total binding; black bars) or excess unlabelled chemokine (non-specific binding; grey bars). Panels A and B show binding of Y117A, Y122A, and Y258A. Panels C and D show binding of E205A, E205D, E205Q, Y117F and Y122F. Panels E and F shows the binding of L118A. Panels G and H show binding of L92A and I286A. Panels I and J show binding of E290A, E290D and E290Q. Data are the mean ± SEM of three independent experiments and analysed with two-way ANOVA, with the exception of panels C and D, which are from two experiments. Significance stars *, ** and *** represent p values of 0.05, 0.01, and 0.001 respectively.

4.2.4 – Inhibition of WT and mutant CCR4-induced chemotaxis to CCL17 and CCL22 by the site 1 antagonists

The allosteric antagonists were hypothesised to bind the receptor and prevent it from shifting into an active conformation, inhibiting its functional response. Since the primary response of chemokine receptors is to induce cell migration, assaying the ability of the antagonist to inhibit this migration would provide a measure of the antagonists' activity. To investigate the ability of the CCR4 antagonists to block CCL17- and CCL22-induced migration, chemotaxis assays were performed. In these assays, cells were tested for their ability to migrate to solutions of a fixed concentration of chemokine and an increasing concentration of antagonist. For mutant transfectants that migrated to chemokine with a reduced potency, the fixed chemokine dose in the antagonist assays was changed accordingly. For example, the most efficacious chemokine concentration for E205A transfectants was 10 nM, which was used as the fixed chemokine concentration in the antagonist assays. By comparing the total migration for each antagonist concentration against the migration to chemokine without antagonist, the ability of the antagonist to inhibit chemotaxis could be determined.

This dose-response of antagonist was used to determine its potency; at a low concentration of antagonist we would expect to see minimal inhibition compared to chemokine alone, whereas a high concentration would be expected to fully inhibit chemokine-induced migration. By plotting a non-linear regression curve using the results of this dose response, the IC_{50} could be measured to give a measure of the potency of the antagonist. The IC_{50} is the concentration causing half of the maximal inhibitory response, in this case half maximal migration. A lower IC_{50} would show that the compound is more potent as half maximal migration is reached at a lower concentration. IC_{50} values can be expressed in the concentration units of the data they are calculated from - in this case nM - or alternatively, in logarithmic form as a $logIC_{50}$. An IC_{50} of 1 nM would be -9 when expressed as a $logIC_{50}$. Antagonist potencies are shown here as $logIC_{50}$ values.

Figure 4-9 shows the results of inhibition of chemotaxis of L1.2 transfectants expressing WT CCR4 to 1 nM CCL17 and CCL22. The four site 1 compounds are used to antagonise the migration of these cells. The antagonists were used at increasing concentrations, from 1 nM to 30 μM. Migration to chemokine alone was

set at 100% and the inhibition of migration calculated relative to this value. Panel A shows that antagonists 3 and 7 inhibited CCL17-induced migration with similar potency; their $logIC_{50}$ values were -8.00 and -8.06, respectively. Complete inhibition of migration occurred at 100 nM of antagonists 3 and 7. Antagonist 4 was less potent at inhibiting the response, with a $logIC_{50}$ of -7.09, and complete inhibition occurring at 1 μM. Antagonist 1 was the least potent, with a $logIC_{50}$ of -6.23, and full inhibition of the response not occurring even with 30 μM of antagonist 1.

Panel B shows the inhibition of CCL22 migration by the antagonists. In contrast to panel A, antagonists 3 and 7 inhibited the response with different potencies; they had $logIC_{50}$ values of -7.43 and -7.97, respectively. Antagonist 4 was poorer at inhibiting CCL22-induced migration compared to CCL17-induced migration, with a $logIC_{50}$ of -6.06. Similarly, antagonist 1 was poorer at inhibiting CCL22-induced migration, with a very low $logIC_{50}$ of -5.43. Even at 30 μM antagonist 1, there was still 25% migration occurring.

Thus, antagonist 1 was shown to be the least potent at inhibiting CCL17- and CCL22-induced migration. Antagonists 3 and 7 were the most potent at inhibiting CCL17-induced migration. Antagonists 1, 3, and 4 were all less potent at inhibiting CCL22-induced migration.

Of the CCR4 point mutants that were functional - those that showed a functional chemotactic response in figure 4-6 – several were then tested for their sensitivity to antagonist in the same manner as described above. Figure 4-10 shows the responses of L1.2 transfectants expressing WT CCR4 and L118A CCR4 to 1 nM CCL17 and CCL22 in the presence of three of the site 1 antagonists; antagonists 3, 4, and 7. Antagonist 1 is not shown due to variability in the datasets arising from the poor solubility of the compound. Rather than compare the response of each mutant to the original dose-response curves shown in figure 4-9, separate WT response curve were generated for each independent assay.

Table 4-11 shows the $logIC_{50}$ values from figure 4-10. Antagonist 3 $logIC_{50}$ values were not significantly different for WT or L118A for both inhibition of CCL17- and CCL22-induced migration. The same was true for antagonist 4 inhibition of migration, with the exception of a small reduction in potency against I125A-induced migration to CCL17. Antagonist 7 however showed a large and significantly reduced potency against L118A CCR4 transfectants. WT CCL17 and CCL22

responses were inhibited with $logIC_{50}$ values of -8.19 and -7.66 respectively, while L118A responses were inhibited with $logIC_{50}$ values of -6.20 and -5.34 respectively. These reductions in potency were statistically significant when analysed with a t-test, with p values of 0.0059 and 0.000023, respectively.

This comparison of mutant versus WT chemotaxis inhibition was then repeated for many of the other CCR4 point mutants. The inhibition of Y122F and I125A migration by site 2 antagonists is shown in figure 4-12. The effectiveness of the site 1 antagonists at inhibiting point mutant-induced migration was compared to WT by testing the significance of the differences between $logIC_{50}$ values. The $logIC_{50}$ values from all of the chemotaxis assays are summarised in table 4-13 along with the data from figure 4-10. Table 4-13 shows that along with L118A, two other site 1 point mutants showed reduced sensitivity to antagonist 7 in chemotaxis assay; both Y122F and I125A showed significantly reduced antagonist potency in the inhibition of CCL22-induced migration compared to WT. I125A also showed a reduction in potency to the CCL17 response. These two mutations are of amino acids in transmembrane domain 3, in close proximity to L118. The other mutants that were tested did not show a reduction in antagonist potency.

The remaining site 1 mutants were also tested against antagonist 7, however no loss of potency was observed. The F173A, K188A and Y258F mutants were also tested against antagonist 4; however these experiments were only performed twice rather than three times. As such, statistical analyses were not performed on the $logIC_{50}$ values.

Chapter 5 discusses a class of antagonists that are hypothesised to bind to the CCR4 C-terminus. In chapter 5, C-terminal truncation mutants of CCR4 were made to dissect the role of successive portions of the C-terminus in antagonist binding. The Δ40 CCR4 mutant had the terminal 40 amino acids of its C-terminus truncated, leaving only the short helix VIII region at the end of the transmembrane helix VII. Since this truncation mutant did not contain any mutated site 1 amino acids, it was tested against the site 1 antagonists in this chapter to confirm that the C-terminus was not required for their function. As can be seen from the table of $logIC_{50}$ values in table 4-13, the Δ40 truncation mutants did not significantly differ in their response to antagonists 3, 4, and 7 compared to WT transfectants.

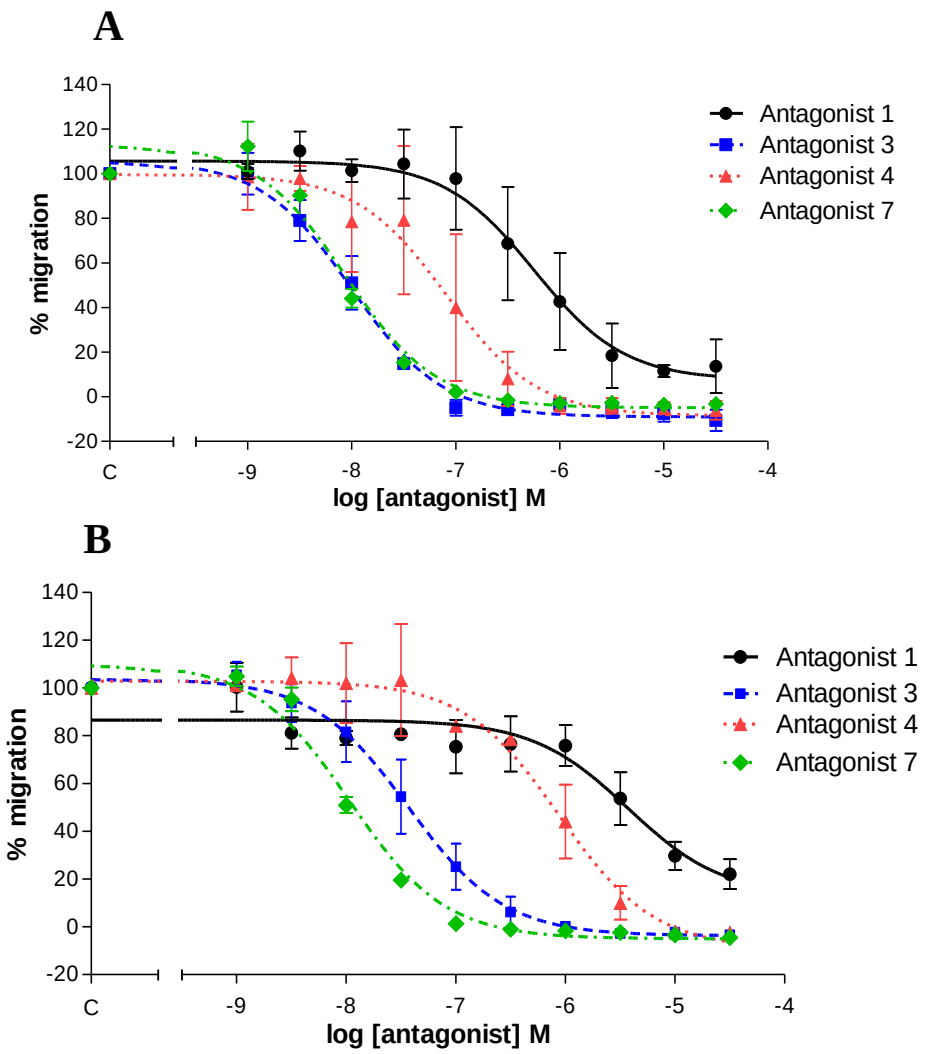

Figure 4-9 – Antagonism of WT CCR4-induced migration of L1.2 transfectants

CCR4 transfectants were tested for their sensitivity to the four site 1 antagonists by measuring migration toward 1 nM CCL17 (A) or CCL22 (B) and increasing concentrations of antagonist, and expressing the data as a percentage of migration to chemokine alone. logIC_{50} values for panel A - 1: -6.23 ± 0.21. 3: -8.00 ± 0.08. 4: -7.09 ± 0.13. 7: -8.06 ± 0.07. Panel B – 1: -5.43 ± 0.23. 3: -7.43 ± 0.10. 4: -6.06 ± 0.09. 7: -7.97 ± 0.05 (B). logIC_{50}s were calculated using non-linear regression analysis. Data points and logIC_{50}s are the mean ± SEM of three independent experiments.

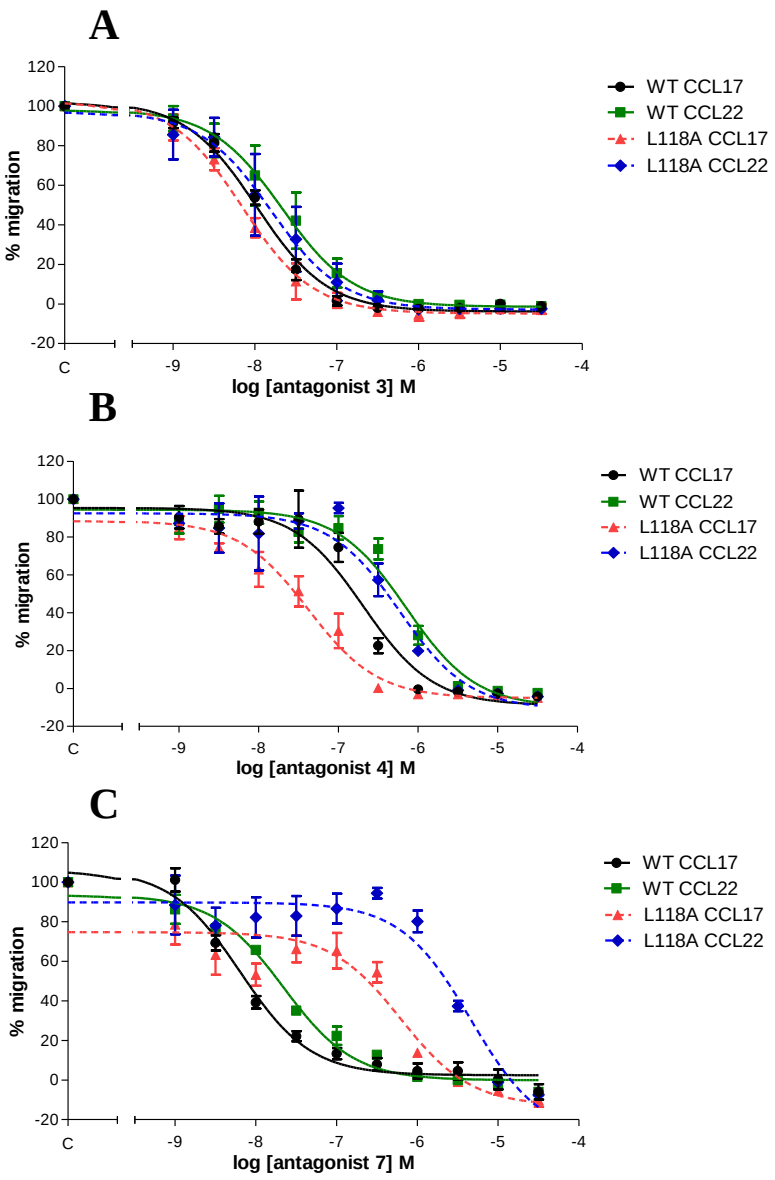

Figure 4-10 – L118A transfectants are less sensitive to chemotactic inhibition by antagonist 7

The sensitivity of L118A transfectants to the site 1 antagonists in chemotaxis assays was compared to WT transfectants. Increasing concentrations of antagonists 3 (A), 4 (B), and 7 (C) inhibited migration to 1 nM CCL17 and CCL22. Data are the mean ± SEM of three independent experiments.

	CCL17			CCL22		
CCR4 construct	*Antagonist 3 $logIC_{50}$*	*Antagonist 4 $logIC_{50}$*	*Antagonist 7 $logIC_{50}$*	*Antagonist 3 $logIC_{50}$*	*Antagonist 4 $logIC_{50}$*	*Antagonist 7 $logIC_{50}$*
WT	-7.98 ± 0.06	-6.68 ± 0.10	-8.23 ± 0.04	-7.71 ± 0.27	-6.16 ± 0.13	-7.64 ± 0.06
L118A	-8.13 ± 0.12	-7.39 ± 0.27	-6.19 ± 0.20	-7.82 ± 0.29	-6.22 ± 0.03	-5.31 ± 0.06 (p=0.000012)

Table 4-11 – Potency of site 1 antagonist inhibition of WT and L118A transfectants
$logIC_{50}$ values from the inhibition of WT and L118A CCR4 transfectants from figure 4-10. $logIC_{50}$ values were calculated using non-linear regression analysis, and two-tailed t-test used to compare values. Blue shaded columns indicate statistically significant differences between $logIC_{50}$ values; p values of 0.007 and 0.000012 for CCL17 and CCL22, respectively. $logIC_{50}$s are the mean ± SEM of three independent experiments.

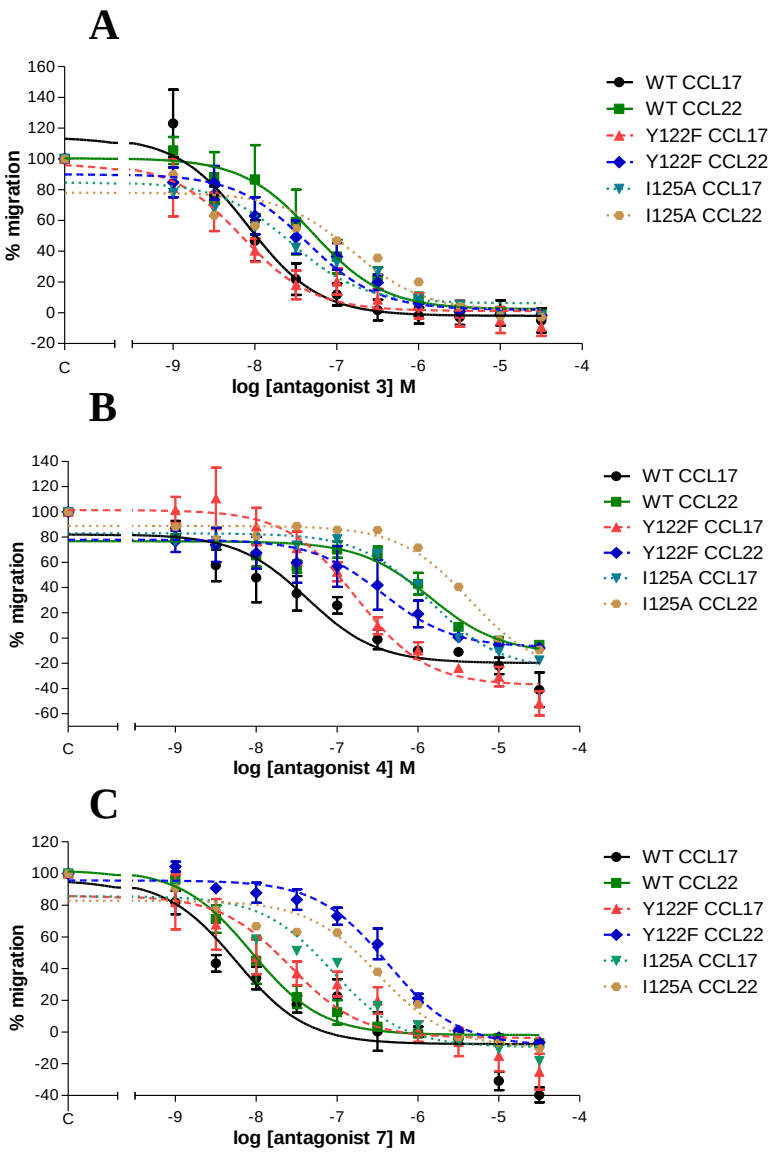

Figure 4-12 – Inhibition of Y122F and I125A transfectant migration by antagonists 3, 4 and 7

The sensitivity of Y122F and I125A transfectants to the site 1 antagonists in chemotaxis assays was compared to WT transfectants. Increasing concentrations of antagonists 3 (A), 4 (B), and 7 (C) inhibited migration to 1 nM CCL17 and CCL22. Data are the mean ± SEM of three independent experiments.

A

CCR4 Construct	Antagonist 3 $logIC_{50}$	Antagonist 4 $logIC_{50}$	Antagonist 7 $logIC_{50}$
WT	-7.94 ± 0.08	-6.84 ± 0.13	-8.23 ± 0.04
I113A	-8.03 ± 0.03	-7.29 ± 0.10	-8.31 ± 0.08
WT	-7.97 ± 0.16	-7.71 ± 0.46	-8.04 ± 0.21
Y117F	-7.35 ± 0.38	-7.57 ± 0.23	-7.86 ± 0.24
WT	-7.98 ± 0.06	-6.68 ± 0.10	-8.23 ± 0.04
L118A	-8.13 ± 0.12	-7.39 ± 0.27	-6.19 ± 0.20 (p=0.007)
WT	-7.74 ± 0.12	ND	ND
F121A	-8.03 ± 0.23	ND	ND
WT	-7.97 ± 0.16	-7.71 ± 0.46	-8.04 ± 0.21
Y122F	-7.51 ± 0.48	-6.80 ± 0.18	-7.09 ± 0.39 (p=0.12)
WT	-7.97 ± 0.16	-7.71 ± 0.46	-8.04 ± 0.18
I125A	-6.97 ± 0.50	-5.81 ± 0.07 (p=0.05)	-7.16 ± 0.25 (p=0.007)
WT	ND	ND	-7.30 ± 0.38
F126A	ND	ND	-7.83 ± 0.18
WT	ND	*-7.03 ± 0.03*	-7.45 ± 0.47
F173A	ND	*-6.70 ± 0.38*	-7.66 ± 0.50
WT	ND	*-7.03 ± 0.03*	-7.45 ± 0.47
K188A	ND	*-7.19 ± 0.08*	-7.91 ± 0.30
WT	ND	ND	-7.30 ± 0.38
S202A	ND	ND	-7.72 ± 0.33
WT	ND	ND	-7.30 ± 0.38
I206A	ND	ND	-7.40 ± 0.28
WT	ND	*-7.03 ± 0.03*	-7.45 ± 0.47
Y258F	ND	*-6.48 ± 0.14*	-7.85 ± 0.37
WT	-8.04 ± 0.11	-7.15 ± 0.24	-8.06 ± 0.01
Δ40	-7.76 ± 0.34	-7.50 ± 0.15	-7.54 ± 0.17

B

CCR4 Construct	Antagonist 3 $logIC_{50}$	Antagonist 4 $logIC_{50}$	Antagonist 7 $logIC_{50}$
WT	-7.50 ± 0.10	-6.37 ± 0.08	-7.64 ± 0.06
I113A	-7.41 ± 0.12	-6.28 ± 0.10	-7.70 ± 0.18
WT	-7.45 ± 0.27	-5.79 ± 0.07	-8.04 ± 0.24
Y117F	-7.16 ± 0.66	-6.68 ± 0.13	-7.65 ± 0.21
WT	-7.71 ± 0.27	-6.16 ± 0.13	-7.64 ± 0.06
L118A	-7.82 ± 0.29	-6.22 ± 0.03	-5.31 ± 0.06 (p=0.000012)
WT	-7.25 ± 0.10	ND	ND
F121A	-7.30 ± 0.13	ND	ND
WT	-7.45 ± 0.27	-5.79 ± 0.07	-8.04 ± 0.24
Y122F	-7.25 ± 0.26	-6.12 ± 0.08	-6.41 ± 0.11 (p=0.01)
WT	-7.45 ± 0.27	-5.79 ± 0.07	-8.04 ± 0.24
I125A	-6.56 ± 0.66	-5.30 ± 0.13 (p=0.04)	-6.51 ± 0.17 (p=0.009)
WT	ND	ND	-6.92 ± 0.33
F126A	ND	ND	-7.71 ± 0.17
WT	ND	*-6.16 ± 0.10*	-7.45 ± 0.47
F173A	ND	*-5.87 ± 0.05*	-7.25 ± 0.54
WT	ND	*-6.16 ± 0.10*	-6.92 ± 0.44
K188A	ND	*-6.24 ± 0.11*	-7.10 ± 0.57
WT	ND	ND	-6.92 ± 0.33
S202A	ND	ND	-6.95 ± 0.32
WT	ND	ND	-6.92 ± 0.33
I206A	ND	ND	-6.93 ± 0.40
WT	ND	*-6.16 ± 0.10*	-7.45 ± 0.47
Y258F	ND	*-5.05 ± 0.21*	-7.19 ± 0.60
WT	-7.45 ± 0.21	-6.05 ± 0.11	-7.97 ± 0.05
Δ40	-7.16 ± 0.32	-6.50 ± 0.15	-7.64 ± 0.17

Table 4-13 – Antagonist 7 has reduced potency against three site 1 mutants in inhibition of chemotaxis assays

Non-linear regression was used to calculate the $logIC_{50}$ values for the site 1 antagonist inhibition of CCR4 point mutant migration to CCL17 (A) and CCL22 (B). Mutant $logIC_{50}$ values that were significantly different to WT are highlighted in blue, and the p-values of the t-tests shown in brackets. Data are the mean ± SEM of three independent experiments. Italicised $logIC_{50}$ values are two independent experiments, upon which statistical analyses were not performed. ND = not done.

4.2.5 – Inhibition of ^{125}I-chemokine binding to WT and mutant CCR4 transfectants by site 1 antagonists

In section 4.2.4 it was shown that L118A transfectants had reduced sensitivity to antagonist 7 in chemotaxis assays. Following this, the ability of the antagonist to antagonise chemokine binding was tested, in order to ascertain whether the reduction in functional potency was due to the antagonist inhibiting ligand binding. Whole-cell binding of chemokine was performed in a similar manner to that described previously (section 4.2.3). L118A transfectants were incubated with a fixed concentration of 0.1 nM ^{125}I-CCL17 or ^{125}I-CCL22 and an increasing concentration of antagonist 7. Data were presented as a percentage of binding without antagonist, after subtraction of non-specific binding (100 nM unlabelled chemokine).

Figure 4-14 shows the inhibition of ^{125}I-CCL17 (panel A) and ^{125}I-CCL22 (panel B) binding to WT and L118A transfectants with antagonist 7, after confirmation of cell-surface expression of the receptors. Binding of ^{125}I-CCL17 to WT CCR4 was inhibited with a logIC_{50} of -6.34, while binding to L118A was inhibited with a logIC_{50} of -5.77. This reduction was statistically significant ($p=0.00022$). Inhibition of CCL22 binding appeared to be reduced in potency by the L118A mutation; however there was no significant reduction, possibly due to variation in the data.

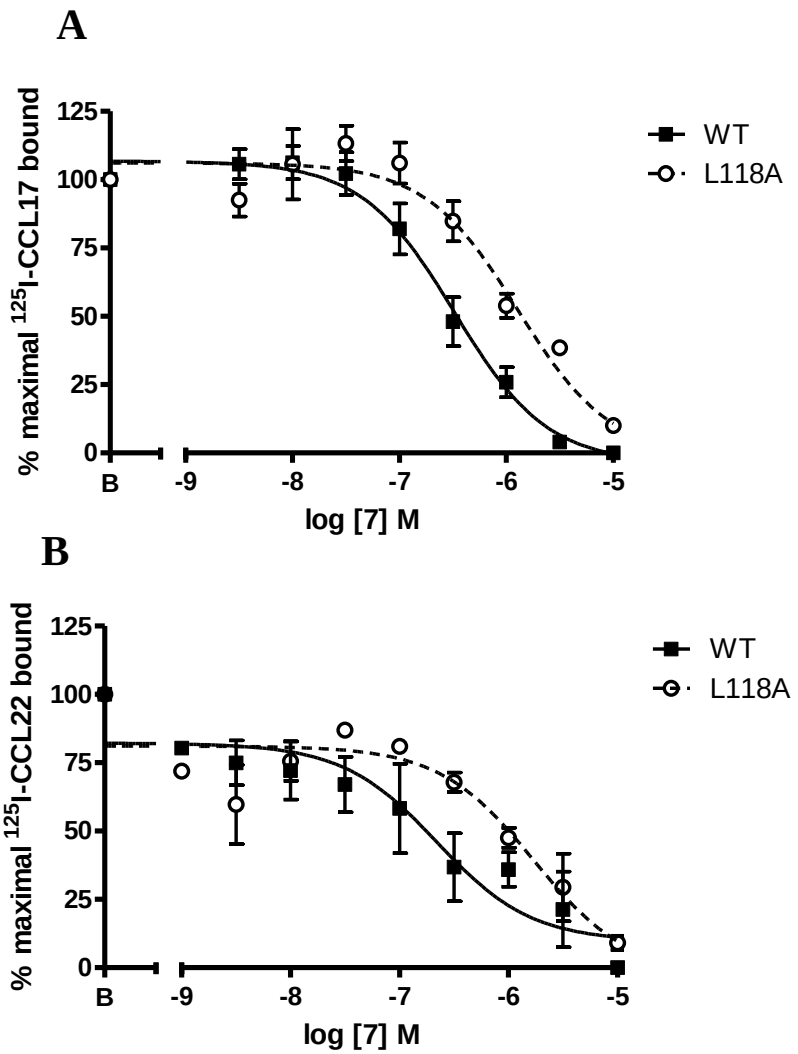

Figure 4-14 – Antagonist 7 inhibition of chemokine binding is less potent against L118A transfectants

Binding of ^{125}I-CCL17 (A) and ^{125}I-CCL22 (B) to WT and L118A transfectants was inhibited by increasing concentrations of antagonist 7. Non-specific binding - 100 nM unlabelled chemokine - was subtracted from each value. logIC_{50} values for panel A – WT: -6.34 ± 0.1. L118A: -5.77 ± 0.16. logIC_{50} values for panel B – WT: -7.92 ± 0.19. L118A: -6.27 ± 0.21. Data are expressed as a percentage of binding without antagonist, and are the mean ± SEM of three independent experiments.

4.3 – Discussion

4.3.1 – The effect of site 1 CCR4 point mutation on cell-surface expression

In this chapter, the amino acids of CCR4 predicted by molecular modelling to be points of site 1 antagonist contact were individually mutated and the effects of these mutations upon receptor function and antagonist activity were measured. The CCR4 site 1 point mutations had a wide variety of effects on receptor cell-surface expression, chemotactic responses and binding of the chemokines CCL17 and CCL22. Some mutations had no effect on receptor phenotype, while others completely removed the ability of the receptor to bind or respond to chemokine.

Following synthesis, proteins are exported via the endoplasmic reticulum and the Golgi apparatus to the cell membrane. The mechanisms by which GPCRs such as chemokine receptors are exported to the cell-surface are not well understood. However, it is believed that various chaperone proteins aid in the trafficking of receptors from the endoplasmic reticulum to the cell membrane, and ensure that the receptors are correctly folded. For example, heat shock proteins have been shown to aid in protein folding, stabilise misfolded proteins, and protect against heat-induced degradation of protein structure. Other accessory proteins have also been demonstrated as important mediators of GPCR expression; for example, Drip78 and ninaA are examples of small proteins that aid the trafficking of the dopamine D_1 receptor and *Drosophila* rhodopsin, respectively. In general, these proteins bind specific motifs in the GPCRs and either stabilise structure or act as chaperones through export pathways (Cooray et al., 2009). The mutation or disruption of motifs or domains required for folding or chaperone interaction may therefore negatively affect cell-surface expression of proteins, such as CCR4. Mutation may have also grossly affected the conformation of the receptor, preventing it from being effectively trafficked and thus targeted for degradation. The mutants of CCR4 that had reduced cell-surface expression included S114A, Y122A, F173A, E205A, E205D, L209A, Y258A, Y258F, and E290D (figure 4-4).

Fifteen site 1 point mutations had no significant effect on receptor cell-surface expression. These were: I113A, Y117A, Y117F, F121A, Y122F, I125A, F126A, K188A, S202A, E205A, E205Q, I206A, I286A, E290A, and E290Q (figure 4-4). The

first seven of these were mutants of amino acids located in transmembrane helix III, while I286A, E290A and E290Q were mutations of helix VII amino acids. The remaining mutants were of amino acids in the second extracellular loop. Since these mutations had no effect on receptor expression, it can thus be surmised that either these mutations were of amino acids not required for receptor trafficking, or that the particular mutation did not perturb an interaction that was necessary for trafficking.

An example of the latter case is highlighted in the case of the E205Q mutant. While E205Q CCR4 retained full receptor expression levels, the E205D mutant showed significantly reduced expression, to approximately 70% of WT levels. Glutamic acid (E) and glutamine (Q) are of similar size but differ in their charge, while aspartic acid (D) is negatively charged like glutamic acid but has a shorter side-chain. Any potential interactions necessary for folding or chaperone binding may have thus been disrupted by the shortening of the E205 side chain. The E205A mutant also showed a trend to reduced receptor expression, to approximately 80% of WT levels. Since the glutamic acid to alanine mutation is a more extreme one than to aspartic acid, it follows that any interactions based on the glutamic acid side chain would also be disrupted upon mutation to alanine.

A similar phenomenon was observed for the mutations of E290, the conserved GluVII:06 amino acid in transmembrane helix VII. The E290D mutant showed a 50% reduction in cell-surface expression relative to WT CCR4, while the E290A and E290Q mutants showed trends to a decrease and increase in expression, respectively. The cause of the reduced cell surface expression of E290D is likely structural rather than related to accessory or chaperone proteins, since this amino acid is buried within helix VII and forms part of the ligand binding pocket and therefore would be inaccessible to other proteins. It is highly conserved and has been shown to be an important structural motif in many chemokine receptors; therefore it is likely that ionic interactions necessary for receptor conformation have been disrupted by the mutations (see chapter 3). In CCR2 and CCR5, an interhelical network of bonds was postulated to exist between conserved tyrosines in transmembrane helices I and III, a tryptophan in helix II and the conserved GluVII:06 in helix VII. Mutagenesis of these residues and validation using cell-surface expression, chemotaxis and chemokine binding assays showed that this network was required to maintain receptor conformation for both cell-surface expression and receptor function (Hall et al., 2009).

In addition to effects upon cell-surface expression, some of the mutations of the various amino acids hypothesised to comprise site 1 had effects on the ability of the receptor to induce chemotaxis to the chemokine CCL17 and CCL22. The E205A and E205D mutants, which as described had reduced cell-surface expression, showed a reduction in efficacy and potency in migration assays using CCL17 and CCL22 (figure 4-6). This implies that the size of the glutamic acid is a determinant of an interaction necessary for receptor function; due its position in the second extracellular loop E205 may be required for chemokine binding or for the formation of a salt bridge with another amino acid in another extracellular loop. The two-step model of chemokine binding describes high affinity binding of chemokines to the receptor N-terminus followed by low affinity binding to the extracellular loops (Monteclaro and Charo, 1997). Mutation of glutamic acid 172 of CCR5 - analogous to E205 of CCR4 - to alanine rendered the mutant unable to bind the chemokine CCL3. It was suggested that this was due to the removal of the negative charge of the amino acid (Blanpain et al., 2003). However, an E172D mutant was not investigated in the course of this study to determine whether amino acid charge or shape was the critical factor in chemokine binding. Mutations of several glutamic acid residues of CCR3 showed that those in the second extracellular loop were required for receptor trafficking to the cell-surface and for binding of CCL26 due to their negative charge. Other charged residues in the third extracellular loop were also required for CCL11 binding to the receptor (Duchesnes et al., 2006).

The ability of the E205 mutants to bind CCL17 and CCL22 was also investigated in this project, and the results mirror those of the expression and chemotaxis assays (figure 4-8). E205Q binding of ^{125}CCL17 did not differ significantly to WT binding of the chemokine, however E205A and E205D showed significantly reduced total binding compared to CCR4. E205A and E205D also showed no significant difference between total and non-specific binding at the 0.1 nM ^{125}I-CCL17 concentration used in the assay. Since these mutants responded to CCL17 in chemotaxis assays with reduced potency, it can be concluded that binding was below the limits of detection in this assay since they likely bound the chemokine with a reduced affinity. Similar results were observed for the binding of ^{125}I-CCL22, however this assay was performed twice and as such statistical analyses could not be carried out.

In conclusion, the E205A and E205D mutations significantly reduced the cell-surface expression, chemotactic ability, and chemokine binding ability of CCR4, likely due to the shortening of the glutamic acid side chain. Since the E205Q mutant retained its cell-surface expression, functional and binding properties, the negative charge of glutamic acid is therefore not a critical requirement for the function of this amino acid. To investigate the precise effect of mutation on chemokine binding, saturation binding assays would need performed using both ^{125}I-CCL17 and ^{125}I-CCL22 in order to determine how chemokine affinities for the mutant receptors may have changed. Saturation assays use increasing concentrations of radiolabelled chemokine in order to determine the binding affinity of the chemokine, the K_d, and also the number of chemokine binding sites, the B_{max}.

The I286A mutant would be another target for saturation binding assays. Transfectants of this mutant migrated to CCL17 at a significantly reduced efficacy and potency, and to CCL22 at a decreased potency and increased efficacy (figure 4-6, panels S and T). This result is interesting in that the mutation had differential effects on the responses of the receptor to the two chemokines. The position of I286 in transmembrane helix VII may signify a role in chemokine activity, since it lies on same side of the helix as the conserved GluVII:06 (E290). Despite the changes in migratory responses of the mutant, there was no detectable binding of 0.1 nM ^{125}I-CCL17 and ^{125}I-CCL22 to the I286A mutant (figure 4-8, panels G and H). As with the E205A and E205D mutants, binding is likely below the limits of detection for this assay, and saturation binding assays would be required to fully investigate the loss of binding affinity that has likely occurred as a result of this mutation.

The E290 mutations had similar effects as the E205 mutants on cell-surface expression; the aspartic acid mutation showed a reduction in cell-surface expression compared to the WT receptor, indicating that the shape of the glutamic acid rather than the charge was important for trafficking. The E290A mutant showed a trend toward a reduction in expression, while the E205Q mutant showed normal expression. As with the E205 mutants, it shows that restoration of side group shape in the form of the glutamine mutation rescued receptor expression.

In addition, the mutation of this residue ablated chemokine binding and function of the receptor. As previously described in section 3.3.2, the conserved

GluVII:06 of CCR4, in this case E290, likely forms networks of bonds necessary for receptor conformations that recognise chemokine.

Apart from the E290 mutants, the other transmembrane mutants that showed a decrease in surface expression were S114A, Y122A, F173A, L209A, Y258A, and Y258F. Like E290, these amino acids have been shown to be required for cell-surface expression of the receptor, possibly due to intramolecular interactions they form with other parts of the receptor. For example, π-stacking, the non-covalent interaction of aromatic rings, can occur between tyrosine and other aromatic amino acids such as phenylalanine. Tyrosines 120 and 124 in helix III of CCR2, analogous to Y117 and Y122 here in CCR4, have been shown to form these π-stacking interactions to stabilise receptor structure. Similar interactions between a tyrosine and a phenylalanine have been shown in CCR5 (Hall et al., 2009). Therefore, mutations of Y122, F173 and Y258 may have perturbed these interactions, leading to a detrimental shift in receptor conformation and ultimately reduced cell-surface expression. Serine is important due to the hydrogen-bonding capacity of its hydroxyl side-group interacting with other membranes of α-helices (Ballesteros et al., 2000). Leucine is commonly a component of transmembrane helices due to its hydrophobicity. This may explain why the S114A and L209A mutants also showed a reduction in cell-surface expression.

While some CCR4 mutants, such as E205A and E205D, showed a concomitant decrease in cell-surface expression, chemotaxis and binding ability, the effects of other mutations on receptor phenotype were more complex. The S114A mutant had reduced expression but only lost chemotactic efficacy to CCL17 but not CCL22, indicating that serine 114 was more important for CCL17-induced conformations of CCR4 than CCL22-induced conformations. This could also be explained by the lower efficacy of CCL17. A similar result was observed for the L209A mutant. The F173A mutant showed reduced expression, but chemotactic responses were normal. Taken together the various mutations show that some amino acids of CCR4 are required for expression, others for functional response to one chemokine and others to both, and some are also required for chemokine binding. This supports the results shown in chapter 3, which suggested that CCR4 has distinct conformations that are stabilised by CCL17 and CCL22

Three major determinants of CCR4 function were the two conserved tyrosines in helix III, Y117 and Y122, and Y258 in helix VI. All three tyrosine to alanine mutations resulted in non-functional CCR4. When these mutants were also tested in binding assays, they showed a lack of binding to ^{125}I-CCL17 and ^{125}I-CCL22, based on two experiments. These data show that the tyrosine side-chain is likely critical for binding of chemokine, and thus receptor function. This may be due to the previously described π-stacking of the aromatic rings of the tyrosine side-chain. This is supported by the fact that mutation to phenylalanine, which also contains an aromatic ring, restored chemotactic ability to all three mutants. However since this restoration was at a reduced level, it may suggest that the hydroxyl group of the tyrosine side chain, lacking in phenylalanine, is necessary for hydrogen bond formation. Binding studies also showed a trend toward restoration of the ability of the Y117 and Y122 phenylalanine mutants to bind ^{125}I-CCL17 and ^{125}I-CCL22.

Interestingly, mutations of the conserved tyrosine residues of helix III in other receptors do not have the same effect upon receptor phenotype. For example, Y113A CCR1 mutant transfectants responded in the same manner as WT transfectants to CCL3 in chemotaxis assays (de Mendonça et al., 2005). A similar mutation in CCR3 was also still able to induce a normal chemotaxis response to CCL11 (Wise et al., 2007). In summary, the CCR4 data demonstrate the importance of the aromatic side chain of these three tyrosines in receptor function, likely due to it forming stabilising interactions necessary for chemokine binding. When compared to the previous studies on CCR3 and CCR1, it may suggest that the importance of particular amino acids in receptor function and chemokine binding are receptor-specific.

Another critical determinant of CCR4 function and chemokine binding was L92, located within the highly conserved TXP motif in transmembrane helix II. This motif is present in nearly all human and murine chemokine receptors; in most receptors the first amino acid is threonine, while in CCR4 and CCR8 it is serine. Leucine is commonly the second amino acid in this motif, while the third is always proline (Govaerts et al., 2001). The L92A mutant of CCR4, despite showing above normal cell-surface expression, was non-functional in chemotaxis assays. Further investigation of this mutant in chemokine binding assays revealed that it did not bind ^{125}I-CCL17 or ^{125}I-CCL22. Mutation of the threonine and proline residues of the TXP motif of CCR5 to alanine reduced the ability of the receptor to bind CCL3 and CCL4.

Mutation of the leucine of this motif was not investigated in this study (Govaerts et al., 2001). An L87A of CCR1 however showed normal binding of CCL3 but impaired receptor activation (de Mendonça et al., 2005).

It was determined that the TXP motif of CCR5, potentially due to the helical kink introduced by the proline, orients the extracellular portion of transmembrane helix II. This portion of the helix is involved in the activation process of the receptor; the high concentration of aromatic residues at the extracellular ends of helices II and III suggest mediation of helical interactions necessary for activation (Govaerts et al., 2001; Govaerts et al., 2003). Mutational studies of CCR5 also suggested an interaction between the N-terminus of chemokines with the TXP motif in the chemokine receptor transmembrane bundle (Blanpain et al., 2003). The L92A CCR4 mutation is therefore likely disrupts this key TXP motif, leading to the observed loss of chemokine binding and receptor functionality.

4.3.2 – The effect of site 1 point CCR4 point mutation on antagonist activity

Following the characterisation of the point mutants, several were then tested against the site 1 antagonists in chemotaxis and chemokine binding assays. The rationale for this was that a residue critical for antagonist activity would result in reduced antagonist effectiveness upon mutation. Since the chemotaxis assays involved the inhibition of migration, only mutants that exhibited a functional response could be antagonised in this manner. The highly conserved GluVII:06 of transmembrane helix VII has previously been implicated in the binding of intrahelical allosteric antagonists (see section 1.4.4.1). However the E290A, E290D and E290Q mutants of this amino acid were non-functional in chemotaxis assays, meaning that these mutant receptors could not be antagonised in chemotaxis assays. The Y117A, Y122A, Y258A and L92A mutants, which were also non-functional could not be tested for the same reasons. The GluVII:06 mutants were however directly tested for their ability to bind radiolabelled antagonist, shown in chapter 6.

The majority of the mutants tested in chemotaxis antagonism assays did not differ significantly to WT CCR4 with respect to inhibition of migration; these were I113A, Y117F, F121A, F126A, F173A, K188A, S202A, I206A and Y258F. Transfectants of the Δ40 truncation, in which the last 40 amino acids of CCR4 were removed, were also tested for their sensitivity to the antagonists in chemotaxis assays. Since the site 1 antagonists were not hypothesised to contact the C-terminus, this truncation should not have resulted in a potency shift of the antagonists. The results of the chemotaxis assays confirmed this.

The I125A mutant showed a significant reduction in potency to inhibition of migration to CCL17 and CCL22 by antagonist 7, indicating that isoleucine 125 within transmembrane helix III was involved in antagonist binding. The Y122F mutant, also in the same region, showed a large drop in potency when inhibition of CCL22 chemotaxis by antagonist 7 was assessed, but interestingly not to migration of CCL17. This suggests that the removal of the hydroxyl group of the tyrosine hindered inhibition of the CCL22-induced response, possibly due to the removal of hydrogen-bonding capacity of this amino acid. This result supports the idea described in chapter 3 that CCL17 and CCL22 activate the receptor in different ways, since an interaction has been identified that inhibits CCL22 but not CCL17.

Modelling of the interaction of the allosteric antagonist BX 741 with CCR1 predicted that strong hydrophobic and π-stacking interactions occurred between the conserved tyrosines of helix III and the piperazine and phenyl rings of the antagonist, and a possible weak hydrogen bond interaction with the urea group (Vaidehi et al., 2006). Antagonist 7 contains three aromatic rings, which have the potential for stacking and hydrophobic interactions. Since the removal of hydrogen-bonding capacity of CCR4 with the Y122F mutant resulted in a reduction in antagonist potency, it may be the case that Y122A mutation removed the stronger hydrophobic and stacking interactions. However, the fact that Y122A was non-functional prevented confirmation of this. In the previously described study, alanine mutations of these tyrosines retained their functionality, which allowed dissection of the relative contribution of hydrogen-bonding and other interactions resulting from the tyrosine side chain (Vaidehi et al., 2006).

The most significant loss of antagonist potency was against the L118A mutant. This mutation significantly reduced the ability of antagonist 7 to inhibit migration to CCL17 and CCL22, with approximately a hundred-fold reduction in potency in the dose-response curves. L118, like Y122 and I125, is located in the third transmembrane helix, which contains a cluster of amino acids predicted to be sites of antagonist binding. This leucine may be involved in hydrophobic interactions with the antagonist; analysis of antagonist binding pockets of β_1- and β_2-adrenergic receptors reveals the presence of a valine residue facing inwards to the pocket (Nygaard et al., 2009). Leucine and valine, along with isoleucine are hydrophobic aliphatic amino acids, meaning that they contain branched carbon chain side groups. Leucine and isoleucine contain four carbons in their side chains in different arrangements while valine contains three.

The ability of antagonist 7 to inhibit ^{125}I-CCL17 and ^{125}I-CCL22 binding to L118A CCR4 was also investigated. Figure 4-8E and F showed that the mutant bound chemokine; in line with the increased cell-surface expression of the receptor, L118A CCR4 bound a higher level of chemokine than the WT receptor. Also in agreement with the chemotaxis inhibition assays, antagonist 7 showed reduced potency against the mutant receptor. Figure 4-14 showed that the antagonist was less able to inhibit binding of ^{125}I-CCL17 and ^{125}I-CCL22. When placed in context with the chemotaxis data these data suggest that antagonist 7 prevents chemokine binding, and that the mutation of leucine 118 to alanine hinders this to a significant degree. This is

consistent with the definition of allosteric modulators, which decrease the activity of the orthosteric ligand of the receptor (Bridges and Lindsley, 2008).

The fact that inhibition only by antagonist 7 was affected by the site 1 CCR4 mutations indicates that this compound has unique features that contact the mutated residues. Since the other antagonists were not affected, it suggests that these did not contain structural features that required the mutated amino acids. Figure 4-1 shows antagonist 7 is of a different structural class to antagonist 3 and 4; the latter are identical apart from the presence of the extra pyridine group in antagonist 3. As described in 4.2.4, the use of antagonist 1 was discontinued due to persistent difficulties regarding its solubility. Inhibition curves using this antagonist were very variable, and often produced inconsistent results.

It is important to note that since the mutants L92A, Y117A, Y122A, Y258A, E290A, E290D, and E290Q were non-functional, it cannot be concluded that the antagonists do not contact that these residues. It may be the case that the effects on L118A, Y122F and I125A result from minor changes in antagonist binding and that the major contact points have yet to be determined. GluVII:06 is involved in the binding of several antagonists to many different chemokine receptors, as it acts as major point of contact for the quaternary nitrogen that is shared by many small molecule inhibitors of these receptors. For example, CCR5 inhibitor Maraviroc, which is clinically approved for the treatment of HIV, is an allosteric antagonist that contacts the conserved GluVII:06 residue (Dorr et al., 2005; Garcia-Perez et al., 2011). Another CCR5 inhibitor, TAK-779, also contacts this residue (Dragic et al., 2000). GluVII:06 of CCR4 is therefore likely a point of antagonist contact; assays investigating direct binding of a site 1 antagonist are presented in chapter 6.

4.3.3 – Summary

In summary, the mutants of amino acids predicted by molecular modelling to be sites of antagonist contact were varied in their phenotype. Several mutants such as I113A, K188A, and S202A showed no difference to WT CCR4 in terms of cell-surface expression and chemotactic ability. Others, such as Y117A, Y122A, Y258A and the GluVII:06 mutations E290A, E290D, and E290Q did not bind chemokine or induce chemotaxis to either ligand. This reflects the critical role these residues play in both chemokine binding and receptor activation, likely due to stabilising interactions they form with ligand and other regions of CCR4.

Antagonism of chemotaxis induced by these mutants revealed that L118A, Y122F and I125A CCR4 responded with reduced potency to inhibition by antagonist 7. Binding of radiolabelled chemokines to L118A CCR4 was poorly inhibited by antagonist 7. The non-functional mutants could not be antagonised in these assays, highlighting the need for further studies using direct methods of investigating the effect of mutations of antagonist activity.

5 – Investigation of intracellular CCR4 antagonists by receptor point mutation and truncation

5.1 – Introduction

Chapter 4 focused on the effects on four intrahelical allosteric antagonists; these were hypothesised to bind within the transmembrane domains and inhibit receptor function. The remaining three antagonists will be investigated in this chapter in a similar manner, by using receptor mutations to identify potential antagonist binding sites.

These three antagonists – denoted 2, 5 and 6 – are hypothesised to bind to an intracellular site on the C-terminus of CCR4 termed ‘site 2’. This intracellular mode of binding is relatively novel compared to the previously described intrahelical antagonist binding (section 4.1), as it was only recently that an intracellular site was described.

As described in section 1.4.4.1, C-terminal exchanges of CCR4 and CCR5 showed that some antagonists were specific to the CCR4 C-terminus. The CCR4-5 chimera (CCR4 with a CCR5 C-terminus) was unable to respond to the antagonists, while the CCR5-4 chimera was able to do so. Carboxylic acid derivatives of the compounds were less able to pass through the membrane and antagonise the CCR4 C-terminus, while ester derivatives were more lipophilic and as such had higher activity. The use of membranes or permeabilised cells also increased the activity of the carboxylic acid derivatives. These findings were therefore taken to shown that some antagonists bound an intracellular site (Andrews et al., 2008). Similar observations were noted regarding CXCR1 and CXCR2; a C-terminal swap between the two receptors transferred antagonist sensitivity, in addition to the fact that antagonists required properties such as lipophilicity and hydrogen bonding capacity in order to pass through the membrane (Nicholls et al., 2008). Further research on CXCR2 showed that in intracellular residue, K320, was an important point of antagonist contact; a K320A mutant had reduced antagonist binding potency by a factor of 5 compared to WT CXCR2 (Salchow et al., 2010).

The three intracellular antagonists described here are pyrazinyl sulphonamides, the structures of which are shown in figure 5-1. The three structures share the same basic core; a sulphur atom bound to two oxygen atoms and two side-groups, including the aromatic pyrazine. Antagonist 2 was previously used in the study that originally identified the intracellular CCR4 antagonists (Andrews et al., 2008).

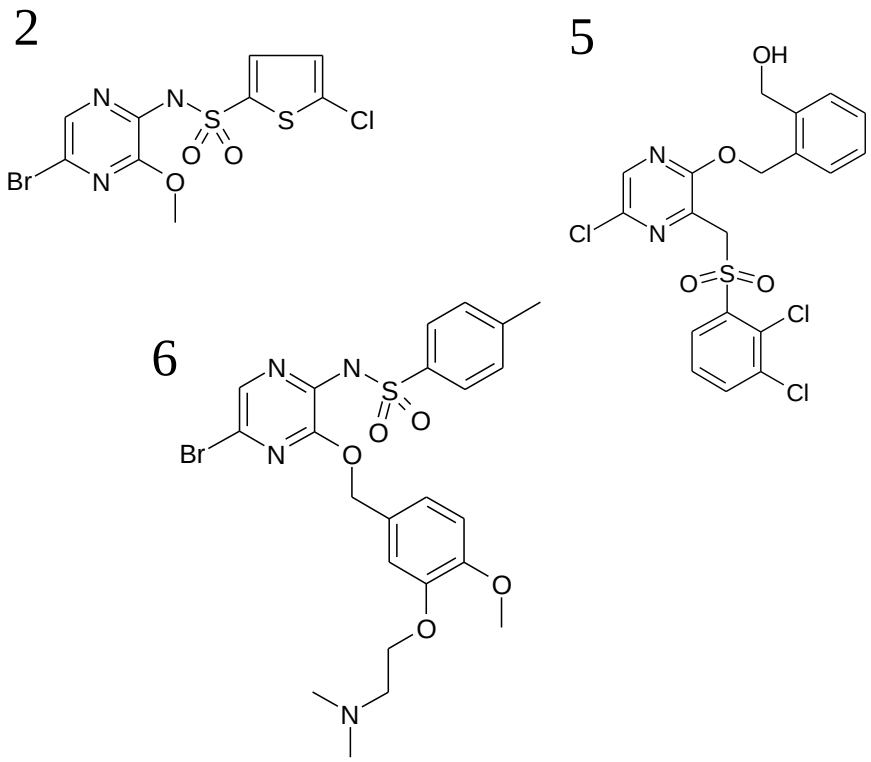

Figure 5-1 – Site 2 antagonists

The structures of the three site 2 (intracellular) allosteric antagonists; denoted 2, 5 and 6. These were supplied by GSK, and based on functional studies and the work by Andrews et al., 2008 were hypothesised to bind to the C-terminus of CCR4. Molecular modelling was performed to identify likely contact points on the receptor.

As in chapter 4, molecular modelling identified several amino acids potentially involved in antagonist binding to site 2; these amino acids were mutated in order determine their contribution to antagonist binding. Figure 5-2 shows a cartoon of CCR4 with the residues highlighted in green. Two amino acids, phenylalanine 305 (F305) and leucine 307 (L307), were located at the end of transmembrane helix VII. Lysine 310 (K310) and leucine 318 (L318) were located in the C-terminus, within the conserved helix VIII region.

Phenylalanine 305 was mutated to alanine, which as previously described in section 4.1 is a small, neutral and non-polar amino acid. Phenylalanine by contrast is much larger due to its benzene ring, but like alanine is hydrophobic. Therefore the mutation removed the bulk associated with phenylalanine but retained the hydrophobicity of the residue. Leucine 307 was mutated to valine, which was a relatively conservative mutation; both have branched aliphatic side-chains, leucine containing one extra carbon in the chain than valine. The differences in structure between leucine and valine are shown in figure 5-3, panels A and B.

The C-terminal helix VIII residue lysine 310 was mutated to asparagine; these two amino acids have different ionisation states at physiological pH (Salchow et al., 2010) but do not differ enough structurally for the mutation to adversely affect helical structure. These amino acids are shown in figure 5-3, panels C and D. Leucine 318 was mutated to alanine.

In addition to the point mutations, three truncations of the receptor were made by mutating the codon at the desired truncation position to a stop codon; the sites of these truncations are labelled in red in figure 5-2. Δ40 CCR4 had the last 40 amino acids of the C-terminus deleted, directly after the end of helix VIII. Δ45 and Δ50 CCR4 were truncations that cut into helix VIII, with Δ50 CCR4 cutting almost to the end of transmembrane helix VII. Receptor truncations have been previously used to investigate receptor function. CCR5 truncations demonstrated that the proximal end of the C-terminus was required for receptor signalling (Gosling et al., 1997); this region is homologous to the helix VIII motif in CCR4, indicating the potential effects CCR4 truncations will have on receptor function. Truncation downstream of this region in CXCR4 resulted in reduced receptor phosphorylation and thus β-arrestin recruitment, leading to poor regulation of receptor-mediated signalling (Cheng et al., 2000). Natural truncations of the distal C-terminus of CXCR4 lead to gain-of-function mutations that result in the rare immunodeficiency disorder WHIM

syndrome (warts, hypogammaglobulinemia, infections and myelokathexis) (Liu et al., 2012b).

Figure 5-3, panel E summarises the CCR4 mutants that were made to investigate site 2 antagonist binding, along with their location within the receptor.

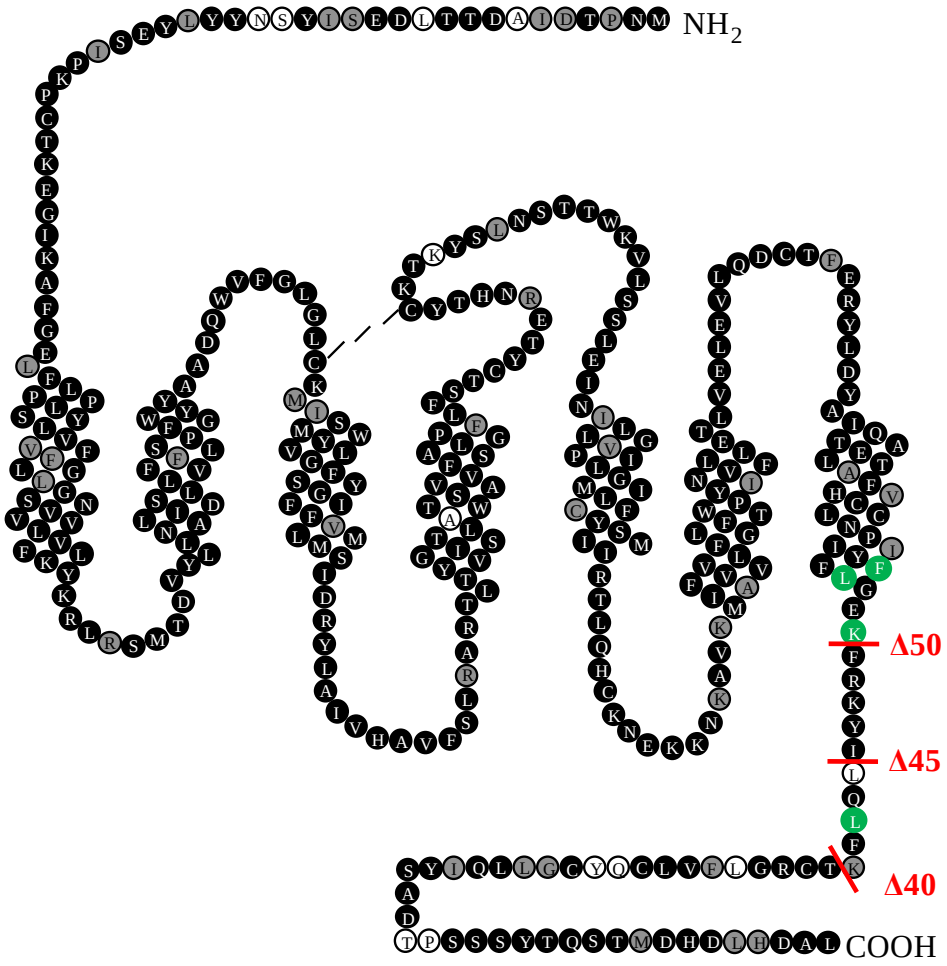

Figure 5-2 – Amino acids and regions implicated in site 2 antagonist binding

Cartoon of CCR4; highlighted in green are amino acids hypothesised to bind the site 2 intrahelical antagonists. Shown in red are sites of three successive C-terminal truncations.

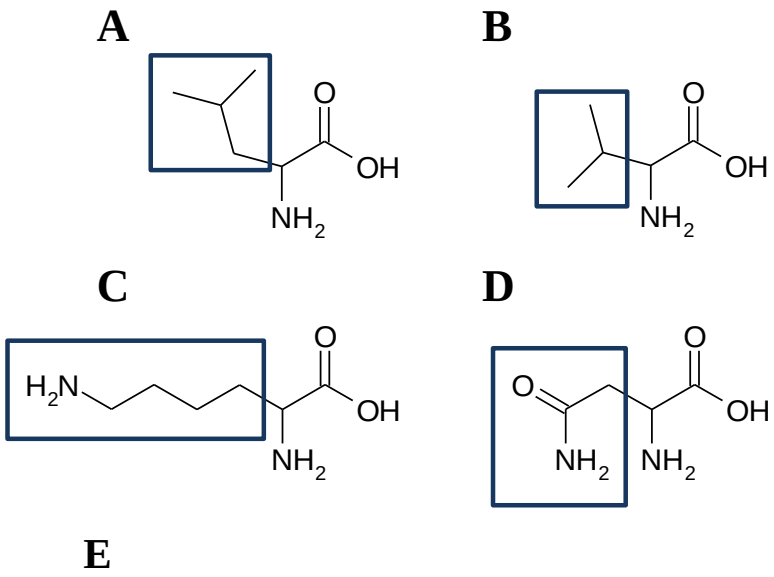

E

Location	TM7	C-terminus
Mutation	F305A	K310N
	L307V	L318A
		Δ50 truncation
		Δ45 truncation
		Δ40 truncation

Figure 5-3 – Site 2 amino acid point mutations and receptor truncations

Structures of amino acids; leucine 307 (A) was mutated to valine (B), and lysine 310 (C) was mutated to asparagines (D). Amino acid side chains are highlighted. Panel E shows a summary table of the site 2 point mutants and truncations along with their location in the receptor.

5.2 – Results

5.2.1 – Cell-surface expression of site 2 CCR4 mutants

Following site-directed mutagenesis of WT CCR4, the plasmids containing the CCR4 constructs were transfected into L1.2 cells, which were analysed the following day for surface expression by flow cytometry.

Figure 5-4 shows the relative cell-surface expression of the CCR4 mutants compared to WT CCR4. Of the point mutants, F305A and L307V showed significant reduction in cell-surface expression relative to WT; 70% and 73% of WT levels, respectively. The other point mutants, K310N and L318A, did not show expression levels significantly different to that of WT. The Δ40 mutant also showed no difference compared to WT with respect to cell-surface expression. The Δ45 and Δ50 mutants however, which were truncations into helix VIII, showed significantly reduced expression; 20% and 30%, respectively. The relative change of each mutant compared to WT is summarised in table 5-5.

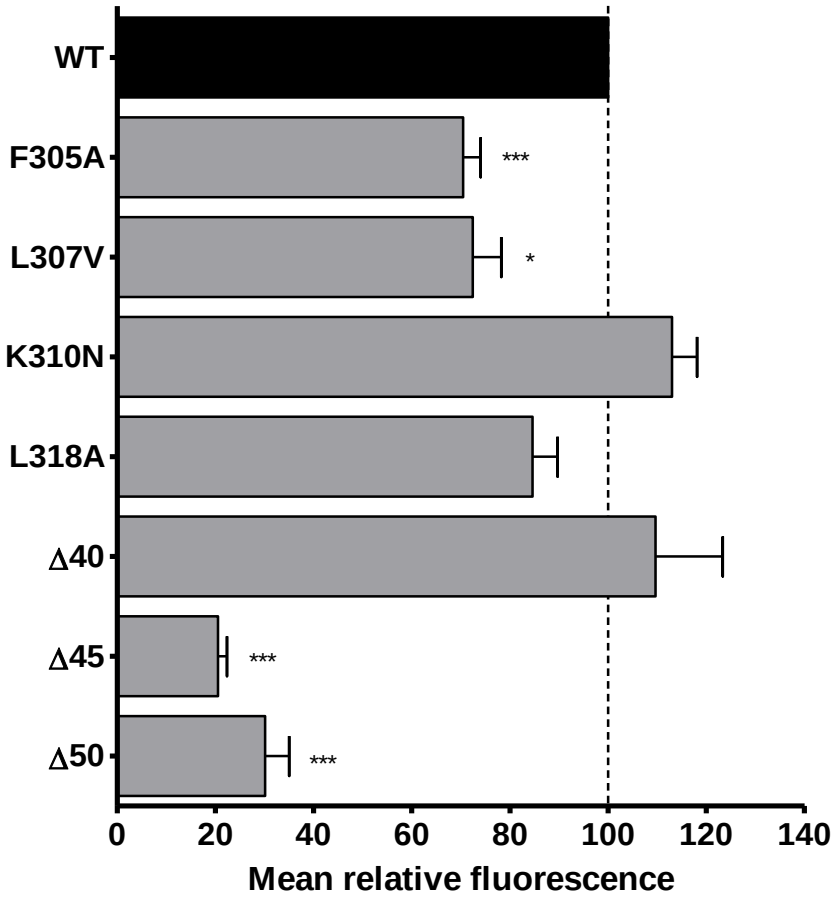

Figure 5-4 – Cell-surface expression of site 2 CCR4 point mutants

L1.2 cells were transiently transfected with WT and mutant CCR4 pcDNA and the following day analysed for cell surface expression by flow cytometry. The black bar shows WT CCR4, grey bars show individual point mutants. Data are presented as percentage of WT expression, and as the mean ± SEM of three independent experiments. Data were analysed by one-way ANOVA. Significance stars *, ** and *** represent p values of 0.05, 0.01, and 0.001 respectively.

Mutant	Relative expression	Mutant	Relative expression
F305A	↓	**Δ40**	-
L307V	↓	**Δ45**	↓
K310N	-	**Δ50**	↓
L318A	-		

Table 5-5 – Change in cell-surface expression of site 2 CCR4 point and truncation mutants

Summary table of the relative expression changes from figure 4-4. - = no change relative to WT, ↑ = increase relative to WT, ↓ = decrease relative to WT.

5.2.2 – Migratory potential of site 2 CCR4 mutants transfectants to CCL17 and CCL22

Following analysis of cell-surface expression, L1.2 cells transfected with the CCR4 site 2 point mutants and truncations were assessed for their ability to migrate to CCL17 and CCL22 in chemotaxis assays. As before, these were performed with chemokine concentrations ranging from 0.1 nM to 100 nM. WT CCR4 transfectants were used as a reference in all cases.

Figure 5-6 shows the results of the chemotaxis assays. F305A transfectants showed no difference to WT for either the CCL17 (A) or CCL22 (B) response in terms of efficacy or potency. L307V transfectants showed reduced efficacy to CCL17-induced migration; at 1 nM the chemotactic index was 19, compared to 33 for WT CCR4 transfectants (C). The potency of chemokine was unaffected by this mutation. The CCL22 response was also no different to WT (D). Interestingly the K310N mutant did not induce migration to CCL17 (E), but did induce migration to CCL22 (F); the chemotactic index for CCL17 was significantly reduced compared to WT, and not significantly different to the level of migration observed to buffer. Migration to CCL22 also showed a reduction in efficacy; at 1 nM a chemotactic index of 31 was observed for K310N, compared to 61 for WT. L318A showed a similar phenotype, in that CCL17-induced migration was significantly reduced (G) with CCL22-induced migration being less affected (H). However in this case, it still induced a small chemotactic response to CCL17, with a chemotactic index of 9 compared to 43 for WT.

For the receptor truncations, Δ40 showed a significant increase in chemotactic efficacy for both chemokines. The Δ40 transfectants migrated to CCL17 with a peak chemotactic index of 60, compared to 25 for WT transfectants (I). They migrated to CCL22 with a peak chemotactic index of 100, compared to 60 for WT (J). The Δ45 and Δ50 truncations showed the most marked change in chemotaxis; both mutants did not show migration to either chemokine at any concentration. For all data points, the chemotactic indices were no different to those observed for migration to buffer alone (K and L). This may be explained in part by the poor truncation surface expression.

Table 5-7 shows a summary table of the point mutants and truncations, indicating the relative changes in potency and efficacy of migration compared to WT CCR4.

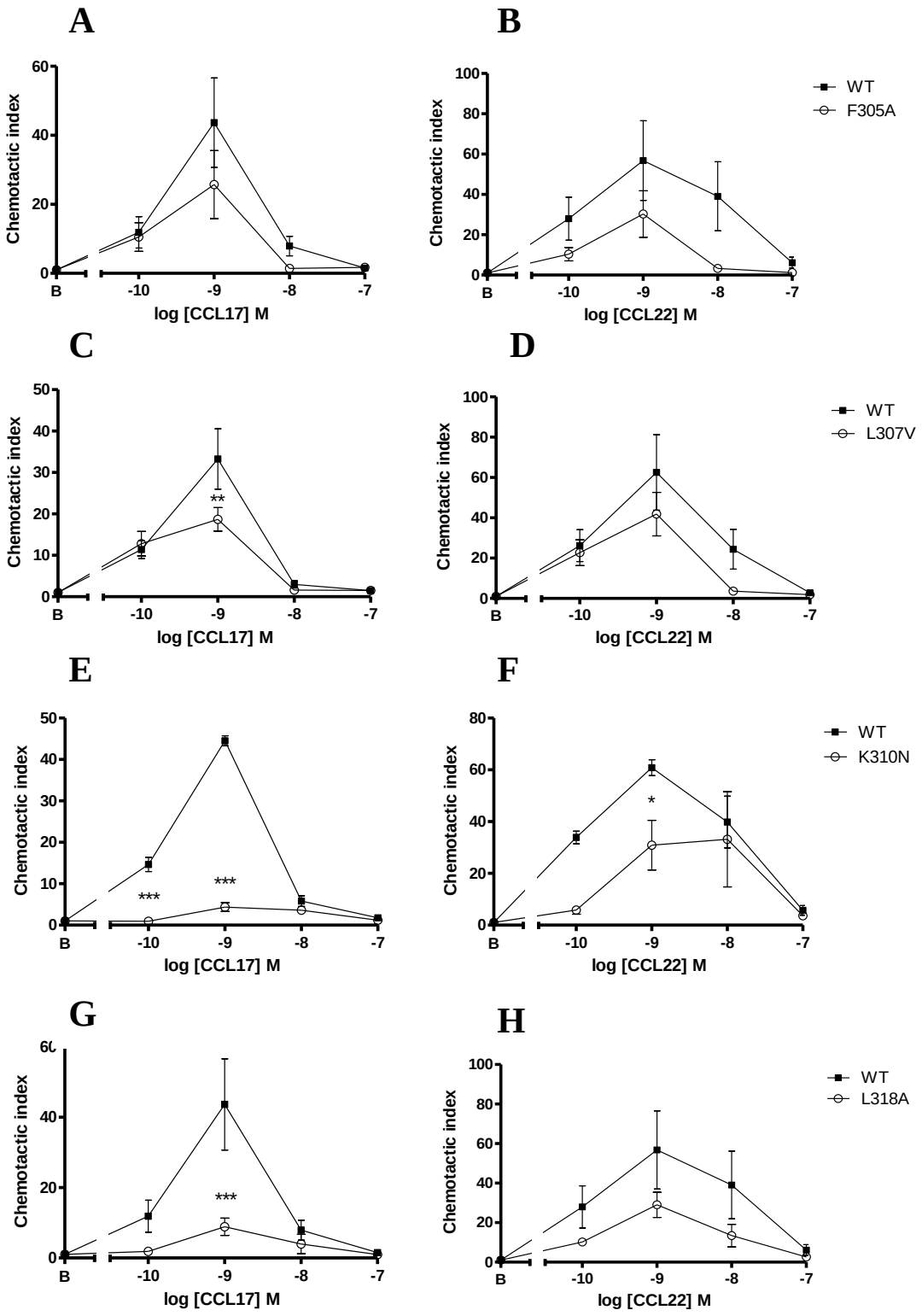
A
B
C
D
E
F
G
H
Chemotactic index
log [CCL17] M
log [CCL22] M
B
-10
-9
-8
-7
WT
F305A
L307V
K310N
L318A
**
***
*

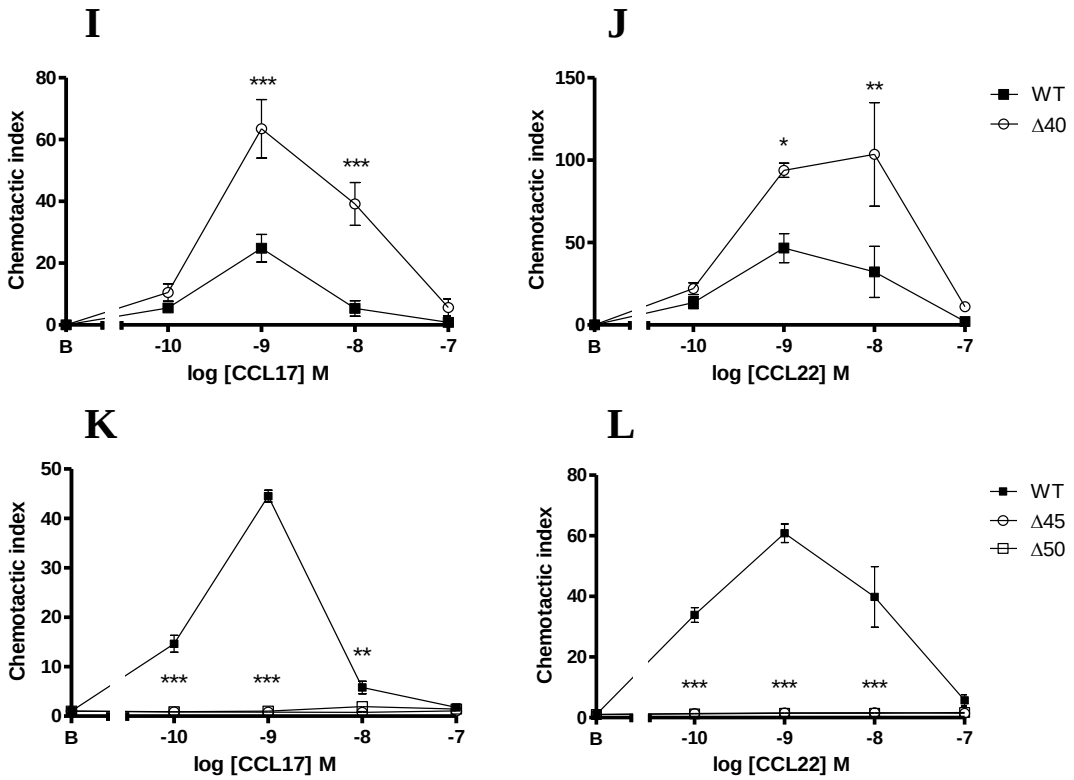

Figure 5-6 – CCR4 point mutation and truncation affects chemotaxis of transfectants to both CCL17 and CCL22

Panels A-L: Following analysis of cell-surface expression, WT and mutant CCR4 transfectants were assessed for their ability to migrate to soluble CCL17 (left-hand column) and CCL22 (right-hand column). WT responses are shown as filled squares; mutants as open circles, squares and triangles. Data are the mean ± SEM of three independent experiments, and were analysed by two-way ANOVA and a Bonferroni post-test. Significance stars *, ** and *** represent p values of 0.05, 0.01, and 0.001 respectively.

	CCL17		CCL22	
	Efficacy	Potency	Efficacy	Potency
F305A	-	-	-	-
L307V	↓	-	-	-
K310N	NR	NR	↓	-
L318A	↓	-	-	-
Δ40	↑	-	↑	-
Δ45	NR	NR	NR	NR
Δ50	NR	NR	NR	NR

Table 5-7 – Changes in chemotactic responses resulting from CCR4 site 2 point mutation and truncation

Summary table of the effect of point mutations on efficacy and potency of the chemotactic response from figure 5-6. - = no change, NR = no response, ↑ = increase in efficacy/potency, ↓ = decrease in efficacy/potency.

5.2.3 – Binding of radiolabelled chemokine to site 2 CCR4 mutant transfectants

After receptor cell-surface expression was confirmed, and chemotaxis assays had been performed, the K310N and Δ40 CCR4 mutants were investigated for their ability to bind ^{125}I-CCL17 and ^{125}I-CCL22. These mutants were chosen due to the distinct phenotypes they induced in chemotaxis assays.

Figure 5-8 shows the results of a whole-cell binding assay in which WT and K310N transfectants were incubated with 0.1 nM ^{125}I-CCL17 (A) or ^{125}I-CCL22 (B) and either buffer or 100 nM unlabelled chemokine. The binding window for WT and K310N CCR4 was the same, indicating that the mutation did not affect chemokine binding. A t-test of the mean total binding values for both WT and K310N transfectants for both chemokines did not shown any significant difference.

The Δ40 mutant showed increased chemotactic efficacy in response to CCL17 and CCL22 (figure 5-6). When this truncation mutant was compared to WT CCR4 in binding assays, there was no observed increase in chemokine binding; in fact chemokine binding decreased compared to WT for both ^{125}I-CCL17 (C) and ^{125}I-CCL22 (D). These data however are from one experiment, which must be taken into consideration when comparing them to the more robust chemotactic data.

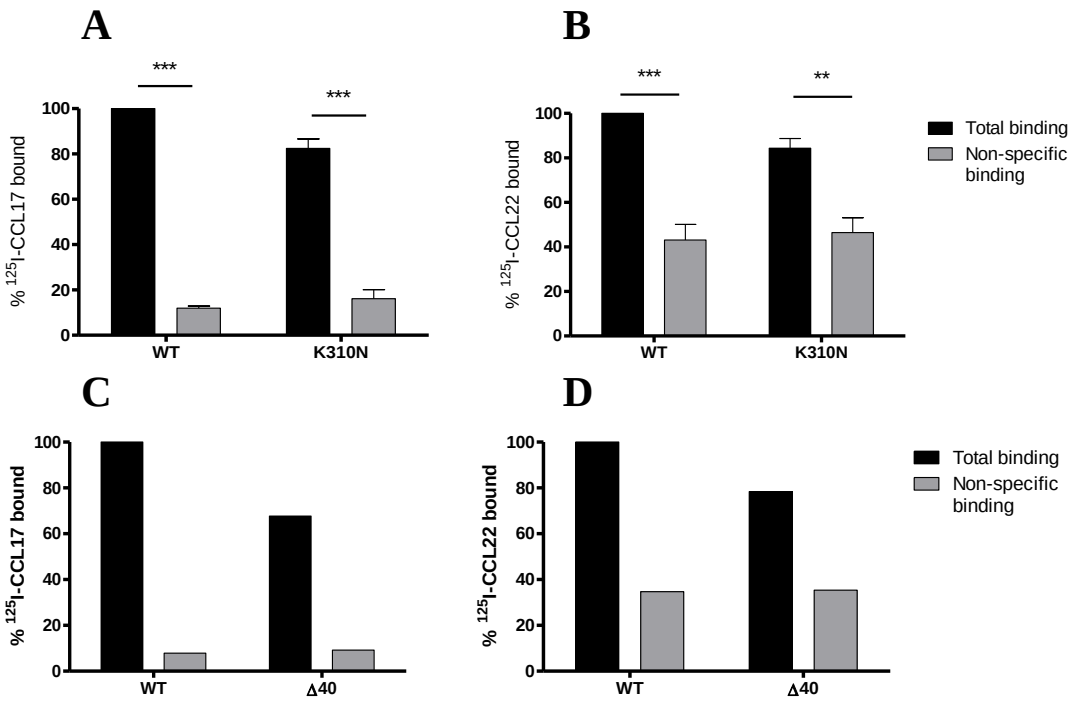

Figure 5-8 – Whole-cell chemokine binding of CCR4 point mutant and truncation transfectants

CCR4 transfectants were incubated with ^{125}I-CCL17 (left-hand column) or ^{125}I-CCL22 (right-hand column) and buffer (total binding; black bars) or excess unlabelled chemokine (non-specific binding; grey bars). Panels A and B show binding of K310N CCR4, panels C and D shown binding of Δ40 CCR4. Panels A and B are the mean ± SEM of three independent experiments, panels C and D are from one experiment. Significance stars ** and *** represent p values of 0.01 and 0.001 respectively.

5.2.4 – Antagonism of site 2 mutant chemotaxis

Following the investigation of site 2 mutant expression, function and chemokine binding, their sensitivity to antagonists was determined. As shown in figure 5-2, the site 2 antagonists were hypothesised to bind to an intracellular site on CCR4. This site included the C-terminal end of transmembrane domain 7 in addition to helix VIII, a highly conserved region located in the proximal portion of the C-terminus. By mutating these regions, their importance in antagonist activity could be determined; if a mutant lost sensitivity to an antagonist it could be inferred that the mutated residue was required for the activity of the antagonist.

Since figure 5-6 showed that the point mutants F305A, L307V, K310N and L318A were able to induce migration to chemokine, this chemotaxis was inhibited with the antagonists and the potency of the inhibition compared to WT. The Δ40 truncation was also tested since it showed a functional response. The Δ45 and Δ50 truncations however were not tested since they did not induce a functional response (figure 5-6 panels K and L). The K310N mutant only induced chemotaxis of transfectants to CCL22. Therefore, responses to CCL22 alone were subjected to antagonism with the compounds.

Figure 5-9 shows the results of the antagonism of WT and L307V CCR4-induced migration to CCL17 and CCL22. Increasing concentrations of the antagonists were used to inhibit maximal migration, and the data analysed using non-linear regression to generate $\log IC_{50}$ values. The values from the mutants were compared to those from the WT to determine whether antagonist potency was affected. This was performed with the three site 2 antagonists. Antagonist 7 was also tested against these transfectants as a control, since this antagonist was not hypothesised to bind the intracellular antagonist binding site. A summary table of the $\log IC_{50}$ values is shown in table 5-10. Antagonist 7 proved to be more potent that the others in inhibiting chemotaxis to both CCL17 and CCL22. Antagonist 2 was the least potent.

The data show that compared to WT, antagonist 2 was less potent at inhibiting CCL17-induced migration; it had a $\log IC_{50}$ of -5.74, compared to -6.30 for WT. This difference was statistically significant, with a p-value of 0.005. Antagonist 5 was less potent at inhibiting CCL22-induced migration of the L307V mutant, with a $\log IC_{50}$ of -6.45 compared to -7.70 for WT. This difference was also significant, with a p-value of 0.00086. T-tests of the remaining $\log IC_{50}$ values did not show a statistical

difference between WT and L307V. There was no difference between the $logIC_{50}$ values for antagonist 7.

This process was repeated for the other functional mutants, such as F305A, the results of which are shown in figure 5-11. The $logIC_{50}$ values from these experiments are shown in table 5-12, along with the results from table 5-10. F305A CCR4 showed a significant decrease in potency in the antagonist 5 inhibition of CCL22; WT transfectant migration was inhibited with a $logIC_{50}$ of -6.88 while F305A transfectant migration was inhibited with a $logIC_{50}$ of -5.71. This difference was significant with a p-value of 0.0031. Both L318A and Δ40 CCR4 did not affect the activity of the antagonists. K310N transfectants also did not show a reduction in antagonist potency.

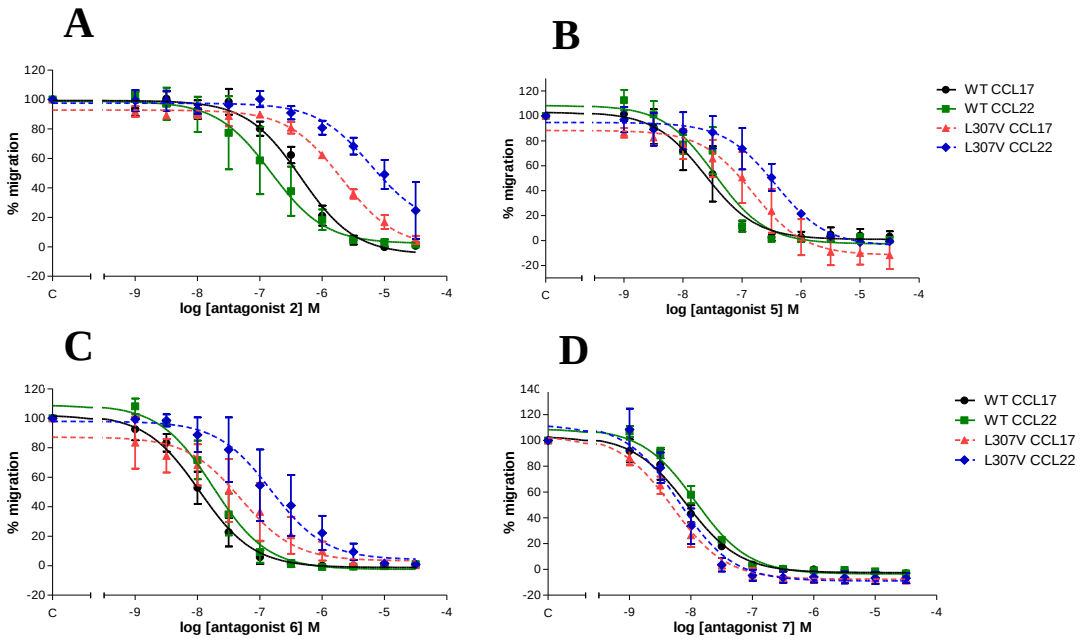

Figure 5-9 – Antagonism of L307V transfectant chemotaxis

Chemotaxis of L307V transfectants to CCL17 or CCL22 was inhibited with increasing concentrations of the site 2 antagonists, and compared to WT. Increasing concentrations of antagonists 2 (A), 5 (B), 6 (C), and 7 (D) inhibited migration to 1 nM CCL17 and CCL22. Data are the mean ± SEM of three independent experiments.

	CCL17			
CCR4 construct	*Antagonist 2* $logIC_{50}$	*Antagonist 5* $logIC_{50}$	*Antagonist 6* $logIC_{50}$	*Antagonist 7* $logIC_{50}$
WT	-6.30 ± 0.10	-7.72 ± 0.32	-7.97 ± 0.16	-8.11 ± 0.12
L307V	-5.74 ± 0.08	-6.79 ± 0.24	-7.03 ± 0.42	-8.30 ± 0.05
	CCL22			
CCR4 construct	*Antagonist 2* $logIC_{50}$	*Antagonist 5* $logIC_{50}$	*Antagonist 6* $logIC_{50}$	*Antagonist 7* $logIC_{50}$
WT	-6.07 ± 0.36	-7.70 ± 0.07	-7.74 ± 0.18	-7.94 ± 0.04
L307V	-5.29 ± 0.15	-6.45 ± 0.10	-6.77 ± 0.47	-8.20 ± 0.12

Table 5-10 – Potency of site 2 antagonist inhibition of WT and L307V transfectants
$logIC_{50}$ values are shown from figure 5-9. $logIC_{50}$ values were calculated using non-linear regression analysis, and two-tailed t-test used to compare values. Blue shaded columns indicate statistically significant differences between $logIC_{50}$ values; p values of 0.005 and 0.00086 for CCL17 and CCL22, respectively. $logIC_{50}$ values are from three independent experiments.

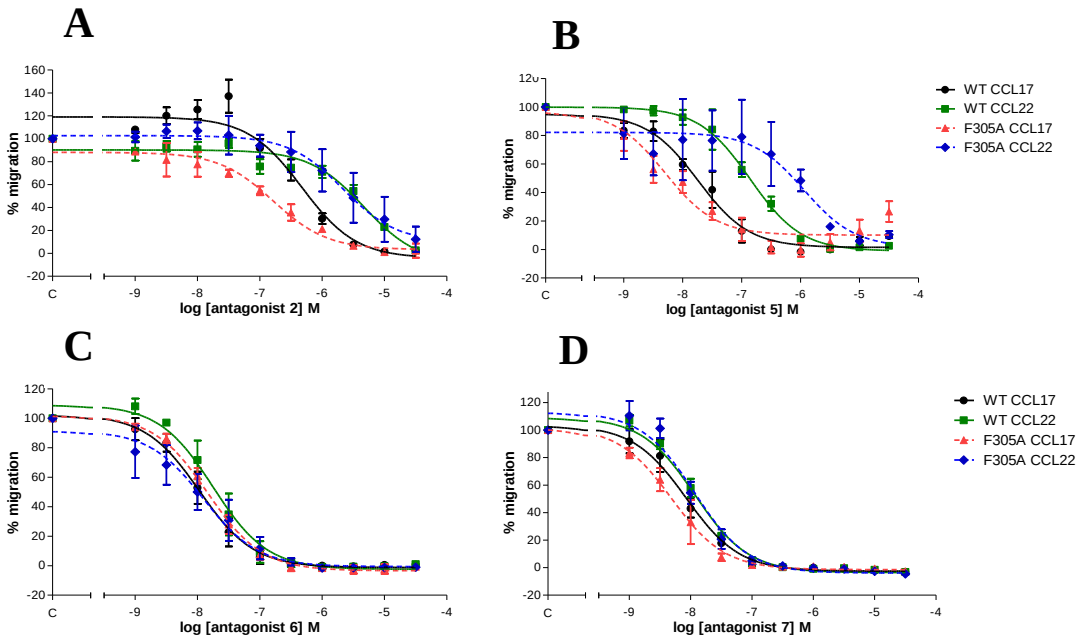

Figure 5-11 – Antagonism of F305A transfectant chemotaxis

Chemotaxis of F305A transfectants to CCL17 or CCL22 was inhibited with increasing concentrations of the site 2 antagonists, and compared to WT. Increasing concentrations of antagonists 2 (A), 5 (B), 6 (C), and 7 (D) inhibited migration to 1 nM CCL17 and CCL22. Data are the mean ± SEM of three independent experiments.

A

CCR4 Construct	Antagonist 2 $logIC_{50}$	Antagonist 5 $logIC_{50}$	Antagonist 6 $logIC_{50}$	Antagonist 7 $logIC_{50}$
WT	-6.34 ± 0.09	-7.70 ± 0.17	-7.97 ± 0.16	-8.11 ± 0.12
F305A	-6.72 ± 0.25	-7.94 ± 0.28	-7.83 ± 0.10	-8.32 ± 0.19
WT	-6.30 ± 0.10	-7.72 ± 0.32	-7.97 ± 0.16	-8.11 ± 0.12
L307V	-5.74 ± 0.08 (p=0.005)	-6.79 ± 0.24	-7.03 ± 0.42	-8.30 ± 0.05
WT	ND	ND	ND	ND
K310N	ND	ND	ND	ND
WT	-6.34 ± 0.09	-7.70 ± 0.17	-7.97 ± 0.16	-8.06 ± 0.01
L318A	-6.42 ± 0.08	-7.77 ± 0.11	-7.55 ± 0.43	-8.30 ± 0.19
WT	-6.33 ± 0.28	-7.62 ± 0.33	-7.83 ± 0.24	-8.06 ± 0.01
Δ40	-6.07 ± 0.18	-7.46 ± 0.21	-7.61 ± 0.11	-7.54 ± 0.17

B

CCR4 Construct	Antagonist 2 $logIC_{50}$	Antagonist 5 $logIC_{50}$	Antagonist 6 $logIC_{50}$	Antagonist 7 $logIC_{50}$
WT	-5.70 ± 0.34	-6.88 ± 0.15	-7.74 ± 0.18	-7.94 ± 0.04
F305A	-5.61 ± 0.44	-5.71 ± 0.09 (p=0.0031)	-7.64 ± 0.23	-7.94 ± 0.08
WT	-6.07 ± 0.36	-7.70 ± 0.07	-7.74 ± 0.18	-7.94 ± 0.04
L307V	-5.29 ± 0.15	-6.45 ± 0.10 (p=0.00086)	-6.77 ± 0.47	-8.20 ± 0.12
WT	-5.71 ± 0.49	-6.96 ± 0.35	ND	ND
K310N	-6.15 ± 0.53	-7.44 ± 0.38	ND	ND
WT	-5.35 ± 0.20	-6.88 ± 0.14	-7.74 ± 0.18	-7.97 ± 0.05
L318A	-5.66 ± 0.20	-6.92 ± 0.07	-7.25 ± 0.37	-8.29 ± 0.21
WT	-5.52 ± 0.76	-6.77 ± 0.27	-7.20 ± 0.10	-7.97 ± 0.05
Δ40	-5.39 ± 0.07	-6.64 ± 0.16	-7.16 ± 0.07	-7.64 ± 0.17

Table 5-12 – F305A and L307V CCR4 transfectant migration is inhibited with reduced potency by the site 2 antagonists

Non-linear regression was used to calculate the $logIC_{50}$ values for the site 2 antagonist inhibition of CCR4 point mutant migration to CCL17 (A) and CCL22 (B). Mutant $logIC_{50}$ values that were significantly different to WT are highlighted in blue, and the p-values of the t-tests shown in brackets. Data are the mean ± SEM of three independent experiments.

5.2.5 – Antagonism of chemokine binding to site 2 mutants

Following the antagonism of CCR4 mutant chemotaxis, the site 2 antagonists were used to dose-dependently inhibit ^{125}I-chemokine binding to the transfectants. L307V transfectants were investigated since they showed reduced sensitivity to the site 2 antagonists in chemotaxis assays. K310N transfectants were tested due to the unique functional phenotype they presented.

Figure 5-13 shows the inhibition of radiolabelled chemokine binding to CCR4 transfectants by increasing concentrations of the site 2 antagonists. Panel A shows inhibition of ^{125}I-CCL22 binding to WT and L307V CCR4 transfectants by antagonist 2. Binding to WT transfectants was inhibited with a mean logIC_{50} of -6.72 while binding to L307V transfectants was inhibited with a mean logIC_{50} of -5. This difference was statistically significant, with a p value of 0.034, showing that the L307V mutation made CCR4 less sensitive to inhibition of ^{125}I-CCL22 binding by antagonist 2.

Inhibition of chemokine binding to K310N transfectants was also investigated. Figure 5-13B shows inhibition of ^{125}I-CCL22 binding to transfectants by antagonist 5, while figure 5-13C shows inhibition of $^{`125}$I-CCL17 binding by antagonist 2. Both experiments were performed twice, meaning that statistical tests of p-values could not be carried out; however the graphs show that the inhibition curves of the mutants are very similar to the WT curves, indicating that the K310N mutation likely had no effect on antagonist inhibition of chemokine binding to the receptor. The WT and K310N inhibition curves produced similar logIC_{50} values.

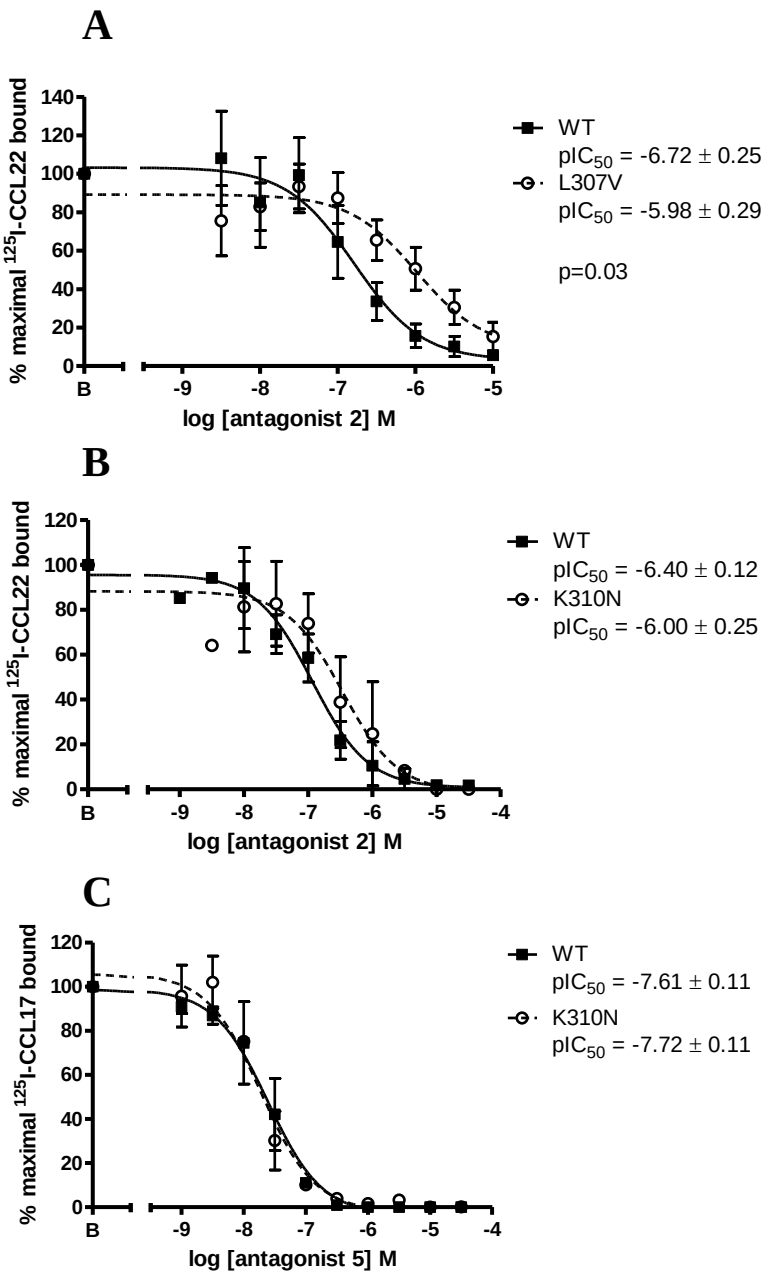

Figure 5-13 – Inhibition of chemokine binding to CCR4 transfectants by site 2 antagonists

Binding of ^{125}I-CCL22 (A and B) and ^{125}I-CCL17 (C) to CCR4 point mutant transfectants was inhibited with increasing concentrations of the site 2 antagonists 2 (A and B) and 5 (C) and compared to WT. Non-specific binding (100 nM unlabelled chemokine) was subtracted and the data presented as a percentage of binding without antagonist. Panel A is the mean ± SEM of four independent experiments; panels B and C are of two experiments. The logIC_{50} values of each dose-response curve are shown; panel A also shows the p value of the t-test of the WT and L307V values.

5.3 – Discussion

5.3.1 – Effect of site 2 mutations and truncations on receptor phenotype

In this chapter, point mutations of CCR4 residues implicated in site 2 antagonist binding were mutated. In addition three receptor truncations, Δ40, Δ45 and Δ50 were made. As in chapter 4, the receptor mutants were assessed for cell-surface expression, chemotactic and chemokine binding abilities. Following this, the potency of the antagonists in the inhibition of migration and chemokine binding was measured, in order to determine the contribution of each residue to antagonist activity.

5.3.1.1 – Phenotype of site 2 CCR4 point mutants

Four CCR4 C-terminal amino acids - F305, L307, K310 and L318 - were predicted by sequence comparison of the CCR4 and CCR5 C-termini to be points of contact for the site 2 antagonists. The mutants of these were F305A, L307V, K310N and L318A. The former two were located at the end of transmembrane helix VII, while the latter two were located in the highly conserved C-terminal helix VIII.

The F305A and L307V CCR4 mutants both showed reduced cell-surface expression, at approximately 75% of WT levels. L307V transfectants showed a significant reduction in migration to CCL17 compared to WT; however there was still a robust response. Migration to CCL22 was unaffected by this mutation. F305A-mediated migration to both chemokines was normal. These data show that despite the reduction in cell surface expression and migration of L307V transfectants to CCL17, both F305 and L307 are not critical for receptor function.

The K310N mutation was previously described in chapter 3, in context of biased agonism through CCR4. This mutant had normal cell surface expression and chemokine binding, but only mediated chemotaxis to CCL22 and not CCL17. This suggested that CCL22 and CCL17 stabilised distinct conformations and that K310 was required for the CCL17-induced conformation (see section 3.3.3).

The mutation of L318 to alanine did not have an effect on receptor expression (figure 5-4), but did however affect chemotaxis. L318A-mediated chemotaxis to CCL17 was significantly decreased in efficacy, although a reduced response still

occurred. Chemotaxis to CCL22 showed a trend to a reduction but this was not significant (figure 5-6). These results were similar to the K310N data, in that chemotaxis to CCL17 was more adversely affected than chemotaxis to CCL22. However the K310N mutant showed a complete lack of response to CCL17 while L318A retained a reduced response, albeit reduced compared to WT.

K310 and L318 lie within helix VIII, a highly conserved C-terminal region located in many receptors. Since the helix lies parallel to the membrane, one side faces the lipid membrane and the other faces the cytosol. Previous studies on helix VIII in other receptors have used helical wheel analysis to show that the helix is amphipathic, with hydrophobic residues of the helix clustered on one side, and polar and hydrophilic residues on the other. For example, helix VIII of rhodopsin was analysed using this tool and shown to have hydrophobic residues such as leucine and phenylalanine on the hydrophobic side, in contrast to hydrophilic and charged residues such as glutamic acid and lysine on the other (Krishna et al., 2002). Similar analyses were performed on the leukotriene B4 receptor 1 (Okuno et al., 2005; Aratake et al., 2012), the β_2-adrenergic receptor (Katragadda et al., 2004) and the cannabinoid receptor 1 (Ahn et al., 2010). Mutational analysis of the cannabinoid receptor 1, in which the hydrophobic residues were replaced with alanine, showed that they were required for ligand binding due to their role in receptor conformation (Ahn et al., 2010). In many GPCRs, the tyrosine of the conserved NPXXY motif of transmembrane helix VII forms π-stacking interactions with a conserved phenylalanine on the hydrophobic side of helix VIII, and is required for receptor activation in the chemokine receptor CCR5 (Fritze et al., 2003; Nygaard et al., 2009; Kraft et al., 2001).

Helical wheel analysis of the putative helix VIII region of CCR4 is shown in figure 5-14. A clear clustering of hydrophobic and charged/hydrophilic residues is present, indicating that the former likely faces the lipid membrane and the latter likely faces the cytosol. K310 is located on the hydrophilic side and L318 on the hydrophobic side. Helix VIII of CCR4 shares the conserved phenylalanine 311 that potentially interacts with the tyrosine of the NPXXY motif, meaning it too is likely required for receptor activation.

The cytosolic face of helix VIII is also important for receptor function, since in other GPCRs it has been shown to bind G proteins. Modelling of helix VIII of the β_1-adrenergic receptor along with mutational studies showed that G proteins

interacted with this region (Delos Santos et al., 2006). In addition, removal of the C-terminus of the viral chemokine receptor ORF74 prevented coupling of the receptor to $G\alpha_q$ proteins (Verzijl et al., 2006). K321 of squid rhodopsin was shown to interact with the detergent octyl glucoside, believed to mimic $G\alpha_q$ binding (Murakami and Kouyama, 2008). Thus the hydrophilic face of helix VIII of CCR4, including the amino acid K310, are likely involved in coupling to signalling partners of the receptor.

In summary, due to the importance of each side of the amphipathic helix VIII in other GPCRs, and the fact that helical wheel analysis of this helix VIII mirrors previous studies, the respective mutations of K310 and L318 have likely disrupted key regions involved in receptor function. L318 may be required for maintenance of helical structure due to its hydrophobicity, since hydrophobic residues would need to orient away from the cytosol and into the lipid membrane. L318 could also possibly stabilise an interaction of the tyrosine of the NPXXY motif with phenylalanine 311. Neighbouring aromatic resides such as this phenylalanine may also be required for anchoring of helix VIII to transmembrane helix VII. K310 on the other hand likely faces the cytosol along with other hydrophilic and charged residues on its side of the helix and is directly implicated in receptor signalling.

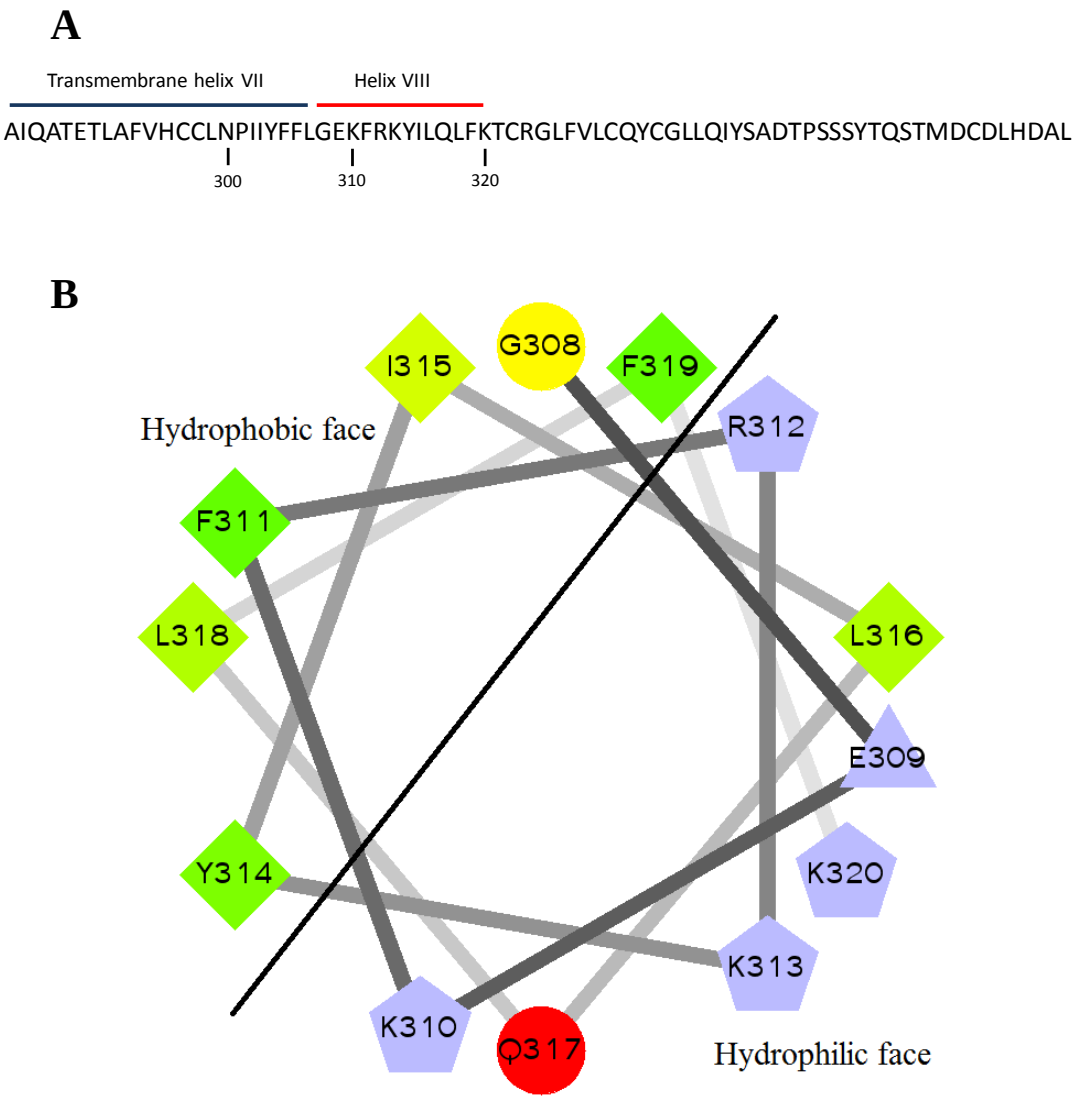

Figure 5-14 – Helical wheel projection of CCR4 helix VIII

Panel A shows the sequence of the helix VII and the C-terminus of CCR4, including helix VIII. Panel B is a helical wheel projection of the thirteen predicted residues of helix VIII, based on sequence conservation and homology modelling. Hydrophobic residues are shown as diamonds, and hydrophilic residues as circles. Negatively charged residues are shown as triangles, and positive ones shown as pentagons. Hydrophobicity is also colour-coded green to yellow, indicating reducing levels of hydrophobicity. Red indicates hydrophilic residues, while charged residues are light blue. The line intersecting the projection indicates the likely divide between the hydrophobic and hydrophilic sides of the helix. Helical wheel program from Zidovetzki et al., 2003.

5.3.1.2 – Phenotype of CCR4 C-terminal truncations

In addition to the four site 2 point mutants, three successive CCR4 C-terminal truncation mutants were made. The Δ40 mutant cut outside the conserved helix VIII after K320, Δ45 cut into helix VIII directly after I315, while the Δ50 mutant had most of helix VIII removed since it cut directly after K310 (figure 5-2). The Δ40 mutant showed normal cell-surface expression while the Δ45 and Δ50 mutants showed significantly reduced expression (figure 5-4). These data demonstrate that the last 40 amino acids of CCR4 are not required for expression, while cutting into the conserved helix VIII region is severely detrimental to receptor trafficking.

Previous studies that disrupted the C-terminal helix VIII produced similar defects in receptors trafficking. A cannabinoid receptor 1 mutant in which three helix VIII hydrophobic residues were substituted with alanine had reduced trafficking to the cell surface. Confocal microscopy revealed that the receptor localised within the endoplasmic reticulum, explaining its failure to export to the cell-surface (Ahn et al., 2010). Earlier studies on the vasopressin V2 receptor showed that the hydrophobic residues of helix VIII were required to maintain folding of the receptor (Thielen et al., 2005). Truncation mutants of the leukotriene B_4 type-2 receptor, similar to those described here for CCR4, also showed that cutting into this region reduced receptor expression. This was determined to be due to incorrect folding of the receptor, causing it to fail to be exported from the endoplasmic reticulum following synthesis (Yasuda et al., 2009). In addition, disruption of the bradykinin B_2 helix VIII structure also negatively impacted trafficking; mutation of lysine 315 of this receptor to proline introduced a kink in the helix and thus substantially disrupted the normal alignment of the helix, leading to its localisation within the cell rather than on the membrane (Feierler et al., 2011).

Therefore, the Δ45 and Δ50 truncations of CCR4 have likely disrupted a key element required for receptor folding, significantly reducing the trafficking of the protein to the cell surface. Placed in context with these data, previously described K310N and L318A mutants have likely not impacted helix VIII structure due to their normal levels of cell-surface expression. Further point mutations of this region designed to disrupt helical structure, such as through the introduction of a proline, would likely result in similar defects in receptor trafficking.

In chemotaxis assays, Δ40 transfectants migrated with increased efficacy to both chemokines while Δ45 and Δ50 transfectants did not migrate to either chemokine (figure 5-6). Since the latter two truncations cut into helix VIII, and considering the impact they had on expression, the inability of the Δ45 and Δ50 mutants to induce chemotaxis is hardly surprising. Several studies of other chemokine receptors have shown similar results. A truncation outside of helix VIII of CCR5 did not affect expression and had a modest effect on chemokine-induced calcium release, however a truncation within helix VIII significantly reduced both expression and the calcium response (Gosling et al., 1997). In a similar manner to data presented here on CCR4, a truncation into helix VIII of CCR3 rendered the receptor unable to mediate chemotaxis to CCL11, CCL13 or CCL5. This truncation exhibited a reduced ability to bind the chemokine CCL11 (Sabroe et al., 2005).

In another chemokine receptor, CCR7, three truncations of the receptor were made; two of these were analogous to the Δ40 and Δ50 CCR4 truncations presented here while the third cut further down into the C-terminus. While all three of these mutants had normal cell-surface expression, the Δ50 analogue did not migrate to either of the CCR7 chemokines CCL19 or CCL21. This CCR7 truncation mutant had a lower level of G protein activation than WT CCR7 or the other truncations, again demonstrating that this region is required for receptor signalling (Otero et al., 2008).

An interesting phenotype observed from the Δ40 CCR4 truncation was that it induced a more efficacious chemotactic response to both CCL17 and CCL22. This increase implies that a mechanism of attenuation had been removed, thus increasing the response induced by the receptor. Further replicates of the ^{125}I-CCL17 and ^{125}I-CCL22 binding assays would need to be performed to determine whether the Δ40 truncation affected chemokine binding of the receptor. If it was unaffected it would suggest that the increase in chemotactic efficacy was due to another factor.

The previously described paper on CCR3 also investigated similar truncations to the CCR4 Δ40 mutant and observed the same chemotactic increase; a truncation mutant of approximately 20 amino acids further down the C-terminus compared to CCR4 showed increased efficacy in chemotaxis assays to CCL11 and CCL13. The CCR3 truncation mutant internalised to a lesser degree after chemokine treatment; this failure to fully remove the receptor from the cell surface after stimulation may account for the observed increase in chemotactic efficacy (Sabroe et al., 2005).

The post-helix VIII portions of chemokine receptors, including CCR4, contain several serine and threonine residues. In CCR5, these residue were shown to be phosphorylated by GPCR kinases (GRKs), which subsequently caused the recruitment of β-arrestins and attenuation of chemokine receptor signalling (Oppermann et al., 1999). As described in section 1.3.2.2, β-arrestins prevent the receptor from further G protein coupling, and also act as a scaffold for recruitment of other proteins that in turn internalise the receptor. β-arrestins can also activate signalling pathways (Borroni et al., 2010; Vroon et al., 2006). The Δ40 CCR4 truncation, lacking these GRK phosphorylation sites, is likely not being phosphorylated at a normal level in response to ligand. The resulting reduction in β-arrestin recruitment and subsequent internalisation would therefore explain the observed increase in chemotactic efficacy. This would also suggest that CCR4-mediated chemotaxis does not require β-arrestin signalling.

5.3.2 – Effect of site 2 mutation on antagonist activity

Following characterisation of their phenotype, the site 2 point mutants and truncations were then tested against the site 2 antagonists in chemotaxis assays (figure 5-9, tables 5-10 and 5-12). The Δ45 and Δ50 truncations were not examined since they did not show a functional response. K310N transfectant responses to CCL17 could not be antagonised for the same reason. F305A, L307V, and L318A transfectants were also tested against antagonist 7, which was hypothesised to target site 1. This was performed as a control to determine that these mutations did not affect the hypothesised first site. The $\log IC_{50}$ values for antagonist 7 did not differ between WT and mutant transfectants, indicating that the activity of this antagonist was not affected by the site 2 mutations.

Both F305 and L307 are hydrophobic amino acids, and modelling by GlaxoSmithKline suggested that they form part of a hydrophobic antagonist binding pocket. Since the site 2 antagonists and phenylalanine contain aromatic rings, π-stacking interactions may occur. Studies of CXCR2 using the rhodopsin crystal structure have identified a hydrophobic antagonist binding pocket on the intracellular face of the receptor, consisting of residues from helices 2, 3, 6, 7 and 8 (Okada and Palczewski, 2001; Nicholls et al., 2008).

The L318A transfectants did not show reduced potency to any of the three site 2 antagonists in chemotaxis assays to both CCL17 and CCL22. K310N transfectants also did not show reduced potency to antagonists 2 and 5. The L307V transfectants however did show a reduced sensitivity to the antagonists; in CCL17 chemotaxis assays L307V transfectants were inhibited with reduced sensitivity to antagonist 2, and in CCL22 assays with reduced sensitivity to antagonist 5.

Inhibition of binding of ^{125}I-CCL22 to L307V by antagonist 2 resulted in a reduced potency of the antagonist compared to WT (figure 5-13). In chemotaxis assays however inhibition of L307V-induced migration by this antagonist did not differ to WT. Since binding assays showed a reduction in potency and the chemotaxis assays did not, it may indicate that the subtle effects on chemokine binding were being obscured by the amplification of signal that occurs after ligand binding to GPCRs. Ligand binding sets off a signalling cascade, in which G protein subunits trigger further activation of downstream signalling partners such as adenylyl cyclase,

phospholipase C, and kinases that in turn activate other proteins (see section 1.3.2.2). Due to the multiple and complex cellular events that arise from ligand binding and receptor signalling, relatively minor changes in chemokine binding may not translate through to observable differences in functional assays. This therefore may explain the observed discrepancy between antagonist potency in binding and chemotaxis assays. Another possible explanation is statistical rather than biological. The chemotaxis inhibition assays were variable in some cases, and further replicates may be needed to confirm whether certain mutations resulted in a reduction of antagonist sensitivity.

Another interesting phenomenon is that the effect of F305A or L307V mutation on the inhibition of migration was chemokine-dependent. The decrease F305A transfectant sensitivity to antagonist 2 only occurred in response to CCL22 migration, while the decrease in L307V transfectant sensitivity to antagonist 2 only occurred in response to CCL17. This suggests that the two chemokines utilise different sets of amino acids in order to transduce signal, and that the two chemokines may stabilise different receptor conformations. Since antagonist 2 is less effective at inhibiting CCL22-induced signalling through the L307V mutant, it implies that L307 was required for full antagonist activity and therefore CCL22 signalling too required that amino acid. Antagonism of CCL17 was not affected, implying that L307 was dispensable for its signalling. This is reminiscent of the data described in chapter 3, regarding the stabilisation of distinct receptor conformations by the two chemokines. However in this case it is the unique responses of the antagonists that reveal the differences between the two ligands.

The binding of ^{125}I-CCL17 and ^{125}I-CCL22 to K310N transfectants was also inhibited using antagonists 5 and 2, respectively (figure 5-13). It was previously described in this chapter and in chapter 3 that the K310N mutant, while being unable to induce chemotaxis to CCL17, still bound ^{125}I-CCL17. It is interesting to note that antagonism of ^{125}I-CCL17 binding was also unaffected by the mutant. This indicates that the K310N mutation affected receptor signalling while not affecting chemokine binding or antagonist activity. Inhibition of ^{125}I-CCL22 binding was similarly unaffected. These data show that K310 is not required to maintain the site 2 antagonist binding site.

Since the Δ40 transfectants did not show any difference to WT transfectants with respect to inhibition of migration, it can be concluded that the last 40 amino

acids of the CCR4 C-terminus are dispensable for antagonism by both the site 1 and site 2 compounds. The binding site of the site 2 antagonists therefore likely lies in the region not truncated, namely helix VIII.

The identification of intracellular CCR4 antagonists (Andrews et al., 2008) used C-terminal domain exchanges between CCR4 and CCR5; these receptors have a highly conserved group of amino acids around the NPXXY motif in transmembrane helix VII. It was here that the C-termini were exchanged. Antagonists active against CCR4 were also active against CCR5/4 (CCR5 with a CCR4 C-terminus). The antagonists could not inhibit CCR5 or CCR4/5 responses, indicating that they were specific for the C-terminal end of helix VII and the C-terminus of CCR4 (Andrews et al., 2008). The previously described F305A and L307V mutants are located within this exchanged region, supporting this finding. CCR5 also possesses a residue analogous to F305, and has the structurally related aliphatic valine instead of a leucine at position 307. In addition, data presented here on the CCR4 Δ40 truncation have narrowed down this binding site. Since the C-terminal swaps between CCR4 and CCR5 were from histidine 296 in helix VII, and that data here show that the amino acids downstream of lysine 320 of CCR4 are not required for antagonist activity, the site 2 antagonist most likely bind to a region between these two points.

C-terminal exchanges of the chemokine receptors CXCR1 and CXCR2 revealed the presence of a similar intracellular allosteric site, and that K320 (analogous to K310 of CCR4) of helix VIII of CXCR2 formed part of this binding pocket since mutation to asparagine reduced the level of antagonism of the receptor (Nicholls et al., 2008).

Further mutational analyses of CXCR2 were performed to determine the specific interactions of the antagonists and intracellular binding sites. K320 of CXCR2 was mutated to alanine rather than asparagine, in order to disrupt ion pair interactions between the amino acid and the antagonist. Y314, part of the conserved NPXXY motif at the end of transmembrane helix VII, was also mutated to alanine to disrupt any π-stacking interactions of the binding pocket. D84 in the first intracellular loop was predicted to form an ion pair interaction with K320; this was also mutated to alanine to disrupt this interaction. All three mutations resulted in reduced antagonist affinity for the receptor, demonstrating that these residues were part of the intracellular antagonist binding pocket (Salchow et al., 2010).

The data presented here on CCR4 show that the site 2 antagonist binding site is not located in the last 40 amino acids of the receptor, and thus is likely made up of residues from the end of helix VII and in helix VIII. The F305A transfectants showed a small but significant increase in antagonist 2 potency while the L307V transfectants showed a decrease in potency, rather than a complete loss of sensitivity. The K310N and L318A mutants had no effect on antagonism.

Based on previous studies on CXCR2, further mutation of K310 to alanine may be required to probe the importance of this amino acid in antagonist activity on the C-terminus of CCR4. The lysine to asparagine mutation performed in this project is fairly conservative, in that it changed the ionisation state of the residue with completely removing the bulk of the lysine side chain. Mutation to alanine, as was done for the majority of potential antagonist-binding amino acids in CCR4, may prove more effective in elucidating the role of K310.

Since the Δ45 and Δ50 truncation mutants were non-functional and had severely reduced cell-surface expression levels, generation of additional helix VIII point mutants would allow further examination of their contribution to both receptor biology and antagonist activity. Mutation of hydrophobic residues such as F311, Y314, and F319 could be performed to determine the role of these residues in stabilisation of helical structure, and also their potential hydrophobic interactions in the intracellular antagonist binding pocket. Hydrophilic and charged residues within helix VIII such as K313 and K320 could be mutated to determine if they form interactions that are necessary for antagonist activity. Q317, a polar neighbour to K313, may form interactions with other residues in the receptor or with functional groups in the antagonists.

In addition, while the current CCR4 homology model does not include this residue as part of the antagonist binding site, mutation of the conserved aspartic acid of the DRYLAIV motif may prove useful since CXCR2 it was shown to form part of the antagonist binding pocket as a partner for the analogous residues to K310, K320 (Salchow et al., 2010). Despite its potential role in antagonism, mutation of this residue would allow investigation into a likely important domain required for CCR4 function.

5.3.3 – Summary

In conclusion, it has been shown in this chapter that the F305A and L307V mutants of CCR4 had reduced cell-surface expression relative to WT CCR4, with L307V transfectants migrating to CCL17 with a lower efficacy. Despite this, both mutants exhibited the typical chemotactic dose response, indicating that the mutated residues were not critical for receptor function. L307V transfectants showed reduced antagonist potencies in chemotaxis assays, and F305A transfectants showed a slight increase in potency. This highlights the role of these residues in antagonist binding, and suggests that the F305A mutation allowed the antagonist better access to the binding pocket.

The L318A and K310N mutations had no effect on receptor antagonism; L318A also had no effect on receptor phenotype. K310N however was unresponsive to CCL17 in chemotaxis assays, meaning that its functional response could not be antagonised. This mutant did retain the ability to bind ^{125}I-CCL17, which was easily antagonised by antagonist 5 with no differences to WT. Thus, while K310 was important for CCL17-induced function it was not shown to be required for antagonist activity. Based on previous studies in CXCR2, further study of this residue by mutation to other side chains may be required.

The three successive C-terminal truncations of the CCR4 C-terminus highlight the importance of the putative helix VIII region, as the Δ45 and Δ50 truncations were non-functional. The Δ40 truncation showed increased chemotactic efficacy, possibly due to the removal of serine and threonine phosphorylation sites required for β-arrestin recruitment. Antagonism of Δ40-induced chemotaxis did not show any differences to WT, showing that the last 40 amino acids of CCR4 are not part of the site 2 antagonist binding site.

6 – Probing antagonist binding sites within CCR4

6.1 – Introduction

Molecular modelling performed by GlaxoSmithKline identified several amino acids within CCR4 that potentially were sites of antagonist contact. The CCR4 antagonists were hypothesised to bind either a classical intrahelical site (site 1) or a novel intracellular site (site 2). In chapter 4, amino acids predicted to contact site 1 antagonists were mutated; the resulting receptor point mutants were then transfected into L1.2 cells and assessed for cell-surface expression and chemotactic ability. Mutants that were both expressed and functional were then tested for their sensitivity to antagonism in chemotaxis assays. If a mutant was insensitive to an antagonist, it implied that the amino acid that had been mutated was required for antagonist activity. The ability of the antagonists to inhibit chemokine binding was also investigated. It was shown that the L118A, Y122F, and I125A mutants had reduced sensitivity to one of the site 1 antagonists in chemotaxis assays. L118A was also shown to have reduced sensitivity to inhibition of chemokine binding.

The same process was repeated in chapter 5, for the site 2 compounds, which involved the mutation of residues in the C-terminus, including the highly conserved helix VIII region, in addition to truncations of the C-terminus of the receptor. The F305A and L307V mutants, located at the distal end of helix VII were shown to have reduced sensitivity to two of the site 2 compounds.

The preceding chapters have thus used indirect methods to investigate the effects of point mutation on antagonist binding. In this chapter, the effects were directly measured using radiolabelled antagonists. GlaxoSmithKline provided ^{3}H-labelled versions of antagonist 3, which targets site 1, and antagonist 5, which targets site 2.

Tritiated antagonists contain the radioactive isotope of hydrogen, ^{3}H, in place of normal hydrogen atoms. The specific activities of the radioactively labelled compound 3 (^{3}H-3) and compound 5 (^{3}H-5) were 37 and 53 Ci/mmol, respectively. Since the maximum theoretical specific activity per tritium is 29 Ci/mmol, on average these antagonists contain more than one tritium atom. The structures of antagonist 3 and 5 are shown in figure 6-1. Tritium decays into helium-3 by β-decay, resulting in the release of β particles, which are electrons. Since β particles emitted from ^{3}H are relatively low energy compared to other forms of ionising radiation such as gamma rays (see chapters 4 and 5 for gamma-emitting ^{125}I-chemokines), they cannot be

directly detected. Scintillants are therefore used to detect the radioactive emissions. Scintillants are compounds that emit light when excited by particles such as electrons. The light emission is then detected by a scintillation counter, which allows quantification of the amount of radiation released by the particle. This phenomenon was exploited in the antagonist binding assays used in this chapter.

Saturation binding assays are commonly used assays that employ radiolabelled ligand. They involve incubating a cell or membrane expressing a receptor of interest with increasing and ultimately saturating concentrations of radiolabelled ligand. This allows the determination of the affinity of the ligand for the receptor, the K_d, and the number of binding sites for the ligand, the B_{max}.

Previous research involving point mutation of the chemokine receptor CXCR1 and CXCR2 putatively identified an intracellular antagonist binding site (Nicholls et al., 2008), analogous to the intracellular CCR4 site hypothesised here. Subsequent research employed tritium-labelled antagonists to further investigate this site. A CXCR2 antagonist, SB265610, was labelled with tritium and used in membrane-based assays. It was shown to be specific to CXCR2, since incubation with CXCR1-expressing membranes did not result in the detection of light emitted from scintillant. This compound was also shown to have rapid dissociation kinetics; after 2.7 minutes the level of bound ^{3}H-SB265610 was reduced by 50%. Saturation assays were used to determine its K_d and B_{max}; these were 2.5 nM and 50 pmol/mg, respectively. Competition binding assays in which increasing concentrations of other CXCR2 ligands were incubated with a fixed concentration of ^{3}H-SB265610 showed that CXCL8 could not displace the antagonist. This demonstrated that the antagonist bound a site distinct to CXCL8. In addition, another CXCR2 antagonist could not displace the compound, indicating that ^{3}H-SB265610 bound to a distinct site on CXCR2. This was believed to be the intracellular site previously described (de Kruijf et al., 2009). Further research used ^{3}H-265610 and other radiolabelled CXCR2 antagonists with a panel of point mutants to provide further information regarding the antagonist binding site. Several point mutants were made of amino acids believed to form the intracellular allosteric site. Mutants of K320 and Y314 in the C-terminus and D84 in the first intracellular loop showed reduced binding affinity for the antagonists, showing that these residues were required for antagonist contact (Salchow et al., 2010). These studies show that radiolabelled antagonists are an important and useful tool in probing antagonist binding to a receptor.

^{3}H-3

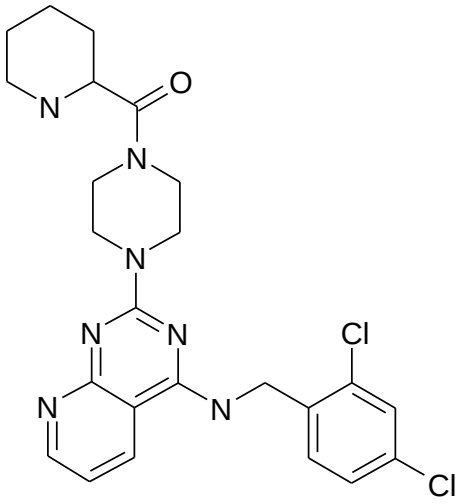

^{3}H-5

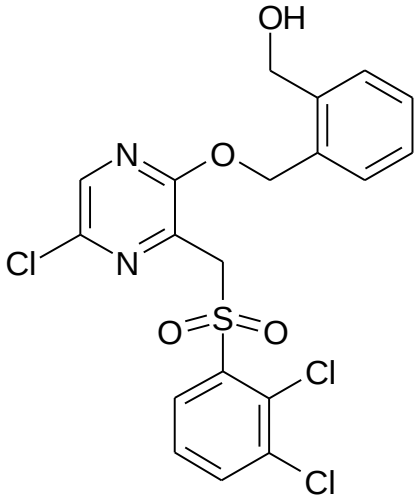

Figure 6-1 – Structures of antagonists 3 and 5

Antagonist 3 and antagonist 5 were radioactively labelled with tritium. Tritium is an isotope of hydrogen that contains two neutrons, denoted as ^{3}H. On average each antagonist molecule would contain 1-2 tritium atoms.

6.2 – Binding of intrahelical allosteric CCR4 antagonists

6.2.1 – Preparation of L1.2 cell membranes

L1.2 cells were transiently transfected with the pcDNA3 plasmid containing the CCR4 insert, as previously described in section 3.2.1. Following confirmation of cell-surface expression of the receptor, the cells were homogenised and centrifuged, resulting in a stock of membranes expressing the receptor. The absorbance values of BSA standards in a BCA assay were analysed by linear regression, and the resulting equation used to determine the concentrations membrane stocks. Figure 6-2A shows the graph of the BSA standards; the linear regression equation generated from these data was:

$$y = 0.0496(x + 0.0078)$$

Measurement of neat and serially diluted membrane concentration gave absorbance values, which were used to solve the equation by setting these values as *y*. The average of these concentration values was then used to determine the stock concentration. In this case, the WT CCR4-L1.2 membrane stock was at 2.05 mg/ml. This was aliquoted and stored at -80ºC until use in subsequent binding assays.

A

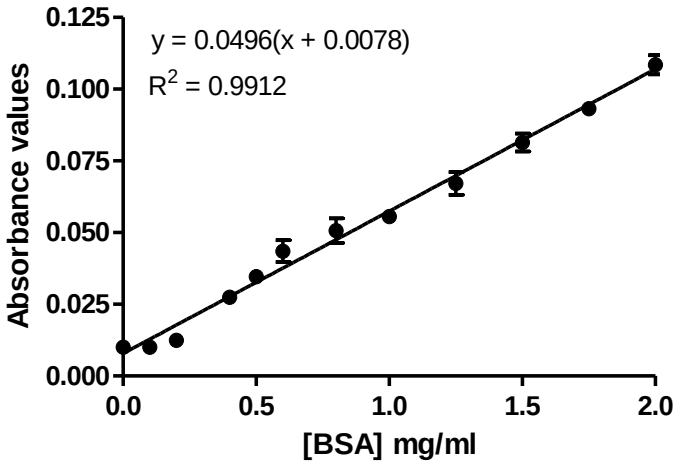

B

Dilution	**Neat**	**1:3**	**1:6**	**1:9**
Absorbance values	0.074	0.032	0.020	0.013
Concentration (mg/ml)	1.48	0.65	0.40	0.26
Concentration of stock (mg/ml)	1.48	1.94	2.42	2.35
Mean stock concentration (mg/ml)	2.05			

Figure 6-2 – Determination of membrane concentration with BCA assay

BSA standards were incubated with the BCA assay reagents, and the results analysed by linear regression (A). The linear regression equation was used to calculate the concentrations of serial dilutions of WT CCR4-L1.2 membrane preps; these were used to generate an average stock concentrate to use in further assays (B).

6.2.2 – Comparison of SPA and filtration binding assays

Two antagonist binding assays were available to use. The first was the scintillation proximity assay (SPA). In this assay, beads containing scintillant were coated with CCR4-expressing membranes. Wheat germ agglutinin (WGA) beads were used since this protein binds various carbohydrates commonly present on cell surfaces. The bead-membrane mixture was incubated with radiolabelled antagonist and either buffer or excess unlabelled antagonist. The emitted β-particles from tritium have a path length of 1.5 μm through water, meaning that scintillant is only excited if it is within this distance. The binding of the tritium-labelled antagonist to the receptor brought it in close enough proximity to the beads to allow excitation of the scintillant by the emitted β-particles. This emission was then detected using a MicroBeta scintillation counter.

Figure 6-3A shows the results of SPA using control CCR4-CHO membranes and WT CCR4-L1.2 membranes. SPA gave a small window of 100 counts between total and non-specific binding for WT CCR4 L1.2 membranes. The binding window for the control CCR4-CHO membranes was also small, approximately 350 counts. These binding windows were too small to produce reliable results, meaning that another binding assay was tested.

The second assay used involved filtration. Membranes were incubated with radiolabelled antagonist and then filtered using vacuum pressure through a glass fibre mat; the membranes were retained on the mat while free ligand was washed away. The mat was then cut into pieces, and each piece immersed in tubes containing liquid scintillant. The emission of light was then quantified using a Tri-Carb liquid scintillation counter. Total binding was measured by incubating the membranes and radiolabelled antagonist with buffer, while non-specific binding was measuring by incubating with 10 μM unlabelled antagonist.

Figure 6-3B shows the results of filtration binding of control CCR4-CHO and WT CCR4-L1.2 membranes. This assay gave a large 7800 count window for the CHO membranes. WT CCR4 L1.2 membranes gave a window of 1600 counts. To confirm that this binding window was specific to the receptor, membranes from naive L1.2 cells were tested in the same assay. Figure 6-3C shows that there was no difference between total and non-specific binding, indicating that ^{3}H-3 did not bind

non-specifically to the L1.2 membranes. Due to these results, filtration binding was used in subsequent antagonist binding assays.

The data shown in figure 6-3 are those generated from the result of several rounds of optimisation, since initial tests showed high non-specific binding to L1.2 membranes when compared to CCR4-CHO controls. The filtration assay was optimised in several ways; as described in section 2.2.4.4, the filter mat was soaked in 0.3% PEI prior to filtration in order to neutralise its negative charge and thus reduce charge-dependent non-specific binding of the antagonist to the mat. Various assay membrane concentrations were also tested in order to give the optimal binding window and to ensure that ligand depletion did not occur. The optimised assay involved 20 μg of membrane per assay well and filtration through a mat pre-soaked for 3 hours in 0.3% PEI.

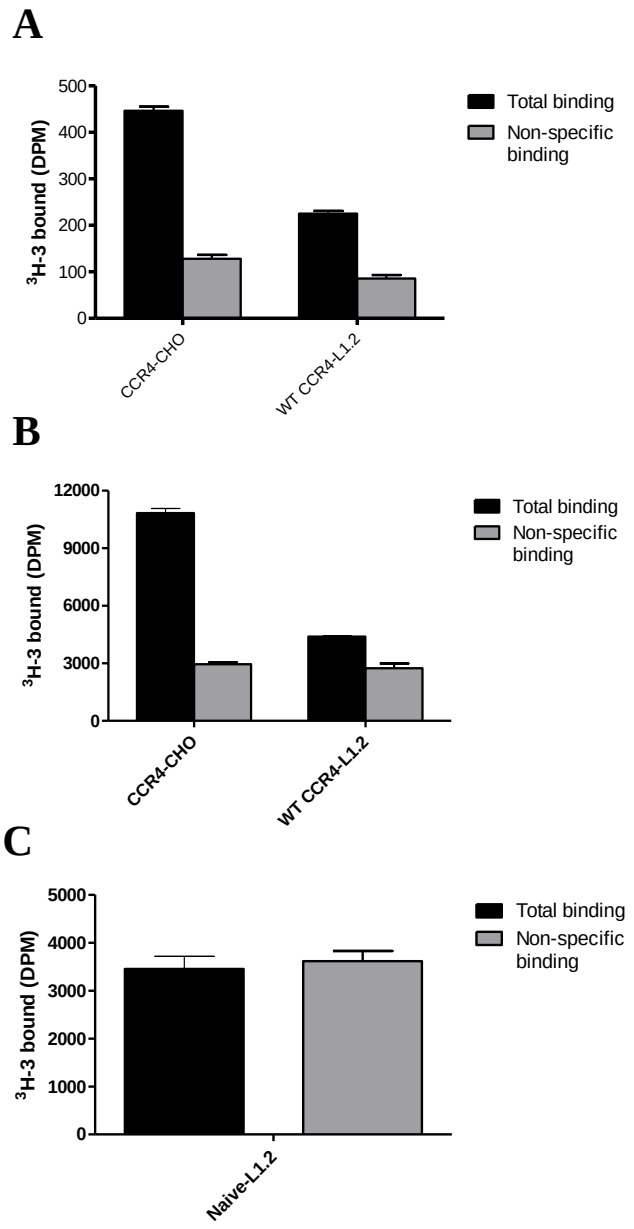

Figure 6-3 – SPA and filtration binding of CCR4-expressing and naive membranes
CCR4-CHO and WT CCR4-L1.2 membranes were assayed for ^{3}H-3 binding in SPA (A) and filtration binding (B). Membranes were incubated with 0.1 nM (A) or 1 nM (B and C) ^{3}H-3 and either buffer (total binding; black bars) or 10 μM unlabelled antagonist 3 (non-specific binding; grey bars). Data are shown as DPM, and are the mean ± SEM of one experiment.

6.2.3 – Saturation of WT CCR4-L1.2 membranes

Following optimisation of the filtration binding assay, saturation binding assays were performed on WT CCR4-L1.2 membranes. These assays involved the incubation of the membranes with increasing concentrations of radiolabelled antagonist, up to a level that saturated the antagonist binding sites. Membranes were also incubated with buffer or 10 µM unlabelled antagonist; thus for each concentration of ^{3}H-3, total and non-specific binding values were generated. Saturation binding assays can be used to determine the affinity of the ligand for the receptor, the K_d, and the maximum number of ligand binding sites, the B_{max}.

Figure 6-4 shows the results of saturation binding on WT CCR4-L1.2 membranes. Panel A shows both total and non-specific binding for a dose response of ^{3}H-3. 0.03 nM ^{3}H-3 showed a low level of binding; total binding for this concentration was 144 DPM, whereas non-specific binding was 127 DPM. As ^{3}H-3 concentration increased, so did the total radioactivity bound. Total binding for 6.15 nM ^{3}H-3 was 15733, while non-specific binding was 14254.

Panel B shows specific binding plotted against ^{3}H-3 concentration; this was calculated by subtracting the non-specific binding values from the total binding values from panel A. The specific binding data were analysed using non-linear regression, and the steepness of the curve quantified by the Hill slope. A Hill slope factor of 1 indicates that the slope is of standard steepness and that no cooperativity is occurring. A slope factor of greater than 1 indicates that multiple binding sites are present with positive cooperativity. The slope factor from this experiment was 1.34, shown in panel C.

The K_d obtained from this fit was 0.85 nM, indicating that at a concentration of 0.85 nM ^{3}H-3, half of the ^{3}H-3 binding sites were occupied. The non-linear fit shows that the specific binding plateaued at higher ^{3}H-3 concentrations, indicating that the antagonist binding sites were saturated. The B_{max} obtained from the fit was 1588 DPM. To convert this value into pmol/mg, the specific activity of ^{3}H-3, 37 Ci/mmol, was multiplied by 2.22 x 10^{12}, since 1 Ci is equal to this value in DPM. These values were also divided by 10^{9} in order to derive DPM/mmol:

$$\frac{37\ x\ 2.22\ x\ 10^{12}}{10^{9}} = 8214$$

The B_{max} was then divided by this number and the concentration of membrane in mg, to determine pmol/mg:

$$\frac{1588}{8214\ x\ 0.04} = 4.83$$

Therefore, the B_{max} of ^{3}H-3 on WT CCR4-L1.2 membranes was 4.83 pmol/mg.

This assay was repeated several times; however these repeats provided very variable results. The non-specific binding of ^{3}H-3 was often high enough to obscure the binding window shown in figure 6-4, such that saturation curves could not be plotted. The data shown in figure 6-4 are representative of two experiments that produced non-linear regression fits that gave K_d and B_{max} values. In subsequent experiments, the non-specific binding of ^{3}H-3 was too variable to produce consistent results.

A

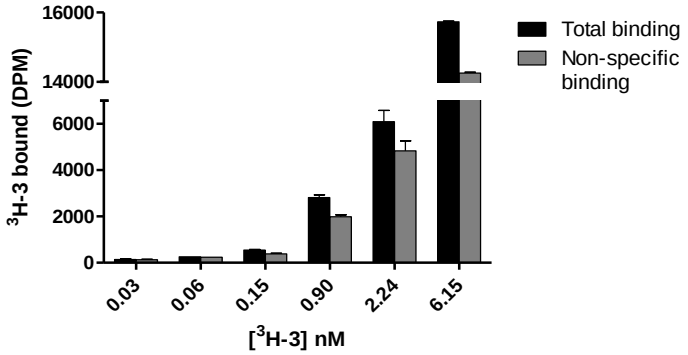

B

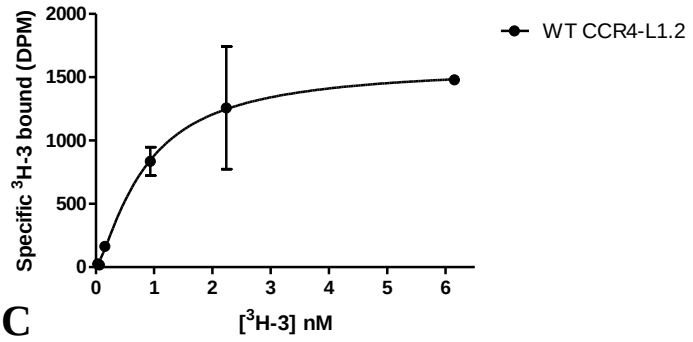

C

B_{max} (DPM)	1588
B_{max} (pmol/mg)	4.83
K_d (nM)	0.85
h	1.34

Figure 6-4 – Saturation of WT CCR4-L1.2 membranes with ^{3}H-3

40 μg of WT CCR4-L1.2 membranes were incubated with increasing concentrations of ^{3}H-3, and either buffer or excess antagonist 3 (A). Specific binding against ^{3}H-3 concentration, and analysed with non-linear regression and Hill slope (B); this was used to the generate B_{max} and K_d values shown in panel C. The Hill slope factor is also shown in panel C. Data are representative of two independent experiments.

6.2.4 – E290 mutant binding to antagonists

Mutants of the conserved glutamine E290 (GluVII:06) in transmembrane helix VII of CCR4 have previously been shown to be unable to bind the chemokines CCL17 and CCL22 and thus render transfectants of these mutants unresponsive in chemotaxis assays (see sections 4.2.2 and 4.2.3). GluVII:06 is a highly conserved amino acid, and was predicted by scientists at GlaxoSmithKline using molecular modelling to be a major point of contact for the site 1 antagonists. The effect of the E290 mutations on antagonist binding was therefore directly probed using the radiolabelled antagonist 3, which was hypothesised to bind the intrahelical site 1.

Figure 6-5 shows the results of saturation binding assays on WT (A), E290A (B), E290D (C) and E290Q (D) CCR4-L1.2 membranes. WT CCR4 gave a binding window at each ^{3}H-3 concentration; for 0.08 nM ^{3}H-3 total binding was 326 DPM and non-specific binding was 160 DPM, while at the highest concentration of ^{3}H-3, 12.64 nM, total binding and non-specific binding were 29466 DPM and 23216 DPM, respectively. The E290 mutants however showed a distinct lack of difference between total and non-specific binding at any ^{3}H-3 concentration, indicating that they did not bind the radiolabelled antagonist. Panel E of figure 6-5 shows specific binding of the WT and E290 mutants plotted against ^{3}H-3 concentration and analysed using non-linear regression. As in figure 6-4, the WT saturation curves were variable; in this case the curve did not plateau, meaning that the K_d and B_{max} could not be calculated. However from this graph and the bar charts it can still be seen that WT CCR4 bound antagonist 3, whereas the E290 mutants did not.

As an alternative to saturation binding, homologous competition assays were performed on the E290 mutants in an attempt to provide as estimate of the K_d, since the saturation assays failed to provide repeatable results. Homologous competition assays were performed in a similar manner to saturation assays, except that the radiolabelled antagonist concentration remained fixed while the unlabelled concentration varied. In this case, the assay was performed with two fixed radiolabelled antagonist concentrations to provide a better estimate of the K_d.

Figure 6-6A shows the results of a homologous competition assay performed on control CCR4-CHO membranes. Two curves are shown, one for 1.36 nM ^{3}H-3 and another for 5.22 nM ^{3}H-3. Total binding in the absence of unlabelled antagonist

was 20777 DPM for 5.22 nM ^{3}H-3 and 8901 DPM for 1.36 nM ^{3}H-3, as was binding in the presence of 10 μM unlabelled antagonist; 7005 DPM for 5.22 nM ^{3}H-3 and 2315 DPM for 1.36 nM ^{3}H-3. The graph shows that binding of both concentrations of ^{3}H-3 was dose-dependently competed with by the increasing concentration of unlabelled antagonist 3. A shared non-linear regression analysis of the two curves gave a logK_d of -8.72 (K_d = 1.9 nM).

Since this assay proved successful in control CCR4-CHO membranes, it was performed on WT and E290 mutant L1.2 membranes. Figure 6-6, panels B-D show the results of these assays. In contrast to panel A, there was no sigmoidal curve generated from the competition data. The addition of unlabelled antagonist did not reduce ^{3}H-3 binding to a low enough level to allow estimation of the K_d. Similar results were observed for two repeats of this experiment.

Figures 6-5 and 6-6 therefore show that both saturation and homologous competition binding assays for ^{3}H-3 are variable, likely due to the high non-specific binding of the compound. Despite this, it was determined that WT CCR4 was able to bind the radiolabelled antagonist, while mutation of E290 to alanine, aspartic acid and glutamic acid removed this binding site.

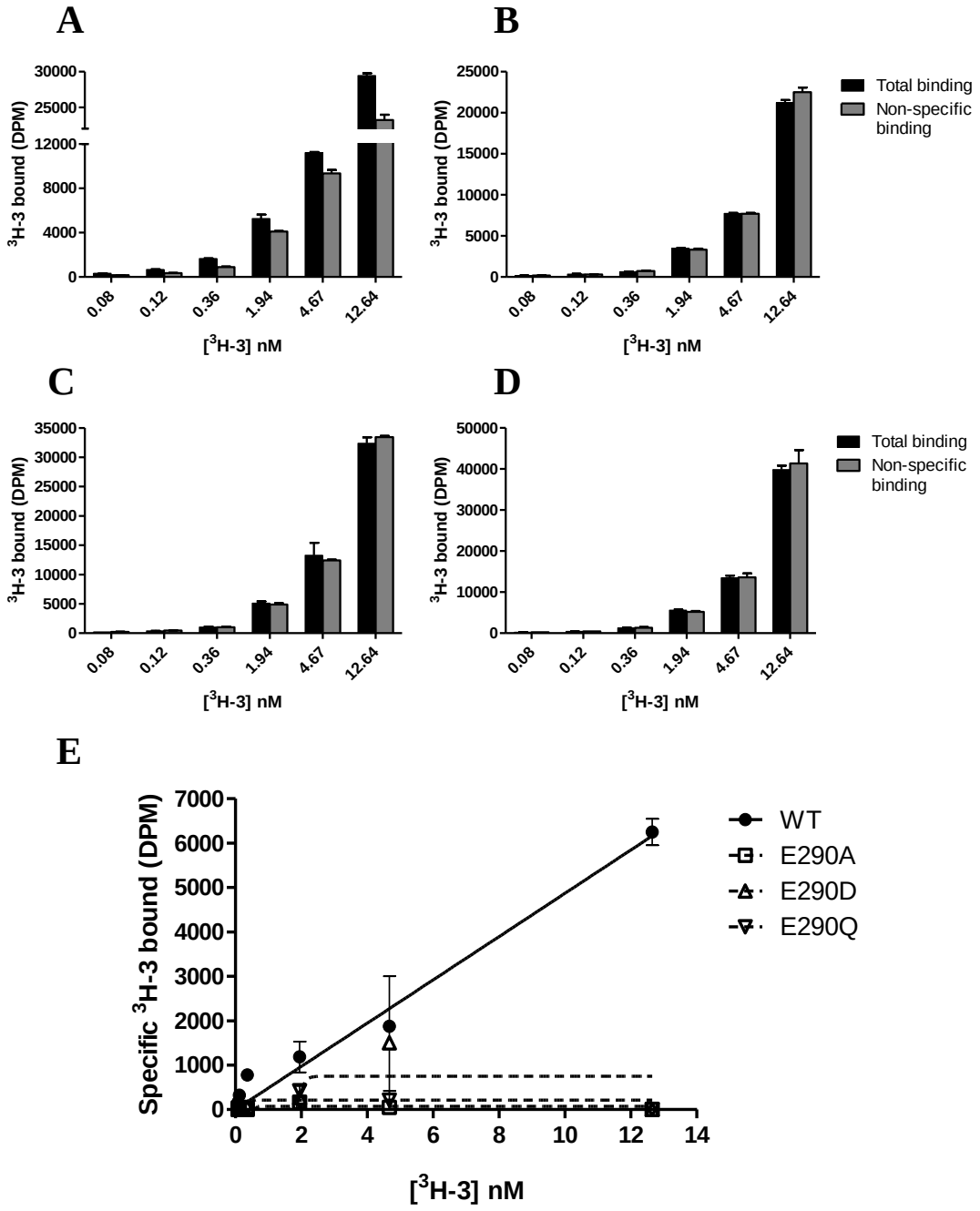

Figure 6-5 – E290 mutants do not bind ^{3}H-3 in saturation assays

40 µg of WT (A), E290A (B), E290D (C), and E290Q (D) CCR4-L1.2 membranes were incubated with increasing concentrations of ^{3}H-3 and either buffer or excess antagonist 3. The specific binding was then plotted against ^{3}H-3 concentration and analysed using non-linear regression with a Hill slope (D). Data are representative of three independent experiments; due to the variability of this assay K_d and B_{max} values could not be generated.

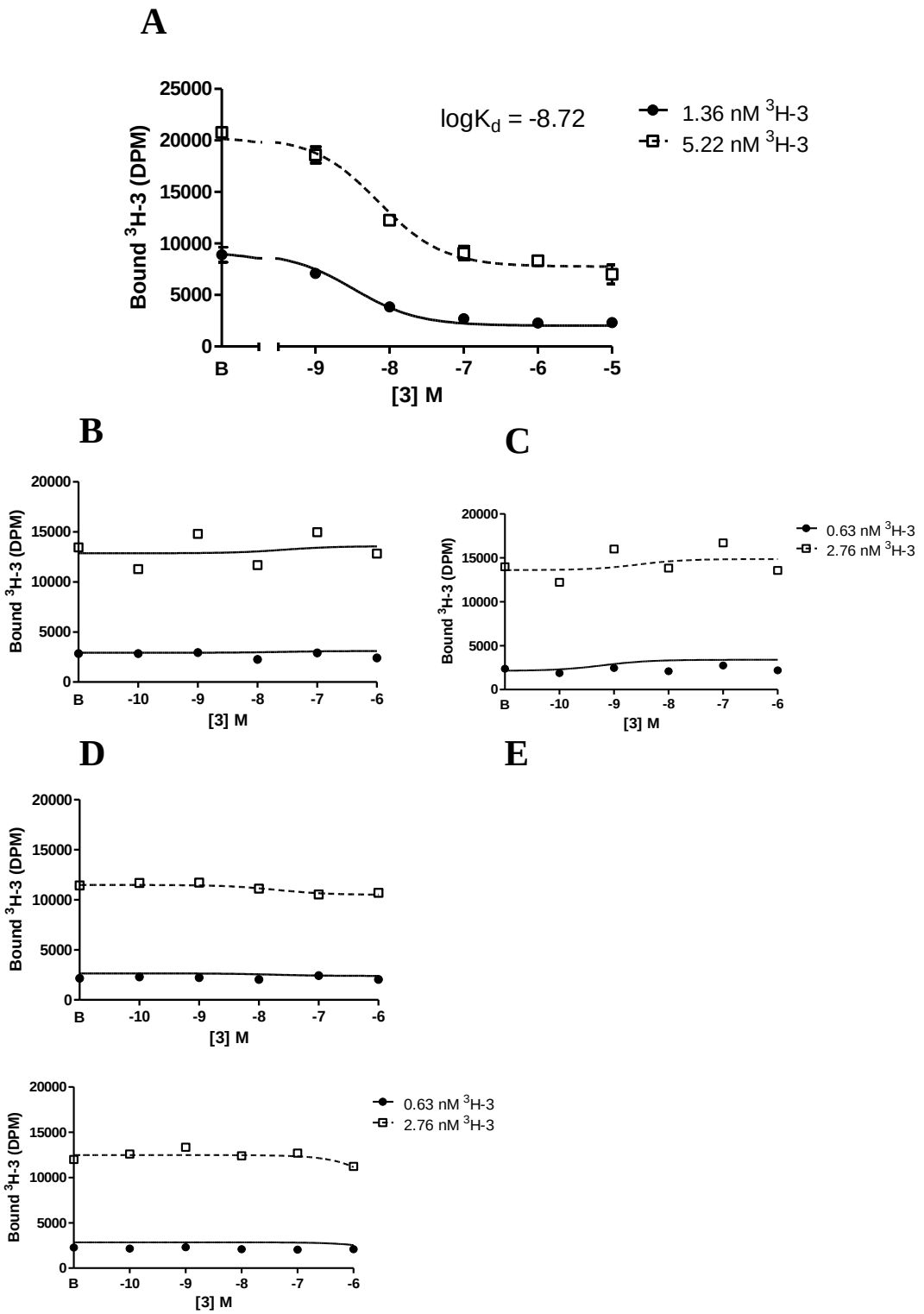
A
logKd = -8.72
1.36 nM 3H-3
5.22 nM 3H-3
Bound 3H-3 (DPM)
[3] M
B
C
D
E
0.63 nM 3H-3
2.76 nM 3H-3

Figure 6-6 – ^{3}H-3 homologous competition assays of E290 mutants

Homologous competition filtration assays were performed in which 5 μg CCR4-CHO membranes (A) and 40 μg WT (B), E290A (C), E290D (D), and E290Q (E) CCR4 L1.2 membranes were incubated with fixed concentrations of ^{3}H-3 and increasing concentrations of antagonist 3. Data were analysed using non-linear regression, and are representative of 3 independent experiments.

6.2.5 – Saturation binding of ^{3}H-3 to L118A CCR4

Saturation binding assays were also performed on the L118A mutant. This mutant has previously been shown to have reduced sensitivity to antagonist 7 in chemotaxis and chemokine binding assays. Antagonist 7 is a site 1 compound, and while it is not very structurally similar to antagonist 3, they both are hypothesised to bind to the same region of CCR4. Therefore, this mutant was investigated in ^{3}H-3 binding assays in order to determine whether this mutation had directly perturbed antagonist binding.

Figure 6-7 shows the results of a saturation binding assay performed on WT and L118A CCR4-L1.2 membranes. As in figures 6-3 and 6-4, WT CCR4 bound ^{3}H-3, giving a window between total and non-specific binding, shown in panel A. L118A also gave a binding window, shown in panel B. Specific binding is shown in panel C, plotted against increasing ^{3}H-3 concentration. Both curves plateaued, indicating that ^{3}H-3 binding sites were saturated at the highest concentration. The L118A curve plateaued at a lower specific binding value that the WT curve; the maximum values were 1094 and 1693 DPM, respectively.

The non-linear regression fit was used to calculate K_d and B_{max}, shown in panel C. The B_{max} of L118A CCR4 was lower than that of WT CCR4; 1120 DPM compared to 1904 DPM. These values were converted to 5.79 and 3.41 pmol/mg, respectively. They indicated that the L118A mutant had fewer ^{3}H-3 binding sites. The K_d of L118A was also lower than the WT; 0.77 nM compared to 1.22 nM. This shows that the mutant receptor had a higher affinity for ^{3}H-3 than the WT receptor. The Hill slope factors were 1.15 and 1.61, indicating positive cooperativity between multiple sites. However, these results could not be reliably reproduced. Due to the variability of the assay, other saturation curves resulted in ambiguous regression curve fits. Other assays showed binding windows for WT and L118A similar to those seen in panel A, but more complex analysis was hindered by the high non-specific binding of ^{3}H-3. Therefore, making strong conclusions regarding the affinity and number of binding sites of ^{3}H-3 may be premature. It can however be concluded that L118A was still able to bind ^{3}H-3 due to the presence of a binding window.

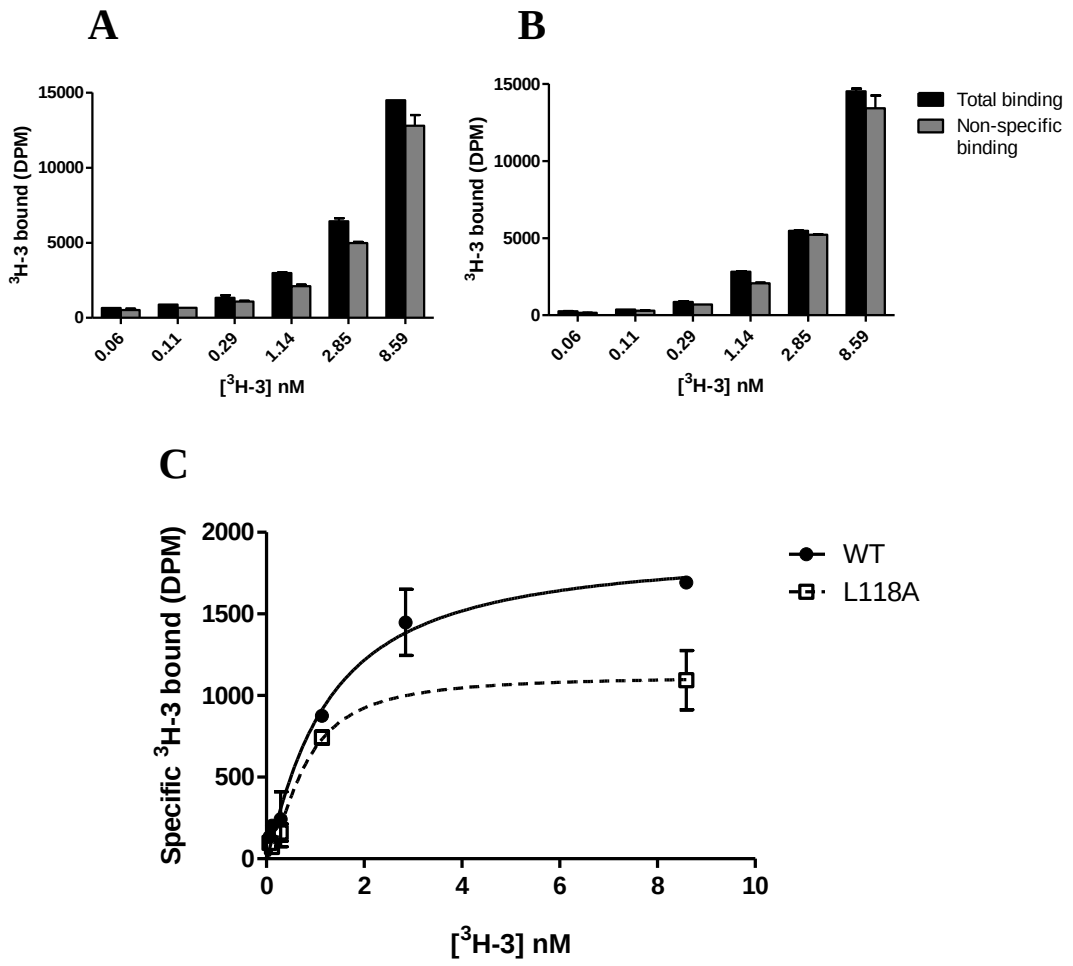

D

	WT CCR4	L118A CCR4
B_{max} (DPM)	1904	1120
B_{max} (pmol/mg)	5.79	3.41
K_d (nM)	1.22	0.77
h	1.15	1.61

Figure 6-7 – L118A mutation reduces total ^{3}H-3 binding in saturation assays

40 μg of WT (A) and L118A (B) CCR4-L1.2 membranes were incubated with increasing concentrations of ^{3}H-3 and either buffer or excess antagonist 3. The specific binding was then plotted against ^{3}H-3 concentration and analysed using non-linear regression with a Hill slope (C), which was used to determine B_{max} and K_d values (D) Data are from one experiment.

6.2.6 – ^{3}H-3 binding to the L92A and Y117A mutants

The mutants L92A and Y117A were shown in section 4.2.2 to not induce migration of transfectants to either CCL17 or CCL22 in chemotaxis assays. Therefore, their sensitivity to antagonists in chemotaxis assays could not be investigated since this assay requires functional receptor to induce a chemotactic response.

Previous data in this chapter have shown that saturation and competition assays using ^{3}H-3 are variable due to high non-specific binding. Therefore, simple total/non-specific binding assays were performed in which WT, L92A and Y117A membranes were incubated with either 1.39 nM or 4.72 nM ^{3}H-3 and either buffer or 10 μM unlabelled antagonist 3. This was performed in order to test whether a binding window was observable at these concentrations of ^{3}H-3. Since these ^{3}H-3 concentrations were lower than previously used in saturation assays, 20 μg rather than 40 μg of membrane was used per well in order to reduce ligand depletion.

Figure 6-8 shows the results of this assay, demonstrating that WT, L92A and Y117A bind ^{3}H-3. Panel A shows binding of 1.39 nM ^{3}H-3, while panel B shows binding of 4.72 nM ^{3}H-3. Specific binding was calculated by subtracting non-specific binding from total binding, the results of which are shown in panel C. For both ^{3}H-3 concentrations, WT and L92A showed similar specific binding levels, while Y117A showed levels approximately 400-600 DPM higher. Figure 6-3C showed that naive L1.2 membranes did not bind ^{3}H-3, demonstrating that results shown in figure 6-8 were specific for the CCR4-expressing membranes.

A

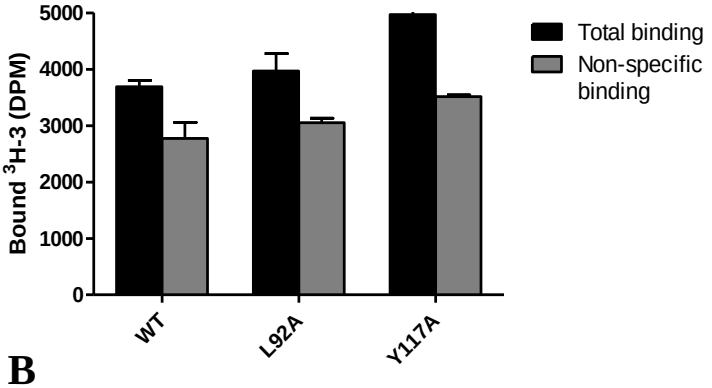

B

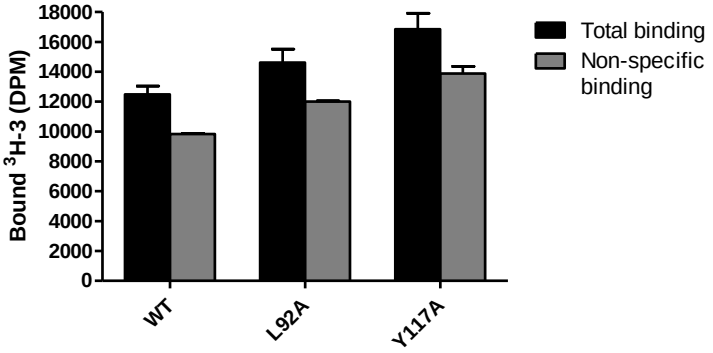

C

Receptor	1.39 nM ^{3}H-3 specific	4.72 nM ^{3}H-3 specific
WT	918	2654
L92A	917	2615
Y117A	1451	2973

Figure 6-8 – Y117A and L92A CCR4 mutants retain the ability to bind ^{3}H-3

20 μg of WT, L92A, and Y117A CCR4-L1.2 membranes were incubated with two concentrations of ^{3}H-3; 1.39 nM (A) or 4.72 nM (B) bars, and either buffer (total binding; black bars) or 10 μM unlabelled antagonist 3 (non-specific binding; grey bars). Panel C shows the specific binding windows resulting from the subtraction of NSB from TB, in DPM. Data are representative of four independent experiments.

6.3 – Binding of intracellular allosteric CCR4 antagonists

6.3.1 – ^{3}H-5 saturation assays

Saturation binding assays were performed on CCR4-expressing membranes in a similar manner to those described previously; however in this case the radiolabelled site 2 antagonist, ^{3}H-5, was used. Figure 6-9A shows a saturation assay using ^{3}H-5 performed on control CCR4-CHO membranes; as in previous figures, specific binding was calculated after subtraction of non-specific from total binding after incubation of membranes with increasing concentrations of the radiolabelled antagonist. The non-linear regression analysis gave a K_d of 1.29 nM, a B_{max} of 41552 DPM (472 pmol/mg), and a hill slope factor of 0.95. These results show that the antagonist bound to CCR4 with nanomolar affinity and without cooperativity, in agreement with previous observations by GlaxoSmithKline (personal communication).

The same assay was performed for WT and mutant CCR4 membranes. L307V and K310N are mutants of C-terminal amino acids, predicted to be sites of intracellular antagonist contact. L307V CCR4 transfectants previously showed reduced sensitivity to antagonist 2 and 5 (see section 5.3.1) in chemotaxis assays; the direct effect of this mutation on antagonist binding was therefore investigated in this chapter using the radiolabelled antagonist ^{3}H-5. K310 is located within the highly conserved helix VIII region, and has been shown to be important for receptor function. An analogous residue in CXCR2 has also been implicated in antagonist binding (Nicholls et al., 2008; Salchow et al., 2010); therefore the effect of this mutation on site 2 antagonist binding was also tested.

Figure 6-9B shows the non-linear regression fit generated from a ^{3}H-5 saturation binding assay performed on WT, L307V and K310N CCR4-L1.2 membranes. Unlike the CCR4-CHO control shown in panel A, the curves for the L1.2 membranes did not plateau, and therefore K_d and B_{max} values could not be generated. Figure 6-9C shows a similar assay performed on WT and E290 mutant CCR4-L1.2 membranes, in which the same non-saturating results were observed. The concentrations of ^{3}H-5 used for the saturation assay were five times higher than those in panel A, indicating that the concentration of radiolabelled antagonist was not an issue.

In addition, the specific activity of ^{3}H-5 was 53 Ci/mmol compared to 37 Ci/mmol for ^{3}H-3. Since saturation had been observed for ^{3}H-3 at 8 nM, using ^{3}H-5 at comparable concentrations should have resulted in saturation since ^{3}H-5 has a higher specific activity than ^{3}H-3.

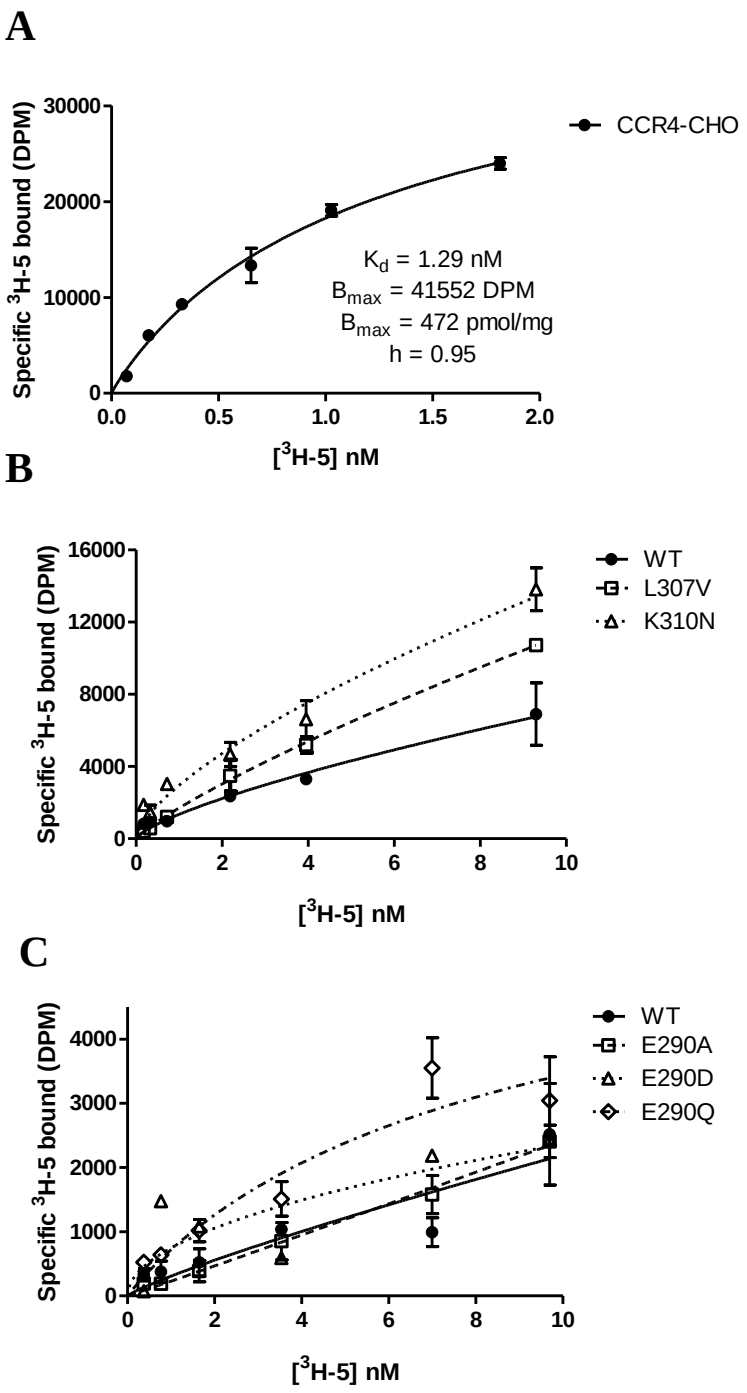

Figure 6-9 – CCR4-L1.2 membranes cannot be saturated with ^{3}H-5

Saturation assays were performed on 5 μg CCR4-CHO membranes, and specific binding plotted with a Hill slope; this generated a K_d of 1.29 nM and a B_{max} of 41552 DPM (472 pmol/mg). Saturation assays were also performed on 40μg L307V and K310N (B) and E290A, E290D, and E290Q (C) CCR4-L1.2 membranes along with WT CCR4-L1.2 membranes. These were not saturated, so K_d and B_{max} values could not be generated. Data are representative of four independent experiments.

6.3.2 – Identification of low affinity binding site on L1.2 membranes

The results of section 6.3.1 showed that high concentrations of ^{3}H-5 were not saturating the membranes, indicating a possible binding site on the L1.2 membranes for the antagonist. To investigate this, a saturation binding assay was performed on naive L1.2 membranes in the same manner as described previously. As can be seen from figure 6-10A, a binding window clearly exists on these naive membranes; at the highest concentration of 10.33 nM ^{3}H-5, total binding was 90027 DPM while non-specific binding was 62464 DPM. Figure 6-10B shows that this binding was not saturated even at this high concentration, in agreement with data shown in figure 6-9.

These data indicated that a low-affinity site for ^{3}H-5 was present on the naive L1.2 membranes. Since high concentrations of ^{3}H-5 were used for the saturation assays shown in panels A and B, lower concentrations were thus used in an attempt to saturate the high-affinity site without hitting the low-affinity site. Panel C shows the results of this; even at low concentrations the binding did not saturate, indicating that the low affinity site was still being bound by ^{3}H-5.

In order to further probe this low affinity site, other site 2 compounds were used in place of unlabelled antagonist 5 to measure non-specific binding. Antagonist 8, a compound structurally related to antagonist 5, was used in an effort to define non-specific binding in a ^{3}H-5 saturation assay of naive L1.2 membranes. Figure 6-11A shows that this compound gave similar results to figure 6-10. This shows that antagonist 8 acted in the same manner as antagonist 5, and did bind to the low-affinity site on the naive L1.2 membranes.

Antagonist 9 is another site 2 compound, structurally distinct from antagonist 5. This was also used as a competing ligand in an effort to define the non-specific binding of antagonist 5. Figure 6-11B shows the results of a saturation assay on naive membranes; this compound removed the window observed for these membranes. However, when this antagonist was used to define NSB for a ^{3}H-5 WT CCR4 saturation assay, no binding window was observed. Figure 6-11C shows no difference between TB and NSB when antagonist 9 was used as NSB. This indicates that antagonist 9 failed to compete with the radiolabelled ligand for specific antagonist binding sites; this compound therefore cannot be used to investigate receptor binding. Ideally, it would have removed the binding window observed in the naive membranes

while preserving a window in CCR4 membranes. These data show that the low affinity site for ^{3}H-5 cannot be blocked using alternative site 2 antagonists. Therefore, no further assays using ^{3}H-5 were performed on L1.2 membranes.

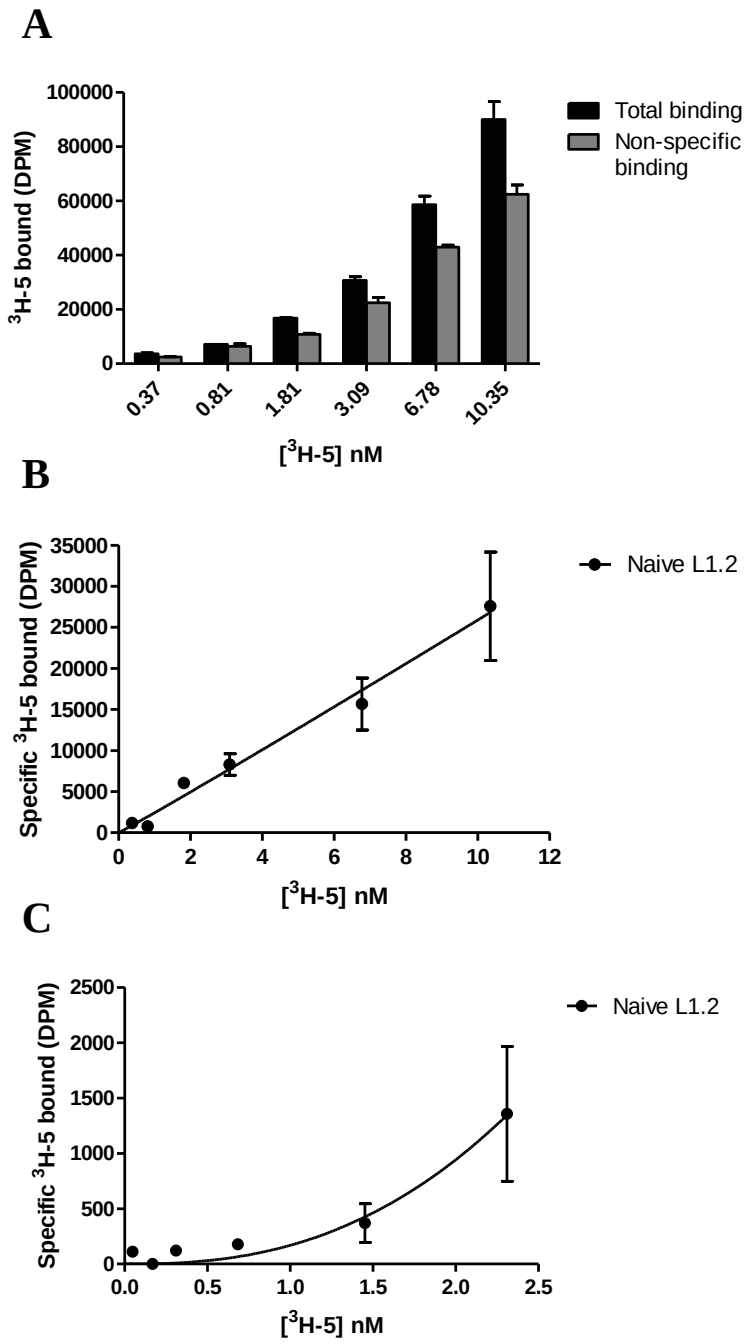

Figure 6-10 – ^{3}H-5 saturation assay reveals binding site on naive L1.2 membranes

A ^{3}H-5 saturation assay was performed on 20 μg naive L1.2 membranes; total and non-specific binding (A) showed the presence of a binding window. Specific binding plotted with a Hill slope showed that this binding site could not be saturated even with high ^{3}H-5 concentrations (B). Lower concentrations of radiolabelled antagonist, on 5 μg of membranes (C), showed similar results. Data are representative of two independent experiments.

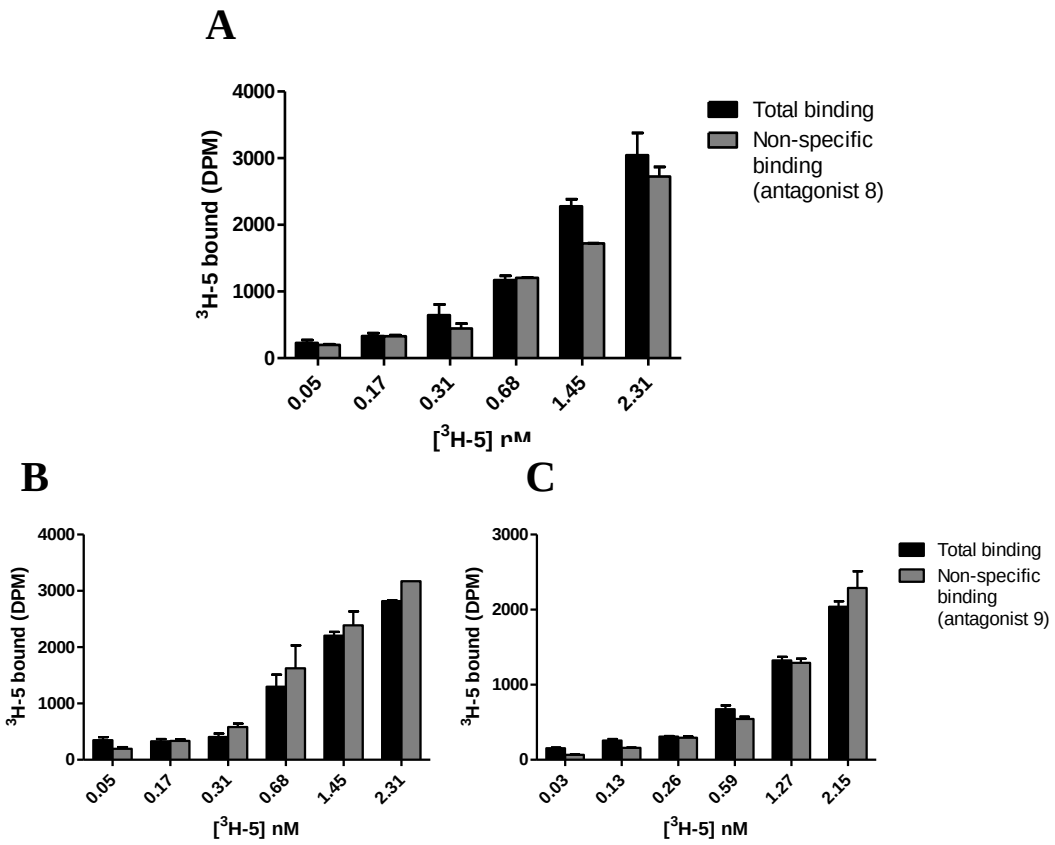

Figure 6-11 – Alternative site 2 antagonists do not define non-specific binding site

Saturation assays were performed on 5 μg naive L1.2 membranes using a different site 2 compound to define non-specific binding (A), however a binding window was still observed. Another compound was used on naive membranes which removed the window (B). This compound also removed the binding window on 5 μg WT CCR4-L1.2 membranes (C). Data are representative of two independent experiments.

6.4 – Discussion

6.4.1 – Direct binding of antagonists to CCR4

In the preceding two chapters, the effects of CCR4 point mutation and truncation on receptor biology and antagonist potency were investigated. The antagonist assays used indirect methods to infer whether the mutation of a particular residue had disrupted an antagonist binding site. For example, chemotaxis assays were performed in which the migration of WT and mutant transfectants to chemokine was dose-dependently inhibited by an increasing concentration of antagonist. This was used to generate $\log IC_{50}$ values to determine potency. The $\log IC_{50}$ values for WT and the mutant were then compared, and if the mutant showed a reduction in antagonist potency then the site of mutation was concluded to be a site of antagonist contact. Similar assays were performed by inhibiting binding of radiolabelled chemokine to the transfectants.

In this chapter, direct assays were performed on membranes expressing WT or mutant CCR4. These involved using radiolabelled antagonists to directly confirm whether a CCR4 mutation had disrupted antagonist binding. Two radiolabelled antagonists were provided by GlaxoSmithKline, which were tritiated versions of antagonists 3 and 5. ^{3}H-3 was hypothesised to bind to the intrahelical site 1, and ^{3}H-5 was hypothesised to bind to the intracellular site 2.

Initially, the scintillation proximity assay (SPA) and filtration binding assay were compared to determine which provided the largest window between total and non-specific binding. Both assays used membrane preparations of previously transfected L1.2 cells. The concentrations of the membrane preparations were measured using a BCA assay so that the assay concentration could be controlled (figure 6-2). This assay allowed reliable determination of the concentration of several L1.2 membrane preparations that were performed prior to binding assays.

The comparison of SPA and filtration binding using ^{3}H-3 (figure 6-3) showed that the latter gave the largest window between total and non-specific binding. For the control CHO cells, 0.1 nM ^{3}H-3 gave a window of 350 counts in SPA whereas 1 nM ^{3}H-3 gave a window of 7800 counts the filtration assay. The WT CCR4-expressing L1.2 membranes also gave a larger binding window in the filtration assay relative to the concentration of radiolabelled antagonist used. Filtration binding was therefore

used in subsequent binding assays. Naive L1.2 membranes were also shown to not bind ^{3}H-3.

Membrane preparations from Chinese hamster ovary (CHO) cells stably expressing CCR4 were used as a positive control in these assays. These had been optimised by GlaxoSmithKline to express high levels of the receptor in order to give a large binding window. In addition, since they were a non-leukocyte cell line the non-specific effects associated with using chemokines and chemokine receptor antagonists could be minimised. L1.2 membranes however were used to investigate the effect of point mutation of receptor antagonism. Due to time constraints, stably-expressing mutant CCR4 in CHO cells would have been unfeasible, and would have meant switching cell lines when previous assays were carried out using the L1.2s.

6.4.2 – Binding of ^{3}H-3 to site 1 CCR4 mutants

The first radiolabelled antagonist to be investigated was ^{3}H-3. Before it was tested against the CCR4 mutant membranes, it was used in saturation assays on WT CCR4 membranes. Figure 6-4 shows a saturation assay of WT CCR4-L1.2 membranes; the plateau of the specific binding curve shows that the ^{3}H-3 binding sites on the membranes were saturated at the highest antagonist concentration. This assay gave a K_d of 0.85 nM, which was similar to previous studies at GSK which had obtained a K_d of approximately 1 nM for this compound when using the control CHO membranes (personal communication).

The non-specific binding of this compound when using the L1.2 membranes was higher than when compared to CHO membranes, which hindered the replication of the saturation assay shown in figure 6-4. The high non-specific binding often resulted in a loss of the binding window at several ^{3}H-3 concentrations, which thus prevented the plotting of a saturation curve. The curve shown in figure 6-4 was thus representative of two experiments that provided curves with a reasonable Hill slope factor, which as described denotes the steepness of the curve.

There are several possible reasons for the high non-specific binding observed here. ^{3}H-3 has been shown to have a higher level of non-specific binding compared to ^{3}H-5 in previous assays (personal communication). This is reflected in the use of different glass fibre mats in the filtration assays; thicker GF/B mats were used during the filtration step of ^{3}H-5 assays, while thinner GF/C mats were used for ^{3}H-3 assays (see section 2.2.4.4). The thinner mats were used in an effort to prevent excess ^{3}H-3 binding to the mats, which would have resulted in higher non-specific binding. In addition, GF/C mats were pre-soaked in a 0.3% solution of polyethyleneimine (PEI). PEI is a cationic polymer that is used to neutralise the negative charge of the glass fibre mat, preventing charge-dependent interactions of the compound with the filter mat. The filtration assay was also optimised in this project by soaking the mats in 0.3% PEI for 3 hours rather than 10 seconds as the protocol initially described.

Despite the high non-specific binding of ^{3}H-3 and the variability of the saturation assays, it was clear that ^{3}H-3 bound the WT CCR4 L1.2 membrane. The same assays were then repeated for mutant CCR4 membranes in order to determine the effect of the mutation on antagonist binding.

6.4.2.1 – Binding of ^{3}H-3 to GluVII:06 mutants

Saturation assays using ^{3}H-3 were then performed on L1.2 membranes expressing WT CCR4 or those expressing one of the three GluVII:06 mutants, E290A, E290D and E290Q (figure 6-5). As with the WT assays described previously, the data were variable and often high non-specific binding of ^{3}H-3 prevented the generation of a saturation curve, thus K_d and B_{max} values could not be obtained. The bar charts however do show the presence of a binding window for the WT membranes. The E290A, E290D and E290Q mutants did not show a difference between total and non-specific binding. This indicates that all three E290 mutations prevented the site 1 antagonist from binding the receptor.

Since the variability of the non-specific binding of ^{3}H-3 prevented the determination of the K_d and B_{max} of the antagonist in the saturation assays, homologous competition assays were performed as a way of estimating the K_d. These used a fixed ^{3}H-3 concentration and an increasing concentration of unlabelled antagonist 3. To provide a better estimate of the K_d, two ^{3}H-3 concentrations were used. As the variability of the saturation assays often occurred at higher concentrations, ^{3}H-3 concentrations of lower than 6 nM were used since these often gave a binding window in the saturation assays.

The use of CCR4-CHO membranes in homologous competition assays showed that increasing concentrations of unlabelled antagonist could compete with ^{3}H-3, and provide an estimate of the K_d (figure 6-6). However when WT, E290A, E290D, and E290Q CCR4 L1.2 membranes were used, a sigmoidal inhibition curve could not be generated. If the E290 mutations disrupted the ^{3}H-3 binding site, this would have been expected. However, the results of the competition assay using WT membranes also failed to produce a sigmoidal curve. The affinity of ^{3}H-3 for WT membranes could thus not be estimated, meaning that a comparison to the E290 mutants could not be performed. For the higher ^{3}H-3 concentration, increasing unlabelled antagonist 3 did not reduce ^{3}H-3 binding. For the lower concentration however, like the saturation assay bar charts of figure 6-5, a difference was observed between total binding in the absence of unlabelled ligand and non-specific binding in the presence of 10 μM unlabelled ligand.

It can be concluded from the saturation and homologous competition assays that the data were too variable to reliably determine the K_d or B_{max} of ^{3}H-3. The data did however show that ^{3}H-3 bound WT CCR4 L1.2 membranes, and that when tested

against the three E290 mutant membranes the binding window was lost. The three E290 mutations therefore removed the ability of the antagonist to bind CCR4. The three mutations were designed to investigate the respective roles of amino acid size and charge in antagonist binding; mutation to aspartic acid reduced the amino acid side group while retaining its negative charge, mutation to glutamine removed the negative charge while retaining side group size, while mutation to alanine removed both size and charge of the side group. Since each mutation resulted in the same loss of binding window, it indicates that both the size and charge of the glutamic acid side group were necessary for antagonist binding.

These data are in agreement with previous studies that investigated the role of this conserved residue in antagonist binding. GluVII:06, as previously described is a highly conserved amino acid in the seventh transmembrane helix of chemokine receptors and has been shown in this project to be required for chemokine binding and thus receptor function (see chapter 3). Several studies have shown this amino acid is required for antagonist activity. For example, mutation of GluVII:06 in CCR5 was used to determine that the antagonist TAK-779 bound a site within the transmembrane domains of the chemokine receptor (Dragic et al., 2000). Mutation of GluVII:06 of CCR1 to glutamine, removing the negative charge of glutamic acid, conferred resistance to the antagonist UCB35625, as migration of mutant transfectants was poorly inhibited by the antagonist. The basic quaternary nitrogen of the compound was modelled to form a salt bridge with the negatively charged GluVII:06, with the mutation disrupting this interaction (de Mendonça et al., 2005). The same compound was also used to investigate the role of GluVII:06 in CCR3 antagonism; transfectants of CCR3 GluvII:06 mutants were similarly resistant to inhibition by UCB35625 (Wise et al., 2007).

Another mutagenesis study identified GluVII:06 of CXCR4 as an important residue for the binding of the antagonist AMD3100 (Rosenkilde et al., 2004). This antagonist is atypical compared to other chemokine receptor antagonists, which often contain two or more aromatic and hydrophobic rings connected through bonds that constrain the conformation of the compound. AMD3100 however consists of two non-aromatic cyclam rings connected by a single aromatic phenyl group. Despite this, GluVII:06 of CXCR4 still was an important interaction point for the antagonist, indicating that basic groups within the compound were interacting with this negatively charged amino acid. It was hypothesised that a cyclam ring of this

compound was ‘sandwiched’ between GluVII:06 and an aspartic acid in transmembrane helix VI of CXCR4 (Rosenkilde et al., 2004). Interestingly, GluVII:06 of CCR1 and CCR8 was required for the activity of the small molecule agonist LMD-559, indicating that the intrahelical binding site for antagonists is also used by non-peptide agonists (Jensen et al., 2012).

More recently, receptor modelling and alanine-scanning mutagenesis studies identified that a hydrogen atom bound to the quaternary nitrogen of DF2156A, a CXCR1/CXCR2 antagonist, formed hydrogen bonds with the negatively charged side group of GluVII:06 in both receptors. For CXCR2, another binding model was also proposed that instead involved an interaction of the compound with an aspartic acid residue in the seventh transmembrane helix (Bertini et al., 2012). In both cases, a negatively charged amino acid was interacting with a positively charged group on the compound, indicating the importance of these basic nitrogen atoms and the bonds they form with acidic amino acids in the receptor helices.

The data presented in this chapter on CCR4 agree with the described studies. GluVII:06 of CCR4 (E290) likely forms a salt bridge with a positively charged side group of antagonist 3. Mutation of this residue to alanine, aspartic acid or glutamine disrupted this interaction and thus prevented binding of the compound to the receptor.

6.4.2.2 – Binding of ^{3}H-3 to L118A CCR4

Saturation binding assays using ^{3}H-3 were also performed on L118A CCR4-expressing L1.2 membranes (figure 6-7). These were performed due to the fact that in section 4.3 L118A transfectants were less sensitive to inhibition of migration and chemokine binding by antagonist 7. Antagonist 7 was hypothesised to bind to the same intrahelical site as antagonist 3, and while antagonist 3 did not show a reduction in potency in these assays it was the only available tritiated site 1 antagonist and was therefore used to investigate the effect of mutations on site 1 antagonist binding. The β_1- and β_2-adrenergic receptors contain a valine residue in their antagonist binding pockets (Nygaard et al., 2009). Like valine, leucine is an aliphatic amino acid; L118 in CCR4 may form hydrophobic interactions with the antagonists.

Like the previous saturation experiments using WT and the GluVII:06 mutants, the data were variable due to the high non-specific binding of ^{3}H-3. For the saturation curve shown in figure 6-7, B_{max} and K_d values were generated. These

suggest that the L118A mutation caused a reduction in the number of ^{3}H-3 binding sites and a slight increase in affinity. It is important to note however that due to the variability of the assay it should not be concluded that the mutation had this effect on ligand binding. In addition, the flow cytometry data from chapter 4 showed an increase in L118A cell-surface expression compared to WT CCR4 (figure 4-4). It would be very surprising if a mutant caused a decrease in maximum binding but an increase in affinity, especially considering the observed increase in cell-surface expression of the mutant receptor; previous studies using mutagenesis to investigate antagonist binding show a reduction in K_d or a concomitant reduction in both B_{max} and K_d. For example, mutation of C-terminal residues K320A and Y314A of CXCR2 decreased both the maximum binding of the intracellular antagonist ^{3}H-SB265610 as well as its affinity for the receptor (Salchow et al., 2010).

The data presented here do however show that the L118A mutant retained the ability to bind ^{3}H-3, since a window was observed between total and non-specific binding in the saturation bar charts. Since antagonist 3 did not show a reduction in the potency in chemotaxis and chemokine binding assays, the presence of a binding site in the tritiated antagonist assays may be due to the mutation not affecting the ability of this antagonist to interact with the receptor. Antagonist 7 only showed a reduction in potency in these assays and not a complete loss of activity, so it is may be possible that the L118A mutation perturbed ^{3}H-3 to a small degree that is not apparent from the limited data presented here.

6.4.2.3 – Binding of ^{3}H-3 to Y117A and L92A

The Y117A and L92A mutants were also investigated for their ability to bind ^{3}H-3. Transfectants expressing both mutants were non-functional in chemotaxis assays and as such their migration could not be inhibited to determine if antagonist potency was affected. Due to the variability of the saturation binding assays, simple total and non-specific binding for these mutants was compared to WT CCR4 membranes at two ^{3}H-concentrations (figure 6-8). These data show that at these two ^{3}H-3 concentrations, the mutants bound the radiolabelled antagonist.

Mutation of Y113A in CCR1, analogous to the Y117A mutation here, conferred resistance to the antagonist UCB36525 in chemotaxis assays (de Mendonça et al., 2005), while the same mutation in CCR1 prevented the antagonist BX 741 from

inhibiting CCL3 binding to the receptor (Vaidehi et al., 2006). While these studies did not directly measure the effect of receptor mutation on antagonist binding, they showed that mutation of this conserved tyrosine inhibited antagonist activity. While it has been shown here in CCR4 that at two concentrations Y117A CCR4 membranes bound ^{3}H-3, full saturation assays would be needed to determine the effect of the mutation on antagonist binding. Considering the fact that this tyrosine along with Y122 is highly conserved amongst chemokine receptors and plays a role in their antagonism, it is likely that Y117 plays a role in CCR4 antagonism.

L92 is located within the TXP motif, a highly conserved motif located in the second transmembrane helix. While there are no previous studies indicating the importance of this amino acid in receptor antagonism, the TXP motif as a whole may play a role. This motif is important in receptor structure and thus chemokine binding, due to the kink the proline confers upon the helix of this region (Govaerts et al., 2001). As we have seen with the GluVII:06 mutants, amino acids that have important roles in receptor function can also be involved in receptor antagonism. As with the Y117A mutant, saturation assays would be needed to determine whether this was the case for the L92A mutant.

6.4.3 – Binding of ^{3}H-5 to site 2 mutants and identification of a low-affinity site

To investigate the binding of site 2 antagonists to the site 2 CCR4 mutants, ^{3}H-5 was used in saturation assays. The L307V and K310N CCR4 mutations were investigated in these assays since they were mutants of C-terminal regions. L307V transfectants were previously shown to have reduced potency to inhibition of chemotaxis to CCL17 and CCL22 by antagonist 2 and antagonist 5, respectively. The GluVII:06 mutants were also tested for their ability to bind ^{3}H-5 to confirm that this mutation had not adversely affected receptor structure and disrupted the intrahelical antagonist binding pocket. As described in sections 5.4.2, L307 is located at the end of transmembrane helix VII and may form hydrophobic interactions with the site 2 CCR4 antagonists. K320, an analogous residue to K310 in CXCR2, was involved in binding to intrahelical antagonists (Salchow et al., 2010).

However after performing these saturation assays it became apparent that even at high ^{3}H-5 concentrations the antagonist was not saturating its binding sites on the membranes, since specific binding did not plateau and instead increased with antagonist concentration (figure 6-9). To confirm that CCR4 could be saturated, ^{3}H-5 was used in saturation assays with CHO-CCR4 membranes, and in agreement with previous studies at GlaxoSmithKline a K_d of 1.29 nM was generated. The CCR4-L1.2 membrane ^{3}H-5 specific binding curves however did not produce a K_d value due to the inability of the compound to saturate the membranes.

Due to this finding, it was speculated that a low-affinity binding site for ^{3}H-5 was present on the L1.2 membranes. This would explain the observation that high ^{3}H-5 concentrations were not saturating the binding sites for the ligand. While the CCR4 expressed on the membranes may have been fully saturated, another low-affinity site would have continued to bind the antagonist even at high concentrations. To confirm the presence of another ^{3}H-5 binding site, saturation assays were performed using naive L1.2 membranes, which had been prepared from untransfected cells that did not express CCR4 (figure 6-10). These naive membranes also showed a window between total and non-specific binding for ^{3}H-5, indicating that a binding site was present. Like the previous saturation curves with WT, L307V, K310N, E290A, E290D, and E290Q membranes, the specific binding did not plateau and instead increased with ^{3}H-5 concentration.

Since the inability to saturate the ^{3}H-5 occurred up to high concentrations such as 10 nM, the concentrations used in the saturation assay were lowered to a maximum of 2 nM. This was done to determine whether the binding site on the naive membranes was of low enough affinity that it would not be detectable in assays of low concentration. If this was the case then saturation assays could be performed on CCR4 membranes using low concentrations, since at this range the low-affinity binding site would not be bound. However, when this lower concentration range was tested on naive L1.2 membranes, a ^{3}H-5 binding site was still present. This indicated that the L1.2 ^{3}H-5 binding site was not of low enough affinity to be undetectable at low concentrations.

Following on from the identification of the ^{3}H-5 L1.2 binding site, different site 2 antagonists were used to define non-specific binding in an effort to remove the binding window present on the naive L1.2 membranes. If a compound was used that removed the binding window on naive L1.2 membranes while preserving a window on WT CCR4 L1.2 membranes, this could be used in subsequent saturation assays.

Non-specific binding occurs when a ligand binds to sites not on the receptor of interest, such as to filter mats or the surface of the cell membranes. To measure non-specific binding (NSB), radiolabelled ligand and membranes expressing the receptor of interest are incubated with excess unlabelled antagonist. The unlabelled antagonist competes with the radiolabelled antagonist for binding to receptor, meaning that the radiolabelled antagonist can only bind to non-specific sites. Total binding (TB) is measured without unlabelled antagonist, meaning that radiolabelled antagonist binds to both specific and non-specific sites. The specific binding window is then calculated by subtracting non-specific values from total binding values. When there is only one specific site for the radiolabelled antagonist, the binding window is therefore specific to the receptor of interest.

In the case of the saturation assays presented here, the low-affinity site for ^{3}H-5 acted as another specific site rather than as a non-specific site. This meant that in NSB wells, the excess unlabelled antagonist 5 competed with ^{3}H-5 for the low-affinity site, resulting in a binding window after subtraction of NSB from TB. This was likely the reason for the observed binding window in naive L1.2 membranes. A more suitable antagonist was therefore needed, one that did not compete with ^{3}H-5

for the low-affinity site and thus allow ^{3}H-5 to bind it as it would any other non-specific site on the membrane.

Antagonist 8, another site 2 CCR4 antagonist supplied by GlaxoSmithKline, was used to define non-specific binding in the ^{3}H-5 saturation assays on naive L1.2 membranes. This compound was structurally similar to antagonist 5. It was hoped that in NSB wells it would not compete with the low-affinity site, allowing ^{3}H-5 to bind the low-affinity site in the same manner as non-specific sites. However, this did not prove to be the case since a binding window was still observed on the naive L1.2 membranes (figure 6-11A). This shows that on naive L1.2 membranes, excess antagonist 8 in the NSB wells competed with ^{3}H-5, such that the radiolabelled ligand only bound non-specific sites on the filter mats and membranes and not the low-affinity site since these were filled by antagonist 8. Subtraction of non-specific binding from total binding thus gave a low-affinity site-specific window.

Antagonist 9 was then used, which was another site 2 compound of a different structural class to antagonist 5. In the naive L1.2 membranes, no binding window was observed. This may have suggested that antagonist 9 did not outcompete ^{3}H-5 for the low affinity site, allowing the radiolabelled ligand to bind it. To confirm this, antagonist 9 was used in a saturation assay of WT CCR4 L1.2 membranes. This assay also did not show a binding window. This result suggests that in addition to not competing with ^{3}H-5 for the low-affinity site, antagonist 9 also did not compete with ^{3}H-5 for binding to CCR4.

In summary, the identification of a low-affinity binding site for ^{3}H-5 on naive L1.2 membranes prevented the investigation of the effect of receptor mutation on the binding of the site 2 antagonist. Using different site 2 compounds as non-specific binding did not provide a solution to this, as antagonist 8 gave similar results to antagonist 5 while antagonist 9 was not of high enough affinity to compete at CCR4 effectively.

Following from these data, the next step was to determine what factor was binding ^{3}H-5 at low-affinity. Previous studies at GlaxoSmithKline indicate that the site may be comprised of other chemokine receptors endogenously expressed on L1.2 cells. Selectivity studies performed on antagonist 5 using [^{35}S]GTPγS binding assays showed that the compound gave a logIC_{50} value of -8.2 (IC_{50} = 6.3 nM) for CCR4, indicating it was active against this receptor.

[^{35}S]GTPγS binding assays measure GPCR activation using the non-hydrolysable GTP analogue, [^{35}S]GTPγS. As described in section 1.3, GPCR activation results in the displacement of GDP from the Gα subunit, allowing it to bind GTP. Gα-GTP then goes on to activate downstream signalling partners. This Gα-GTP dimer is then hydrolysed by GTPase activity of the Gα subunit, returning it to the inactive Gα-GDP form. The presence of [^{35}S]GTPγS prevents hydrolysis to GDP, leading to accumulation of the [^{35}S]GTPγS complex on the membrane. Due to its radioactivity, this accumulation can be measured (Harrison and Traynor, 2003). In the [^{35}S]GTPγS binding assays, antagonist can be used to inhibit GPCR activation, and thus the potency of the antagonist quantified.

These assays also showed activity against other chemokine receptors, shown in table 6-12. Antagonist 5 also showed activity against CCR5, with a logIC_{50} value of -7.5 (IC_{50} = 31.6 nM). CCR1 also showed sensitivity to the antagonist, with a logIC_{50} of -6.5 (IC_{50} = 316 nM). These data show that antagonist 5 is not specific for CCR4, and in fact antagonises other chemokine receptors.

Receptor	CCR1	CCR2	CCR4	CCR5	CCR8	CCR10	CXCR1	CXCR3	CXCR4
logIC_{50}	-6.5	-5.8	-8.2	-7.5	-5.2	<5	<5	<5	<5

Table 6-12 – Antagonist 5 selectivity data

[^{35}S]GTPγS accumulation was inhibited using antagonist 5. The table shows the logIC_{50} values for each receptor. Data are from GlaxoSmithKline selectivity studies.

L1.2 cells are a pre-B cell lymphoma line, and therefore likely endogenously express chemokine receptors. No data were available on the specific chemokine receptor expression of these cells, however previous studies have shown that pre-B cells can express CCR5 (Honczarenko et al., 2002). It has been previously shown however that L1.2 cells respond to the CXCR4 ligand, CXCL12, and the CCR7 ligands, CCL19 and CCL21, in chemotaxis assays (James Pease, personal communication).

Figure 6-13 shows an alignment of the C-termini of the chemokine receptors. It shows the strong degree of conservation between these receptors in the putative helix VIII region. Since previous data shown in chapter 5 demonstrated that the last 40 amino acids of CCR4 were not required by site 2 antagonists, they were concluded to therefore likely bind to helix VIII of the receptor. Considering the high homology of this region between receptors, the selectivity data showing antagonist 5 activity against CCR5 and CCR1 is perhaps unsurprising.

These findings are in contrast to the previously published data on the identification of the intracellular allosteric site on CCR4. In this study, both WT CCR5 and a chimeric CCR4 construct with a CCR5 C-terminus showed a 50-fold reduction in antagonist potency compared to WT CCR4 and chimeric CCR5 construct with a CCR4 C-terminus (Andrews et al., 2008). It is important to note however that this study used compounds of a different structural class to antagonist 5; one compound in particular was antagonist 2 presented in chapter 5. Therefore the differences in CCR4/CCR5 selectivity between antagonist 5 shown here and antagonist 2 shown in the study may be due to structural differences of the compounds themselves. Saturation binding assays using radiolabelled antagonist 2 on naive L1.2 cells would determine whether the low-affinity site was specific to antagonist 5.

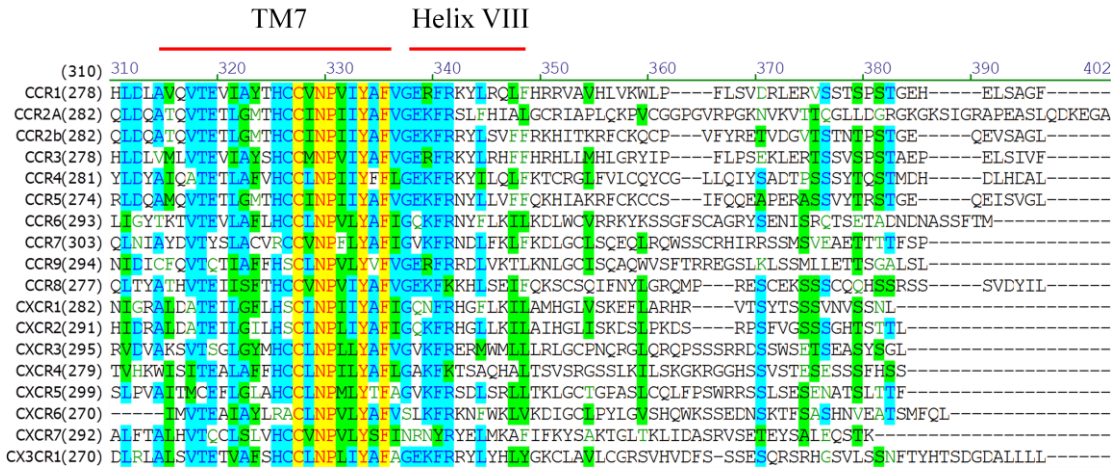

Figure 6-13 – Alignment of chemokine receptor C-termini

Aligned sequences of 16 chemokine receptors show transmembrane helices VII and the C-terminus including helix VIII. Yellow highlights indicate amino acids conserved between all receptors, turquoise between the majority of the receptors. Green highlights indicate conservation of amino acid type, e.g. the polar serines and threonines. From James Pease (personal communication).

The identification of a low-affinity ^{3}H-5 binding site on naive L1.2 membranes prevented analysis of binding of the compound of site 2 mutants. It also highlights a potential problem in the future development of this antagonist for treatment of CCR4-driven pathologies since the antagonist is not specific for CCR4. However, antagonists that bind more than one chemokine receptor may have potential uses in therapy.

6.4.4 – Summary

In summary, the use of the intrahelical antagonist ^{3}H-3 to investigate site 1 mutants revealed that the GluVII:06 mutants E290A, E290D, and E290Q did not bind the antagonist, indicating that this conserved residue was required for antagonist contact. The ^{3}H-3 saturation assays were variable due to high non-specific binding of the antagonist, which prevented the generation of reproducible K_d and B_{max} values for WT CCR4 in addition to the mutants L118A, Y117A and L92A. These mutants however were shown to contain a binding site for ^{3}H-3.

Saturation binding assays performed using the intracellular antagonist ^{3}H-5 to investigate site 2 mutants were hindered due to the identification of a low-affinity site for this compound. Naive L1.2 membranes confirmed the presence of this site, and the use of other site 2 compounds as non-specific binding did not remedy the problem. Selectivity data for antagonist 5 from GlaxoSmithKline suggest this site may be comprised of other chemokine receptors. This compound therefore may have potential use as a promiscuous chemokine receptor antagonist.

7 – General discussion

7.1 – The biology of CCR4

In this project, point mutants of CCR4 were made along with three receptor truncations. Chapter 3 investigated the impact of the mutations of GluVII:06 in transmembrane domain helix VII and K310 in the C-terminal helix VIII region. In chapters 4 and 5, point mutants of CCR4 were made to determine the role of the mutated regions in the activity of CCR4 antagonists. In doing so these mutants were also characterised in terms of their cell-surface expression, chemotactic and chemokine-binding ability. Thus in addition to the mutants of chapter 3, the mutants of chapters 4 and 5 revealed key determinants of CCR4 expression and function.

The three GluVII:06 mutations, E290A, E290D, and E290Q were shown to remove the ability of the receptor to bind chemokine and thus induce chemotaxis of transfectants. This supported previous studies of this conserved residue in other chemokine receptors. Mutations of GluVII:06 in other chemokine receptors such as CCR1, CCR2, CCR3 and CCR5 showed that it was often required for chemotaxis and chemokine-binding. It is important to note however that in CCR1 and CCR5 GluVII:06 mutants were still functional, in contrast to the CCR4 GluVII:06 mutants described here (Mirzadegan et al., 2000; de Mendonça et al., 2005; Wise et al., 2007; Hall et al., 2009).

Figure 6-13 in chapter 6 shows an alignment of helices VII and the C-termini of 18 chemokine receptors, including CCR4. Of these 18, GluVII:06 is present in 14. It is only CCR7, CCR9, CXCR3 and CXCR7 that do not contain this residue. CCR9 and CXCR7 contain a glutamine, which while polar is not charged at physiological pH. CCR7 has a bulky hydrophobic tyrosine while CXCR3 has a small polar serine. These may indicate potential π-stacking interactions and hydrogen bonds, respectively, as possible alternatives to salt bridges in this region. Due to its conservation with other receptors, and from the data presented here on CCR4, GluVII:06 has been shown to be a major determinant of CCR4 function.

From the data presented in chapters 4 and 5, other CCR4 point mutants also revealed other amino acids required for receptor function. The most striking examples of CCR4 mutants that resulted in non-functional receptor were the Y117A, Y122A, and Y258A mutants. The Y117A mutation had no effect on CCR4 cell-surface expression, while the Y122A and Y258A mutations significantly reduced surface

levels of the receptor. All three mutants however had a significant effect on chemotaxis to CCL17 and CCL22; the mutants did not allow chemotaxis to either ligand at any concentration. The Y258A transfectants showed a slight increase in chemotactic index at high concentrations of CCL22, however this was not significant. As with GluVII:06, other chemokine receptors such as CCR3 and CCR5 possess conserved tyrosines in similar helical positions to the ones shown here for CCR4, although these residues were not critical for chemotaxis (de Mendonça et al., 2005; Wise et al., 2007). Another mutant that showed no chemotactic ability was L92A. This was a mutation of a residue within the TXP motif, which as described is a highly conserved structural determinant of receptor function (Govaerts et al., 2001, 2003; Blanpain et al., 2003).

K310, located in the C-terminal helix VIII region of CCR4, was mutated to asparagine. This mutation was relatively conservative in that it changed the ionisation state of the amino acid at physiological pH but did not cause a large enough change to disrupt helical structure. Despite this, the K310N CCR4 mutant produced an interesting phenotype in that the receptor was able to bind both ^{125}I-CCL17 and ^{125}I-CCL22 while only being able to mediate chemotaxis to CCL22. These data along with others presented in chapter 3 signified that CCL17 and CCL22 stabilise distinct conformations of CCR4, and that K310 is required for the functionality of one of the receptor states. As will be described in section 7.2.2, proteins such as FROUNT have been identified that bind to the C-termini of chemokine receptors. Since we hypothesise that K310 is required for the functionality of one CCR4 state, it may indicate that this amino acid requires an interaction with proteins that bind the CCR4 C-terminus.

Another mutant that exhibited differential effects upon chemokine binding and chemokine-induced migration was I286A CCR4, in which isoleucine 286 at the N-terminal face of transmembrane helix VII was mutated to alanine (see chapter 4). This mutant had normal cell-surface expression, but in chemotaxis assays the effects on CCL17 and CCL22 differed. CCL17-induced migration was significantly reduced in efficacy and potency, and only at 100 nM CCL17 was a low degree of migration observed. Chemotaxis to CCL22 was also reduced in potency, in that the response peaked at 10 nM rather than 1 nM (figure 4-5S). Interestingly, the efficacy of this response was significantly increased, as the chemotactic index for I286A transfectants at 10 nM was three-fold greater than the chemotactic index for WT transfectants at 1

nM (figure 4-5T). Assays investigating the ability of this mutant to bind chemokine however showed that the receptor did not bind either 0.1 nM ^{125}I-CCL17 or ^{125}I-CCL22. Clearly, due to the observed chemotaxis of the mutant transfectant, I286A bound chemokine. Therefore, the affinity of the chemokines for the receptor has likely been reduced as a result of the mutation.

As such, in contrast to the K310N mutant the apparent differential activity of the chemokines through the I286A mutant is likely due to an affinity change of the chemokines. I286 lies on the same side of transmembrane helix VII as the previously described GluVII:06 (E290), which was required for both receptor expression and chemokine binding. The I286 side chain may therefore be involved in similar interactions to GluVII:06 that are required for chemokine activity; the loss of the isoleucine in the I286A mutation may have disrupted interactions necessary for CCL17 binding. Alanine is a much less bulky residue than isoleucine, which may suggest that the I286A mutation has allowed a greater degree of helical movement to occur during CCL22-mediated activation of CCR4. As described in section 1.3.2.2, receptor activation according to the toggle switch model results in movement of the transmembrane helices, leading to an outward shift of the extracellular face of the receptor. This occurs along with intracellular portions of the receptor moving inwards, allowing the initiation of signalling. Since I286 is located at the top of transmembrane helix VII, it likely shifts during receptor activation. The mutation of this residue to alanine therefore may have facilitated this helical movement, resulting in the observed increase in CCL22 efficacy.

To further investigate this, saturation assays would need to be performed with increasing ^{125}I-chemokine concentrations in order to determine whether the I286A mutation caused a reduction in chemokine affinity.

In addition to point mutation, CCR4 was also C-terminally truncated and the resulting mutants investigated for their cell-surface expression and ability to induce chemotaxis of transfectants. The Δ40 truncation cut downstream of the putative helix VIII region, and the resulting mutant had normal cell-surface expression but chemotactic responses that were significantly increased in efficacy. This was attributed to the removal of serine and threonines, which as described are phosphorylated by GRKs, leading to the recruitment of arrestins and subsequent

receptor desensitisation and internalisation (Oppermann et al., 1999; Borroni et al., 2010; Vroon et al., 2006).

The Δ45 and Δ50 C-terminal truncations were also made; these cut into the putative helix VIII region. These had reduced cell-surface expression, and in chemotaxis assays were non-functional, indicating the importance of this region in receptor function. Analogous truncations of the chemokine receptors CCR5, CCR3 and CCR7 C-terminus have been shown to reduce receptor activation (Gosling et al., 1997; Sabroe et al., 2005; Otero et al., 2008). As described in section 1.3.2.3, studies of other GPCRs such as BLT1 and PAR1 indicated that this region, which is highly conserved across GPCRs, is involved in G protein activation (Okuno et al., 2003, 2005; Swift et al., 2006). In the crystal structure of squid rhodopsin, the detergent octyl glucoside bound to helix VIII and was believed to mimic $G\alpha_q$ (Murakami and Kouyama, 2008). The phenotypes of the Δ45 and Δ50 C-terminal truncations of CCR4 may therefore indicate a loss of G protein activation by the receptor.

Many of the CCR4 point mutations from chapters 4 and 5 had little or no effect on cell-surface expression or chemotactic ability of the receptor. For example, mutation of isoleucine 113 in transmembrane helix 3 to alanine did not perturb expression or function of the receptor. Mutation of lysine 188 in the second extracellular loop to alanine similarly had no effect on receptor phenotype. Other mutations such as F121A resulted in normal cell-surface expression but a reduction in chemokine potency in chemotaxis assays. These results suggest that, as would be expected, some amino acids of CCR4 do not directly interact with chemokine or signalling partners. Others such as I113 likely do not provide critical structural stabilisation required for the shift in transmembrane helix conformation that occurs during receptor activation (see section 1.3.2.2).

The data here presented have thus identified key regions of CCR4 that are required for its function. The residues that had the most drastic effect on CCR4 phenotype are highlighted on a cartoon diagram of CCR4 shown in figure 7-1, along with the regions identified by the truncation mutants.

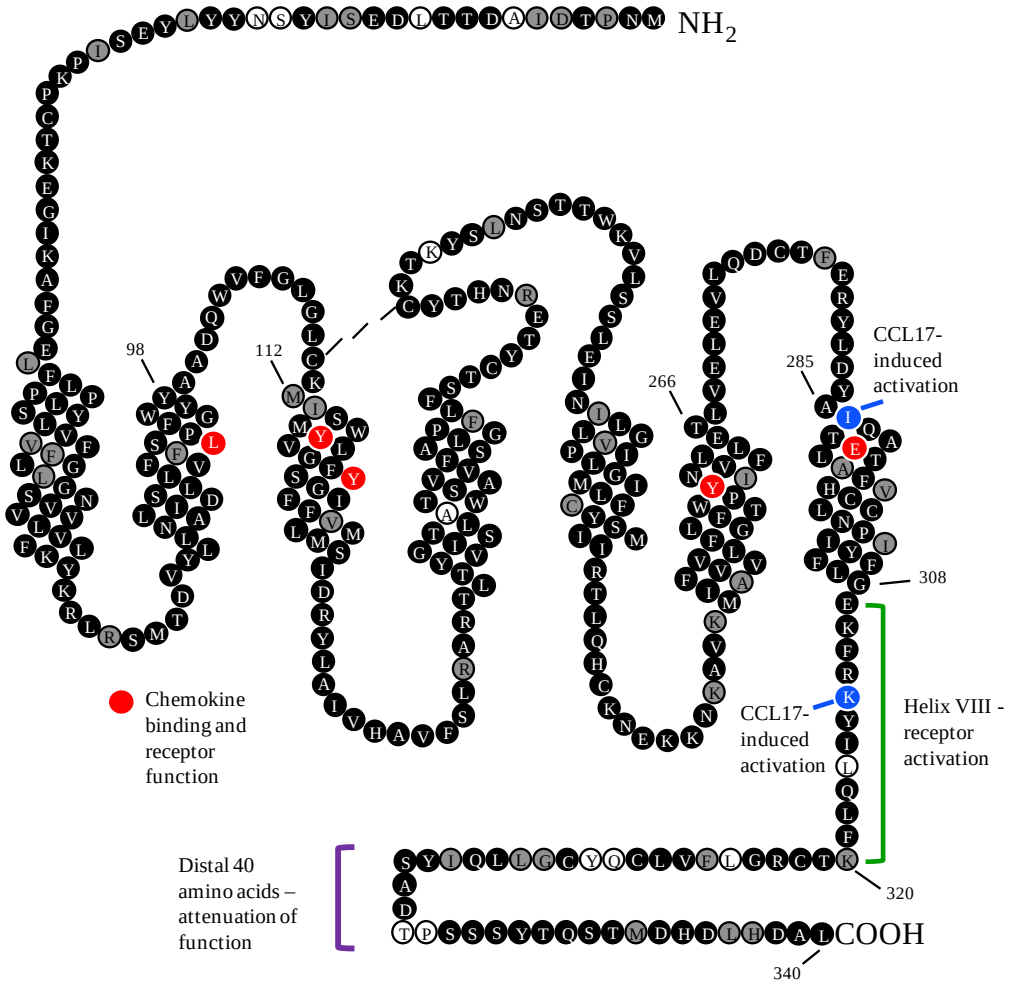

Figure 7-1 – Key regions of CCR4

Cartoon of CCR4, showing the extracellular N-terminus and loops, the transmembrane helices, and the intracellular loops and C-terminus. Residues that were determined to be critical for chemokine binding and receptor function are highlighted in red. K310 and I286, which are required for CCL17-induced chemotaxis, are highlighted in blue. The green and purple brackets denote the roles of specific regions of the C-terminus.

7.1.1 – Further work on the biology of CCR4

In section 1.3.2.2 the role of G proteins and β-arrestins in biased agonism was discussed; two ligands for the same receptor can induce differential effects on receptors signalling, such as the preferential recruitment of G proteins over β-arrestins, or vice versa. The chemokine receptor CCR7 is phosphorylated on its C-terminal serine and threonine residues by GRKs in response to CCL19 binding, but not in response to CCL21 binding. The receptor was thus internalised in response to one ligand and not the other (Bardi et al., 2001; Kohout et al., 2004).

The data from the K310N mutant indicate that CCL17 and CCL22 may stabilise distinct conformations of CCR4, as described in section 3.3.3. The chemokines CCL17 and CCL22 also induce differential effects upon the receptor, such as the inability of CCL17 to fully desensitise CCR4 against CCL22 treatment or for it to completely displace CCL22 in homologous binding assays (chapter 3).

We hypothesised that two populations of CCR4 exist; the first major population signals in response to CCL17 and CCL22 while the second minor population only signals in response to CCL22. We also hypothesised that K310 in the C-terminus played a role in the maintenance of the first population, as its mutation resulted in only CCL22-induced chemotaxis. To investigate these hypotheses, assays examining receptor activation and β-arrestin recruitment could be performed.

One method of directly comparing the potential biased signalling outputs of CCR4 would be to perform fluorescence resonance energy transfer (FRET) assays. These assays can be used to investigate protein-protein interactions. The proteins of interests are labelled with fluorescent proteins such as cyan fluorescent protein (CFP) or yellow fluorescent protein (YFP). CFP, the donor fluorophore, is excited leading to the emission of cyan light (wavelength = 527 nM). If the two proteins of interest are in close proximity, excited CFP transfers energy to YFP, leading to the emission of yellow light. If the two proteins are not in proximity, only cyan light is emitted (wavelength = 477 nM). The interaction of two proteins can therefore be measured (Lohse et al., 2012).

This assay has previously been used to examine interactions of G proteins and β-arrestins with the β_2-adrenergic receptor (β_2-AR). G protein activation was measured using FRET-based detection of cAMP, a secondary messenger produced as a result of GPCR activation. The formation of receptor/β-arrestin complexes were

also detected using FRET. The relative activation of these two signalling pathways were then compared for various ligands of β_2-AR, and used to determine which generated biased outputs; for example the ligand CPB showed a relatively higher level of β-arrestin recruitment compared to cAMP production, while the ligand isoproterenol was unbiased in its signalling (Drake et al., 2008). This assay could be performed on CCR4, using both CCL17 and CCL22 to determine the potential bias of each ligand in terms of G protein activation or β-arrestin recruitment. To explore the role of K310 in the activity of the ligands, the K310N mutant could also be tested alongside the WT receptor. Since the K310N mutation rendered the receptor unresponsive to CCL17, it would not be expected to activate G proteins. However, CCL17 may still cause β-arrestin recruitment to the receptor. This FRET-based assay would allow direct investigation of the relative roles of both CCL17 and CCL22 and the signalling pathways they utilise.

Murine embryonic fibroblast (MEF) β-arrestin knockouts have previously been used to investigate the role of β-arrestins in β_2-adrenergic and angiotensin II type 1A receptor internalisation; it was found that the receptors internalised to a lower degree in the β-arrestin knockout cells when compared to WT cells (Kohout et al., 2001). Since β-arrestins are involved in the desensitisation, endocytosis, and signalling of GPCRs including chemokine receptors (see section 1.3.2.2), their role in CCR4 could be determined through the use of β-arrestin knockout cells. The Δ40 CCR4 truncation in particular would be an interesting target for this assay, as it was hypothesised that the truncation removed serine and threonine sites required for GRK phosphorylation and thus β-arrestin recruitment (chapter 5).

7.2 – Allosteric antagonism of CCR4

The second portion of this project, encompassing chapters 4 – 6, addressed the action of allosteric antagonists of CCR4 and how they interacted with the receptor. Two classes of allosteric CCR4 antagonists were supplied by GlaxoSmithKline; the first class was hypothesised to bind to the intrahelical site 1 while the second class was hypothesised to bind to the intracellular site 2.

Chapters 4 and 5 probed the effect of CCR4 mutation on the ability of antagonists to inhibit chemotaxis or chemokine binding. These assays were indirect in that they inferred a loss of binding site if a mutant was less sensitive to inhibition. Chapter 6 however used direct assays to measure the effects of CCR4 mutation, by investigating the binding of radiolabelled antagonists to the mutant receptors.

7.2.1 – Site 1 antagonists

It was hypothesised that the first class of CCR4 antagonists bound to site 1, within the transmembrane helices of the receptor. Chemotaxis and chemokine-binding assays were performed in chapter 4 on site 1 mutants, and assays using ^{3}H-3 were performed in chapter 6. The hypothesis was confirmed, due to the fact that several site 1 mutants showed reduced sensitivity to the site 1 antagonists.

In chapter 4 it was shown that L118A transfectants had significantly reduced potency in chemotaxis assays to 1 nM CCL17 and CCL22 when inhibited by antagonist 7. This result was supported by binding assays, in which the same transfectants showed reduced sensitivity to inhibition of ^{125}I-CCL17 and ^{125}I-CCL22 by antagonist 7. The L118A mutation was of a residue in the third transmembrane domain, in a cluster of amino acids that were predicted to form part of the intrahelical antagonist binding site. Two other mutants, Y122F and I125A, also showed reductions in antagonist potency in chemotaxis assays.

Assays in chapter 6 revealed that mutants of the highly conserved amino acid GluVII:06 in the seventh transmembrane helix did not bind the tritium-labelled antagonist 3 (^{3}H-3). However, due to issues regarding the non-specific binding of this compound to L1.2 membranes, the variability of the ^{3}H-3 assays was high and as such saturation assays to determine ligand affinity for the mutant receptors could not be performed. This assay also prevented detailed investigation of other site 1 mutants such as L118A, Y117A, and L92A. These mutants were assayed with limited

concentration ranges of ^{3}H-3, at which they showed the ability to bind the antagonist. However, due to the variability of the assay any change in affinity resulting from the receptor mutation could not be investigated.

This loss of the ^{3}H-3 binding site in the GluVII:06 mutants supports previous studies into the role of this amino acid in receptor antagonism. As has been described in chapter 6, this conserved amino acid was involved in the binding of antagonists such as TAK-779, UCB3625 and AMD3100 to the receptors CCR5, CCR1 & CCR3, and CXCR4 (Dragic et al., 2000; de Mendonça et al., 2005; Wise et al., 2007; Rosenkilde et al., 2004).

From the eighteen residues predicted to form the site 1 antagonist binding site, the results from these assays have shown that three from the third transmembrane helix and one from the seventh helix are involved in antagonist binding to CCR4. Figure 7-2 shows the location of the residues identified to be contact points for antagonist.

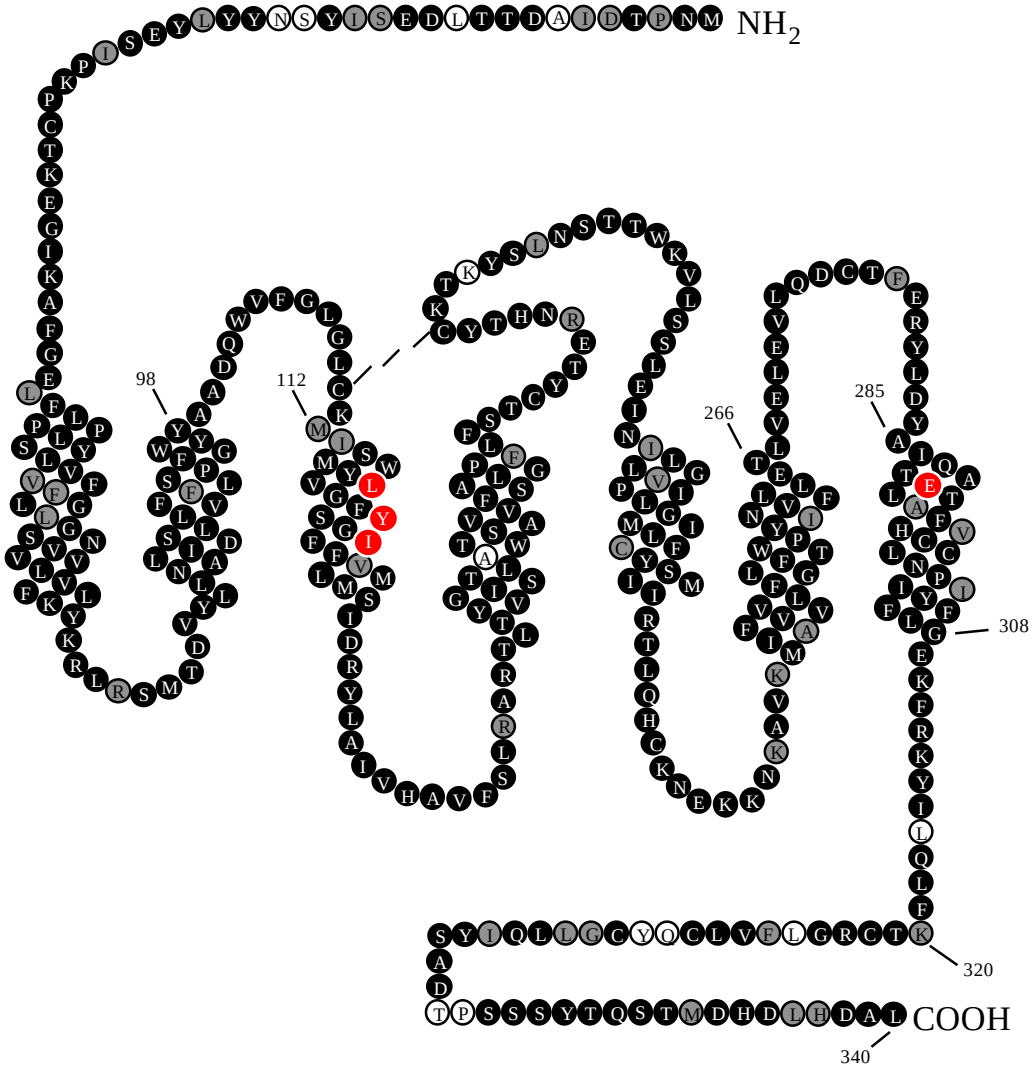

Figure 7-2 – CCR4 residues involved in site 1 antagonist activity

Chapters 4 and 6 used indirect and direct antagonist-based assays to investigate the role of several helical and extracellular loop mutants in site 1 antagonist activity. The residues that when mutated showed reduced ability to antagonise or bind the receptor are highlighted in red. L118, Y122, and I125 in transmembrane helix III were identified using chemotaxis assays. E290/GluVII:06 in transmembrane helix VII was identified using ^{3}H-3 binding assays.

These results of the site 1 study can be used to suggest putative interactions for these residues with elements of the antagonist structures. In WT CCR4, GluVII:06 likely forms ionic interactions with positively charged groups in the site 1 antagonists. This interaction requires both the acidic nature of glutamic acid in addition to its size, since mutation to both aspartic acid and alanine rendered it unable to bind ^{3}H-3.

The transmembrane domain mutants, L118A, Y122F, and I125A, suggest that this region in WT CCR4 forms hydrophobic interactions with the antagonists. Tyrosine contains an aromatic group, which as described can form π-stacking interactions with other aromatic groups. These groups are present in the antagonists. In addition, the hydroxyl group of tyrosine can also form hydrogen bonds; mutation of a conserved tyrosine of CCR5 to phenylalanine reduced antagonist binding, indicating that the hydrogen bonding capacity of tyrosine is also required for receptor-antagonist interactions (James Pease, personal communication). Branched chain hydrophobic amino acids such as leucine and isoleucine may supply hydrophobic interactions in the antagonist binding pocket, as has been suggested for the antagonists aplaviroc, UCB36525, and reparixin that bind the receptors CCR5, CCR1, and CXCR4, respectively (Allegretti et al., 2008).

The site 1 antagonists have been shown to inhibit CCR4-induced migration, and also to bind to an intracellular pocket in a similar manner to previously described chemokine receptor antagonists, in that they bind GluVII:06 in transmembrane helix VII and several residues in helix III (see section 6.4.2.1). These CCR4 antagonists may therefore be useful as therapeutic agents in the treatment of CCR4-driven diseases. Such diseases include asthma, atopic dermatitis, and various cancers such as non-Hodgkin lymphoma and adult T-cell leukaemia (see section 1.4.2).

Allosteric antagonists of other chemokine receptors have had mixed success in clinical trials, as described in section 1.4.4. For example, the CCR5 antagonist Maraviroc binds in an allosteric manner to a similar helical pocket to the one described here for CCR4, as does the CCR1 antagonist BX 741. However, while Maraviroc is currently approved for HIV therapy, the development of BX 741 for the treatment of multiple sclerosis was halted due to a lack of efficacy. This may be explained by the fact that inflammatory disease involve multiple chemokines and chemokine receptors, while HIV can only enter macrophages through CCR5,

meaning that a chemokine receptor-specific drug would be more effective in this case (Dorr et al., 2005; Watson et al., 2005; Garcia-Perez et al., 2011; Pease and Horuk, 2009; Allegretti et al., 2012).

It has been suggested that the clinical failure of some chemokine receptor antagonists may be in part due to the effective dose of the antagonist used in the trials. As described in section 1.4.4, over 90% of receptors need to be occupied by the antagonist in order to give an efficacious response, since a small number of unoccupied receptors can drive inflammation through positive feedback. An effective antagonist would also need to be potent, in order to reduce the concentration of compound required to inhibit a response. In the *in vitro* chemotaxis assays shown in figure 4-7, antagonist 7 proved to be the most potent at inhibiting both CCL17 and CCL22-induced migration of transfected cells. While further assays would be needed to determine if this translated to an *in vivo* setting, antagonist 7 would likely be the most attractive target for therapy in this regard. This antagonist could be further developed by examining the structure-activity relationship (SAR) of the compound and modifying it to improve its potency or specificity for the receptor.

CCR4 antagonists have been previously optimised for potency by exploring the SAR of three functional groups. An initial screen of an antagonist library resulted in the identification of several thiazolidinone-based compounds. These contained an amide linker, a central aromatic ring, and an amide group. The modification of these three groups by introduction of halogens, sulphonamides and phenyl rings in various combinations resulted in compounds that could inhibit CCL22 binding to CCR4 with IC_{50} values of between 100 and 200 nM, compared to the initial compound which had an IC_{50} of 2.4 μM (Allen et al., 2004). The antagonists presented in this project, particularly antagonist 7, could therefore be further developed in order to improve their activity against CCR4.

7.2.2 – Site 2 antagonists

It was hypothesised that the site 2 antagonists bound to an intracellular site on the C-terminus of CCR4. In chapter 4, the F305A and L307V mutants showed reduced sensitivity to two of the site 2 antagonists, confirming this hypothesis. These mutants however did not show a complete lack of sensitivity to the antagonists, indicating that other regions of the C-terminus were involved in antagonist binding.

Three truncation mutants were created in order to determine the role of successive portions of the CCR4 C-terminus in antagonist binding to this site. The Δ45 and Δ50 truncation mutants, which cut into the highly conserved helix VIII region, were non-functional. Transfectants of these mutants could therefore not be investigated for their ability to be inhibited by the site 2 antagonists in chemotaxis assays. The Δ40 construct however did prove to be functional, and in chemotaxis assays it was determined that it did not differ to WT with respect to inhibition of migration. The last 40 amino acids of CCR4 were thus shown to be dispensable for the action of the site 2 antagonists, meaning that they must bind to a site upstream of the truncation point. This site likely lies within the conserved helix VIII region, since other studies of chemokine receptors have identified an intracellular antagonist site involving the helix VIII region (Nicholls et al., 2008; Salchow et al., 2010).

K310N transfectants, which did not migrate to CCL17, were assayed in CCL22 chemotaxis antagonism assays and showed no difference to WT transfectants. L318A transfectants also showed no difference to WT transfectants in chemotaxis antagonism assays.

These data therefore showed that F305 and L307 at the end of transmembrane helix VII are involved in site 2 antagonist activity, while the last 40 amino acids of CCR4 are not required for antagonist activity. A summary of this is shown in figure 7-3.

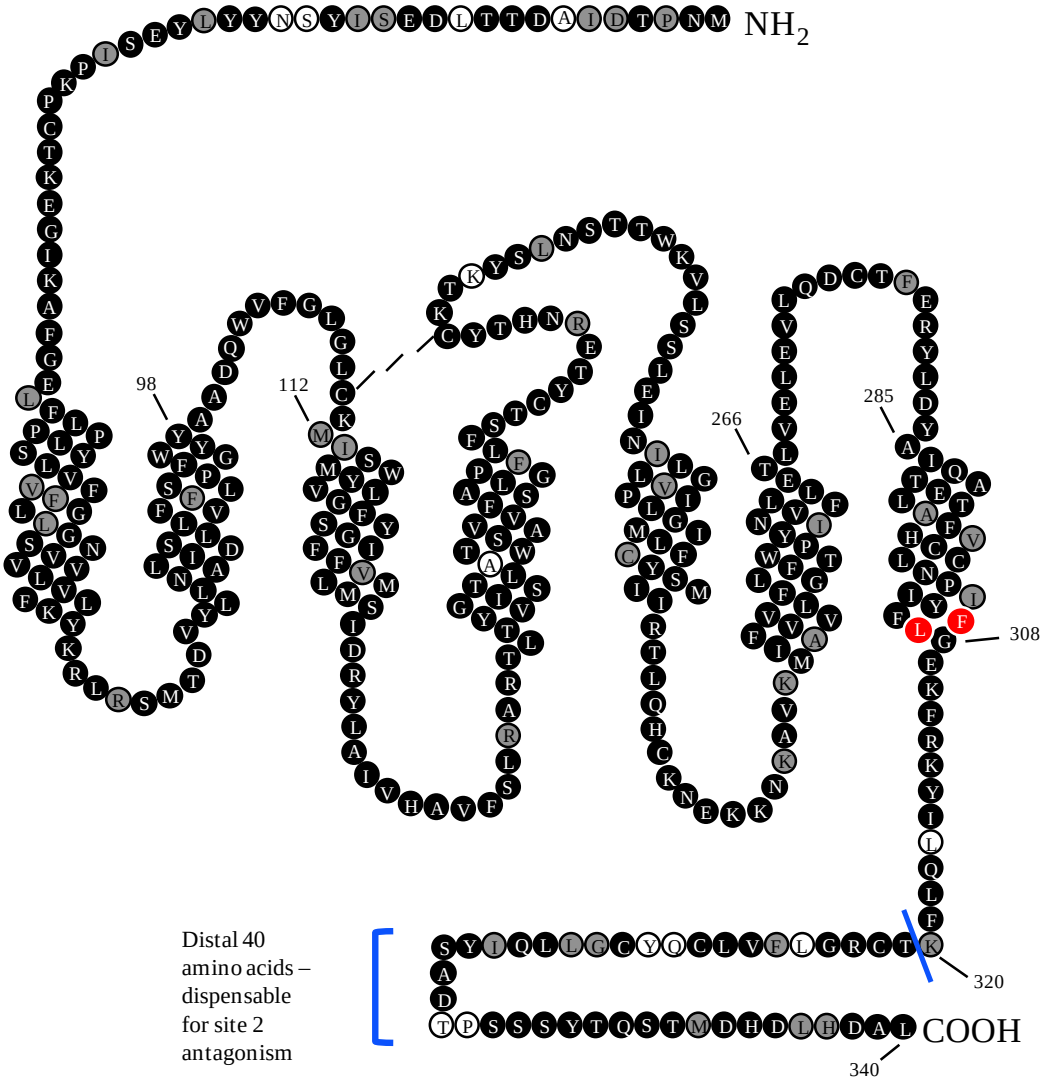

Figure 7-3 – CCR4 residues involved in site 2 antagonist activity

Chapter 5 used indirect antagonist-based assays to investigate the role of several helical and extracellular loop mutants in site 1 antagonist activity. F305 and L307 were identified in chemotaxis assays as having a role in antagonist activity. Truncation mutants demonstrated that the distal 40 amino acids of the C-terminus of CCR4 were not required for antagonism.

Chapter 6 involved the use of ^{3}H-5, a tritiated site 2 antagonist, to investigate binding of antagonist to L1.2 membranes expressing the site 2 mutants. This analysis however was hindered by the identification of a low-affinity binding site for ^{3}H-5 on the L1.2 membranes. Even at high ^{3}H-5 concentrations, the CCR4-expressing membranes were not saturated, indicating the presence of another site for the compound. This site was confirmed using naïve L1.2 membranes, and the use of different site 2 compounds to define non-specific binding did not remedy the problem.

Selectivity data provided by GlaxoSmithKline showed that antagonist 5 had some activity against other chemokine receptors, particularly CCR1 and CCR5. Since the C-termini of chemokine receptors are highly conserved, it is perhaps unsurprising that antagonist 5 showed activity against other receptors. L1.2 cells are a leukocyte line and therefore likely endogenously express chemokine receptors, which may explain the presence of a ^{3}H-5 binding site on the L1.2 membranes.

While this finding prevented analysis of the direct binding of ^{3}H-5 to the site 2 mutants, it does suggest that antagonist 5 may have potential as a promiscuous antagonist of chemokine receptors. As described in section 6.4.3, several promiscuous receptor antagonists have been discovered. If antagonist 5 showed activity against multiple chemokine receptors in further studies, it may have the potential to be developed for therapy for disease involving multiple chemokine receptors.

Asthma for example involves CCR7-expressing dendritic cells presenting antigen to CCR7-expressing naïve T cells, which differentiate into CCR4- and CCR8-expressing T_H2 cells. These T_H2 cells produce IL-5, which drives the production and survival of CCR3-expressing eosinophils. T_H2 cells also produce IL-13, which stimulates CXCR5-expressing B cells to produce IgE which activates CCR2-expressing mast cells (see section 1.1). A CCR4-specific antagonist would only target T_H2 cells in this disease, while a more promiscuous antagonist could potentially target multiple cell types. Antagonist 5 for example could be used to inhibit both T_H2 and mast cell migration, since it was shown that it had activity against CCR2. CCR2 is expressed on mast cells, which as described in section 1.1 release the inflammatory mediator histamine in response to binding of IgE cross-linked by antigen. By blocking CCR2-mediated migration of mast cells the histamine response could be

prevented from occurring in tissues, along with the inflammation caused by CCR4-expressing T_H2 cells.

Research into interaction partners of chemokine receptors may shed light on the action of intracellular allosteric antagonists. The protein FROUNT was identified to bind the CCR2 C-terminus, and was shown to play an important role in the function of this receptor. Upon stimulation by the CCR2 ligand CCL2, FROUNT trafficks to the cell membrane and interacts with CCR2 at the leading edge of the migrating cell. FROUNT was also shown to mediate the formation of CCR2 clusters at this leading edge, which led to the formation of pseudopodia and ultimately cell migration (Terashima et al., 2005). It was later shown that CCR5 also bound FROUNT. A dominant-negative version of FROUNT inhibited CCR5-mediated chemotaxis of cells, and as with CCR2, FROUNT was shown to co-localise with the receptor at the leading edge of the cell upon chemokine stimulation (Toda et al., 2009).

Truncations of CCR2 and CCR5 had previously been shown to result in impaired chemotaxis of cells expressing these receptor mutants (Arai et al., 1997; Le Gouill et al., 1999; Kraft et al., 2001). It was hypothesised that these truncations prevented the binding of FROUNT, and due to the role this protein played in receptor-mediated chemotaxis, perturbed the ability of the truncated receptors to induce cell migration (Toda et al., 2009).

The region truncated in CCR2 and CCR5 corresponds to the helix VIII region previously described (see section 1.3.2.3). The Δ45 and Δ50 truncations shown in chapter 5 are also truncations of this region. It was speculated that due to the conservation of this C-terminal region, there may be other FROUNT-like proteins that mediate chemotaxis of other chemokine receptors. Helix VIII is believed to interact with G proteins and play a role in receptor activation. The Δ45 and Δ50 CCR4 truncations were therefore hypothesised to have removed the ability of CCR4 to couple to G proteins and initiate signalling (see section 5.4.1.2). It may also be the case that helix VIII of CCR4 is necessary for the recruitment of FROUNT-like proteins to facilitate cell migration.

The identification of FROUNT and the possibility of FROUNT-like proteins mediating CCR4 chemotaxis also has implications for the mechanism of the site 2

allosteric CCR4 antagonists. As described above, helix VIII was hypothesised to couple to G proteins. This may suggest that this class of antagonists inhibit receptor signalling by preventing their coupling to G proteins.

Considering the high degree of conservation of the C-terminal helix VIII region between chemokine receptors, it would not be surprising if a FROUNT-like protein was discovered that mediated cell migration in a similar manner to that described for CCR2 and CCR5. The cytoplasmic end of transmembrane helix VII and the beginning of helix VIII in particular are almost identical across all chemokine receptors, and compared to CCR2 and CCR5, CCR4 only differs in this region in one amino acid; it contains a phenylalanine directly after the NPXXY motif (F305) rather than an alanine in CCR2 and CCR5. FROUNT-like proteins may bind to this region as it possesses the same amino acids that would facilitate these interactions. Therefore, a possible alternative mechanism for site 2 antagonist inhibition of CCR4 may be the blocking of an interaction between a FROUNT-like protein and the CCR4 helix VIII region.

One way to examine the potential interactions that helix VIII has with other proteins would be to perform yeast two-hybrid screening. This technique is used to discover protein-protein interactions. The ‘bait’ protein, in this case CCR4, is cloned into a plasmid containing the sequence for the DNA binding domain (BD) of the *Gal4* transcription factor. Fragments of genomic DNA are cloned into plasmid vectors containing the sequence for the *Gal4* activation domain (AD). When these two plasmids are transformed into yeast cells, bait-BD and prey-AD are expressed. If the prey protein is a binding partner for the bait protein, the two domains of the Gal4 transcription factor are able to activate transcription of a reporter gene (Brückner et al., 2009). This assay could therefore be used to identify possible FROUNT-like proteins that bind the CCR4 C-terminus.

7.2.3 – Further work on the CCR4 allosteric antagonists

There are many potential avenues for further work on the CCR4 antagonists. Some of the site 1 mutants were not tested against all the site 1 antagonists in chemotaxis assays; these assays would need to be performed in order to provide a complete picture of the effect of receptor mutation on the activity of the antagonists.

Additional CCR4 point mutants could also be made to further investigate the role of various residues in antagonist activity. For example, K310 could be mutated to alanine (K310A) instead of asparagine (K310N) to determine whether this more extreme mutation had any effect on antagonist activity. In CXCR2, K320 was mutated to alanine in order to disrupt an ion-pair interaction between the receptor and an intracellular antagonist (Salchow et al., 2010). Since the CCR4 Δ45 and Δ50 truncation mutants were non-functional, additional point mutation of specific helix VIII residues would allow the contribution of this region to antagonist activity to be determined.

Another major avenue for investigation would be optimising the use of the tritiated antagonists in the filtration binding assays. Ideally the CCR4 point mutants would be stably-transfected into CHO cells; these are a non-leukocyte line and have a low degree of non-specific binding for the radioactively labelled antagonists. The high variability of ^{3}H-3 in the investigation of the GluVII:06 and other site 1 mutants prevented detailed analysis of the effect of the mutation on antagonist affinity and binding sites. CHO-transfectants may provide a way to determine potential reductions in antagonist affinity as a result of CCR4 mutation.

The use of CHO membranes would also allow investigation of the site 2 mutants, since L1.2 membranes possessed a low-affinity binding site for ^{3}H-5. It has been established that this site is not present on CHO membranes, meaning that CHO-transfectants would provide a way to determine if site 2 point mutation or truncation resulted in reduced ^{3}H-5 affinity.

The non-functional CCR4 mutants such as the Δ45 and Δ50 truncations would be of particular interest for ^{3}H-5 saturation assays, since there was no data regarding the effect of these truncations on the activity of the site 2 antagonists. Since it was determined that the antagonists did not require the amino acids downstream of helix VIII for activity, it was hypothesised that these intracellular antagonists bound to a

site within helix VIII. Performing saturation assays on membranes expressing these truncations would determine the contribution of this region to antagonist binding and conclusively determine the role of helix VIII in CCR4 antagonism.

While only two tritiated antagonists were available, ^{3}H-3 and ^{3}H-5, the effect of receptor mutation on the binding of the remaining five antagonists could also be determined using competition assays in which membranes expressing CCR4 are incubated with a fixed concentration of a tritiated antagonist and an increasing concentration of unlabelled antagonist. This heterologous competition assay could be used to determine the IC_{50} of the unlabelled antagonist for WT and mutant CCR4; if a receptor mutation disrupted antagonist binding we would expect to see a less potent competition of the radiolabelled antagonist by the unlabelled antagonist.

Assays to investigate the kinetics of the radiolabelled ligands could also be performed, which would involve measuring specific binding at various intervals. Binding of the ligand to receptor can take time to equilibrate, which would require association assays to be performed to determine at what time equilibrium occurs. The assays performed in chapter 6 were incubated for 3 hours, which was after the equilibrium point. An association assay using intervals from 0 hours up to 3 hours could be performed. In addition, measuring specific binding at time points after 3 hours could also be performed in order to investigate the dissociation rate of the ligand. By performing these assays on both WT CCR4- and mutant CCR4-CHO membranes the potential effects of ligand kinetics resulting from the mutations could be determined.

Another potential avenue for investigation would be to determine which chemokine receptors L1.2 cells endogenously express. Flow cytometry using a panel of chemokine receptor antibodies could be performed on naïve L1.2 cells to determine cell-surface expression of the receptors. Following identification of these receptors, plasmids containing receptor cDNA could be transfected into CHO cells, and the resulting membranes used in ^{3}H-5 saturation assays and compared to CCR4-expressing membranes. This would allow the relative affinity of the ligand for the different receptors to be determined.

As described in section 7.2.2, broad-spectrum chemokine receptor antagonists could have therapeutic potential. Several such antagonists have previously been

identified. An example of such an antagonist is TAK-779, an allosteric antagonist that binds an intrahelical pocket of the chemokine receptors CCR2 and CCR5 (Baba et al., 1999; Shiraishi et al., 2000). TAK-779 was later shown to target the chemokine receptor CXCR3 (Gao et al., 2003). TAK-779 and its derivative TAK-652 were investigated for their ability to inhibit HIV-1 replication, since the virus uses CCR5 to enter macrophages (Moore et al., 1997). The agonist UCB35625 inhibits activity of the related receptors CCR1 and CCR3 (Sabroe et al., 2000), and was shown to bind similar intrahelical residues including GluVII:06 of both receptors (de Mendonça et al., 2005; Wise et al., 2007).

Therapies targeting multiple receptors have had some success. Zyprexa is a benzodiazepine used to treat schizophrenia, which binds to multiple GPCRs including those from the dopamine, histamine, and serotonin families (Pease and Horuk, 2009). Broad-spectrum antagonists may provide potential for chemokine receptor-driven diseases, since these pathologies involve multiple immune cells each of which express many different receptors. For example, asthma involves migration to the lung of T_H2 cells expressing both CCR4 and CCR8; these then release cytokines such as IL-5 which causes the development and recruitment of eosinophils expressing CCR3. CCR2-expressing mast cells are also involved in the pathogenesis of the disease (see section 1.4.1). Therefore, an antagonist targeting multiple receptors could provide a way to target the multi-faceted aspects of an inflammatory condition such as asthma.

7.3 – Summary

This project investigated both the biology of the human chemokine receptor CCR4 and the action of seven allosteric antagonists.

The highly conserved GluVII:06 of transmembrane helix VII was determined to be critical for chemokine binding and thus receptor function. Mutation of K310, an amino acid located within the highly conserved helix VIII region, rendered the receptor unable to induce migration to CCL17; however the mutant receptor was still able to induce migration to CCL22. Both chemokines bound the receptor in the same manner as WT CCR4, indicating that the mutation affected activation of the receptor in response to CCL17. This finding was novel in that it was the first identified case of an amino acid change causing differential effects on ligand-induced responses. Previous studies highlighted the dominance of CCL22 over CCL17 in CCR4-desensitisation, internalisation, and chemokine binding assays. In conjunction with the data presented in this project it was concluded that CCL17 and CCL22 stabilise distinct conformations of CCR4.

Mutations of other regions within CCR4, such as conserved tyrosines in transmembrane helix III and L92 of the TXP motif demonstrated that these amino acids were required for receptor function.

Two classes of allosteric CCR4 antagonists were supplied by GlaxoSmithKline. The first class was hypothesised to bind to a classical intrahelical site, while the second hypothesised to bind to a novel intracellular site. Residues of CCR4 were mutated to confirm these hypotheses.

The investigation of the site 1 antagonists showed that L118, Y122, and I125 of transmembrane helix III and E290 (GluVII:06) of transmembrane helix VII were involved in the activity of these antagonist, through the use of both indirect and direct antagonist-based assays. The indirect antagonists assays were also used to determine that F305 and L307 at the extracellular face of transmembrane helix VII were involved in site 2 antagonist activity.

Direct assays using a radiolabelled site 2 antagonist were hindered by the identification of a low-affinity binding site for the antagonist on the L1.2 membranes used in the binding assays. This site was hypothesised to be comprised of other chemokine receptors endogenously expressed on the cells, possibly CCR2 and CCR5,

based on antagonist selectivity data provided by GlaxoSmithKline. Despite this, the site 2 antagonist may have potential as a promiscuous chemokine receptor antagonist. Since many inflammatory conditions involve multiple cell types expressing a range of chemokine receptors, an antagonist that targets a variety of receptors may prove to be an effective therapeutic agent.

8 – References

Abi-Younes, S., Si-Tahar, M., and Luster, A D. (2001). The CC chemokines MDC and TARC induce platelet activation via CCR4. Thrombosis research *101*, 279–289.

Abraham, S. N., and St John, A. L. (2010). Mast cell-orchestrated immunity to pathogens. Nature reviews. Immunology *10*, 440–452.

Ahn, K. H., Nishiyama, A., Mierke, D. F., and Kendall, D. A. (2010). Hydrophobic residues in helix 8 of cannabinoid receptor 1 are critical for structural and functional properties. Biochemistry *49*, 502–511.

Ai, L., and Liao, F. (2002). Mutating the Four Extracellular Cysteines in the Chemokine Receptor CCR6 Reveals Their Differing Roles in Receptor Trafficking, Ligand Binding, and Signaling. Biochemistry, 8332–8341.

Allegretti, M., Bertini, R., Bizzarri, C., Beccari, A., Mantovani, A., and Locati, M. (2008). Allosteric inhibitors of chemoattractant receptors: opportunities and pitfalls. Trends in pharmacological sciences *29*, 280–286.

Allegretti, M., Cesta, M. C., Garin, A., and Proudfoot, A. E. I. (2012). Current status of chemokine receptor inhibitors in development. Immunology letters *145*, 68–78.

Allen, S. J., Crown, S. E., and Handel, T. M. (2007). Chemokine: receptor structure, interactions, and antagonism. Annual review of immunology *25*, 787–820.

Allen, S., Newhouse, B., Anderson, A. S., Fauber, B., Allen, A., Chantry, D., Eberhardt, C., Odingo, J., and Burgess, L. E. (2004). Discovery and SAR of trisubstituted thiazolidinones as CCR4 antagonists. Bioorganic & medicinal chemistry letters *14*, 1619–1624.

Andrew, D. P., Chang, M. S., McNinch, J., Wathen, S. T., Rihanek, M., Tseng, J., Spellberg, J. P., and Elias, C. G. (1998). STCP-1 (MDC) CC chemokine acts specifically on chronically activated Th2 lymphocytes and is produced by monocytes on stimulation with Th2 cytokines IL-4 and IL-13. Journal of immunology (Baltimore, Md. : 1950) *161*, 5027–5038.

Andrews, G., Jones, C., and Wreggett, K. A. (2008). An Intracellular Allosteric Site for a Specific Class of Antagonists of the CC Chemokine G Protein-Coupled Receptors CCR4 and CCR5. Molecular Pharmacology *73*, 855–867.

Annunziato, F., Cosmi, L., Galli, G., Beltrame, C., Romagnani, P., Manetti, R., Romagnani, S., and Maggi, E. (1999). Assessment of chemokine receptor expression by human Th1 and Th2 cells in vitro and in vivo. Journal of leukocyte biology *65*, 691–699.

Arai, H., Monteclaro, F. S., Tsou, C. L., Franci, C., and Charo, I. F. (1997). Dissociation of chemotaxis from agonist-induced receptor internalization in a lymphocyte cell line transfected with CCR2B. Evidence that directed migration

does not require rapid modulation of signaling at the receptor level. The Journal of biological chemistry *272*, 25037–25042.

Aramori, I., Zhang, J., Ferguson, S. S. G., Bieniasz, P. D., Cullen, B. R., and Caron, M. G. (1997). Molecular mechanism of desensitization of the chemokine receptor CCR-5: receptor signaling and internalization are dissociable from its role as an HIV-1 co-receptor. The EMBO journal *16*, 4606–4616.

Aratake, Y., Okuno, T., Matsunobu, T., Saeki, K., Takayanagi, R., Furuya, S., and Yokomizo, T. (2012). Helix 8 of leukotriene B4 receptor 1 inhibits ligand-induced internalization. FASEB, 1–11.

Auger, G. A., Pease, J. E., Shen, X., Xanthou, G., and Barker, M. D. (2002). Alanine scanning mutagenesis of CCR3 reveals that the three intracellular loops are essential for functional receptor expression. European journal of immunology *32*, 1052–1058.

Baba, M., Nishimura, O., Kanzaki, N., Okamoto, M., Sawada, H., Iizawa, Y., Shiraishi, M., Aramaki, Y., Okonogi, K., Ogawa, Y., et al. (1999). A small-molecule, nonpeptide CCR5 antagonist with highly potent and selective anti-HIV-1 activity. Proceedings of the National Academy of Sciences of the United States of America *96*, 5698–5703.

Ballesteros, J. A, Deupi, X., Olivella, M., Haaksma, E. E., and Pardo, L. (2000). Serine and threonine residues bend alpha-helices in the chi(1)=g(-) conformation. Biophysical journal *79*, 2754–2760.

Bannert, N., Craig, S., Farzan, M., Sogah, D., Santo, N. V., Choe, H., and Sodroski, J. (2001). Sialylated O-glycans and sulfated tyrosines in the NH2-terminal domain of CC chemokine receptor 5 contribute to high affinity binding of chemokines. The Journal of experimental medicine *194*, 1661–1673.

Barak, L. S., Menard, L., Ferguson, S. S. G., Colapietro, A., and Caron, M. G. (1995). The Conserved Seven-Transmembrane Sequence NPXXY of the G-protein-Coupled Receptor Superfamily Regulates Multiple Properties of the beta2-adrenergic receptor. Biochemistry, 15407–15414.

Bardi, G., Lipp, M., Baggiolini, M., and Loetscher, P. (2001). The T cell chemokine receptor CCR7 is internalized on stimulation with ELC, but not with SLC. European journal of immunology *31*, 3291–3297.

Barlic, J., Khandaker, M. H., Mahon, E., Andrews, J., Devries, M. E., Mitchell, G. B., Rahimpour, R., Tan, C. M., Ferguson, S. S. G., and Kelvin, D. J. (1999). Beta Arrestins Regulate Interleukin-8-induced CXCR1 Internalization. The Journal of biological chemistry *274*, 16287–16294.

Barton, G. M. (2008). A calculated response: control of inflammation by the innate immune system. The Journal of clinical investigation *118*.

Beck, A., and Reichert, J. M. (2012). Marketing approval of mogamulizumab. Landes Bioscience, 1–7.

Belisle, B., and Abo, A. (2000). N-Formyl peptide receptor ligation induces rac-dependent actin reorganization through Gbeta gamma subunits and class Ia phosphoinositide 3-kinases. The Journal of biological chemistry *275*, 26225–26232.

Benard, V., Bohl, B. P., and Bokoch, G. M. (1999). Characterization of rac and cdc42 activation in chemoattractant-stimulated human neutrophils using a novel assay for active GTPases. The Journal of biological chemistry *274*, 13198–13204.

Bennett, G. L., and Horuk, R. (1997). Iodination of Chemokines for Use in Receptor Binding Analysis. Methods in Enzymology *529*, 134–148.

Bertini, R., Barcelos, L. S., Beccari, a R., Cavalieri, B., Moriconi, A., Bizzarri, C., Di Benedetto, P., Di Giacinto, C., Gloaguen, I., Galliera, E., et al. (2012). Receptor binding mode and pharmacological characterization of a potent and selective dual CXCR1/CXCR2 non-competitive allosteric inhibitor. British journal of pharmacology *165*, 436–454.

Bjarnadóttir, T. K., Gloriam, D. E., Hellstrand, S. H., Kristiansson, H., Fredriksson, R., and Schiöth, H. B. (2006). Comprehensive repertoire and phylogenetic analysis of the G protein-coupled receptors in human and mouse. Genomics *88*, 263–273.

Blackburn, P. E., Simpson, C. V., Nibbs, R. J. B., O'Hara, M., Booth, R., Poulos, J., Isaacs, N. W., and Graham, G. J. (2004). Purification and biochemical characterization of the D6 chemokine receptor. The Biochemical journal *379*, 263–272.

Blanpain, C., Doranz, B. J., Bondue, A., Govaerts, C., De Leener, A., Vassart, G., Doms, R. W., Proudfoot, A., and Parmentier, M. (2003). The core domain of chemokines binds CCR5 extracellular domains while their amino terminus interacts with the transmembrane helix bundle. The Journal of biological chemistry *278*, 5179–5187.

Blanpain, C., Wittamer, V., Vanderwinden, J. M., Boom, A., Renneboog, B., Lee, B., Le Poul, E., El Asmar, L., Govaerts, C., Vassart, G., et al. (2001). Palmitoylation of CCR5 is critical for receptor trafficking and efficient activation of intracellular signaling pathways. The Journal of biological chemistry *276*, 23795–23804.

Bockaert, J., and Pin, J. P. (1999). Molecular tinkering of G protein-coupled receptors: an evolutionary success. The EMBO journal *18*, 1723–1729.

Bonecchi, R., Bianchi, G., Bordignon, P. P., D'Ambrosio, D., Lang, R., Borsatti, A., Sozzani, S., Allavena, P., Gray, P. A., Mantovani, A., et al. (1998). Differential expression of chemokine receptors and chemotactic responsiveness of type 1 T

helper cells (Th1s) and Th2s. The Journal of experimental medicine *187*, 129–134.

Borroni, E. M., Mantovani, A., Locati, M., and Bonecchi, R. (2010). Chemokine receptors intracellular trafficking. Pharmacology & therapeutics *127*, 1–8.

Bridges, T. M., and Lindsley, C. W. (2008). G-protein-coupled receptors: from classical modes of modulation to allosteric mechanisms. ACS chemical biology *3*, 530–541.

Brückner, A., Polge, C., Lentze, N., Auerbach, D., and Schlattner, U. (2009). Yeast two-hybrid, a powerful tool for systems biology. International journal of molecular sciences *10*, 2763–2788.

Burns, D. L. (1988). Subunit structure and enzymic activity of pertussis toxin. Microbiol Sci *5*, 285–287.

Byers, M. A., Calloway, P. A., Shannon, L., Cunningham, H. D., Smith, S., Li, F., Fassold, B. C., and Vines, C. M. (2008). Arrestin 3 mediates endocytosis of CCR7 following ligation of CCL19 but not CCL21. Journal of immunology (Baltimore, Md. : 1950) *181*, 4723–4732.

Campbell, J. J., Brightling, C. E., Symon, F. A., Qin, S., Murphy, K. E., Hodge, M., Andrew, D. P., Wu, L., Butcher, E. C., and Wardlaw, A. J. (2001). Expression of chemokine receptors by lung T cells from normal and asthmatic subjects. Journal of immunology (Baltimore, Md. : 1950) *166*, 2842–2848.

Campbell, J. J., and Butcher, E. C. (2000). Chemokines in tissue-specific and microenvironment-specific lymphocyte homing. Current opinion in immunology *12*, 336–341.

Campbell, J. J., Haraldsen, G., Pan, J., Rottman, J., Qin, S., Ponath, P., Andrew, D. P., Warnke, R., Ruffing, N., Kassam, N., et al. (1999a). The chemokine receptor CCR4 in vascular recognition by cutaneous but not intestinal memory T cells. Nature *400*, 776–780.

Campbell, J. J., Pan, J., and Butcher, E. C. (1999b). Cutting edge: developmental switches in chemokine responses during T cell maturation. Journal of immunology (Baltimore, Md. : 1950) *163*, 2353–2357.

Carman, C. V., Sage, P. T., Sciuto, T. E., Fuente, M. A. D., Geha, S., Ochs, H. D., Dvorak, H. F., Dvorak, A. M., and Springer, T. A. (2007). Transcellular Diapedesis Is Initiated by Invasine Podosomes. Immunity *26*, 784–797.

Casarosa, P., Waldhoer, M., LiWang, P. J., Vischer, H. F., Kledal, T., Timmerman, H., Schwartz, T. W., Smit, M. J., and Leurs, R. (2005). CC and CX3C chemokines differentially interact with the N terminus of the human cytomegalovirus-encoded US28 receptor. The Journal of biological chemistry *280*, 3275–3285.

Chantry, D., Romagnani, P., Raport, C. J., Wood, C. L., Epp, A., Romagnani, S., and Gray, P. W. (1999). Macrophage-derived chemokine is localized to thymic medullary epithelial cells and is a chemoattractant for CD3(+), CD4(+), CD8(low) thymocytes. Blood *94*, 1890–1898.

Chao, T. S., Byron, K. L., Lee, K. M., Villereal, M., and Rosner, M. R. (1992). Activation of MAP kinases by calcium-dependent and calcium-independent pathways. Stimulation by thapsigargin and epidermal growth factor. The Journal of biological chemistry *267*, 19876–19883.

Chaplin, D. (2003). Overview of the immune response. Journal of Allergy and Clinical Immunology *111*, 442–459.

Charo, I. F., Myers, S. J., Herman, A., Franci, C., Connolly, A. J., and Coughlin, S. R. (1994). Molecular cloning and functional expression of two monocyte chemoattractant protein 1 receptors reveals alternative splicing of the carboxyl-terminal tails. Proceedings of the National Academy of Sciences of the United States of America *91*, 2752–2756.

Chen, Y., Green, S. R., Almazan, F., and Quehenberger, O. (2006). The Amino Terminus and the Third Extracellular Loop of CX3CR1 Contain Determinants Critical for Distinct Receptor Functions. Molecular pharmacology *69*, 857–865.

Cheng, Y.-C., and Prusoff, W. H. (1973). Relationship between the inhibition constant (Ki) and the concentration of inhibitor which causes 50 per cent inhibition (I50) of an enzymatic reaction. Biochemical Pharmacology *22*, 3099–3108.

Cheng, Z. J., Zhao, J., Sun, Y., Hu, W., Wu, Y. L., Cen, B., Wu, G. X., and Pei, G. (2000). beta-arrestin differentially regulates the chemokine receptor CXCR4-mediated signaling and receptor internalization, and this implicates multiple interaction sites between beta-arrestin and CXCR4. The Journal of biological chemistry *275*, 2479–2485.

Chensue, S. W., Lukacs, N. W., Yang, T. Y., Shang, X., Frait, K. A., Kunkel, S. L., Kung, T., Wiekowski, M. T., Hedrick, J. A., Cook, D. N., et al. (2001). Aberrant in vivo T helper type 2 cell response and impaired eosinophil recruitment in CC chemokine receptor 8 knockout mice. The Journal of experimental medicine *193*, 573–584.

Cherezov, V., Rosenbaum, D. M., Hanson, M. A., Rasmussen, S. G. F., Thian, F. S., Kobilka, T. S., Choi, H.-J., Kuhn, P., Weis, W. I., Kobilka, B. K., et al. (2007). High-resolution crystal structure of an engineered human beta2-adrenergic G protein-coupled receptor. Science (New York, N.Y.) *318*, 1258–1265.

Chung, C. D., Kuo, F., Kumer, J., Alykhan, S., Lawrence, C. E., Henderson, W. R., and Venkataraman, C. (2012). CCR8 Is Not Essential for the Development of Inflammation in a Mouse Model of Allergic Airway Disease. Journal of immunology (Baltimore, Md. : 1950) *170*, 581–587.

Chvatchko, Y., Hoogewerf, a J., Meyer, A., Alouani, S., Juillard, P., Buser, R., Conquet, F., Proudfoot, a E., Wells, T. N., and Power, C. a (2000). A key role for CC chemokine receptor 4 in lipopolysaccharide-induced endotoxic shock. The Journal of experimental medicine *191*, 1755–1764.

De Clercq, E. (2010). Recent advances on the use of the CXCR4 antagonist plerixafor (AMD3100, Mozobil™) and potential of other CXCR4 antagonists as stem cell mobilizers. Pharmacology & therapeutics *128*, 509–518.

Colvin, R. A., Campanella, G. S. V., Manice, L. A., and Luster, A. D. (2006). CXCR3 requires tyrosine sulfation for ligand binding and a second extracellular loop arginine residue for ligand-induced chemotaxis. Molecular and cellular biology *26*, 5838–5849.

Conn, P. J., Christopoulos, A., and Lindsley, C. W. (2009). Allosteric modulators of GPCRs: a novel approach for the treatment of CNS disorders. Nature reviews. Drug discovery *8*, 41–54.

Conroy, D. M., Jopling, L. A., Lloyd, C. M., Hodge, M. R., Andrew, D. P., Williams, T. J., Pease, J. E., and Sabroe, I. (2003). CCR4 blockade does not inhibit allergic airways inflammation. Journal of leukocyte biology *74*, 558–563.

Cooray, S. N., Chan, L., Webb, T. R., Metherell, L., and Clark, A. J. L. (2009). Accessory proteins are vital for the functional expression of certain G protein-coupled receptors. Molecular and cellular endocrinology *300*, 17–24.

Cox, M. A., Jenh, C. H., Gonsiorek, W., Fine, J., Narula, S. K., Zavodny, P. J., and Hipkin, R. W. (2001). Human interferon-inducible 10-kDa protein and human interferon-inducible T cell alpha chemoattractant are allotopic ligands for human CXCR3: differential binding to receptor states. Molecular pharmacology *59*, 707–715.

Cronshaw, D. G., Owen, C., Brown, Z., Ward, S. G., and Chemotaxis, L. (2004). Activation of Phosphoinositide 3-Kinases by the CCR4 Ligand Macrophage-Derived Chemokine Is a Dispensable Signal for T Lymphocyte Chemotaxis. Journal of immunology (Baltimore, Md. : 1950) *172*, 7761–7770.

Cullen, P. J., and Lockyer, P. J. (2002). Integration of calcium and Ras signalling. Nature reviews. Molecular cell biology *3*, 339–348.

Cyster, J. G., and Goodnow, C. C. (1995). Pertussis Toxin Inhibits Migration of B and T Lymphocytes into Splenic White Pulp Cords. The Journal of experimental medicine *182*, 581–586.

Dagan-Berger, M. (2006). Role of CXCR3 carboxyl terminus and third intracellular loop in receptor-mediated migration, adhesion and internalization in response to CXCL11. Blood *107*, 3821–3831.

Daugherty, B. L., Siciliano, S. J., and Springer, M. S. (2000). Radiolabeled chemokine binding assays. Methods in molecular biology (Clifton, N.J.) *138*, 129–134.

Delos Santos, N. M., Gardner, L. A., White, S. W., and Bahouth, S. W. (2006). Characterization of the residues in helix 8 of the human beta1-adrenergic receptor that are involved in coupling the receptor to G proteins. The Journal of biological chemistry *281*, 12896–12907.

Devreotes, P. N., and Zigmond, S. H. (1988). Chemotaxis in eukaryotic cells: a focus on leukocytes and Dictyostelium. Annual review of cell biology *4*, 649–686.

Dong, C. (2008). TH17 cells in development: an updated view of their molecular identity and genetic programming. Nature reviews. Immunology *8*, 337–348.

Dorr, P., Westby, M., Dobbs, S., Griffin, P., Irvine, B., Macartney, M., Mori, J., Rickett, G., Smith-burchnell, C., Napier, C., et al. (2005). Maraviroc (UK-427,857), a Potent, Orally Bioavailable, and Selective Small-Molecule Inhibitor of Chemokine Receptor CCR5 with Broad-Spectrum Anti-Human Immunodeficiency Virus Type 1 Activity. Antimicrobial Agents and Chemotherapy *49*, 4721–4732.

Dragic, T., Trkola, A., Thompson, D. A., Cormier, E. G., Kajumo, F.A. Maxwell, E., Lin, S. W., Ying, W., Smith, S. O., Sakmar, T. P., et al. (2000). A binding pocket for a small molecule inhibitor of HIV-1 entry within the transmembrane helices of CCR5. Proceedings of the National Academy of Sciences of the United States of America *97*, 5639–5644.

Drake, M. T., Violin, J. D., Whalen, E. J., Wisler, J. W., Shenoy, S. K., and Lefkowitz, R. J. (2008). Beta-Arrestin-Biased Agonism At the Beta2-Adrenergic Receptor. The Journal of biological chemistry *283*, 5669–5676.

Duchesnes, C. E., Murphy, P. M., Williams, T. J., and Pease, J. E. (2006). Alanine scanning mutagenesis of the chemokine receptor CCR3 reveals distinct extracellular residues involved in recognition of the eotaxin family of chemokines. Molecular immunology *43*, 1221–1231.

D'Ambrosio, D., Albanesi, C., Lang, R., Girolomoni, G., and Sinigaglia, F. (2002). Quantitative differences in chemokine receptor engagement generate diversity in intregrin-dependent lymphocyte adhesion. Journal of immunology (Baltimore, Md. : 1950) *169*, 2303–2312.

Farzan, M., Chung, S., Li, W., Vasilieva, N., Wright, P. L., Schnitzler, C. E., Marchione, R. J., Gerard, C., Gerard, N. P., Sodroski, J., et al. (2002). Tyrosine-sulfated peptides functionally reconstitute a CCR5 variant lacking a critical amino-terminal region. The Journal of biological chemistry *277*, 40397–40402.

Farzan, M., Mirzabekov, T., Kolchinsky, P., Wyatt, R., Cayabyab, M., Gerard, N. P., Gerard, C., Sodroski, J., and Choe, H. (1999). Tyrosine Sulfation of the Amino Terminus of CCR5 Facilitates HIV-1 Entry. Cell *96*, 667–676.

Feierler, J., Wirth, M., Welte, B., Schüssler, S., Jochum, M., and Faussner, A. (2011). Helix 8 plays a crucial role in bradykinin b2 receptor trafficking and signaling. The Journal of biological chemistry *286*, 43282–43293.

Fernandez, E. J., and Lolis, E. (2002). Structure, function, and inhibition of chemokines. Annual review of pharmacology and toxicology *42*, 469–499.

Filidoza, M., and Devi, L. A. (2012). How opioid drugs bind to receptors. Nature *485*, 314–316.

Flier, J., Boorsma, D. M., Bruynzeel, D. P., Beek, P. J. V., Stoof, T. J., Scheper, R. J., Willemze, R., and Tensen, C. P. (1999). The CXCR3 Activating Chemokines IP-10, Mig, and IP-9 are Expressed in Allergic but not Irritant Patch Test Reactions. The Society for Investigative Dermatology, 574–578.

Fong, A. M., Alam, S. M., Imai, T., Haribabu, B., and Patel, D. D. (2002a). CX3CR1 tyrosine sulfation enhances fractalkine-induced cell adhesion. The Journal of biological chemistry *277*, 19418–19423.

Fong, A. M., Premont, R. T., Richardson, R. M., Yu, Y.-R.A. Lefkowitz, R. J., and Patel, D. D. (2002b). Defective lymphocyte chemotaxis in beta-arrestin2- and GRK6-deficient mice. Proceedings of the National Academy of Sciences of the United States of America *99*, 7478–7483.

Fox, J. M., Najarro, P., Smith, G. L., Struyf, S., Proost, P., and Pease, J. E. (2006). Structure/function relationships of CCR8 agonists and antagonists. Amino-terminal extension of CCL1 by a single amino acid generates a partial agonist. The Journal of biological chemistry *281*, 36652–36661.

Fredriksson, R., Lagerström, M. C., Lundin, L.-G., and Schiöth, H. B. (2003). The G-protein-coupled receptors in the human genome form five main families. Phylogenetic analysis, paralogon groups, and fingerprints. Molecular pharmacology *63*, 1256–1272.

Frishman, W. H. (2003). Beta-adrenergic blockers. Circulation *107*, e117–9.

Fritze, O., Filipek, S., Kuksa, V., Palczewski, K., Hofmann, K. P., and Ernst, O. P. (2003). Role of the conserved NPxxY(x)5,6F motif in the rhodopsin ground state and during activation. Proceedings of the National Academy of Sciences of the United States of America *100*, 2290–2295.

Förster, R., Davalos-Misslitz, A. C., and Rot, A. (2008). CCR7 and its ligands: balancing immunity and tolerance. Nature reviews. Immunology *8*, 362–371.

Galandrin, S., Oligny-Longpré, G., and Bouvier, M. (2007). The evasive nature of drug efficacy: implications for drug discovery. Trends in pharmacological sciences *28*, 423–430.

Galliera, E., Jala, V. R., Trent, J. O., Bonecchi, R., Signorelli, P., Lefkowitz, R. J., Mantovani, A., Locati, M., and Haribabu, B. (2004). beta-Arrestin-dependent

constitutive internalization of the human chemokine decoy receptor D6. The Journal of biological chemistry *279*, 25590–25597.

Gao, P., Zhou, X., Yashiro-ohtani, Y., Yang, Y., Sugimoto, N., Ono, S., Nagasawa, T., Fujiwara, H., and Hamaoka, T. (2003). The unique target specificity of a nonpeptide chemokine receptor antagonist: selective blockade of two Th1 chemokine receptors CCR5 and CXCR3. Journal of leukocyte biology *73*, 273–280.

Garcia-Perez, J., Rueda, P., Alcami, J., Rognan, D., Arenzana-Seisdedos, F., Lagane, B., and Kellenberger, E. (2011). Allosteric model of maraviroc binding to CC chemokine receptor 5 (CCR5). The Journal of biological chemistry *286*, 33409–33421.

Gehret, A. U., Jones, B. W., Tran, P. N., Cook, L. B., Greuber, E. K., and Hinkle, P. M. (2010). Role of Helix 8 of the Thyrotropin-Releasing Hormone Receptor in Phosphorylation by G Protein-Coupled Receptor Kinase. Molecular pharmacology *77*, 288–297.

Geissmann, F., Manz, M. G., Jung, S., Sieweke, M. H., Merad, M., and Ley, K. (2010). Development of monocytes, macrophages, and dendritic cells. Science (New York, N.Y.) *327*, 656–661.

Glass, W. G., McDermott, D. H., Lim, J. K., Lekhong, S., Yu, S. F., Frank, W.A., Pape, J., Cheshier, R. C., and Murphy, P. M. (2006). CCR5 deficiency increases risk of symptomatic West Nile virus infection. The Journal of experimental medicine *203*, 35–40.

Gonzalo, J., Qiu, Y., Lora, J. M., Villeval, J., Boyce, J. A., Marquez, G., Goya, I., Hamid, Q., Fraser, C. C., Picarella, D., et al. (2012). Coordinated Involvement of Mast Cells and T cells in Allergic Mucosal Inflammation: Critical Role of the CC Chemokine Ligand 1:CCR8 Axis. Journal of immunology (Baltimore, Md. : 1950) *179*, 1740–1750.

Gordon, J. R., and Galli, S. J. (1990). Mast cells as a source of both preformed and immunologically inducible TNF-alpha/cachetin. Nature.

Gorman, C. M., and Howard, B. H. (1983). Expression of recombinant plasmids in mammalian cells is enhanced by sodium butyrate. Nucleic Acids Research *1*, 7631–7648.

Gosling, J., Monteclaro, F. S., Atchison, R. E., Arai, H., Tsou, C. L., Goldsmith, M.A., and Charo, I. F. (1997). Molecular uncoupling of C-C chemokine receptor 5-induced chemotaxis and signal transduction from HIV-1 coreceptor activity. Proceedings of the National Academy of Sciences of the United States of America *94*, 5061–5066.

Le Gouill, C., Parent, J. L., Caron, C.A., Gaudreau, R., Volkov, L., Rola-Pleszczynski, M., and Stanková, J. (1999). Selective modulation of wild type

receptor functions by mutants of G-protein-coupled receptors. The Journal of biological chemistry *274*, 12548–12554.

Govaerts, C., Blanpain, C., Deupi, X., Ballet, S., Ballesteros, J.A., Wodak, S. J., Vassart, G., Pardo, L., and Parmentier, M. (2001). The TXP motif in the second transmembrane helix of CCR5. A structural determinant of chemokine-induced activation. The Journal of biological chemistry *276*, 13217–13225.

Govaerts, C., Bondue, A., Springael, J.-Y., Olivella, M., Deupi, X., Le Poul, E., Wodak, S. J., Parmentier, M., Pardo, L., and Blanpain, C. (2003). Activation of CCR5 by chemokines involves an aromatic cluster between transmembrane helices 2 and 3. The Journal of biological chemistry *278*, 1892–1903.

Goya, I., Villares, R., Zaballos, A., Gutiérrez, J., Kremer, L., Gonzalo, J.-A., Varona, R., Carramolino, L., Serrano, A., Pallarés, P., et al. (2003). Absence of CCR8 does not impair the response to ovalbumin-induced allergic airway disease. Journal of immunology (Baltimore, Md. : 1950) *170*, 2138–2146.

Granier, S., and Kobilka, B. (2012). A new era of GPCR structural and chemical biology. Nature Chemical Biology *8*, 670–673.

Granier, S., Manglik, A., Kruse, A. C., Kobilka, T. S., Thian, F. S., Weis, W. I., and Kobilka, B. K. (2012). Structure of the δ-opioid receptor bound to naltrindole. Nature *485*, 400–404.

Gurevich, V. V., and Gurevich, E. V. (2008). GPCR monomers and oligomers: it takes all kinds. Trends neuroscience *31*, 74–81.

Gutiérrez, J., Kremer, L., Zaballos, A., Goya, I., Martínez-A, C., and Márquez, G. (2004). Analysis of post-translational CCR8 modifications and their influence on receptor activity. The Journal of biological chemistry *279*, 14726–14733.

Hall, S. E., Mao, A., Nicolaidou, V., Finelli, M., Wise, E. L., Nedjai, B., Kanjanapangka, J., Harirchian, P., Chen, D., Selchau, V., et al. (2009). Elucidation of Binding Sites of Dual Antagonists in the Human Chemokine Receptors CCR2 and CCR5. Molecular pharmacology *75*, 1325–1336.

Harrison, C., and Traynor, J. R. (2003). The [35S]GTPγS binding assay: approaches and applications in pharmacology. Life Sciences *74*, 489–508.

Harrison, J. K., and Lukacs, N. W. (2007). The Chemokine Receptors (Humana Press).

Heijink, I. H., and Van Oosterhout, A. J. M. (2005). Targeting T cells for asthma. Current opinion in pharmacology *5*, 227–231.

Henderson, R., and Unwin, P. (1975). Three-dimensional model of purple membrane obtained by electron microscopy. Nature *257*, 28–32.

Hoffmann, C., Zürn, A., Bünemann, M., and Lohse, M. J. (2008). Conformational changes in G-protein-coupled receptors-the quest for functionally selective conformations is open. British journal of pharmacology *153*, S358–66.

Holmes, W., Lee, J., Kuang, W., Rice, G., and Wood, W. (1991). Structure and functional expression of a human interleukin-8 receptor. Science (New York, N.Y.) *253*, 1278–1280.

Holst, P. J., Rosenkilde, M. M., Manfra, D., Chen, S., Wiekowski, M. T., Holst, B., Cifire, F., Lipp, M., Schwartz, T. W., and Lira, S. A. (2001). Tumorigenesis induced by the HHV8-encoded chemokine receptor requires ligand modulation of high constitutive activity. Journal of clinical investigation *108*, 1789–1796.

Honczarenko, M., Le, Y., Glodek, A. M., Majka, M., Campbell, J. J., Ratajczak, M. Z., and Silberstein, L. E. (2002). CCR5-binding chemokines modulate CXCL12 (SDF-1)-induced responses of progenitor B cells in human bone marrow through heterologous desensitization of the CXCR4 chemokine receptor. Blood *100*, 2321–2329.

Iellem, A., Mariani, M., Lang, R., Recalde, H., Panina-Bordignon, P., Sinigaglia, F., and D'Ambrosio, D. (2001). Unique chemotactic response profile and specific expression of chemokine receptors CCR4 and CCR8 by CD4(+)CD25(+) regulatory T cells. The Journal of experimental medicine *194*, 847–853.

Imai, T., Baba, M., Nishimura, M., Kakizaki, M., Takagi, S., and Yoshie, O. (1997). The T cell-directed CC chemokine TARC is a highly specific biological ligand for CC chemokine receptor 4. The Journal of biological chemistry *272*, 15036–15042.

Imai, T., Chantry, D., Raport, C. J., Wood, C. L., Nishimura, M., Godiska, R., Yoshie, O., and Gray, P. W. (1998). Macrophage-derived chemokine is a functional ligand for the CC chemokine receptor 4. The Journal of biological chemistry *273*, 1764–1768.

Ishida, T., Ishii, T., Inagaki, A., Yano, H., Komatsu, H., Iida, S., Inagaki, H., and Ueda, R. (2006). Specific recruitment of CC chemokine receptor 4-positive regulatory T cells in Hodgkin lymphoma fosters immune privilege. Cancer research *66*, 5716–5722.

Ishida, T., and Ueda, R. (2011). Immunopathogenesis of lymphoma: focus on CCR4. Cancer science *102*, 44–50.

Jaakola, V.-P., Griffith, M. T., Hanson, M. A., Cherezov, V., Chien, E. Y. T., Lane, J. R., Ijzerman, A. P., and Stevens, R. C. (2008). The 2.6 Angstrom Crystal Structure of a Human A2A Adenosine Receptor Bound to an Antagonist. Science (New York, N.Y.) *322*, 1211–1217.

Jensen, P. C., Thiele, S., Steen,A., Elder, A., Kolbeck, R., Ghosh, S., Frimurer, T. M., and Rosenkilde, M. M. (2012). Reversed binding of a small molecule ligand in

homologous chemokine receptors - differential role of extracellular loop 2. British journal of pharmacology *166*, 258–275.

Jensen, P. C., Thiele, S., Ulven, T., Schwartz, T. W., and Rosenkilde, M. M. (2008). Positive versus negative modulation of different endogenous chemokines for CC-chemokine receptor 1 by small molecule agonists through allosteric versus orthosteric binding. The Journal of biological chemistry *283*, 23121–23128.

Ji, T., Grossman, M., Ji, I., and Receptors, G. P. (1998). G Protein-coupled Receptors. Biochemistry *273*, 17299–17302.

Johnston, C. A., and Siderovski, D. P. (2007). Receptor-Mediated Activation of Heterotrimeric G-Proteins: Current Structural Insights. Molecular pharmacology *72*, 219–230.

Jopling, L. A., Sabroe, I., Andrew, D. P., Mitchell, T. J., Li, Y., Hodge, M. R., Williams, T. J., and Pease, J. E. (2002). The identification, characterization, and distribution of guinea pig CCR4 and epitope mapping of a blocking antibody. The Journal of biological chemistry *277*, 6864–6873.

Juremalm, M., Olsson, N., and Nilsson, G. (2005). CCL17 and CCL22 attenuate CCL5-induced mast cell migration. Clinical and experimental allergy : journal of the British Society for Allergy and Clinical Immunology *35*, 708–712.

Juremalm, M., Olsson, N., and Nilsson, G. (2002). Selective CCL5/RANTES-induced mast cell migration through interactions with chemokine receptors CCR1 and CCR4. Biochemical and biophysical research communications *297*, 480–485.

Kakinuma, T., Nakamura, K., Wakugawa, M., Mitsui, H., Tada, Y., Saeki, H., Torii, H., Asahina, A., Onai, N., Matsushima, K., et al. (2001). Thymus and activation-regulated chemokine in atopic dermatitis: Serum thymus and activation-regulated chemokine level is closely related with disease activity. The Journal of allergy and clinical immunology *107*, 535–541.

Katragadda, M., Maciejewski, M. W., and Yeagle, P. L. (2004). Structural studies of the putative helix 8 in the human beta(2) adrenergic receptor: an NMR study. Biochimica et biophysica acta *1663*, 74–81.

Katritch, V., Cherezov, V., and Stevens, R. C. (2012). Diversity and modularity of G protein-coupled receptor structures. Trends in pharmacological sciences *33*, 17–27.

Katschke, K. J., Rottman, J. B., Ruth, J. H., Qin, S., Wu, L., LaRosa, G., Ponath, P., Park, C. C., Pope, R. M., and Koch, a E. (2001). Differential expression of chemokine receptors on peripheral blood, synovial fluid, and synovial tissue monocytes/macrophages in rheumatoid arthritis. Arthritis and rheumatism *44*, 1022–1032.

Kaur, S., Gupta, V. K., Shah, A., Thiel, S., Sarma, P. U., and Madan, T. (2005). CC chemokine receptors CCR1 and CCR4 are expressed on airway mast cells in allergic asthma. The Journal of allergy and clinical immunology *116*, 1381–1383.

Kawasaki, S., Takizawa, H., Yoneyama, H., Nakayama, T., Fujisawa, R., Izumizaki, M., Imai, T., Yoshie, O., Homma, I., Yamamoto, K., et al. (2001). Intervention of thymus and activation-regulated chemokine attenuates the development of allergic airway inflammation and hyperresponsiveness in mice. Journal of immunology (Baltimore, Md. : 1950) *166*, 2055–2062.

Kenakin, T. (2009). Biased agonism. F1000 biology reports *1*, 1–5.

Kledal, T. N., Rosenkilde, M. M., and Schwartz, T. W. (1998). Selective recognition of the membrane-bound CX3C chemokine, fractalkine, by the human cytomegalovirus-encoded broad-spectrum receptor US28. FEBS letters *441*, 209–214.

Kohout, T. A., Lin, F., Perry, S. J., Conner, D. A., and Lefkowitz, R. J. (2001). Beta-arrestin 1 and 2 differentially regulate heptahelical receptor signaling and trafficking. PNAS *98*, 1601–1606.

Kohout, T. A., Nicholas, S. L., Perry, S. J., Reinhart, G., Junger, S., and Struthers, R. S. (2004). Differential desensitization, receptor phosphorylation, beta-arrestin recruitment, and ERK1/2 activation by the two endogenous ligands for the CC chemokine receptor 7. The Journal of biological chemistry *279*, 23214–23222.

Kraft, K., Olbrich, H., Majoul, I., Mack, M., Proudfoot, A., and Oppermann, M. (2001). Characterization of Sequence Determinants within the Carboxyl-terminal Domain of Chemokine Receptor CCR5 That Regulate Signaling and Receptor Internalization. The Journal of biological chemistry *276*, 34408–34418.

Krishna, A. G., Menon, S. T., Terry, T. J., and Sakmar, T. P. (2002). Evidence that helix 8 of rhodopsin acts as a membrane-dependent conformational switch. Biochemistry *41*, 8298–8309.

de Kruijf, P., Heteren, J. V., Lim, H. D., Conti, P. G. M., Lee, M. M. C. V. D., Bosch, L., Ho, K., Auld, D., Ohlmeyer, M., Smit, M. J., et al. (2009). Nonpeptidergic Allosteric Antagonists Differentially Bind to the CXCR2 Chemokine Receptor. Journal of Pharmacology and Experimental Therapeutics *329*, 783–790.

Kuhn, D. E., Beall, C. J., and Kolattukudy, P. E. (1995). The cytomegalovirus US28 protein binds multiple CC chemokines with high affinity. Biochemical and biophysical research communications *211*, 325–330.

Lacy, P. (2006). Mechanisms of Degranulation in Neutrophils. Allergy, Asthma, and Clinical Immunology *2*, 98–108.

Lagane, B., Planchenault, T., Balabanian, K., Poul, E. L., Percherancier, Y., Staropoli, I., Vassart, G., Oppermann, M., and Parmentier, M. (2005). Mutation

of the DRY Motif Reveals Different Structural Requirements for the CC Chemokine Receptor 5-Mediated Signaling and Receptor Endocytosis. Molecular pharmacology *67*, 1966–1976.

Lagerström, M. C., and Schiöth, H. B. (2008). Structural diversity of G protein-coupled receptors and significance for drug discovery. Nature reviews. Drug discovery *7*, 339–357.

Laing, K. J., and Secombes, C. J. (2004). Chemokines. Developmental and comparative immunology *28*, 443–460.

Lakshminarayanan, V., Beno, D. W. A., Costa, R. H., and Roebuck, K. A. (1997). Differential regulation of interleukin-8 and intercellular adhesion molecule-1 by H2O2 and tumor necrosis factor-alpha in endothelial and epithelial cells. The Journal of biological chemistry *272*, 32910–32918.

Laurence, A., Tato, C. M., Davidson, T. S., Kanno, Y., Chen, Z., Yao, Z., Blank, R. B., Meylan, F., Siegel, R., Hennighausen, L., et al. (2007). Interleukin-2 signaling via STAT5 constrains T helper 17 cell generation. Immunity *26*, 371–381.

Lefkowitz, R. J., and Whalen, E. J. (2004). Beta-Arrestins: Traffic Cops of Cell Signaling. Current opinion in cell biology *16*, 162–168.

Leurs, R., Church, M. K., and Taglialatela, M. (2002). H1-antihistamines: inverse agonism, anti-inflammatory actions and cardiac effects. Clinical and experimental allergy : journal of the British Society for Allergy and Clinical Immunology *32*, 489–498.

Ley, K., Laudanna, C., Cybulsky, M. I., and Nourshargh, S. (2007). Getting to the site of inflammation: the leukocyte adhesion cascade updated. Nature reviews. Immunology *7*, 678–689.

Lim, H. W., Lee, J., Hillsamer, P., Kim, C. H., and Chang, H. (2008). Human Th17 Cells Share Major Trafficking Receptors with Both Polarized Effector T Cells and FOXP3+ Regulatory T Cells. Journal of immunology (Baltimore, Md. : 1950) *180*, 122–129.

Liu, J. J., Horst, R., Katritch, V., Stevens, R. C., and Wüthrich, K. (2012a). Biased signaling pathways in β2-adrenergic receptor characterized by 19F-NMR. Science (New York, N.Y.) *335*, 1106–1110.

Liu, Q., Chen, H., Ojode, T., Gao, X., Anaya-O'Brien, S., Turner, N. A., Ulrick, J., Decastro, R., Kelly, C., Cardones, A. R., et al. (2012b). WHIM syndrome caused by a single amino acid substitution in the carboxy-tail of chemokine receptor CXCR4. Blood *120*, 181–189.

Lloyd, C. M., Delaney, T., Nguyen, T., Tian, J., Martinez-A, C., Coyle, a J., and Gutierrez-Ramos, J. C. (2000). CC chemokine receptor (CCR)3/eotaxin is followed by CCR4/monocyte-derived chemokine in mediating pulmonary T

helper lymphocyte type 2 recruitment after serial antigen challenge in vivo. The Journal of experimental medicine *191*, 265–274.

Lloyd, C. M., and Hessel, E. M. (2010). Functions of T cells in asthma: more than just T(H)2 cells. Nature reviews. Immunology *10*, 838–848.

Loetscher, P., Uguccioni, M., Bordoli, L., Baggiolini, M., and Moser, B. (1998). CCR5 is characteristic of Th1 lymphocytes. Nature *391*, 344–345.

Lohse, M. J., Nuber, S., and Hoffmann, C. (2012). Fluorescence/Bioluminescence Resonance Energy Transfer Techniques to Study G-Protein-Coupled Receptor Activation and Signaling. Pharmacological reviews *64*, 299–336.

Lukacs, N. W., Oliveira, S. H. P., and Hogaboam, C. M. (1999). Chemokines and asthma: redundancy of function or a coordinated effort? Journal of clinical investigation *104*, 995–999.

Luster, A. D., and Rothenberg, M. E. (1997). Role of the monocyte chemoattractant protein and eotaxin subfamily of chemokines in allergic inflammation. Journal of leukocyte biology *62*, 620–633.

Manglik, A., Kruse, A. C., Kobilka, T. S., Thian, F. S., Mathiesen, J. M., Sunahara, R. K., Pardo, L., Weis, W. I., Kobilka, B. K., and Granier, S. (2012). Crystal structure of the μ-opioid receptor bound to a morphinan antagonist. Nature *485*, 321–327.

Mantovani, A. (1999). The chemokine system: redundancy for robust outputs. Immunology today *5699*, 254–257.

Mariani, M., Lang, R., Binda, E., Panina-Bordignon, P., and D'Ambrosio, D. (2004). Dominance of CCL22 over CCL17 in induction of chemokine receptor CCR4 desensitization and internalization on human Th2 cells. European journal of immunology *34*, 231–240.

Meiser, A., Mueller, A., Wise, E. L., McDonagh, E. M., Petit, S. J., Saran, N., Clark, P. C., Williams, T. J., and Pease, J. E. (2008). The chemokine receptor CXCR3 is degraded following internalization and is replenished at the cell surface by de novo synthesis of receptor. Journal of immunology (Baltimore, Md. : 1950) *180*, 6713–6724.

de Mendonça, F. L., da Fonseca, P. C. A., Phillips, R. M., Saldanha, J. W., Williams, T. J., and Pease, J. E. (2005). Site-directed mutagenesis of CC chemokine receptor 1 reveals the mechanism of action of UCB 35625, a small molecule chemokine receptor antagonist. The Journal of biological chemistry *280*, 4808–4816.

Mikhak, Z., Fukui, M., Farsidjani, A., Medoff, B. D., Tager, A. M., and Luster, A. D. (2010). Contribution of CCR4 and CCR8 to antigen-specific Th2 cell trafficking in allergic pulmonary inflammation. Journal of Allergy and Clinical Immunology *123*, 67–73.

Miller, W. E., Houtz, D. A., Nelson, C. D., Kolattukudy, P. E., and Lefkowitz, R. J. (2003). G-protein-coupled receptor (GPCR) kinase phosphorylation and beta-arrestin recruitment regulate the constitutive signaling activity of the human cytomegalovirus US28 GPCR. The Journal of biological chemistry *278*, 21663–21671.

Mirzadegan, T., Diehl, F., Ebi, B., Bhakta, S., Polsky, I., McCarley, D., Mulkins, M., Weatherhead, G. S., Lapierre, J. M., Dankwardt, J., et al. (2000). Identification of the binding site for a novel class of CCR2b chemokine receptor antagonists: binding to a common chemokine receptor motif within the helical bundle. The Journal of biological chemistry *275*, 25562–25571.

Monteclaro, F. S., and Charo, I. F. (1997). The Amino-terminal Domain of CCR2 Is Both Necessary and Sufficient for High Affinity Binding of Monocyte Chemoattractant Protein 1. The Journal of biological chemistry *272*, 23186–23190.

Montes-Vizuet, R., Vega-Miranda, A., Valencia-Maqueda, E., Negrete-García, M. C., Velásquez, J. R., and Teran, L. M. (2006). CC chemokine ligand 1 is released into the airways of atopic asthmatics. The European respiratory journal : official journal of the European Society for Clinical Respiratory Physiology *28*, 59–67.

Moore, J. P., Trkola, A., and Dragic, T. (1997). Co-receptors for HIV-1 entry. Current opinion in immunology *9*, 551–562.

Moore, K. L. (2009). Protein tyrosine sulfation: a critical posttranslation modification in plants and animals. Proceedings of the National Academy of Sciences of the United States of America *106*, 14741–14742.

Moser, B., and Willimann, K. (2004). Chemokines: role in inflammation and immune surveillance. Annals of the rheumatic diseases *63*, ii84–ii89.

Mosmann, T. R., Cherwinski, H., Bond, M. W., Giedlin, M. A., and Coffman, R. L. (1986). Two types of murine helper T cell clone. Journal of immunology (Baltimore, Md. : 1950) *136*, 2348–2357.

Mosmann, T. R., and Sad, S. (1996). The expanding universe of T-cell subsets: Th1, Th2 and more. Immunology today *17*, 138–146.

Motulsky, H., and Christopoulos, A. (2004). Fitting Models to Biological Data Using Linear and Nonlinear Regression: A Practical Guide to Curve Fitting 1st ed. (Oxford University Press).

Mueller, A., Meiser, A., McDonagh, E. M., Fox, J. M., Petit, S. J., Xanthou, G., Williams, T. J., and Pease, J. E. (2008). CXCL4-induced migration of activated T lymphocytes is mediated by the chemokine receptor CXCR3. Journal of leukocyte biology *83*, 875–882.

Murakami, M., and Kouyama, T. (2008). Crystal structure of squid rhodopsin. Nature *453*, 363–367.

Murphy, K. (2011). Immunobiology 8th ed.

Murphy, P. M., Baggiolini, M., Charo, I. F., Hébert, C. A., Horuk, R., Matsushima, K., Miller, L. H., Oppenheim, J. J., and Power, C. a (2000). International union of pharmacology. XXII. Nomenclature for chemokine receptors. Pharmacological reviews *52*, 145–176.

Murphy, P. M., and Tiffany, H. L. (1991). Cloning of complementary DNA encoding a functional human interleukin-8 receptor. Science (New York, N.Y.) *253*, 1280–1283.

Mutalithas, K., Guillen, C., Raport, C., Kolbeck, R., Soler, D., Brightling, C. E., Pavord, I. D., and Wardlaw, a J. (2010). Expression of CCR8 is increased in asthma. Clinical and experimental allergy : journal of the British Society for Allergy and Clinical Immunology *40*, 1175–1185.

Müller, C. E., Schiedel, A. C., and Baqi, Y. (2012). Allosteric modulators of rhodopsin-like G protein-coupled receptors: Opportunities in drug development. Pharmacology & therapeutics.

Nagase, H., Kudo, K., Izumi, S., Ohta, K., Kobayashi, N., Yamaguchi, M., Matsushima, K., Morita, Y., Yamamoto, K., and Hirai, K. (2001). Chemokine receptor expression profile of eosinophils at inflamed tissue sites: Decreased CCR3 and increased CXCR4 expression by lung eosinophils. The Journal of allergy and clinical immunology *108*, 563–569.

Nagira, M., Imai, T., Hieshima, K., Kusuda, J., Ridanpää, M., Takagi, S., Nishimura, M., Kakizaki, M., Nomiyama, H., and Yoshie, O. (1997). Molecular cloning of a novel human CC chemokine secondary lymphoid-tissue chemokine that is a potent chemoattractant for lymphocytes and mapped to chromosome 9p13. The Journal of biological chemistry *272*, 19518–19524.

Nathan, C. (2006). Neutrophils and immunity: challenges and opportunities. Nature reviews. Immunology *6*, 173–182.

Nathans, J., and Hogness, D. S. (1983). Isolation, sequence analysis, and intron-exon arrangement of the gene encoding bovine rhodopsin. Cell *34*, 807–814.

Nedjai, B., Li, H., Stroke, I. L., Wise, E. L., Webb, M. L., Merritt, J. R., Henderson, I., Klon, A. E., Cole, A. G., Horuk, R., et al. (2012). Small molecule chemokine mimetics suggest a molecular basis for the observation that CXCL10 and CXCL11 are allosteric ligands of CXCR3. British journal of pharmacology *166*, 912–923.

Neel, N. F., and Richmond, A. (2005). Chemokine receptor internalization and intracellular trafficking. Cytokine growth factor rev *16*, 637–658.

Neote, K., Darbonne, W., Ogez, J., Honk, R., and Schall, T. J. (1993a). Identification of a Promiscuous Inflammatory Peptide Receptor on the Surface of Red Blood Cells. The Journal of biological chemistry, 12247–12249.

Neote, K., Digregorlo, D., Mak, J. Y., Horuk, R., and Schall, T. J. (1993b). Molecular Cloning, Functional Expression, and Signaling Characteristics of a C-C Chemokine Receptor. Cell *72*, 415–425.

Nibbs, R. J. B., McLean, P., McCulloch, C., Riboldi-Tunnicliffe, A., Blair, E., Zhu, Y., Isaacs, N., and Graham, G. J. (2009). Structure-function dissection of D6, an atypical scavenger receptor. Methods in Enzymology *460*, 245–261.

Nicholls, D. J., Tomkinson, N. P., Wiley, K. E., Brammall, A., Bowers, L., Grahames, C., Gaw, A., Meghani, P., Shelton, P., Wright, T. J., et al. (2008). Identification of a Putative Intracellular Allosteric Antagonist Binding-Site in the CXC Chemokine Receptors 1 and 2. Molecular pharmacology *74*, 1193–1202.

Nobles, K. N., Xiao, K., Ahn, S., Shukla, A. K., Lam, C. M., Rajagopal, S., Strachan, R. T., Huang, T.-Y., Bressler, E. A., Hara, M. R., Shenoy, Sudha K., Gygi, Steven P., Lefkowitz, Robert J. (2011). Distinct phosphorylation sites on the β(2)-adrenergic receptor establish a barcode that encodes differential functions of β-arrestin. Science signaling *4*, 1–10.

Noda, K., Saad, Y., Graham, R. M., and Karnik, S. S. (1994). The high affinity state of the beta 2-adrenergic receptor requires unique interaction between conserved and non-conserved extracellular loop cysteines. The Journal of biological chemistry *269*, 6743–6752.

Nomiyama, H., Imai, T., Kusuda, J., Miura, R., Callen, D. F., and Yoshie, O. (1998). Human chemokines fractalkine (SCYD1), MDC (SCYA22) and TARC (SCYA17) are clustered on chromosome 16q13. Cytogenetics and cell genetics *81*, 10–11.

Nomiyama, H., Osada, N., and Yoshie, O. (2010). The evolution of mammalian chemokine genes. Cytokine & growth factor reviews *21*, 253–262.

Nygaard, R., Frimurer, T. M., Holst, B., Rosenkilde, M. M., and Schwartz, T. W. (2009). Ligand binding and micro-switches in 7TM receptor structures. Trends in pharmacological sciences *30*, 249–259.

Offermanns, S. (2003). G-proteins as transducers in transmembrane signalling. Progress in Biophysics and Molecular Biology *83*, 101–130.

Okada, T., and Palczewski, K. (2001). Crystal structure of rhodopsin: implications for vision and beyond. Current Opinion in Structural Biology, 420–426.

Okuno, T., Ago, H., Terawaki, K., Miyano, M., Shimizu, T., and Yokomizo, T. (2003). Helix 8 of the leukotriene B4 receptor is required for the conformational

change to the low affinity state after G-protein activation. The Journal of biological chemistry *278*, 41500–41509.

Okuno, T., Yokomizo, T., Hori, T., Miyano, M., and Shimizu, T. (2005). Leukotriene B4 receptor and the function of its helix 8. The Journal of biological chemistry *280*, 32049–32052.

Olkhanud, P. B., Baatar, D., Bodogai, M., Hakim, F., Gress, R., Anderson, R. L., Deng, J., Xu, M., Briest, S., and Biragyn, A. (2009). Breast cancer lung metastasis requires expression of chemokine receptor CCR4 and regulatory T cells. Cancer research *69*, 5996–6004.

Oppermann, M., Mack, M., Proudfoot, A. E. I., and Olbrich, H. (1999). Differential effects of CC chemokines on CC chemokine receptor 5 (CCR5) phosphorylation and identification of phosphorylation sites on the CCR5 carboxyl terminus. The Journal of biological chemistry *274*, 8875–8885.

Otero, C., Eisele, P. S., Schaeuble, K., Groettrup, M., and Legler, D. F. (2008). Distinct motifs in the chemokine receptor CCR7 regulate signal transduction, receptor trafficking and chemotaxis. Journal of Cell Science *121*, 2759–2767.

Ott, T. R., Lio, F. M., Olshefski, D., Liu, X.-J., Struthers, R. S., and Ling, N. (2004). Determinants of High-Affinity Binding and Receptor Activation in the N-Terminus of CCL-19 (MIP-3β). Biochemistry *43*, 3670–3678.

Ovchinnikov, Y. A., Abdulaev, N. G., and Bogachuk, A. S. (1988). Two adjacent cysteine residues in the C-terminal cytoplasmic fragment of bovine rhodopsin are palmitylated. FEBS letters *230*, 1–5.

Palczewski, K. (2000). Crystal Structure of Rhodopsin: A G Protein-Coupled Receptor. Science (New York, N.Y.) *289*, 739–745.

Panina-Bordignon, P., Papi, A., Mariani, M., Di Lucia, P., Casoni, G., Bellettato, C., Buonsanti, C., Miotto, D., Mapp, C., Villa, A., et al. (2001). The C-C chemokine receptors CCR4 and CCR8 identify airway T cells of allergen-challenged atopic asthmatics. The Journal of clinical investigation *107*, 1357–1364.

Park, J. H., Scheerer, P., Hofmann, K. P., Choe, H.-W., and Ernst, O. P. (2008). Crystal structure of the ligand-free G-protein-coupled receptor opsin. Nature *454*, 183–187.

Pease, J. E. (2011). Targeting chemokine receptors in allergic disease. The Biochemical journal *434*, 11–24.

Pease, J. E., and Horuk, R. (2009). Chemokine receptor antagonists: part 1. Expert opinion on therapeutic patents *19*, 199–221.

Pease, J. E., Wang, J., Ponath, P. D., and Murphy, P. M. (1998). The N-terminal Extracellular Segments of the Chemokine Receptors CCR1 and CCR3 Are Determinants for MIP-1 and Eotaxin Binding, Respectively, but a Second

Domain Is Essential for Efficient Receptor Activation. The Journal of biological chemistry *273*, 19972–19976.

Percherancier, Y., Planchenault, T., Valenzuela-Fernandez, A., Virelizier, J. L., Arenzana-Seisdedos, F., and Bachelerie, F. (2001). Palmitoylation-dependent control of degradation, life span, and membrane expression of the CCR5 receptor. The Journal of biological chemistry *276*, 31936–31944.

Petit, S. J., Chayen, N. E., and Pease, J. E. (2008). Site-directed mutagenesis of the chemokine receptor CXCR6 suggests a novel paradigm for interactions with the ligand CXCL16. European journal of immunology *38*, 2337–2350.

Peverelli, E., Lania, A. G., Mantovani, G., Beck-Peccoz, P., and Spada, A. (2009). Characterization of Intracellular Signaling Mediated by Human Somatostatin Receptor 5: Role of the DRY Motif and the Third Intracellular Loop. Endocrinology *150*, 3169–3176.

Power, C. A. (2003). Knock out models to dissect chemokine receptor function in vivo. Journal of Immunological Methods *273*, 73–82.

Power, C. A., Meyer, A., Nemeth, K., Bacon, K. B., Hoogewerf, A. J., Proudfoot, A. E. I., and Wells, T. N. C. (1995). Molecular cloning and functional expression of a novel CC chemokine receptor cDNA from a human basophilic line. The Journal of biological chemistry *270*, 19495–19500.

Preobrazhensky, A A., Dragan, S., Kawano, T., Gavrilin, M. A., Gulina, I. V., Chakravarty, L., and Kolattukudy, P. E. (2000). Monocyte chemotactic protein-1 receptor CCR2B is a glycoprotein that has tyrosine sulfation in a conserved extracellular N-terminal region. Journal of immunology (Baltimore, Md. : 1950) *165*, 5295–5303.

Pruenster, M., Mudde, L., Bombosi, P., Dimitrova, S., Zsak, M., Middleton, J., Richmond, A., Graham, G. J., Segerer, S., Nibbs, R. J. B., et al. (2009). The Duffy antigen receptor for chemokines transports chemokines and supports their promigratory activity. Nature immunology *10*, 101–108.

Qian, B.-F., and Wahl, S. M. (2009). TGF-beta can leave you breathless. Current opinion in pharmacology *9*, 454–461.

Rajagopal, S., Rajagopal, K., and Lefkowitz, R. J. (2010). Teaching old receptors new tricks: biasing seven-transmembrane receptors. Nature reviews. Drug discovery *9*, 373–386.

Rands, E., Candelore, M. R., Cheung, a H., Hill, W. S., Strader, C. D., and Dixon, R. a (1990). Mutational analysis of beta-adrenergic receptor glycosylation. The Journal of biological chemistry *265*, 10759–10764.

Rasmussen, S. G. F., Choi, H.-J., Rosenbaum, D. M., Kobilka, T. S., Thian, F. S., Edwards, P. C., Burghammer, M., Ratnala, V. R. P., Sanishvili, R., Fischetti, R.

F., et al. (2007). Crystal structure of the human beta2 adrenergic G-protein-coupled receptor. Nature *450*, 383–387.

Rasmussen, S. G. F., DeVree, B. T., Zou, Y., Kruse, A. C., Chung, K. Y., Kobilka, T. S., Thian, F. S., Chae, P. S., Pardon, E., Calinski, D., et al. (2011). Crystal structure of the β2 adrenergic receptor–Gs protein complex. Nature *477*, 549–555.

Reiter, E., and Lefkowitz, R. J. (2006). GRKs and beta-arrestins: roles in receptor silencing, trafficking and signaling. Trends in endocrinology and metabolism: TEM *17*, 159–165.

Roland, J., Murphy, B. J., Ahr, B., Robert-Hebmann, V., Delauzun, V., Nye, K. E., Devaux, C., and Biard-Piechaczyk, M. (2003). Role of the intracellular domains of CXCR4 in SDF-1-mediated signaling. Blood *101*, 399–406.

Roos, R. S., Loetscher, M., Legler, D. F., Clark-lewis, I., Baggiolini, M., and Moser, B. (1997). Identification of CCR8, the Receptor for the Human CC Chemokine I-309. Journal of Biological Chemistry *272*, 17251–17254.

Rosenbaum, D. M., Cherezov, V., Hanson, M. A., Rasmussen, S. G. F., Thian, F. S., Kobilka, T. S., Choi, H.-J., Yao, X.-J., Weis, W. I., Stevens, R. C., et al. (2007). GPCR engineering yields high-resolution structural insights into beta2-adrenergic receptor function. Science (New York, N.Y.) *318*, 1266–1273.

Rosenkilde, M. M., Gerlach, L.-O., Jakobsen, J. S., Skerlj, R. T., Bridger, G. J., and Schwartz, T. W. (2004). Molecular Mechanism of AMD3100 Antagonism in the CXCR4 Receptor. Journal of Biological Chemistry *279*, 3033–3041.

Rot, A., and von Andrian, U. H. (2004). Chemokines in innate and adaptive host defense: basic chemokinese grammar for immune cells. Annual review of immunology *22*, 891–928.

Rothenberg, M. E., and Hogan, S. P. (2006). The eosinophil. Annual review of immunology *24*, 147–174.

Rovati, G. E., and Neubig, R. R. (2007). The Highly Conserved DRY Motif of Class A G Protein-Coupled Receptors: Beyond the Ground State. Molecular pharmacology *71*, 959–964.

Sabroe, I., Jorritsma, A., Stubbs, V. E. L., Xanthou, G., Jopling, L. A., Ponath, P. D., Williams, T. J., Murphy, P. M., and Pease, J. E. (2005). The carboxyl terminus of the chemokine receptor CCR3 contains distinct domains which regulate chemotactic signaling and receptor down-regulation in a ligand-dependent manner. European journal of immunology *35*, 1301–1310.

Sabroe, I., Peck, M. J., Van Keulen, B. J., Jorritsma, A., Simmons, G., Clapham, P. R., Williams, T. J., and Pease, J. E. (2000). A small molecule antagonist of chemokine receptors CCR1 and CCR3. Potent inhibition of eosinophil function

and CCR3-mediated HIV-1 entry. The Journal of biological chemistry *275*, 25985–25992.

Saeki, H., and Tamaki, K. (2006). Thymus and activation regulated chemokine (TARC)/CCL17 and skin diseases. Journal of dermatological science *43*, 75–84.

Sakaguchi, S., Yamaguchi, T., Nomura, T., and Ono, M. (2008). Regulatory T cells and immune tolerance. Cell *133*, 775–787.

Salchow, K., Bond, M. E., Evans, S. C., Press, N. J., Charlton, S. J., Hunt, P. A., and Bradley, M. E. (2010). A common intracellular allosteric binding site for antagonists of the CXCR2 receptor. British journal of pharmacology *159*, 1429–1439.

Sallusto, F., Palermo, B., Lenig, D., Miettinen, M., Matikainen, S., Julkunen, I., Forster, R., Burgstahler, R., Lipp, M., and Lanzavecchia, a (1999). Distinct patterns and kinetics of chemokine production regulate dendritic cell function. European journal of immunology *29*, 1617–1625.

Sanderson, C. J. (1992). Interleukin-5, eosinophils, and disease. Blood *79*, 3101–3109.

Sanguinetti, M. C., and Tristani-Firouzi, M. (2006). hERG potassium channels and cardiac arrhythmia. Nature *440*, 463–469.

Savareses, T. M., Wang, C., and Fraserll, C. M. (1992). Site-directed Mutagenesis of the Rat m1 Muscarinic Acetylcholine Receptor imply. The Journal of biological chemistry *267*, 11439–11448.

Schall, T. J., Bacon, K., Toy, K. J., and Goeddel, D. V. (1990). Selective attraction of monocytes and T lymphocytes of the memory phenotype by cytokine RANTES. Nature.

Schall, T. J., and Proudfoot, A. E. I. (2011). Overcoming hurdles in developing successful drugs targeting chemokine receptors. Nature reviews. Immunology *11*, 355–363.

Scheerer, P., Park, J. H., Hildebrand, P. W., Kim, Y. J., Krauss, N., Choe, H.-W., Hofmann, K. P., and Ernst, O. P. (2008). Crystal structure of opsin in its G-protein-interacting conformation. Nature *455*, 497–502.

Schiöth, H. B., and Fredriksson, R. (2005). The GRAFS classification system of G-protein coupled receptors in comparative perspective. General and comparative endocrinology *142*, 94–101.

Scholten, D., Canals, M., Maussang, D., Roumen, L., Smit, M., Wijtmans, M., de Graaf, C., Vischer, H., and Leurs, R. (2012a). Pharmacological modulation of chemokine receptor function. British journal of pharmacology *165*, 1617–1643.

Scholten, D., Canals, M., Wijtmans, M., de Munnik, S., Nguyen, P., Verzijl, D., de Esch, I., Vischer, H., Smit, M., and Leurs, R. (2012b). Pharmacological characterization of a small-molecule agonist for the chemokine receptor CXCR3. British journal of pharmacology *166*, 898–911.

Schroeder, J. T. (2009). Basophils beyond effector cells of allergic inflammation. 1st ed. (Elsevier Inc.).

Schwartz, T. W., Frimurer, T. M., Holst, B., Rosenkilde, M. M., and Elling, C. E. (2006). Molecular mechanism of 7TM receptor activation--a global toggle switch model. Annual review of pharmacology and toxicology *46*, 481–519.

Sebastiani, S., Danelon, G., Gerber, B., and Uguccioni, M. (2005). CCL22-induced responses are powerfully enhanced by synergy inducing chemokines via CCR4: evidence for the involvement of first beta-strand of chemokine. European journal of immunology *35*, 746–756.

Shiraishi, M., Aramaki, Y., Seto, M., Imoto, H., Nishikawa, Y., Kanzaki, N., Okamoto, M., Sawada, H., Nishimura, O., Baba, M., et al. (2000). Discovery of novel, potent, and selective small-molecule CCR5 antagonists as anti-HIV-1 agents: synthesis and biological evaluation of anilide derivatives with a quaternary ammonium moiety. Journal of medicinal chemistry *43*, 2049–2063.

Shulman, Z., Cohen, S. J., Roediger, B., Kalchenko, V., Jain, R., Grabovsky, V., Klein, E., Shinder, V., Stoler-Barak, L., Feigelson, S. W., et al. (2011). Transendothelial migration of lymphocytes mediated by intraendothelial vesicle stores rather than by extracellular chemokine depots. Nature immunology *13*.

Shulman, Z., Shinder, V., Klein, E., Grabovsky, V., Yeger, O., Geron, E., Montresor, A., Bolomini-Vittori, M., Feigelson, S. W., Kirchhausen, T., et al. (2009). Lymphocyte crawling and transendothelial migration require chemokine triggering of high-affinity LFA-1 integrin. Immunity *30*, 384–396.

Singh, S. P., Zhang, H. H., Foley, J. F., Hedrick, M. N., and Farber, J. M. (2008). Human T cells that are able to produce IL-17 express the chemokine receptor CCR6. Journal of immunology (Baltimore, Md. : 1950) *180*, 214–221.

Smart, S. J., and Casale, T. B. (1994). TNF-a-induced transendothelial is IL-8 dependent neutrophil migration. American journal of physiology.

Spangrude, G. J., Braaten, B. A., and Raymond, A. D. (1984). Molecular Mechanisms of Lympocyte Extravasation. Journal of immunology (Baltimore, Md. : 1950), 354–362.

Spangrude, G. J., Sacchi, F., Hill, H. R., Van Epps, D. E., and Daynes, R. a (1985). Inhibition of lymphocyte and neutrophil chemotaxis by pertussis toxin. Journal of immunology (Baltimore, Md. : 1950) *135*, 4135–4143.

Spiro, R. G. (2002). Protein glycosylation: nature, distribution, enzymatic formation, and disease implications of glycopeptide bonds. Glycobiology *12*, 43R–56R.

Strader, C. D., Sigal, I. S., and Dixon, R. A. (1989). Structural bases of beta-adrenergic receptor function. FASEB, 1825–1832.

Sugiyama, T., Kohara, H., Noda, M., and Nagasawa, T. (2006). Maintenance of the hematopoietic stem cell pool by CXCL12-CXCR4 chemokine signaling in bone marrow stromal cell niches. Immunity *25*, 977–988.

Sullivan, S. K., Mcgrath, D. A., Grigoriadis, D., and Bacon, K. B. (2000). Pharmacological and Signaling Analysis of Human Chemokine Receptor CCR-7 Stably Expressed in HEK- 293 Cells: High-Affinity Binding of Recombinant Ligands MIP-3beta and SLC Stimulates Multiple Signaling Cascades. Biochemical and biophysical research communications *690*, 685–690.

Sun, Y., Cheng, Z., Ma, L., and Pei, G. (2002). Beta-arrestin2 is critically involved in CXCR4-mediated chemotaxis, and this is mediated by its enhancement of p38 MAPK activation. The Journal of biological chemistry *277*, 49212–49219.

Swaminath, G., Xiang, Y., Lee, T. W., Steenhuis, J., Parnot, C., and Kobilka, B. K. (2004). Sequential binding of agonists to the beta2 adrenoceptor. Kinetic evidence for intermediate conformational states. The Journal of biological chemistry *279*, 686–691.

Swift, S., Leger, A. J., Talavera, J., Zhang, L., Bohm, A., and Kuliopulos, A. (2006). Role of the PAR1 receptor 8th helix in signaling: the 7-8-1 receptor activation mechanism. The Journal of biological chemistry *281*, 4109–4116.

Swillens, S., Waelbroeck, M., and Champeil, P. (1995). Does a radiolabelled ligand bind to a homogeneous population of non-interacting receptor sites? Trends in pharmacological sciences *16*, 151–155.

Tang, H. L., and Cyster, J. G. (1999). Chemokine Up-Regulation and Activated T Cell Attraction by Maturing Dendritic Cells. Science (New York, N.Y.) *284*, 819–822.

Terashima, Y., Onai, N., Murai, M., Enomoto, M., Poonpiriya, V., Hamada, T., Motomura, K., Suwa, M., Ezaki, T., Haga, T., et al. (2005). Pivotal function for cytoplasmic protein FROUNT in CCR2-mediated monocyte chemotaxis. Nature immunology *6*, 827–835.

Tesmer, J. J. G. (2010). The quest to understand heterotrimeric G protein signaling. Nature structural & molecular biology *17*, 650–652.

Thiele, S., Steen, A., Jensen, P. C., Mokrosinski, J., Frimurer, T. M., and Rosenkilde, M. M. (2011). Allosteric and orthosteric sites in CC chemokine receptor (CCR5), a chimeric receptor approach. The Journal of biological chemistry *286*, 37543–37554.

Thielen, A., Oueslati, M., Hermosilla, R., Krause, G., Oksche, A., Rosenthal, W., and Schülein, R. (2005). The hydrophobic amino acid residues in the membrane-

proximal C tail of the G protein-coupled vasopressin V2 receptor are necessary for transport-competent receptor folding. FEBS letters *579*, 5227–5235.

Thompson, A. A., Liu, W., Chun, E., Katritch, V., Wu, H., Vardy, E., Huang, X.-P., Trapella, C., Guerrini, R., Calo, G., et al. (2012). Structure of the nociceptin/orphanin FQ receptor in complex with a peptide mimetic. Nature *485*, 395–399.

Thompson, B. D., Jin, Y., Wu, K. H., Colvin, R. A., Luster, A. D., Birnbaumer, L., and Wu, M. X. (2007). Inhibition of G alpha i2 activation by G alpha i3 in CXCR3-mediated signaling. The Journal of biological chemistry *282*, 9547–9555.

Toda, E., Terashima, Y., Sato, T., Hirose, K., Kanegasaki, S., and Matsushima, K. (2009). FROUNT is a common regulator of CCR2 and CCR5 signaling to control directional migration. Journal of immunology (Baltimore, Md. : 1950) *183*, 6387–6394.

Vaidehi, N., Schlyer, S., Trabanino, R. J., Floriano, W. B., Abrol, R., Sharma, S., Kochanny, M., Koovakat, S., Dunning, L., Liang, M., et al. (2006). Predictions of CCR1 chemokine receptor structure and BX 471 antagonist binding followed by experimental validation. The Journal of biological chemistry *281*, 27613–27620.

Vassilatis, D. K., Hohmann, J. G., Zeng, H., Li, F., Ranchalis, J. E., Mortrud, M. T., Brown, A., Rodriguez, S. S., Weller, J. R., Wright, A. C., et al. (2003). The G protein-coupled receptor repertoires of human and mouse. Proceedings of the National Academy of Sciences of the United States of America *100*, 4903–4908.

Venter, J. C., Adams, M. D., Myers, E. W., Li, P. W., Mural, R. J., Sutton, G. G., Smith, H. O., Yandell, M., Evans, C. A., Holt, R. A., et al. (2001). The sequence of the human genome. Science (New York, N.Y.) *291*, 1304–1351.

Verzijl, D., Pardo, L., van Dijk, M., Gruijthuijsen, Y. K., Jongejan, A., Timmerman, H., Nicholas, J., Schwarz, M., Murphy, P. M., Leurs, R., et al. (2006). Helix 8 of the viral chemokine receptor ORF74 directs chemokine binding. The Journal of biological chemistry *281*, 35327–35335.

Vestergaard, C., Bang, K., Gesser, B., Yoneyama, H., Matsushima, K., and Larsen, C. G. (2000). A Th2 Chemokine, TARC, Produced by Keratinocytes May Recruit CLA+ CCR4+ Lymphocytes into Lesional Atopic Dermatitis Skin. The Journal of Investigate Dermatology *4*, 640–646.

Vijayanand, P., Durkin, K., Hartmann, G., Morjaria, J., Seumois, G., Staples, K. J., Hall, D., Bessant, C., Bartholomew, M., Howarth, P. H., et al. (2010). Chemokine receptor 4 plays a key role in T cell recruitment into the airways of asthmatic patients. Journal of immunology (Baltimore, Md. : 1950) *184*, 4568–4574.

Viney, J. M., Andrew, D. P., Phillips, R. M., Meiser, A., Barton, N. P., Hall, D. A., and Pease, J. E (in preparation). The chemokines CCL22 and CCL17 interact with distinct conformations of CCR4.

Viola, A., and Luster, A. D. (2008). Chemokines and their receptors: drug targets in immunity and inflammation. Annual review of pharmacology and toxicology *48*, 171–197.

Vroon, A., Heijnen, C. J., and Kavelaars, A. (2006). GRKs and arrestins : regulators of migration and inflammation. Journal of leukocyte biology *80*, 1214–1221.

Vu, T. K., Hung, D. T., Wheaton, V. I., and Coughlin, S. R. (1991). Molecular cloning of a functional thrombin receptor reveals a novel proteolytic mechanism of receptor activation. Cell *64*, 1057–1068.

Wang, Y., Zhang, Y., Yang, X., Han, W., Liu, Y., Xu, Q., Zhao, R., Di, C., Song, Q., and Ma, D. (2006). Chemokine-like factor 1 is a functional ligand for CC chemokine receptor 4 (CCR4). Life Sciences *78*, 614–621.

Warne, T., Serrano-Vega, M. J., Baker, J. G., Moukhametzianov, R., Edwards, P. C., Henderson, R., Leslie, A. G. W., Tate, C. G., and Schertler, G. F. X. (2008). Structure of a beta1-adrenergic G-protein-coupled receptor. Nature *454*, 486–491.

Waterhouse, P., Penninger, J. M., Timms, E., Wakeham, A., Shahinian, A., Lee, K. P., Thompson, C. B., Griesser, H., and Mak, T. W. (1995). Lymphoproliferative disorders with early lethality in mice deficient in Ctla-4. Science (New York, N.Y.) *270*, 985–988.

Watson, C., Jenkinson, S., Kazmierski, W., and Kenakin, T. (2005). The CCR5 Receptor-Based Mechanism of Action of 873140, a Potent Allosteric Noncompetitive HIV Entry Inhibitor. Molecular pharmacology, 1268–1282.

Wess, J., Nanavati, S., Vogel, Z., and Maggio, R. (1993). Functional role of proline and tryptophan residues highly conserved among G protein-coupled receptors studied by mutational analysis of the m3 muscarinic receptor. The EMBO journal *12*, 331–338.

Westfield, G. H., Rasmussen, S. G. F., Su, M., Dutta, S., Devree, B. T., and Young, K. (2011). Structural flexibility of the Gαs α-helical domain in the β2-adrenoceptor Gs complex. Proceedings of the National Academy of Sciences *108*, 16086–16091.

Williams, C. M., and Galli, S. J. (2000). The diverse potential effector and immunoregulatory roles of mast cells in allergic disease. The Journal of allergy and clinical immunology *105*, 847–859.

Wise, E. L., Duchesnes, C., da Fonseca, P. C. A., Allen, R. A., Williams, T. J., and Pease, J. E. (2007). Small molecule receptor agonists and antagonists of CCR3

provide insight into mechanisms of chemokine receptor activation. The Journal of biological chemistry *282*, 27935–27943.

Wu, B., Chien, E. Y. T., Mol, C. D., Fenalti, G., Liu, W., Katritch, V., Abagyan, R., Wells, P., Bi, F. C., Hamel, D. J., et al. (2010). Structures of the CXCR4 Chemokine GPCR with Small-Molecule and Cyclic Peptide Antagonists. Science (New York, N.Y.) *330*, 1066–1071.

Wu, D., Larosa, G. J., and Simon, M. I. (1993). G protein-coupled signal transduction pathways for interleukin-8. Science (New York, N.Y.) *261*, 101–103.

Wu, H., Wacker, D., Mileni, M., Katritch, V., Han, G. W., Vardy, E., Liu, W., Thompson, A. A., Huang, X.-P., Carroll, F. I., et al. (2012). Structure of the human κ-opioid receptor in complex with JDTic. Nature *485*, 327–332.

Xanthou, G., Williams, T. J., and Pease, J. E. (2003). Molecular characterization of the chemokine receptor CXCR3: evidence for the involvement of distinct extracellular domains in a multi-step model of ligand binding and receptor activation. European journal of immunology *33*, 2927–2936.

Yasuda, D., Okuno, T., Yokomizo, T., Hori, T., Hirota, N., Hashidate, T., Miyano, M., Shimizu, T., and Nakamura, M. (2009). Helix 8 of leukotriene B4 type-2 receptor is required for the folding to pass the quality control in the endoplasmic reticulum. FASEB journal : official publication of the Federation of American Societies for Experimental Biology *23*, 1470–1481.

Yoshida, R., Nagira, M., Kitaura, M., Imagawa, N., Imai, T., and Yoshie, O. (1998). Secondary Lymphoid-tissue Chemokine Is a Functional Ligand for the CC Chemokine Receptor CCR7*. The Journal of biological chemistry *273*, 7118–7122.

Yoshie, O. (2005). Expression of CCR4 in adult T-cell leukemia. Leukemia & lymphoma *46*, 185–190.

Zeng, F. Y., Soldner, A., Schöneberg, T., and Wess, J. (1999). Conserved extracellular cysteine pair in the M3 muscarinic acetylcholine receptor is essential for proper receptor cell surface localization but not for G protein coupling. Journal of neurochemistry *72*, 2404–2414.

Zhang, Y., Rodriguez, A. L., and Conn, P. J. (2005). Allosteric Potentiators of Metabotropic Glutamate Receptor Subtype 5 Have Differential Effects on Different Signaling Pathways in Cortical Astrocytes. Journal of Pharmacology and Experimental Therapeutics *315*, 1212–1219.

Zidovetzki, R., Rost, B., Armstrong, D., and Pecht, I. (2003). Transmembrane domains in the functions of Fc receptors. Biophys Chem *100*, 555–575.

Zlotnik, A., and Yoshie, O. (2012). The Chemokine Superfamily Revisited. Immunity *36*, 705–716.

Zlotnik, A., Yoshie, O., and Nomiyama, H. (2006). The chemokine and chemokine receptor superfamilies and their molecular evolution. Genome biology *7*.

Zúñiga-Pflücker, J. C. (2004). T-cell development made simple. Nature reviews. Immunology *4*, 67–72.

9 – Appendix

9.1 – Sequences

9.1.1 – Sequence of CCR4

```
ATGAACCCCACGGATATAGCAGACACCACCCTCGATGAAAGCATATACAGCAATTACTAT
 M  N  P  T  D  I  A  D  T  T  L  D  E  S  I  Y  S  N  Y  Y
CTGTATGAAAGTATCCCCAAGCCTTGCACCAAAGAAGGCATCAAGGCATTTGGGGAGCTC
 L  Y  E  S  I  P  K  P  C  T  K  E  G  I  K  A  F  G  E  L
TTCCTGCCCCCACTGTATTCCTTGGTTTTTGTATTTGGTCTGCTTGGAAATTCTGTGGTG
 F  L  P  P  L  Y  S  L  V  F  V  F  G  L  L  G  N  S  V  V
GTTCTGGTCCTGTTCAAATACAAGCGGCTCAGGTCCATGACTGATGTGTACCTGCTCAAC
 V  L  V  L  F  K  Y  K  R  L  R  S  M  T  D  V  Y  L  L  N
CTTGCCATCTCGGATCTGCTCTTCGTGTTTTCCCTCCCTTTTTGGGGCTACTATGCAGCA
 L  A  I  S  D  L  L  F  V  F  S  L  P  F  W  G  Y  Y  A  A
GACCAGTGGGTTTTTGGGCTAGGTCTGTGCAAGATGATTTCCTGGATGTACTTGGTGGGC
 D  Q  W  V  F  G  L  G  L  C  K  M  I  S  W  M  Y  L  V  G
TTTTACAGTGGCATATTCTTTGTCATGCTCATGAGCATTGATAGATACCTGGCAATTGTG
 F  Y  S  G  I  F  F  V  M  L  M  S  I  D  R  Y  L  A  I  V
CACGCGGTGTTTTCCTTGAGGGCAAGGACCTTGACTTATGGGGTCATCACCAGTTTGGCT
 H  A  V  F  S  L  R  A  R  T  L  T  Y  G  V  I  T  S  L  A
ACATGGTCAGTGGCTGTGTTCGCCTCCCTTCCTGGCTTTCTGTTCAGCACTTGTTATACT
 T  W  S  V  A  V  F  A  S  L  P  G  F  L  F  S  T  C  Y  T
GAGCGCAACCATACCTACTGCAAAACCAAGTACTCTCTCAACTCCACGACGTGGAAGGTT
 E  R  N  H  T  Y  C  K  T  K  Y  S  L  N  S  T  T  W  K  V
CTCAGCTCCCTGGAAATCAACATTCTCGGATTGGTGATCCCCTTAGGGATCATGCTGTTT
 L  S  S  L  E  I  N  I  L  G  L  V  I  P  L  G  I  M  L  F
TGCTACTCCATGATCATCAGGACCTTGCAGCATTGTAAAAATGAGAAGAAGAACAAGGCG
 C  Y  S  M  I  I  R  T  L  Q  H  C  K  N  E  K  K  N  K  A
GTGAAGATGATCTTTGCCGTGGTGGTCCTCTTCCTTGGGTTCTGGACACCTTACAACATA
 V  K  M  I  F  A  V  V  V  L  F  L  G  F  W  T  P  Y  N  I
GTGCTCTTCCTAGAGACCCTGGTGGAGCTAGAAGTCCTTCAGGACTGCACCTTTGAAAGA
 V  L  F  L  E  T  L  V  E  L  E  V  L  Q  D  C  T  F  E  R
TACTTGGACTATGCCATCCAGGCCACAGAAACTCTGGCTTTTGTTCACTGCTGCCTTAAT
 Y  L  D  Y  A  I  Q  A  T  E  T  L  A  F  V  H  C  C  L  N
CCCATCATCTACTTTTTTCTGGGGGAGAAATTTCGCAAGTACATCCTACAGCTCTTCAAA
 P  I  I  Y  F  F  L  G  E  K  F  R  K  Y  I  L  Q  L  F  K
ACCTGCAGGGGCCTTTTTGTGCTCTGCCAATACTGTGGGCTCCTCCAAATTTACTCTGCT
 T  C  R  G  L  F  V  L  C  Q  Y  C  G  L  L  Q  I  Y  S  A
GACACCCCCAGCTCATCTTACACGCAGTCCACCATGGATCATGATCTCCATGATGCTCTG
 D  T  P  S  S  S  Y  T  Q  S  T  M  D  H  D  L  H  D  A  L
```

Figure 9-1 – Sequence of CCR4

DNA and protein sequence of CCR4. Red text denotes extracellular portions of the receptor. Black text denotes transmembrane helices. Green text denotes intracellular portions of the receptor. Purple text corresponds to the C-terminal helix VIII region.

9.1.1 – Primer sequences

9.1.1.1 – Primers for site 1 CCR4 point mutants

L92A forward (F; top) and reverse (R; bottom):

5′ GCTCTTCGTGTTTTCC**GCC**CCTTTTTGGGGCTACTATGC 3′

5′ GCATAGTAGCCCCAAAAAGG**GGC**GGAAAACACGAAGAGC 3′

I113A:

5′ GCTAGGTCTGTGCAAGATG**GCT**TCCTGGATGTACTTGGTGGG 3′

5′ CCCACCAAGTACATCCAGGA**AGC**CATCTTGCACAGACCTAGC 3′

S114A:

5′ GGTCTGTGCAAGATGATT**GCC**TGGATGTACTTGGTGGGC 3′

5′ GCCCACCAAGTACATCCA**GGC**AATCATCTTGCACAGACC 3′

Y117A:

5′ GCAAGATGATTTCCTGGATG**GCC**TTGGTGGGCTTTTACAGTGG 3′

5′ CCACTGTAAAAGCCCACCAA**GGC**CATCCAGGAAATCATCTTGC 3′

Y117F:

5′ GCAAGATGATTTCCTGGATG**TTC**TTGGTGGGCTTTTACAGTGG 3′

5′ CCACTGTAAAAGCCCACCAA**GAA**CATCCAGGAAATCATCTTGC 3′

L118A:

5′ GATGATTTCCTGGATGTAC**GCG**GTGGGCTTTTACAGTGGC 3′

5′ GCCACTGTAAAAGCCCAC**CGC**GTACATCCAGGAAATCATC 3′

F121A:

5′ CCTGGATGTACTTGGTGGGC**GCT**TACAGTGGCATATTCTTTG 3′

5′ CAAAGAATATGCCACTGTA**AGC**GCCCACCAAGTACATCC 3′

Y122A:

5′ GGATGTACTTGGTGGGCTTT**GCC**AGTGGCATATTCTTTGTC 3′

5′ GACAAAGAATATGCCACT**GGC**AAAGCCCACCAAGTACATCC 3′

Y122F:

5′ GGATGTACTTGGTGGGCTTT**TTC**AGTGGCATATTCTTTGTC 3′

5′ GACAAAGAATATGCCACT**GAA**AAAGCCCACCAAGTACATCC 3′

I125A:

5′ GGTGGGCTTTTACAGTGGC**GCA**TTCTTTGTCATGCTCATG 3′

5′ CATGAGCATGACAAAGAA**TGC**GCCACTGTAAAAGCCCACC 3′

F126A:

5′ GGTGGCTTTTACAGTGGCATA**GCC**TTTGTCATGCTCATGAGCATTG 3′

5′ CAATGCTCATGAGCATGACAAA**GGC**TATGCCACTGTAAAAGCCACC 3′

F173A:

5′ GTTCGCCTCCCTTCCTGGC**GCT**CTGTTCAGCACTTGTTATAC 3′

5′ GTATAACAAGTGCTGAACAG**AGC**GCCAGGAAGGGAGGCGAAC 3′

K188A:

5′ CGCAACCATACCTACTGC**GCA**ACCAAGTACTCTCTCAAC 3′

5′ GTTGAGAGAGTACTTGGT**TGC**GCAGTAGGTATGGTTGCG 3′

S202A:

5′ CACGACGTGGAAGGTTCTC**GCC**TCCCTGGAAATCAACATTC 3′

5′ GAATGTTGATTTCCAGGGA**GGC**GAGAACCTTCCACGTCGTG 3′

E205A:

5′ GAGGGTTCTCAGCTCCCTG**GCA**ATCAACATTCTCGGATTG 3′

5′ CAATCCGAGAATGTTGATTGCCAGGGAGCTGAGAACCCTC 3′

E205D:

5′ GAGGGTTCTCAGCTCCCTG**GAC**ATCAACATTCTCGGATTG 3′

5′ CAATCCGAGAATGTTGAT**GTC**CAGGGAGCTGAGAACCCTC 3′

E205Q:

5′ GAGGGTTCTCAGCTCCCTG**CAA**ATCAACATTCTCGGATTG 3′

5′ CAATCCGAGAATGTTGAT**TTG**CAGGGAGCTGAGAACCCTC 3′

I206A:

5′ GTTCTCAGCTCCCTGGAA**GCC**AACATTCTCGGATTGGTG 3′

5′ CACCAATCCGAGAATGTT**GGC**TTCCAGGGAGCTGAGAAC 3′

L209A:

5′ CTCCCTGGAAATCAACATT**GCC**GGATTGGTGATCCCCTTAG 3′

5′ CTAAGGGGATCACCAATCC**GGC**AATGTTGATTTCCAGGGAG 3′

Y258A:

5′ CTTGGGTTCTGGACACCT**GCC**AACATAGTGCTCTTCCTAG 3′

5′ CTAGGAAGAGCACTATGTT**GGC**AGGTGTCCAGAACCCAAG 3′

Y258F:

5′ CTTGGGTTCTGGACACCT**TTC**AACATAGTGCTCTTCCTAG 3′

5′ CTAGGAAGAGCACTATGTT**GAA**AGGTGTCCAGAACCCAAG 3′

I286A:

5′ GATACTTGGACTATGCC**GCC**CAGGCCACAGAAACTCTG 3′

5′ CAGAGTTTCTGTGGCCTG**GGC**GGCATAGTCCAAGTATC 3′

E290A:

5′ GCCATCCAGGCCACA**GCA**ACTCTGGCTTTTGTTC 3′

5′ GAACAAAAGCCAGAGT**TGC**TGTGGCCTGGATGGC 3′

E290D:

5′ GCCATCCAGGCCACA**GAT**ACTCTGGCTTTTGTTC 3′

5′ GAACAAAAGCCAGAGT**ATC**TGTGGCCTGGATGGC 3′

E290Q:

5′ GCCATCCAGGCCACA**CAA**ACTCTGGCTTTTGTTC 3′

5′ GAACAAAAGCCAGAGT**TTG**TGTGGCCTGGATGGC 3′

9.1.1.2 – Primers for site 2 CCR4 point mutants and truncations

F305A:

5′ CCTTAATCCCATCATCTAC**GCT**TTTCTGGGGGAGAAATTTCG 3′

5′ CGAAATTTCTCCCCCAGAAA**AGC**GTAGATGATGGGATTAAGG 3′

L307V:

5′ CCCATCATCTACTTTTTT**GTG**GGGGAGAAATTTCGCAAG 3′

5′ CTTGCGAAATTTCTCCCC**CAC**AAAAAAGTAGATGATGGG 3′

K310N:

5′ CTACTTTTTTCTGGGGGAG**AAC**TTTCGCAAGTACATCCTAC 3′

5′ GTAGGATGTACTTGCGAAA**GTT**CTCCCCCAGAAAAAAGTAG 3′

L318A:

5′ CGCAAGTACATCCTACAG**GCC**TTCAAAACCTGCAGGGGC 3′

5′ GCCCCTGCAGGTTTTGAA**GGC**CTGTAGGATGTACTTGCG 3′

Δ40 truncation:

5′ ATCCTACAGCTCTTCAAA**TGA**TGCAGGGGCCTTTTTGTG 3′

5′ CACAAAAAGGCCCCTGCA**TCA**TTTGAAGAGCTGTAGGAT 3′

Δ45 truncation:

5′ GAGAAATTTCGCAAGTACATC**TGA**CAGCTCTTCAAAACCTGCAGG 3′

5′ CCTGCAGGTTTTGAAGAGCTG**TCA**GATGTACTTGCGAAATTTCTC 3′

Δ50 truncation:

5′ CTTTTTTCTGGGGGAGAAA**TGA**CGCAAGTACATCCTACAGC 3′

5′ GCTGTAGGATGTACTTGCG**TCA**TTTCTCCCCCAGAAAAAAG 3′

9.2 – Plasmid

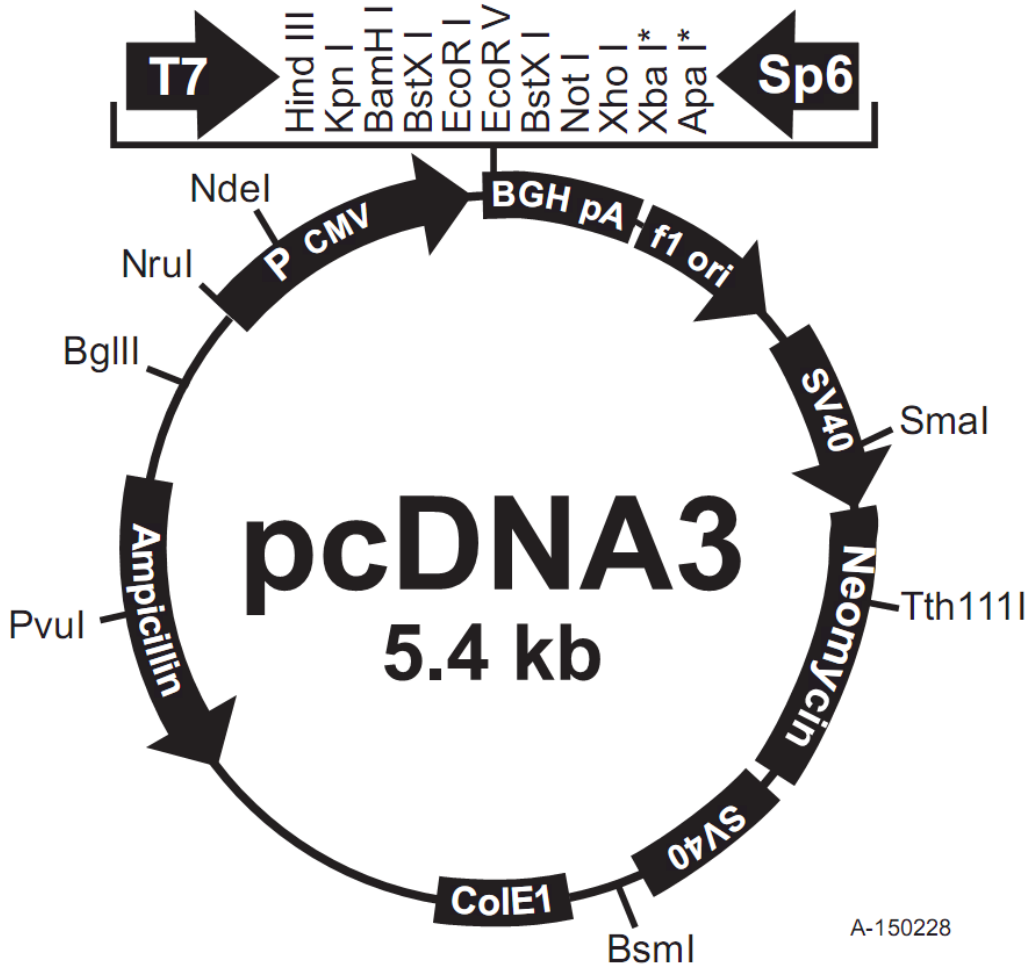

Figure 9-2 – Plasmid map of pcDNA3

Plasmid map of pcDNA3, showing the sites of various promoters, antibiotic resistance genes, origins of replication and the multiple cloning site. * - there is another ATG upstream of the *Xba* I site.